

**Republic of Iraq
Ministry of Higher Education
and Scientific Research
Al-Nahrain University
College of Science
Department of Physics**



**Study of Spectroscopic Properties in
Isotopic Chain of Hf and W Nuclei
Using IBM and IBFM.**

**A Dissertation
Submitted to the College of Science Al-Nahrain University
in Partial Fulfillment of the Requirements for
the Degree of Doctor of Philosophy
in Physics**

**By
Ammar Abdulsattar Z. Alrawi**

**B.Sc., Physics/ College Science / Al-Nahrain University (2000)
M.Sc., Physics/ College Science / Al-Nahrain University (2004)**

2017 A.D.

1438 A.H

Republic of Iraq
Ministry of Higher Education
and Scientific Research
Al-Nahrain University
College of Science
Department of Physics



Study of Spectroscopic Properties in Isotopic Chain of Hf and W Nuclei Using IBM and IBFM.

A Dissertation

Submitted to the College of Science Al-Nahrain University in Partial
Fulfillment of the Requirements for the Degree of Doctor of Philosophy
in Physics

By

Ammar Abdulsattar Z. Alrawi

B.Sc., Physics/ College Science / Al-Nahrain University (2000)

M.Sc., Physics/ College Science / Al-Nahrain University (2004)

Supervised by

Prof. Dr. Saad N. Abood

٢٠١٧

Prof. Dr. Laith A. AL-Ani

١٤٣٨هـ

Supervisors certification

We certify this dissertation entitled " **Study of Spectroscopic Properties in Isotopic Chain of Hf and W Nuclei Using IBM and IBFM** " was prepared by " **Ammar Abdulsattar Z. Alrawi**" under our supervision at the College of Science/ Al-Nahrain University as a partial fulfillment of the requirements for the Degree of Doctor of Philosophy in Physics.

Signature: *Saad N. Abood*
Name: **Dr. Saad N. Abood**
Scientific Degree: Professor
Date: *8/3/2016*

Signature: *Laith A. AL-Ani*
Name: **Dr. Laith A. AL-Ani**
Scientific Degree: Professor
Date: *8/3/2016*

In view of the available recommendations, I forward this dissertation for debate by the examining committee.

Signature: *Saad N. Abood*
Name: **Dr. Saad N. Abood**
Scientific Degree: Professor
Title: Head of Physics Department
Date: *8/3/2016*

Committee certification

We, the examining committee certify that we have read this dissertation entitled " **Study of Spectroscopic Properties in Isotopic Chain of Hf and W Nuclei Using IBM and IBFM** " and examined the student " Ammar Abdulsattar Z. Alrawi " in its contents and that in our opinion, it is accepted for the Degree of Doctor of Philosophy in Physics.

Signature: 

Name: **Dr. Nidhala H. K. Al-Ani**

Scientific Degree: Professor

Date: 5 / 2 / 2017

(Chairman)

Signature: 

Name: **Dr. Nada Fadhal Tawfeq**

Scientific Degree: Professor

Date: 31 / 1 / 2017

(Member)

Signature: 

Name: **Dr. Mohammed Ahmed Salih**

Scientific Degree: Chief Researchers

Date: 1 / 2 / 2017

(Member)


Signature: 

Name: **Dr. Gaith N. Flaiyh**

Scientific Degree: Assist Professor

Date: 31 / 1 / 2017

(Member)

Signature: 

Name: **Dr. Huda Majeed Tawfeek**

Scientific Degree: Assist Professor

Date: 1 / 2 / 2017

(Member)

Signature: 

Name: **Dr. Saad N. Abood**

Scientific Degree: Professor

Date: 31 / 1 / 2017

(Member/ Supervisor)

Signature: 

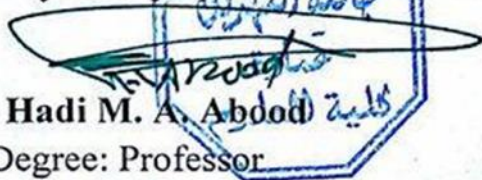
Name: **Dr. Laith A. AL-Ani**

Scientific Degree: Professor

Date: 31 / 1 / 2017

(Member/ Supervisor)

I, hereby certify upon the decision of the examining committee.

Signature: 

Name: **Dr. Hadi M. A. Abood**

Scientific Degree: Professor

Title: Dean of College of Science

Date: 2 / 2 / 2017

ACKNOWLEDGEMENTS

Praise be to **ALLAH** the lord of the whole creation who supported me and gave me the strength and patience to complete this work. The best peace and blessings be upon his Prophet **MOHAMMED** sent a mercy to the world and all his family and companions.

I would like to express my deepest gratitude and sincere thanks to my supervisors **Prof. Dr. Saad N. Abood** and **Prof. Dr. Laith Abdul Aziz Al-Ani** for suggesting this project, their advice guidance which enriched and expanded my understanding to complete this work in the present manner, ask **ALLAH** to protect them.

I would like to thank the Head of the department of physics, and the Dean of the College for their support to perform this work.

I am grateful to **Dr. Fadhel Subhi**, **Dr. Nada F. Tawfeeq**, **Dr. Ibraheem AbdulMahday**, **Dr. Omer Ayad**, **Dr. Ahmad Shaker**, my dearest friend **Belal A. Al-Shaykhli** and all my colleagues and the staff of the Physics department for their support.

I am also thankful to **Dr. A. R. Subber**, Physics Department/collage of education/Al-Basra University, **Dr. Laith A. Najim**, Physics Department/ collage of Science/Al-Mosul University, **Dr. Khalid R. Al-Rawi**, Physics Department/collage of Science for Women/Baghdad University, and **Dr. Ziad R. Al-Rawi**.

I wish I have a word better than thanks to express my feeling to my **Father**, **Mother**, my **Wife** and her family specially her **Father** and sister **Samara**, my **Sisters** and **Brothers**.

Ammar

TABLE OF CONTENTS

Title	Page
Table of Contents	i
List of Figures	iv
List of Tables	vi
List of Symbols	viii
List of Abbreviations	ix
Abstract	x
Chapter One - Introduction	1
1.1 Nuclear Structure	1
1.2 Historical Survey	4
1.2.1 Hf Isotopes	4
1.2.2 W Isotopes	8
1.3 Scientific Motivation of the present work	12
1.4 Thesis Layout	12
Chapter Two - Theoretical Consideration	14
2.1 Group Theoretical Model-The Interacting Boson Model (IBM)	14
2.1.1 Vibrational $SU(5)$ Symmetry	21
2.1.2 Rotational $SU(3)$ Symmetry	24
2.1.3 Gamma Unstable $O(6)$ Symmetry	28
2.2 Interacting Boson Model-2 (IBM-2)	33
2.2.1 Electromagnetic Transitions and Quadrupole Moments in IBM-2	34
2.2.2 Two-neutron Separation Energy	37
2.2.3 The <i>IBM-2</i> Basis States	38
2.2.4 Mixed-Symmetry States	39
2.2.4.1 <i>F-Spin</i>	40
2.3 Interacting Boson-Fermion Model	43
2.3.1 Interacting Boson-Fermion Model-1 (IBFM-1)	43
2.3.1.1 $U^B(5)$ Plus Particle	49
2.3.1.2 $U^B(5)$ plus $j = 4$: The Spin (3) Limit	49
1- Energy Spectra	50
2- Electromagnetic Transition Rates	52
E2 Transitions.	52
M1 Transitions.	53
2.3.1.3 $U^B(5)$ plus $j = 3/2$: The Spin(S) Limit	53
1- Energy Spectra	54
2- Wave Functions	56

3- Electromagnetic Transition Rates E2 Transitions.	57
M1 Transitions.	58
2.3.2 Interacting Boson-Fermion Model-2 (IBFM-2)	58
2.3.2.1 Bosons and fermions	59
1- Boson and fermion operators.	60
2-Isospin	61
3-Basis states	62
2.3.2.2 The IBFM-2 Hamiltonian operator	62
1-Special forms of the interaction	62
2-Transition operators	65
3-Transfer operators	66
4-Algebras: Boson and Fermion Algebras	67
2.3.2.3 Dynamic symmetries	69
1-Lattice of algebras	69
2-Energy Eigenvalues	70
Examples of nuclei with $U_f^B(6) \otimes U_\epsilon^B(6) \otimes U_f^F(4) \otimes U_\epsilon^F(12)$ symmetry.	71
Examples of nuclei with $U_f^B(6) \otimes U_\epsilon^B(6) \otimes U_f^F(4) \otimes U_\epsilon^F(4)$ symmetry.	71
2.3.2.4 Super algebras.	72
1- Supersymmetric chains	72
2- Dynamic supersymmetries	73
2.3.2.5 Numerical studies	75
1- Even-Odd nuclei.	76
2-Energies	78
3-Electromagnetic transitions and moments; E2	78
Chapter Three - Interacting Boson Model Results and Discussion	80
3.1 $^{172-180}\text{Hf}$ Isotopes in IBM-1	80
3.1.1 Hamiltonian Parameters	80
3.1.2 Energy Spectra	80
3.1.3 Electric Transition Probability	86
3.1.4 Magnetic Transition Probability and Mixing Ratio u (E2/M1)	89
3.1.5 Electric Monopole Matrix Element ...($E0$)	93
3.2 $^{182-190}\text{W}$ Isotopes	97
3.2.1 Hamiltonian Parameters Energy Spectra	97
3.2.2 Electric Transition Probability	104
3.2.3 Magnetic Transition Probability and Mixing Ratio δ (E2/M1)	108
3.2.4 Electric Monopole Matrix Element ...($E0$)	112
3.3 $^{172-180}\text{Hf}$ Isotopes in IBM-2	115

3.3.1 Hamiltonian Interaction Parameters	115
3.3.2 Energy Spectra	117
3.3.3 Electric Transition Probability B(E2)	120
3.3.4 Magnetic Transition Probability and Mixing Ratio $u(E2/M1)$	122
3.3.5 Electric Monopole Matrix Element	125
3.3.6 Mixed Symmetry States in $^{172-180}\text{Hf}$ Isotopes	126
3.4 $^{180-190}\text{W}$ Isotopes in IBM-2	131
3.4.1 Hamiltonian Interaction Parameters	131
3.4.2 Energy Spectra	133
3.4.3 Electric Transition Probability B(E2)	135
3.4.4 Magnetic Transition Probability and Mixing Ratio $u(E2/M1)$	138
3.4.5 Electric Monopole Matrix Element	143
3.4.6 Two Neutron Separation Energy	144
3.4.7 Mixed Symmetry States in $^{180-190}\text{W}$ Isotopes	145
Chapter Four- Interacting Boson-Fermion Model Results and Discussion	152
4.1 $^{171-179}\text{Hf}$ Isotopes in IBFM-1	152
4.1.1 Energy Spectra for $^{171-179}\text{Hf}$ isotopes	152
4.1.2 E2 Transitions for $^{171-179}\text{Hf}$ Isotopes	164
4.1.3 M1 Transitions and $^{171-179}\text{Hf}$ Isotopes	167
4.2- $^{181-187}\text{W}$ Isotopes in IBFM-1	169
4.2.1 Energy Levels for $^{181-189}\text{W}$ Isotopes	169
4.2.2 E2 Transitions for $^{181-187}\text{W}$ Isotopes	178
4.2.3 M1 Transitions for $^{181-187}\text{W}$ Isotopes	180
4.3 $^{171-179}\text{Hf}$ Isotopes in IBFM-2	182
4.3.1 Energy Spectra	182
4.3.2 E2 Transitions for $^{171-179}\text{Hf}$ Isotopes	184
4.3.3 M1 Transitions and Mixing Ratio $u(E2/M1)$ for $^{171-179}\text{Hf}$ Isotopes	185
4.4 $^{181-187}\text{W}$ Isotopes in IBFM-2	189
4.4.1 Energy Spectra	189
4.4.2 E2 Transitions for $^{181-189}\text{W}$ Isotopes	190
4.4.3 M1 Transitions and Mixing Ratio $u(E2/M1)$ for $^{181-189}\text{W}$ Isotopes	191
Chapter Five – Conclusions and Suggestions for Future Work	196
5.1 Concluding Remarks	196
Hf Isotopes	196
W Isotopes	198
5.2 Suggestions for Future Work	200
References	202

LIST OF FIGURES

No.	Title	Page
2.1	Energy spectra corresponding to a spherical vibrator, axially deformed rotor, and a deformed χ - unstable nucleus.	21
2.2	Typical spectrum of a nucleus exhibiting the SU (5) symmetry.	26
2.3	An example of a magic square in the Pt-Au region.	74
3.1	Comparison between experimental data, IBM-1 and IBM-2 calculated energy levels for ^{172}Hf .	82
3.2	Comparison between experimental data, IBM-1 and IBM-2 calculated energy levels for ^{174}Hf .	83
3.3	Comparison between experimental data, IBM-1 and IBM-2 calculated energy levels for ^{176}Hf .	84
3.4	Comparison between experimental data, IBM-1 and IBM-2 calculated energy levels for ^{178}Hf .	85
3.5	Comparison between experimental data, IBM-1 and IBM-2 calculated energy levels for ^{180}Hf .	86
3.6	Comparison between experimental data, IBM-1 and IBM-2 calculated energy levels for ^{180}W .	99
3.7	Comparison between experimental data, IBM-1 and IBM-2 calculated energy levels for ^{182}W .	100
3.8	Comparison between experimental data, IBM-1 and IBM-2 calculated energy levels for ^{184}W .	101
3.9	Comparison between experimental data, IBM-1 and IBM-2 calculated energy levels for ^{186}W .	102
3.10	Comparison between experimental data, IBM-1 and IBM-2 calculated energy levels for ^{188}W .	103
3.11	Comparison between experimental data, IBM-1 and IBM-2 calculated energy levels for ^{190}W .	104
3.12	The change in level energy as $\langle_1, \langle_2, \langle_3$.	128
2.13	The F-spin components in the $2_2, 2_3, 2_4$ and 0_3 levels as a function of \langle_2 when all other parameters are as in Table (3-22).	129
3.14	The change in energy of low-lying positive parity states as a function of the Majorana term with $\langle_1 = \langle_3$.	147
3.15	The variation in level energy as a function of \langle_2 .	148
3.16	The F-spin components in the $2_2, 2_3, 2_4$ and 0_3 levels as a function of \langle_2	149
4.1	Comparison between experimental negative parity states data, IBFM-1 and IBFM-2 calculated energy levels for ^{171}Hf .	155

4.2	Comparison between experimental negative parity states data, IBFM-1 and IBFM-2 calculated energy levels for ^{173}Hf .	156
4.3	Comparison between experimental negative parity states data, IBFM-1 and IBFM-2 calculated energy levels for ^{175}Hf .	157
4.4	Comparison between experimental negative parity states data, IBFM-1 and IBFM-2 calculated energy levels for ^{177}Hf .	158
4.5	Comparison between experimental negative parity states data, IBFM-1 and IBFM-2 calculated energy levels for ^{179}Hf .	159
4.6	Comparison between experimental positive parity states data, IBFM-1 and IBFM-2 calculated energy levels for ^{171}Hf .	160
4.7	Comparison between experimental positive parity states data, IBFM-1 and IBFM-2 calculated energy levels for ^{173}Hf .	161
4.8	Comparison between experimental positive parity states data, IBFM-1 and IBFM-2 calculated energy levels for ^{175}Hf .	162
4.9	Comparison between experimental positive parity states data, IBFM-1 and IBFM-2 calculated energy levels for ^{177}Hf .	163
4.10	Comparison between experimental positive parity states data, IBFM-1 and IBFM-2 calculated energy levels for ^{179}Hf .	164
4.11	Comparison between experimental negative parity states data, IBFM-1 and IBFM-2 calculated energy levels for ^{181}W .	171
4.1	Comparison between experimental negative parity states data, IBFM-1 and IBFM-2 calculated energy levels for ^{183}W .	172
4.13	Comparison between experimental negative parity states data, IBFM-1 and IBFM-2 calculated energy levels for ^{185}W .	173
4.14	Comparison between experimental negative parity states data, IBFM-1 and IBFM-2 calculated energy levels for ^{187}W .	174
4.15	Comparison between experimental positive parity states data, IBFM-1 and IBFM-2 calculated energy levels for ^{181}W .	175
4.16	Comparison between experimental positive parity states data, IBFM-1 and IBFM-2 calculated energy levels for ^{183}W .	176
4.16	Comparison between experimental positive parity states data, IBFM-1 and IBFM-2 calculated energy levels for ^{185}W .	177
4.18	Comparison between experimental positive parity states data, IBFM-1 and IBFM-2 calculated energy levels for ^{187}W .	178

LIST OF TABLES

No.	Title	Page
3-1	IBM-1 Hamiltonian parameters for $^{172-180}\text{Hf}$ isotopes.	81
3-2	Experimental and theoretical values of energy ratios in $^{172-180}\text{Hf}$ isotopes.	81
3-3	The root means square deviations (<i>rmsd</i>) between experimental and calculated energy levels for $^{172-180}\text{Hf}$ isotopes.	82
3-4	The reduced matrix element parameters for $^{172-180}\text{Hf}$ isotopes.	86
3-5	Electric Transition Probability $B(E2; J_i \rightarrow J_f)$ for $^{172-180}\text{Hf}$.	88
3-6	Magnetic Transition Probability $B(M1; J_f^+ \rightarrow J_i^+)$ for $^{172-180}\text{Hf}$ isotopes.	91
3-7	Mixing Ratio $u(E2/M1)$ for $^{172-180}\text{Hf}$.	92
3-8	Monopole transition matrix element $...(E0)$ for $^{172-178}\text{Hf}$ isotopes.	95
3-9	Mixing Ratio $X(E0/E2)$ for $^{172-180}\text{Hf}$ isotopes.	96
3-10	IBM-1 Hamiltonian parameters for $^{180-190}\text{W}$ Isotopes.	97
3-11	Energy ratios for $^{180-190}\text{W}$ isotopes in IBM-1 and its dynamical symmetries.	98
3-12	The root mean square deviations (<i>rmsd</i>) between experimental and calculated energy levels for $^{180-190}\text{W}$ isotopes.	98
3-13	The reduced matrix element parameters for $^{180-190}\text{W}$ Isotopes.	105
3-14	Electric transition probability $B(E2; J_i^+ \rightarrow J_f^+)$ for $^{180-186}\text{W}$.	107
3-15	Magnetic transition probability B (M1) for $^{182-188}\text{W}$ isotopes.	109
3-16	Mixing ratio $u(E2/M1)$ for $^{182-186}\text{W}$ Isotopes.	111
3-17	Monopole Matrix Element $...(E0)$ for $^{182-186}\text{W}$ isotopes.	113
3-18	$X(E0/E2)$ for $^{182-186}\text{W}$ Isotopes.	114
3-19	Isomer Shift in fm^2 for $^{182-186}\text{W}$ Isotopes.	114
3-20	Isotopic shifts in fm^2 for $^{182-186}\text{W}$ Isotopes.	115
3-21	IBM-2 Parameters of $^{172-180}\text{Hf}$.	119
3-22	Effective charge used in E2 transition calculations.	120
3-23	IBM-2 Parameters of $^{172-180}\text{Hf}$.	127
3-24	Mixing Ratio $u(E2/M1)$ for $^{172-180}\text{Hf}$ in eb/\sim_N units.	129
3-25	IBM-2 Parameters for $^{180-190}\text{W}$ Isotopes.	134
3-26	Effective charge used in E2 transition calculations.	136

3-27	Branching ratios for $^{182-186}\text{W}$ Isotopes.	138
3-28	Experimental and IBM-2 calculations for g-factors for $^{182-186}\text{W}$.	141
3-29	Two neutron bosons separation energies S_{2n} in MeV units.	145
4-1	Adopted Parameters which used for IBFM-1 calculation.	152
4-2	Adopted values for the parameters used for IBFM calculation.	153
4-3	Effective fermions charge for Hafnium isotopes.	165
4-4	Electric Transition Probability for $^{171-179}\text{Hf}$ $B(E2; J_i^+ \rightarrow J_f^+)$ for Positive Parity States.	166
4-5	Electric Transition Probability for $^{171-179}\text{Hf}$ $B(E2; J_i^+ \rightarrow J_f^+)$ for negative Parity States.	167
4-6	Magnetic Transition Probability $B(M1; J_i \rightarrow J_f)$ for $^{171-179}\text{Hf}$ for positive Parity State.	168
4-7	Magnetic Transition Probability $B(M1; J_i \rightarrow J_f)$ for $^{171-179}\text{Hf}$ for negative Parity State.	169
4-8	Adopted values for the parameters used for IBFM calculation.	170
4-9	Electric Transition Probability $B(E2; J_i^+ \rightarrow J_f^+)$ for $^{181-187}\text{W}$, for Positive Parity States.	179
4-10	Electric Transition Probability $B(E2; J_i^- \rightarrow J_f^-)$ for $^{181-187}\text{W}$, for negative Parity States.	180
4-11	Magnetic Transition Probability $B(M1; J_i^+ \rightarrow J_f^+)$ for $^{181-187}\text{W}$ for Positive Parity States.	181
4-12	Magnetic Transition Probability $B(M1; J_i^- \rightarrow J_f^-)$ for $^{181-187}\text{W}$ for negative Parity States.	181
4-13	Parameters (in MeV) of the boson-fermion interaction for $^{171-179}\text{Hf}$ isotopes	183
4-14	Mixing Ratio $u(E2/M1)$ for $^{171-179}\text{Hf}$ isotopes for positive Parity States.	187
4-15	Mixing Ratio $u(E2/M1)$ for $^{171-179}\text{Hf}$ isotopes for Negative Parity States.	188
4-16	Mixing Ratio $u(E2/M1)$ for $^{181-187}\text{W}$ for Positive Parity States.	193
4-17	Mixing Ratio $u(E2/M1)$ for $^{181-187}\text{W}$ for Negative Parity States.	194

LIST OF SYMBOLS

A	Mass number
$a_{j,m}^\dagger; (\tilde{a}_{j,m})$	Creation (annihilation) operators
Δ	Pairing gap energy
$\Delta\langle r^2 \rangle$	Isotope (isotone) shifts in fm ²
$\delta\langle r^2 \rangle$	Isomer Shift in fm ²
$(E2/M1)$	Mixing ratio in eb / \sim_N
v	Boson energy
v_v	Neutron-boson energy
v_π	Proton-boson energy
\langle_i	Component of Majorana interaction (i=1,2,3)
\vec{l}	Orbital angular momentum quantum no.
$ $	Quadrupole-quadrupole interaction strength
M	Magnetic dipole moment
M_{fv}	Majorana term
\sim_N	Nuclear magnetons
$—$	Boson number
$(E0)$	Monopole transition matrix elements.
$X(E0/E2)$	Branching (mixing)ratios
t	Quadrupole sign parameter

LIST OF ABBREVIATIONS

BCS	Bardon-Cooper-Schrifer parameters
$B(E2)$	Electric quadrupole transition matrix elements in $e^2 \cdot b^2$ units.
$B(M1)$	The magnetic dipole moment matrix elements in ($\sim \frac{2}{N}$).
<i>DDM</i>	Dynamic Deformation Model
e_π	Proton-boson effective charges
e_ν	Neutron-boson effective charges
F_{\max}	Full Symmetry States
g_B	Effective boson is estimated $g = Z/A$
H	Hamiltonian operator
Hf	Hafnium isotopes ($Z=72$)
IBFM	Interacting Boson-Fermion Model
IBM	Interacting boson model
J	Total angular momentum
<i>MSSs</i>	Mixed-Symmetry States
N	Neutron number
n_d	Number of d-boson
N_F	Number of fermion
NPBOS	Neutron –proton- boson (program)
NPBRTN	Neutron- proton boson transition probability (program)
n_s	Number of s-boson
PHINT	Particle-Hole interacting (program)
Q	Quadrupole moments.
<i>rmsd</i>	The root means square deviations
V	Interaction between bosons
W	Tungsten isotopes ($Z = 74$)
Z	Atomic number

Abstract

The interacting boson model (IBM) has been used to make a schematic study of ($^{172-180}\text{Hf}$ and $^{180-190}\text{W}$) isotopes. For each isotope of Hafnium and Tungsten determined the values of the parameters in the Hamiltonian of IBM-1 and IBM-2, which satisfied the best fit to the experimental data for energy levels. Beside on these values, can extrapolate to isotopes are extrapolated for which no experimental data founded and can make predictions for future experiments. We obtain the electromagnetic transition probability $B(E2)$ and $B(M1)$ by using the same values of these parameters for each isotope to, quadrupole moments for first and second excited states, mixing ratios $u(E2/M1)$ and monopole transition probabilities $B(E0)$, isomer and isotopic shifts and two neutron boson separation energy. Where our results had good agreement with the experimental data in general, although more experimental data we needed for the nuclear properties. The long range goal is to understand the origin of the IBM-1 and IBM-2 parameters in terms of a microscopic theory, such as nuclear shell and Nilsson models.

Results of schematic calculations are presented in various terms of F -spin symmetry in the Hamiltonian of the IBM-2. Specific attention is paid to the effect of F -spin symmetry breaking on gamma to ground and gamma to gamma $M1$ transition in deformed nuclei. A comparison with available magnetic dipole moment transition probability $M1$ data in deformed nuclei is presented. The constraints implicit by these data on the form of IBM-2 Hamiltonian in deformed nuclei are discussed.

Mixed symmetry states are also studied. It is found that some of the mixed symmetry states with moderate high spins change very fast with respect to Majorana interaction. Under known conditions, they become the yrast state or yrare state. These states are difficult to decay and become very stable. This study suggests that a possible new mode of isomers may

exist due to the special nature in their proton and neutron degrees of freedom for these isotopes.

The mixed-symmetry 2_3^+ , 2_4^+ , 2_5^+ , 3_2^+ and 1^+ states or at least a fragment of it, have been identified in Hf and W isotopes. This enable us to trace the evolution of the one-phonon and two-phonon states in the even-even Hafnium and Tungsten isotopic chain from the γ -soft nuclei near $N = 82$ to the deformed nuclei towards mid-shell.

In $^{180-190}\text{W}$ isotopes, energy levels, B (E2), B (M1) and mixed symmetry states (*MSS*) have been discussed using IBM-2. The effects of the Majorana parameters on the energy of the highly excited state have been investigated. The variation of these parameters has a great effect on the properties of *MSS*. All the calculated results were compared to the available experimental data and a reasonable agreement was achieved. It is found that the 2_5^+ , in ^{180}W and ^{182}W are the first 2^+ mixed symmetry states, while the 2_4^+ , in ^{184}W and ^{186}W are the first 2^+ mixed symmetry states. The B (*M1*) properties of even $^{180-188}\text{W}$ isotopes are investigated in the IBM-2. The u (*E2/M1*) mixing ratios, g -factors, and summed *M1* strength are calculated. A least-squares fit of the excitation energies is used to fix the IBM-1 projected Hamiltonian parameters, while the *F*-spin-breaking terms are adjusted to reproduce the *M1* properties of low-lying states. The influence of *F*-spin mixing on the summed *M1* strength is studied using the coherent state technique in perturbation theory. The *M1* properties of the low-lying states are described satisfactorily when the standard boson g factors are used, but the summed *M1* strengths are found to be larger than the present experimental values. Possible g factor adjustment, which reconciles the calculated and experimental *M1* strength, is discussed.

The Hafnium ($Z=72$) lies in the deformed region and tungsten isotopes ($Z = 74$) lie in the transitional region that occurs at the upper limit of the range of the deformed nuclei. The γ -ray E2/M1 mixing ratios for the

selected transitions in $^{172-180}\text{Hf}$ and $^{180-188}\text{W}$ are calculated in the IBM-2. The Majorana parameters are found to have a great effect on the energy of mixed-symmetry states as well as on the sign and magnitude of the E2/M1 mixing ratios of transitions between regular (symmetric) states. The results demonstrate the sensitivity of the sign and magnitude of $u(E2/M1)$ values on particular IBM-2 parameters.

In this study, analyzed the positive and negative parity states of odd Hf and W isotopes within framework IBFM-1 and IBFM-2. The results of an IBFM-1 and IBFM-2 multilevel calculations of $2f_{5/2}, 3p_{3/2}$ and $3p_{1/2}$, single particle orbit are reported for the positive and negative parity states of the odd atomic mass number, A, Hf and W isotopes. Also, an IBM-1 and IBM-2 calculation by using ODDA and PBEFM programs is presented for the low-lying states in the even-even $^{170-180}\text{Hf}$ and $^{180-190}\text{W}$ core nucleus. The energy levels, B (E2) and B (M1) transition probabilities and mixing ratios are calculated and compared to the available experimental data. We found that the calculated positive and negative parity low spin state energy spectra of the odd-A $^{171-179}\text{Hf}$ and $^{181-187}\text{W}$ isotopes agree quite well with the experimental data.

CHAPTER ONE

INTRODUCTION

CHAPTER ONE

INTRODUCTION

1.1 Nuclear structure

Nuclear structure has been an active field of research since the discovery of the nucleus. Rutherford found that most of all matter was concentrated in a very small core at the center of the atom in 1911 [1]. Perhaps the next great milestone was the discovery of the neutron by the associate and doctoral student of Rutherford, Chadwick in 1932 [2]. It is noteworthy that by this time special relativity, quantum mechanics, and the relativistic formulation of quantum mechanics were already developed. The existence of the positron was postulated by *Dirac* in his relativistic formulation of quantum mechanics in 1928 [3, 4] and it was subsequently discovered in 1932 by Anderson [5], in the same year the neutron was discovered. The proton and neutron have since been used as the fundamental building blocks in describing the nature of the atomic nucleus to this day.

A number of models have been developed to describe the large array of phenomena and properties displayed by atomic nuclei. The **Liquid Drop Model (LDM)**, first proposed by Gamow in 1928 [6], viewed the nucleus as drop of liquid whose constituent particles were held together by surface tension. This model was able to describe some bulk properties of nuclei. Using the ideas of the liquid drop model, von Weizsäcker developed a semi-empirical mass formula [7] to predict nuclear masses. A large breakthrough in nuclear theory came in 1949 when Maria Goeppert-Mayer [8] and independently Jensen, Haxel and Suess [9] were able to explain the magic numbers in nuclei, where nuclei would exhibit an increased stability, by including a spin-orbit interaction term in a Hamiltonian that considered all nucleons to be orbiting essentially freely in an average field created by all the other nucleons. The magic numbers correspond to closed shells in nuclei analogous to

the filling of electron shells in atoms. Excited states were found that correspond to the excitation of a nucleon into an orbit of a higher lying shell as predicted by the model. The shell model, as this model is called, has been one of the most fundamental ways to describe atomic nuclei. It has been used extensively in the analysis of experimental data.

Apart from the single-particle excitations found in nuclei, another type of excitation, collective excitation, was soon explained. In 1950, Rainwater observed that spherical nuclei could easily be deformed [10]. This led the way in the 1950's for more ground breaking work done by Bohr and Mottelson [11, 12] and also Hill and Wheeler [13] when they presented models for a collective motion in nuclei. These models used shapes to parameterize the nucleus and used their dynamics to derive the collective phenomena observed. Since the discoveries of single-particle and collective motion, these have been the two ways in which excitations in nuclei have been classified. The interplay between single-particle and collective degrees of freedom has long been and continues to be an active field of study. One example is perhaps a variation of the shell model, which was proposed by Nilsson in 1955 [14] where he considered the average potential of the shell model to be deformed. This led to the idea of changing shell structure with deformation.

In 1975, the **Interacting Boson Model (IBM)**, the model used in the present work, was proposed by Iachello and Arima [15], where interacting bosons are used to describe collective excitations in nuclei. From the symmetry properties of the model's boson Hamiltonian, three types of idealized nuclei were found whose properties can be calculated analytically. These three limits of nuclei can be used as benchmarks with which to classify different nuclei. It was found that different regions of the nuclear chart exhibit properties that are similar to one of these idealized limits.

The above account of nuclear physics is very brief and highlights only a few of the main accomplishments in nuclear physics in the twentieth century. Although brief, it can be seen that there is not one single comprehensive theory in nuclear physics, but several models tailored to describe specific phenomena. A quote taken from the book of Eisenbud and Wigner [16] published in 1958 describes the state of nuclear theory in the following way:

"Introduction forces are not yet completely known and it is clear that they have a complex character. Even the consequences of a simple interaction are difficult to obtain for a system containing a large but finite number of particles. A good deal of effort has been expended, therefore, in the search for simple models in terms of which the broad regularities satisfied by nuclei could be understood. This search has led to a number of interesting but only partially successful models; these have proved very fruitful for the stimulation of experimental research, and for the development of further ideas on nuclear structure. One can hope that future investigations will clarify the limitations of these models and provide an understanding of the validity of it different models for different groups of phenomena".

Although written in 1958, the ideas set forth in this quote still serve as a description of present day research in nuclear physics. It is with the aim of better understanding the "broad regularities satisfied by nuclei" and "understanding the validity of different models for different groups of phenomena" that the topic of this present work is introduced. One of the broad regularities in nuclei that will be investigated is the existence of a certain class of collective excitations called mixed-symmetry states defined within the Interacting Boson Model (*IBM*). The data obtained from the experimental investigations of these states will help elucidate the extent of the validity of the *IBM*.

1.2 Historical Survey

During the last two-decade nuclear spin states and high spin states have been the subject of experimental and theoretical studies. The fascinating progress in this new field has been made possible by the essential development in experimental on exciting and detecting the high spin states in Hf-W nuclei. Apart from such interesting expectations as existence of a deformed and super-deformation, the research in this new field can also be considered as providing a tool for testing the validity of **Interacting Boson Model (IBM)** and **Interacting Boson Fermion Model (IBFM)**.

1.2.1 Hf isotopes

K. S. Krane [17] proposed the multipole mixing ratios $u(E2/M1)$ of gamma transitions in even-even deformed nuclei. A summary is presented of the magnitudes and phases of previously measured $u(E2/M1)$ multipole mixing ratios of gamma transition deexciting levels of the beta and gamma bands to the ground state band in even-even deformed nuclei. A uniform phase, with few exceptions is characteristic of transitions depopulating the gamma band, while no systematic behavior is apparent among the nuclei in this region. Although none of the previously proposed theoretical interpretation is sufficient to explain both the magnitudes and relative phases of these mixing ratios, a phenomenological interpretation in terms of $\Delta K = 1$ band mixing through the intermediary of a $K = 1^+$ excitation is successful with regard to the relative magnitudes and phases in a number of cases.

Hamilton *et al.*, [18] have studied $X(E0/E2)$ values of ^{178}Hf and compared with nuclear models. Three of these values are considerably large than the s -vibrational model estimates. Experiments are suggested to test the possibility that large $X(E0/E2)$ values indicate mostly proton excitations.

Chen *et al.*, [19] investigated the Hf isotopes in the boson plus Fermion pair model. Energy spectra, effective moments of inertia and $B(E2)$ values are calculated. It was found that the high spin anomalies qualitatively by the model. Possible extension of the model is disused.

Subber [20] studied the monopole transition in deformed nuclei of Hf isotopes. The structure and monopole transitions of sum neutron rich deformed Hf isotopes have been studied within the framework of the Interacting Boson Model. The level structure for two selected isotopes $Hf^{176-178}$ and $B(E2)$, $... (E0)$ and the $X(E0/E2)$ ratios have been calculated. The numerical results obtained have been compared to the experimental data. Satisfactory results for comparison were obtained.

Abou Salem and El-mageed [21] studied the spectra of even-even Hf isotopes through the selecting of core-cluster decomposition of the parent nucleus. The considered partition should give internal stability of the core-cluster combination. The modified Wood-Saxon and Coulomb potentials were used to reproduce the spectra of even-even Hf isotopes where the core radius was taken as a free parameter. The theoretical calculations of the excitation energies and the transition probabilities $B(E2)$ of the ground state band were compared to the experimental data of the considered Hf isotopes. The obtained results reflect the ability of describing the pure rotational ground state band of even-even Hf isotopes through the core cluster decomposition model.

The two-dimensional total routhian surface calculations have been carried out to study the triaxial super-deformed structured of a neutron-rich nucleus Hf^{178} firstly studied by Shao-Ying *et al.*, [22]. In particular, the effects of the rotational frequency S and pairing-energy gap parameter Δ are discussed in detail in the course of shaping its triaxial super deformed nucleus Hf^{173} . Finally, more systematical results have been investigated for some confirmed super-deformed nuclei experimentally and a few predicted triaxial super deformed nuclei theoretically with

quadrupole deformation $v_2 \approx 0.4$ and triaxial deformation $\chi \approx 20^\circ$ or $\chi \approx 30^\circ$ in the $Z = 72$.

Mansour and Saad [23] studied the properties of high-spin states and the alignment effects in the lighter $^{157-175}\text{Hf}$ isotopes. An interesting nuclear feature emerging from this study concerns the evaluation of the moment of inertia and the yrast line yields conclusion in the Hf isotopes is discussed.

Usmanov *et al.*, [24] investigated the analysis of electromagnetic transitions in nuclei $^{176-178}\text{Hf}$. In this study, the structure of excited states and non-adiabatic effects in manifested in the energies and probabilities of electromagnetic transitions are studied in the context of a phenomenological model taking into account the Coriolis mixing of the low-lying states of positive parity in rotational bands. Energies and the structure of wave functions of excited states are calculated. The calculated energies are in agreement with the experimental data. The mixing effect is demonstrated to play an important role in the wave functions of vibrational states. The probabilities of E2 and M1 transitions are calculated. The theoretical values of ratios and multipole mixing coefficients $u(E2/M1)$ of transitions from the first and second beta and gamma vibrational bands are compared to the available experimental data.

Ohlsson [25] showed that the even-even deformed nuclei present a rotational band built on their ground state 0. In some of these nuclei, higher energy levels are interpreted as members of a rotational band built on the 3-vibrational level.

Al-Maqtary *et al.*, [26] discussed the Interacting Boson Model-1 (IBM-1) and employed for calculating the energy levels and electromagnetic transitions probabilities $B(E2)$ of the even-even $^{174-180}\text{Hf}$ isotopes. These isotopes have been investigated based on two different arrangements; i.e., the dynamical symmetries of $^{174-180}\text{Hf}$ isotopes;

SU(3) (deformed nuclei) and dynamical symmetries of ^{174}Hf isotope in transition region SU(3)-O (6). The determined values using IBM-1 Hamiltonian showed a significant agreement with the experimental reported energy levels data and B(E2) values. The model provides a fast and accurate prediction method of energy levels and B(E2) values.

Nomura *et al.*, [27] studied the collective structural evolution in neutron rich Yb-Hf-W-Os and Pt isotopes. In this study an Interacting Boson Model Hamiltonian determined from Hatree-Fock-Bogoliubov calculation with microscopic Gogny energy density function DIM applied to the spectroscopic analysis of neutron rich Yb-Hf-W-Os and Pt isotopes with mass $A \approx 180 - 200$. Excitation energies and transition rates for the relevant low-lying quadrupole collective states are calculated by this method. Transitions from prolate to oblate ground state shapes are analyzed as a function of neutron number in a given isotopic chain by calculating excitation energies, B(E2) ratios, and correlation energies in the ground state.

Praharaj *et al.*, [28] studied the band structures and deformations of rare-earth nuclei using deformed Hartree-Fock and angular momentum projection theory and some results are presented here.

In 2013, Gupta [29] studied the collective band structure of $^{166-168}\text{Hf}$ in IBM and DPPQ. This study showed the $^{166-168}\text{Hf}$ are the lightest isotopes of Hf for which the spectral information for non-yrast levels is now available from recent experiments. The algebraic Interacting Boson Model-1 (IBM-1) is employed to reproduce their level structure and to produce the E2 transition probabilities. The pairing plus quadrupole model (PPQ) is used to predict their spectra and E2 transition rates and the static moments in a microscopic approach. The spin assignments I^f of new levels and K- and structures are studied. The validity of inclusion of $^{166-168}\text{Hf}$ as members of U(12) super-group is studied using various empirical observations. The potential energy

surfaces for the two isotopes are compared and the fitting of the nucleons in Nilsson orbits is analyzed to yield a consistent comprehensive view of the two $Z=72$ isotopes.

Ma [30] studied in 2014 the triaxial strongly deformed structures in the even-even Hf isotopes. This study showed that the two rotational bands of distinct character have been identified in ^{164}Hf from a recent experiment at Gamma-sphere. They are suggested to correspond to the long anticipated triaxial strongly deformed (TSD) bands predicted by theoretical studies. The bands are substantially stronger in intensity and are located at lower spins than the previously observed TSD bands in ^{164}Hf , and have been linked to the known states, hereby making ^{164}Hf the best even-even system for the study of TSD structures in the $A \approx 160$ mass region. Cranking calculations based on the modified oscillator model suggest that the bands are associated with four quasi-particle configurations involving high- j intruder $(i_{13/2})^2$ proton orbits. Wobbling model has not been observed in Hf^{164} and the possible reasons are discussed.

1.2.2 W Isotopes

The s and x vibrational bands are nearly degenerated around $W^{182-184}$ making these nuclei ideal for probing the interaction between these important collective degrees of freedom in nuclei. A perturbation treatment of the coupling between the various collective degrees of freedom (rotation, s -vibration and x -vibration) is inadequate to reproduce the collective properties in the shape of transitional nuclei, a region of nuclear shape change from spherical to deformed or prolate to oblate. The first attempt at a more exact treatment of such couplings was accomplished by Kumar and Baranger [31] who solved Bohr's Hamiltonian using a pairing plus quadrupole model. Kumar and Baranger predicted some unusual features, such as a prolate-oblate shape transition in Os-Pt nuclei and a strong mixing between the beta and

gamma bands in the more strongly deformed rotational W nuclei. The former has been established [32, 33] by the measurement of the quadrupole moments of the first excited state in Coulomb excitation experiments. A notable consequence of the latter is the reduction of quadrupole moments for the 2_2^+ and 2_3^+ states and the predicted deviation from the Alaga rule for the decay of the beta and gamma bands. For example, the predicted quadrupole moment of the 2_2^+ state of ^{182}W is only 8% of what it would be if it were a pure $K = 2$, gamma band member of a prolate nucleus. Most of the supportive experimental evidence [34,35] for this strong mixing in W nuclei comes from the electromagnetic properties of the 2_2^+ states and the level energies of the lower members of the gamma and beta bands.

Conflicting experimental evidence exists regarding the band mixing in W nuclei. The known E2 transition between the 2_2^+ and 2_3^+ states and the ground-state band can also be well reproduced by means of a three-bands mixing calculation [36], indicating a rather weak mixing between beta and gamma bands. Moreover, the recent theoretical studies of W nuclei using phenomenological model, such as the general collective model by Hess, Maruhn and Greiner [37] and Interacting Boson Model by Duval and Barrett [38], suggest weak mixing between beta and gamma bands.

Although ^{185}W has been proposed [39] as an empirical example of a deformed odd-mass nucleus with pseudo- L symmetry, it remains true that the specific K mixing implied by the pseudo- L scheme makes it applicable in very special case only.

A new limit of the SU(3) symmetry scheme of the Interacting Boson-Fermion model (IBFM) is suggested for deformed-mass nuclei [40]. In this scheme, states are characterized by the intrinsic quantum number K , instead of the pseudo-orbital angular momentum of previous multi-j symmetries of this type. An application to $^{183-187}\text{W}$ is presented.

Wu *et al.*, [41] studied the coupling between the beta and gamma bands in W nuclei. This work was stimulated by the need for a systematic study of the $E2$ transitions between beta, gamma and ground state bands.

Mosbah *et al.*, [42] applied an Interacting Boson Model-2 (IBM-2) to study the multipole mixing ratios for selected transitions in $^{182-186}W$. The results demonstrate the sensitivity of the sign and magnitude of delta values on particular IBM-2 parameters.

The $M1$ properties of even $^{182-186}W$ isotopes are investigated in the Interacting Boson Model-2 (IBM-2) [43]. The $E2/M1$ mixing ratios, g factors, and summed $M1$ strength are calculated. A least-squares fit of the excitation energies is used to fix the IBM-1 projected Hamiltonian parameters, while the F -spin-breaking terms are adjusted to reproduce the $M1$ properties of low-lying states. The influence of F -spin mixing on the summed $M1$ strength is studied using the coherent state technique in perturbation theory. When the standard boson g factors are used, the $M1$ properties of the low-lying states are described satisfactorily, but the summed $M1$ strengths are found to be larger than present experimental values. Possible g factor adjustment, which reconciles the calculated and experimental $M1$ strength, is discussed.

Ameer and AL-Shimmary [44] investigated even-even $^{180-190}W$ isotopes with means IBM-1. For these isotopes, the energy levels, $B(E2)$ transition probabilities, and electric quadrupole moment were calculated. The results are compared to the most recent experimental data. In 2011 Abojassem and AL-Temeame [45] studied the nuclear structure of ^{182}W using IBM-1. In this work, the energy levels and reduced transition probability have been studied. Also, the nucleus shape was determined through the potential energy surface; the square rotational energy and the moment of inertia were calculated.

Sharrad *et al.*, [46] investigated the low-lying states of ^{184}W and ^{184}Os nuclei. The energy levels, $B(E2)$ values, intrinsic quadrupole moment and potential energy surface were calculated using IBM-1. The predicted energy levels and transition probabilities and intrinsic quadrupole moments results are reasonably consistent with the experimental data.

The backbending phenomenon in deformed even-even $^{180-182}\text{W}$ isotopes within IBM-1, have been studied by AL-Ameer and Hussein[47]. $^{180-182}\text{W}$ isotopes near mass region $A \approx 180$ which exhibits feature of the $SU(3)-O(6)$ symmetry at low energy and the backbending phenomenon a high spin, are studied in framework of IBM-1. A reasonable agreement was obtained between the theoretical calculation and the experimental data. The backbending phenomenon was noticed both experimentally and theoretically were in a good agreement.

Mohmmadi and Banafsheh Nemati Giv [48] studied the backbending W isotopes. They developed a special computing code for calculation of nuclear deformation parameters (s) of tungsten isotopes. It has been shown from these calculations that by increasing neutron number, deformation parameter also increases for heavier isotopes which means more deformation from spherical shape. By comparison with Nilsson level diagrams, quadrupole deformation (s_2) of these isotopes can be inferred.

In tungsten isotopes $Z = 74$ ($A=180-186$), energy levels, $B(E2)$, $B(M1)$ and mixed symmetry states (MSS) have been discussed using the Interacting Boson Model (IBM-2) studied by Mahdi *et al.*, [49]. The effect of the Majorana parameters on energy of the highly excited state have been investigated. The variation of these parameters have a great effect on the properties of MSS. All the calculated results were compared with the available experimental data and a reasonable agreement has been achieved. It is found that the 2_4^+ in ^{180}W and ^{182}W

are the first 2^+ mixed symmetry states, while the 2_5^+ in ^{184}W and ^{186}W are the first 2^+ mixed symmetry states.

1.3 Scientific Motivation of the Present Work

The purpose of the present study is to analyze some properties of the nuclear structure of Hf and W isotopes with the framework of IBM and IBFM. Firstly, the low-lying excited energy states for even-even positive parity states and even-odd negative parity states are examined. Secondly, the reduced transition probabilities for quadrupole and dipole $B(E2)$ and $B(M1)$ and $B(E0)$ are determined and thirdly, the theoretical results are compared to the available experimental data. Part of this work is an investigation of the mixed-symmetry states for some states when there is a mixture between the wavefunction for proton and neutron, and then determines the quadrupole moment (Q) to find out the deformation of these isotopes, mixing ratios $u(E2/M1)$ and finally $X(E0/E2)$ ratios.

The $^{172-180}\text{Hf}$ nuclei under consideration have $Z = 72$ and $N = 100$ to 108, which mean that we have (for ^{176}Hf) 22 proton particle outside shell at 50 or 10 proton holes related to the closed shell at the magic number 82. The neutrons number are 104 (^{176}Hf), means that have 22 neutrons outside the major closed shell at 82, or we have 22 holes related to the closed shell at 126, and 106 which means that we have 24 neutrons outside number 82 or 20 holes outside the closed shell at magic number 126. The large numbers of nucleons outside the major shell make the nucleus close to heavy deformed nuclei more like Gd, Er, and Sm nuclei.

The aims of the present study are the following:

- 1- The properties of the even-even Hf-W nuclei are investigated in the framework of Interacting Boson Model (IBM) and Interacting Boson-Fermion model (IBFM), including the neutron-proton degree of freedom. The axially symmetric deformed feature of Hf nuclei to transition from gamma unstable region in W nuclei is shown. This

work the dynamical symmetries are investigated Hf and W nuclei and studies the energy levels, Electromagnetic transition probabilities $B(E2)$, $B(M1)$, mixing ratio $u(E2/M1)$ and monopole transition probability $B(E0)$, quadrupole and magnetic moments and monopole transitions.

- 2- The implementing IBM-2 calculation of the even-even W isotopes in the context of new experimental data.
- 3- Studying the mixed symmetry characters through a study of various quantities, the wave function, the F-spin values and the electromagnetic transition probabilities.
- 4- Identifying the one-phonon and two-phonon mixed symmetry states.
- 5- Studying some even-odd $^{171-179}\text{Hf}$ and $^{181-187}\text{W}$ isotopes purposely for the sake of having alternative testes experimental data. In this study spectroscopic properties such as energy levels, electromagnetic transition probabilities, mixing ratios $u(E2/M1)$, quadrupole and magnetic moments for these isotopes will be investigated using IBM and IBFM.

1.4 Thesis Layout

Finally, a brief outline of the remaining this work will be given. In Chapter two, some background on the Interacting Boson Model (IBM) and interacting Boson-Fermion Model (IBFM) in details, Mixed Symmetry States (MSS). The results of IBM are discussed in Chapter Three, and the results of IBFM are discussed in Chapter four, Chapter five gives the concluding remarks and suggestions for future work.

CHAPTER TWO
THEORETICAL
CONSIDERATIONS

CHAPTER TWO

THEORETICAL CONSIDERATIONS

2.1 Group Theoretical Model-The Interacting Boson Model (IBM)

Iachello and Arima [50, 51, 52] have proposed a model which attempts to describe the collective structure of all nuclei with $A \geq 100$, except those near closed shells. The particles outside of closed shells are treated as bosons, or pairs of particles, which can occupy one of two levels: a ground state with angular momentum equal to zero (called s-bosons) and an excited state with two units of angular momentum (called d-bosons). The d-bosons have energy v_d , the s-bosons v_s ; one can define a boson energy $v = v_d - v_s$. Unlike the more familiar bosons, these bosons may interact with each other. Thus, the model has been called the **Interacting Boson Model (IBM)**. The total number of bosons, equal to the number of d-bosons plus the number of s-bosons, $N = n_d + n_s$, is a constant in the IBM prescription as for a given nucleus. N is the number of pairs of neutrons plus the number of pairs of protons, outside their respective nearest closed shells, without distinguishing between the particle or hole character of the pairs. For example, ${}^{182}_{74}\text{W}_{108}$ is characterized by $N=13$, due to the 8 protons (4 proton pairs) + 18 neutrons (9 neutron pairs) away from the closed shell ${}^{208}_{82}\text{Pb}_{126}$. Alternatively, ${}^{174}\text{Hf}$ would correspond to $N=15$, because of the 20 neutron particles away from the 82 neutron closed shell and 10 proton holes away from the 82 proton closed shell.

As stated earlier, interactions between the s - and d - bosons, and among the s - or d - bosons themselves, may occur. Therefore, in the simplest terms, the Hamiltonian of the system can be written as [53]:

$$H = v_s s^\dagger s + v_d \sum_m d_m^\dagger d_m + V \dots\dots\dots (2-1)$$

where v_s and v_d , are the s - and d -boson energies, $s^\dagger(s)$ is the creation (annihilation) operator for s -bosons, $d^\dagger(d)$ is the creation (annihilation)

operator for d-bosons, the sum is taken over the $5(2(L=2) + 1)$ components of the d-boson state, and V is the interaction(s) between the bosons.

In this description, three natural limits occur. The first [50,54] occurs when $v = v_d - v_s \gg V$, so that the energy spectrum is simply given by $E = v n_d$, the ground state being a C_L zero d-boson state. This first limit is similar to the harmonic oscillator of the geometrical picture described in section (2.1.1) of this chapter. The IBM interpretation will be discussed later. The other two limits occur when $V \gg v$, and correspond to specific interboson interactions. If V is a quadrupole-quadrupole interaction [51,55] between bosons, the system obtained is very similar to a certain kind of deformed rotor. The IBM version will be presented in section (2.1.2). The third limit arises when a repulsive pairing interaction [66] exists between the bosons. As will be seen in the discussion of section (2.1.3), this limit is very-similar to the geometrical description of the x -unstable oscillator of Wilets and Jean [56].

The most general form of the IBM Hamiltonian, in which all possible boson-boson interactions up to second order are explicitly included, is given by [54]:

$$\begin{aligned}
 H = & v_s s^+ s + v_d \sum_m d_m^\dagger d_m + \sum_{J=0,2,4} \frac{1}{2} (2J+1)^{\frac{1}{2}} C_J [(d^\dagger d^\dagger)^{(J)} dd^{(J)}]^{(0)} \\
 & + \frac{1}{2} v_2 \left[(d^\dagger d^\dagger)^{(2)} \cdot (ds)^{(2)} + (s^\dagger d^\dagger)^{(2)} \cdot (dd)^{(2)} \right]^{(0)} \\
 & + \frac{1}{2} v_0 \left[(d^\dagger d^\dagger)^{(0)} \cdot (ss)^{(0)} + (s^\dagger s^\dagger)^{(0)} \cdot (dd)^{(0)} \right]^{(0)} \\
 & + \frac{1}{2} u_2 \left[(d^\dagger s^\dagger)^{(2)} \cdot (ds)^{(2)} \right]^{(0)} + \frac{1}{2} u_0 \left[(s^\dagger s^\dagger)^{(0)} \cdot (ss)^{(0)} \right]^{(0)} \dots\dots\dots(2-2)
 \end{aligned}$$

where v is the boson energy, d^\dagger, d, s^\dagger and s , are as described for Eq. (2-1) and the parentheses denote angular momentum couplings.

The parameters C_J, v_J, u_J are related to the two-body matrix elements by [54]:

$$\begin{aligned} C_J &= \langle d^2 J | V | d^2 J \rangle \\ v_2 &= \langle ds 2 | V | d^2 2 \rangle (5/2)^{1/2} \\ v_0 &= \langle d^2 0 | V | s^2 0 \rangle (1/2)^{1/2} \\ u_2 &= \langle ds 2 | V | ds 2 \rangle 5^{1/2} \\ u_0 &= \langle s^2 0 | V | s^2 0 \rangle \end{aligned} \dots\dots\dots(2-3)$$

The IBM-1 Hamiltonian (Eq. (2-2)) can be written in general form as [55] :

$$\hat{H} = v(\hat{n}_s + \hat{n}_d) + a_0 \hat{P} \cdot \hat{P} + a_1 \hat{L} \cdot \hat{L} + a_2 \hat{Q} \cdot \hat{Q} + a_3 \hat{T}_3 \cdot \hat{T}_3 + a_4 \hat{T}_4 \cdot \hat{T}_4 \dots\dots\dots(2-3a)$$

the operators are:

$$\begin{aligned} \hat{n}_s &= \hat{s}^\dagger \cdot \hat{s} \quad , \quad \hat{n}_d = \hat{d}^\dagger \cdot \hat{d} \quad , \quad \hat{P} = \frac{1}{2}(\hat{d}^- \cdot \hat{d}^-) - \frac{1}{2}(\hat{s} \cdot \hat{s}) \\ \hat{L} &= \sqrt{10}[\hat{d}^\dagger \times \hat{d}^-]^{(1)} \quad , \\ \hat{Q} &= \sqrt{5}[(\hat{d}^\dagger \times \hat{s}^-) + (\hat{s}^\dagger \times \hat{d}^-)]^{(2)} + t[\hat{d}^\dagger \times \hat{d}^-] \\ \hat{T}_3 &= [\hat{d}^\dagger \times \hat{d}^-]^{(3)} \quad , \quad \hat{T}_4 = [\hat{d}^\dagger \times \hat{d}^-]^{(4)} \quad \dots\dots\dots(2-3b) \end{aligned}$$

The phenomenological parameters $a_0, a_1, (a_2, t), a_3, a_4$, represents the strengths of the pairing angular momentum, quadrupole, octupole and hexadecapole interaction between bosons, respectively.

Equation (2-2) appears formidable, especially given the explicit form of the parameters, as introduced in Eq. (2-3). However, the terms correspond to one of four types:

- 1) $v_s s^\dagger s + v_d \sum d_m^\dagger d_m$ - simply counts the number of s -and d -bosons, respectively, and multiplies this number by the appropriate energy;
- 2) the terms with coefficients C_J, u_2 and u_0 represent interactions in which the total number of d -bosons and s -bosons, separately, are conserved, i.e., n_d , is not changed;
- 3) a term (with coefficient v_2) in which n_d , is changed by unity;
- 4) a term (with coefficient v_0) in which n_d is changed by two units.

Returning to the three limits alluded to earlier, the vibrational limit will correspond to a Hamiltonian with only n_d -conserving terms, the

rotational limit to a situation with one and two d-boson number changing terms, and the "x-unstable" limit will represent the situation with two d-boson number changing terms included.

An alternate form, in which the general Hamiltonian may be frequently written, is in terms of the specific interactions between the bosons. In these cases, [54, 57]:

$$H = v \sum_m d_m^\dagger d_m - \left| \sum_{ij} \vec{Q}_i \cdot \vec{Q}_j \right| - \left| \sum_{i<j} L_{ij} \right| - \left| \sum_{i<j} P_{ij} \right| \dots \dots \dots (2-4)$$

where \vec{Q}_i is the quadrupole moment of the i^{th} boson, $L_{ij} = 2\vec{\ell}_i \cdot \vec{\ell}_j$ with $\vec{\ell}_i, \vec{\ell}_j$ being the angular momenta of the i^{th} and j^{th} boson, respectively, P_{ij} is the pairing operator, between bosons, and $|, |', |''$ are the respective strengths of the different interactions. For simplicity, was set equal to zero, so that only $v = v_d - v_s = v_d$ appears in Eq. (2-4).

Associated with the collective states calculated with the IBM are transition operators. In the most general form, the E0, M1, E2, M3, E4 transition operators are, to leading order, given [54,55,58]:

$$T_m^{(\ell)} = r_\ell u_{\ell 2} (d^\dagger s + s^\dagger d)_m^{(2)} + s_\ell (d^\dagger d)_m^{(\ell)} + x_{10} u_{10} u_{m0} (s^\dagger s)_0^{(0)} \dots \dots \dots (2-5)$$

where l denotes the multipolarity with projection m , and r, s, x are the coefficients of the different terms of the operator. In particular, for E2 transitions [54,55,58]:

$$T_m(E2) = r_2 (d^\dagger s + s^\dagger d)_m^{(2)} + s_2 (d^\dagger d)_m^{(2)} \dots \dots \dots (2-6)$$

This operator has two parts $(d^\dagger s + s^\dagger d)^{(2)}$: which satisfies the selection rule $\Delta n_d = \mp 1$, and $(d^\dagger d)^{(2)}$ which satisfies the selection rule $\Delta n_d = 0$. The coefficients and depend on the limit involved or the appropriate intermediate structure. The form of the operator that corresponds to the various limiting symmetries will be discussed later.

Exact forms of the E0, M3, and E4 operators exist. It should be noted that *no M1 transitions can occur* in first order [64, 65, 69]. The reasons lie

in the form of the $M1$ operator [54, 55, 58]:

$$T_m(M1) = S_1 (d^\dagger d)_m^{(1)} \dots\dots\dots (2-7a)$$

As discussed in references [54, 55, 58], the operator $(d^\dagger d)^{(1)}$ proportional to the boson angular momentum operator; therefore, Eq. (2-7a) may be rewritten as

$$T_m(M1) = g_B I_m^{(1)} \dots\dots\dots (2-7b)$$

where g_B is the effective boson g -factor. This form of the operator has no off-diagonal matrix elements, implying that in this approximation $M1$ transitions are forbidden [54, 55, 58]. Some of the transition probabilities obtained from perturbation theory are further discussed in Refs. [54, 55].

The solution of the Hamiltonian, in either the Eq. (2-6) or the Eq. (2-7b) form, may be attempted either analytically or numerically. Arima and Iachello [50, 51, 52] have been able to solve the Hamiltonian analytically in the three -limiting situations described earlier by utilizing the underlying group theoretic aspects of this system. As discussed in Ref.[54], the five components of the $L = 2$ d-boson state and the single component of the $L = 0$ s-boson state span a linear vector space which provides a basis for the totally symmetric representations of the group $SU(6)$, the special unitary group in six dimensions. The group $SU(6)$ is partitioned, with each totally symmetric representation labeled by $[N]$. For a situation where all boson states are degenerate and no boson-boson interaction exists, all states belonging to a particular partition $[N]$ are degenerate. However, given the energy difference $v = v_d - v_s$ and an interaction between the bosons, a definite energy level spectrum will exist. The group $SU(6)$ is characterized by nine parameters which will correspond to the parameters of Eq.(2-6), i.e., N , v , and the coefficients $C_J (J = 0,2,4), \epsilon_2, \epsilon_0, u_2, u_0$.

The E0 operator can be written directly as:

$$\hat{T}(E0) = s_0(d^\dagger d^-) + \chi_0(s^\dagger \tilde{s}) \dots \dots \dots (2-8a)$$

where s_0 and χ_0 are free parameters and the superscript notation indicates spherical tensor coupling. Eq. (2-8a) can be expressed in terms of the boson number operators \hat{n}_s ; \hat{n}_d and $\hat{N} = (\hat{n}_s + \hat{n}_d)$ as [54]:

$$\hat{T}(E0) = \tilde{S}_0 \hat{n}_d + \chi_0 \hat{n}_s = \chi_0 \hat{N} + \tilde{S}_0 \hat{n}_d = S'_0 \hat{N} + \chi'_0 \hat{n}_s \dots \dots \dots (2-8b)$$

where

$$s'_0 = \frac{s_0}{\sqrt{5}}, \tilde{S}_0 = S'_0 - \chi_0, \tilde{\chi}_0 = \chi_0 - S'_0 \dots \dots \dots (2-8c)$$

The IBM-1 possesses simple limiting dynamical symmetries which lead to closed form expressions for the matrix elements of $\hat{T}(E0)$ and, consequently, to selection rules [54]. We deal with the three limiting cases, U(5), SU(3), and O(6), separately.

The isomer shift, $u \langle r^2 \rangle$ is measure r^2 between the first 2^+ state and the ground state,

$$u \langle r^2 \rangle = \tilde{S}_0 \left[\langle \hat{n}_d \rangle_{2^+}^{(N)} - \langle \hat{n}_d \rangle_{0^+}^{(N)} \right] \dots \dots \dots (2-8d)$$

The isotope (isotone) shifts $\Delta \langle r^2 \rangle$, are measure of difference in radii between nuclei one neutron (or proton) pair (one boson) away from each other,

$$\Delta \langle r^2 \rangle^{(N)} = \tilde{\chi}_0 + \tilde{S}_0 \left[\langle r^2 \rangle_{0^+}^{(N+1)} - \langle r^2 \rangle_{0^+}^{(N)} \right] \dots \dots \dots (2-8e)$$

If one can find a subgroup $G \subset SU(6)$ under which the Hamiltonian is invariant, then the diagonalization problem is simplified. In particular, Arima and Iachello have observed that there are three such groups, namely $SU(5)$ [50,54], $SU(3)$ [51,55], and $O(6)$ [59], the special unitary groups in five and three dimensions, and the orthogonal group in six dimensions. The solutions obtained correspond to the same three limits mentioned earlier, the vibrational, rotational, and "x-unstable" limits, respectively.

Frequently, when the subgroup G under which the Hamiltonian is

invariant has been identified, the problem may be written in terms of the forces as given in Eq. (2-8). Then, the eigenvalue problem is reduced to finding the expectation value of the forces. This method of solution in the different limits will be discussed in their separate subsections.

An alternative approach to the eigenvalue problem presented in Eq. (2-6) or Eq. (2-8) is to solve the Hamiltonian numerically. This has advantages in that the entire Hamiltonian may be solved, not only in the limits for which analytic solutions are readily obtainable, but also in the intermediate cases. To this end, Scholten has written a computer code ***PHINT*** [60] which solves the entire IBM Hamiltonian in the Eq. (2-6) or Eq. (2-8) parameterization, or a convenient mixture of the two forms.

The computer code presents the wave functions in the basis $J^f |n_d n_s n_\Delta\rangle$ where J^f is spin-parity, n_d is the number of d-bosons. n_s is the number of pairs of d-bosons coupled to angular momentum zero, and n_Δ is the number of triplets of bosons coupled to angular momentum zero. For example, the 2 d-boson 0^+ state would be denoted $0^+|210\rangle$; the 3 d-boson 0^+ state would be $0^+|310\rangle$; the 3 d-boson 2^+ state would be $2^+|310\rangle$, because the parentage of this state is the $2^+|210\rangle$.

Calculations have been performed with this code to reproduce a number of different situations:

- 1) calculations of the three limiting symmetries which reproduce the analytic solutions;
- 2) calculations of systematic deviations from these limiting cases;
- 3) calculations of, not necessarily physical, situations to understand the operation and interplay of the different parameters contained in the IBM.

The first case will be discussed in subsections (2.1.1), (2.1.2), and (2.1.3). However, since an understanding of the effect of the parameters is essential to the later discussions, the third aspect will be discussed here.

It is more convenient to discuss the forces of the IBM in terms of the parameterization of Eq.(2-8), where the variables are ν , the boson energy, and the strengths of the quadrupole-quadrupole, $\vec{\ell}_i \cdot \vec{\ell}_f$, and pairing interactions between the bosons.

To summarize this section, the IBM model developed by Iachello and Arima aims to predict the structure of collective states of heavy even-even nuclei. This model can be analytically solved for the case of three limiting symmetries; these will be discussed in the next three sections. The model can also be solved numerically with the computer code *PHINT* [60]. A discussion of the transition between the limits will be presented in next section.

2.1.1- The Vibrational $SU(5)$ Symmetry

The first limiting symmetry of the IBM to be discussed was the vibrational limit [8,64]. As described in the last section, a very simple spectrum of collective states, presented in **Figure (2.1)**, arises from a system characterized by a boson energy ν . This limit corresponds to the $O(5)$, orthogonal group in 5 dimensions, symmetry. However, the IBM Hamiltonian can also be solved analytically for the $SU(5)$ representation [50, 54].

6 ⁺ — 4 ⁺ — 3 ⁺ — 2 ⁺ — 0 ⁺ —		6 ⁺ — 4 ⁺ — 3 ⁺ — 0 ⁺ — 2 ⁺ —
4 ⁺ — 2 ⁺ — 0 ⁺ —	4 ⁺ — 4 ⁺ —	0 ⁺ —
	2 ⁺ — 3 ⁺ —	
	0 ⁺ — 2 ⁺ —	
2 ⁺ — Sph. vibrator	6 ⁺ —	4 ⁺ — 2 ⁺ —
U(5)	Sym. rotor	def. γ -unstable
	SU(3)	O(6)
0 ⁺ —	4 ⁺ —	
	2 ⁺ —	
	0 ⁺ —	

Figure (2-1). Energy spectra corresponding to a spherical vibrator, axially deformed rotor, and a deformed χ - unstable nucleus [54].

In the $SU(5)$ representation, the degeneracies of the levels in Figure(2.1) are explicitly broken by the introduction of interactions which

conserve the number of d -bosons. The form of the Hamiltonian in this limit is given by [50,54]:

$$H = \nu \sum_m d_m^\dagger d_m + \sum_J \frac{1}{2} (2J+1)^{\frac{1}{2}} C_J \left[(d^\dagger d^\dagger)^{(J)} \cdot (dd)^{(J)} \right]^{(0)} \dots (2-9)$$

where the C_J 's are given in Eq. (2-3). An analytic solution to this Hamiltonian is presented in detail in Ref. [54]. For the reader's information, the arguments of Arima and Iachello will be repeated here. The Hamiltonian of this symmetry can be written as:

$$\hat{H} = \nu(\hat{n}_s + \hat{n}_d) + a_1 \hat{L} \cdot \hat{L} + a_3 \hat{T}_3 \cdot \hat{T}_3 + a_4 \hat{T}_4 \cdot \hat{T}_4 \dots (2-9a)$$

Where $\nu(\hat{n}_s + \hat{n}_d)$ is the energy of s and d bosons, a_1 is the angular momentum and a_3 is the octupole and a_4 the hexadecapole parameters. The eigenvalue equation may be expressed as:

$$H |n_d \nu n_\Delta JM\rangle = E |n_d \nu n_\Delta JM\rangle \dots (2-10)$$

where H is given by Eq. (2-9) and the states are labelled by the quantum numbers n_d, ν, n_Δ, J, M . The number of d -bosons, n_d , the angular momentum J and its projection M are already familiar; n_d , as discussed earlier, is the number of d -boson triplets coupled to angular momentum zero, and ν is the seniority, which counts the number of d -bosons not coupled to angular momentum zero. An alternate representation involves the quantum number n_s , which counts the number of d -boson pairs coupled to angular momentum zero; ν and n_s are related by $\nu = n_d - 2n_s$. The total number of bosons is partitioned as [54]:

$$n_d = 2n_s + 3n_\Delta + \} \dots (2-11)$$

where $\}$ is the excess bosons and determines the angular momentum range [54]:

$$J = 2\}, 2\} - 2, 2\} - 3, \dots, \} + 1, \} \dots (2-12)$$

The angular momentum $J = 2\} - 1$ is absent because of the requirement that bosons may only be coupled to form symmetric states [61].

An alternate method of solving the Hamiltonian in Eq. (2-9) is to rewrite it in terms of the forces presented earlier in Eq. (2-8). Only three parameters are necessary to describe the interaction between two d -bosons because only three angular momentum couplings can occur [61]: $J = 0, 2, 4$. Therefore, the coefficients $C_J (J = 0, 2, 4)$ in Eq. (2-13), or three alternate parameters r, s, x , are necessary. Iachello and Arima have expressed the interaction as [54]:

$$V = \sum_{i < j} V_{ij} = \sum_{i < j} (r l_{ij} + s P_{ij} + x L_{ij}) \dots \dots \dots (2-13)$$

where l_{ij} is the unit operator, P_{ij} and L_{ij} are the pairing and L interactions discussed earlier. The expectation values of these operators, as given in Ref. [54], are:

$$\begin{aligned} \langle 1 \rangle &= \frac{1}{2} n_d (n_d - 1) \\ \langle L \rangle &= J(J + 1) - 6n_d \\ \langle P \rangle &= (n_d - \nu)(n_d + \nu + 3) \dots \dots \dots (2-14) \end{aligned}$$

Therefore, the eigenvalue of interacting d -boson Hamiltonian are [50, 54]:

$$\begin{aligned} E([N], n_d, \nu, n_\Delta, J, M) &= \nu n_d + r \frac{1}{2} n_d (n_d - 1) \\ &+ s (n_d - \nu)(n_d + \nu + 3) \\ &+ x [J(J + 1) - 6n_d] \dots \dots \dots (2-15) \end{aligned}$$

A typical spectrum in the vibrational limit is presented in **Figure (2.2)**. The spectrum may be divided into several "bands"; this terminology is valid since large $E2$ matrix elements exist between adjacent members of the same band. The states in **Figure (2.2)** are labelled by the quantum numbers n_d, ν, n_Δ . The "bands" are very reminiscent of those occurring in rotational nuclei. The Y -band corresponds to the ground band, X and Z to a x -vibrational band, s to a s -vibrational band and Δ to a

2-phonon χ -vibrational band. The energies of states in some of these bands are given by [54]:

$$\begin{aligned}
 \mathbf{Y \textit{ band}} \quad E_Y(n_d, n_d, 0, J = 2n_d, M) &= \nu n_d + \frac{1}{2} C_4 n_d (n_d - 1) \\
 \mathbf{X \textit{ band}} \quad E_X(n_d, n_d, 0, J = 2n_d - 2, M) &= \nu n_d + \frac{C_4}{2} n_d (n_d - 1) - \chi (8n_d - 2) \\
 \mathbf{Z \textit{ band}} \quad E_Z(n_d, n_d, 0, J = 2n_d - 3, M) &= \nu n_d + \frac{C_4}{2} n_d (n_d - 1) - \chi (12n_d - 6) \\
 \mathbf{S \textit{ band}} \quad E_S(n_d, n_d - 2, 0, J = 2n_d - 4, M) &= \nu n_d + \frac{C_4}{2} n_d (n_d - 1) + \chi (12n_d - 16n_d) + S (4n_d + 1) \\
 \mathbf{\Delta \textit{ band}} \quad E_\Delta(n_d, n_d, 1, J = 2n_d - 6, M) &= \nu n_d + \frac{C_4}{2} n_d (n_d - 1) - 6\chi (4n_d - 5) \dots \dots \dots (2-16)
 \end{aligned}$$

The general form of the electric quadrupole transition operator $T(E2)$ was given in Eq. (2-17). In the limits for which analytic solutions are obtainable, Arima and Iachello require the transition operator to be a generator of the underlying group. For the limit characterized by $SU(5)$, $T(E2)$ is given by [54]:

$$T_m(E2) = r (d^+ s + s^+ d)_m^{(2)} \dots \dots \dots (2-17)$$

for $r = \langle d \| \bar{Q} \| s \rangle (1/5)^{(2)}$, where \bar{Q} is the quadrupole operator. This form of the operator leads to the selection rule $\Delta n_d = \pm 1$.

The $U(5)$ limit of the IBM-1 possesses N and n_d as good quantum numbers [54]. Thus, $T^\wedge(E0)$ is diagonal in this limit and $E0$ transitions are forbidden.

2.1.2- The Rotational $SU(3)$ Symmetry

The second limit of the IBM model is based on the $SU(3)$ group and gives rise to nuclear structures similar to a certain form of the symmetric rotor. This symmetry occurs when there is a dominant quadrupole-quadrupole interaction between bosons, as described in section (2-1). The most general form of the interboson interaction will also include a term of the form $L = l_i^\rightarrow \cdot l_j^\rightarrow$.

In Eq. (2-2), the entire IBM Hamiltonian was presented. Many years ago Elliott [62] showed that if a Hamiltonian could be expressed in terms

Tableaux [61] they represent. Each particle can be represented by a box; boxes may be coupled to form symmetric or antisymmetric states [64].

An example of the collective positive parity states characteristic of the SU(3) symmetry is shown in **Figure (2.2)**, The spectrum is divided into a number of bands according to the (λ, μ) value. The angular momenta J which may occur in each (λ, μ) group are given by [55]:

$$J = K, (K + 1), \dots, (K + \max\{\lambda, \mu\}) \dots \dots \dots (2-24)$$

where $K = \text{integer} = \min\{\lambda, \mu\}, \min\{\lambda, \mu\} - 2, \dots, 1$ or 0 unless $K = 0$.

For $K = 0$, the allowed angular momentum values are [55]:

$$J = \max\{\lambda, \mu\}, \max\{\lambda, \mu\} - 2, \dots, 1 \text{ or } 0 \dots \dots \dots (2-25)$$

The quantum number K is analogous to the K quantum number of a symmetric rotor, namely the projection of the angular momentum J along the nuclear symmetry axis. Therefore, the $K = 0$ and $K = 2$ bands of the $(N-4, 2)$ representation would correspond to the s and x bands, respectively, in the geometrical rotor description of subsection (2.1.2). However, in this limit of the IBM, states with the same angular momentum and (λ, μ) representation are required to be degenerate; e.g., the 2^+_s and 2^+_x states. Also, the transition probabilities between bands are considerably altered, as will be discussed below.

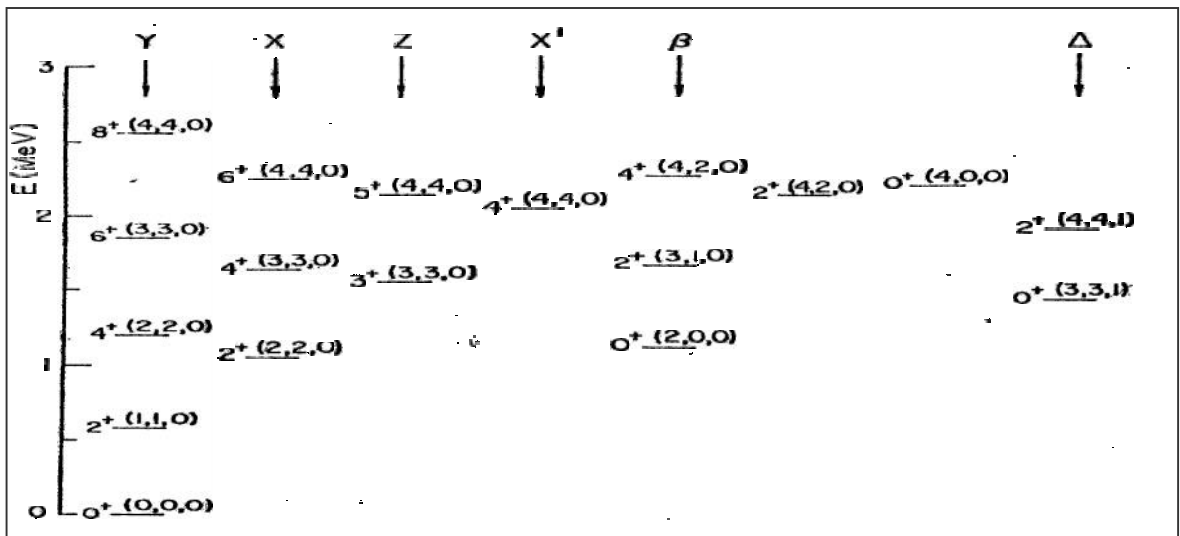


Figure (2.2) Typical spectrum of a nucleus exhibiting the SU(5) symmetry. The states are labeled by the quantum numbers $J^\pi (n_\lambda, \nu, n_x)$. The spectrum is broken up into a number of bands [55].

The most general form of the $E2$ transition operator $T(E2)$ was presented in Eq. (2-17). As for the earlier $SU(5)$ symmetry, Arima and Iachello require this operator to be a generator of the underlying group symmetry. For the case of the $SU(3)$ symmetry, since the operators of Eq. (2-6), namely $d^\dagger s$ and $s^\dagger d$ are already generators of the group [55], the requirement reduces to fixing the values, of the coefficients r_2 and s_2 in Eq.(2-6). The resulting $E2$ operator in the $SU(3)$ symmetry is [55]:

$$T_m(E2) = r_2 \left[(d^\dagger s + s^\dagger d)_m^{(2)} - \frac{1}{2} \sqrt{7} (d^\dagger d)_m^{(2)} \right] \dots \dots \dots (2-26)$$

where r_2 is the effective $E2$ charge, of Eq. (2-6) became $-\frac{1}{2} \sqrt{7} r_2$. Due to the form of the $E2$ operator $T(E2)$ in Eq. (2-26) does not connect states with different (λ, μ) representations [55]. Thus, transitions between the x -band or s -band and the ground band are ***forbidden***. Conversely, transitions between states of the same representation are allowed. Therefore, unlike the predictions of the geometrical rotational model, the 2_x^+ state will preferentially decay to the 0_s^+ state rather than to the 0_g^+ state.

A number of regions of the periodic table have shown evidence of exhibiting a rotational structure characterized by a $J(J+1)$ level sequence. However, the requirement of degenerate β - and γ -vibrations tends to limit the regions of $SU(3)$ symmetry to those where the onset of prolate deformation occurs, such as the Gd isotopes.

$$H = \nu n_d - \left| \sum_{i,j} \vec{Q}_i \cdot \vec{Q}_j \right| - \left| \sum_{i < j} L_{ij} \right| \dots \dots \dots (2-27)$$

where ν , the boson energy, and Q is the quadrupole-quadrupole and L interactions are as previously described. To study a transitional region, they fixed ν and ν' , allowing to linearly decrease as a function of the number of bosons [65].

Equation (2-27) shows that all transition probabilities depend explicitly upon the number of valence nucleons. Now that two limiting symmetries have been presented, the $SU(5)$ and $SU(3)$ limits, it would be

interesting to investigate the transition between these two regions. Such work has recently been conducted by Iachello, Scholten, and Arima. In this investigation, they considered a simpler form of the IBM Hamiltonian in Eq. (2-6), namely [65]:

$$V = v_c - \kappa N_v \dots \dots \dots (2-28)$$

where v_c is a constant and N_v is the number of neutron bosons. This will simulate the transition, since, near $SU(5)$, v is much greater than any interboson interaction, while, near $SU(3)$, the quadrupole-quadrupole interaction dominates the boson energy.

The $SU(3)$ limit of the IBM-1 possesses N as a good quantum number together with the conventional $SU(3)$ quantum numbers (λ, μ) , but n_d is not a good quantum number [55]. However, considering $\hat{T}(E0)$ in the form:

$$\hat{T}(E0) = \kappa_0 \hat{N} + \tilde{\kappa}_0 \sqrt{5} (d^\dagger d)^{(0)} \dots \dots \dots (2-28a)$$

noting that d^\dagger transforms [55] as a $(\lambda, \mu) = (2; 0)$ representation of $SU(3)$; then, e.g., $(\lambda, \mu) = (2N; 0)$ states connect only with $(\lambda, \mu) = (2N-4; 2)$ states via $E0$ transitions. This includes the $E0$ transitions connecting the "s" band ($(2N-4; 2)$ irrep.) with the ground band ($(2N; 0)$ irrep.).

2.1.3- The Gamma Unstable $O(6)$ Symmetry

A third limiting symmetry of the IBM model will occur when the interboson interaction is dominated by a pairing force [52]. Analogous to the $SU(5)$ and $SU(3)$ symmetries, Iachello and Arima have diagonalized the IBM Hamiltonian, generated by $SU(6)$ (Eq. (2-7)), by identifying a subgroup of $SU(6)$ under which the Hamiltonian is invariant. In this case, the subgroup is $O(6)$ which also contains the subgroups $O(5)$ and $O(3)$. By using the group chain, $SU(6) \supset O(6) \supset O(5) \supset O(3)$, the IBM Hamiltonian in the $O(6)$ limit can be written as:

$$H = AP_6 + BC_5 + CC_3 \dots \dots \dots (2-29)$$

where P_6 is the pairing operator in $O(6)$ and C_5 and C_3 are the Casimir operators of $O(5)$ and $O(3)$, respectively. A , B , and C are the strengths of the various components. In terms of the IBM Hamiltonian of Eq. (2-1), corresponds to the term:

$$v_0 \left[(d^\dagger d)^{(0)} (ss)^{(0)} + (s^\dagger s^\dagger)^{(0)} (dd)^{(0)} \right]^{(0)} \dots\dots\dots(2-30)$$

while C_5 and C_3 and correspond to the terms

$$v \sum_m d_m^\dagger d_m + \sum_{J=0,2,4} \frac{1}{2} (2J+1)^{1/2} C_J \left[(d^\dagger d^\dagger)^{(J)} (dd)^{(J)} \right]^{(0)} \dots\dots\dots(2-31)$$

The Hamiltonia of this symmetry is:

$$\hat{H} = a_0 \hat{P}^+ \cdot \hat{P} + a_1 \hat{L} \cdot \hat{L} + a_3 \hat{T}_3 \cdot \hat{T}_3 \dots\dots\dots(2-31a)$$

The symmetric irreducible representations of $O(6)$ are labelled by a quantum number \dagger where [52]:

$$\dagger = N, N-2, N-4, \dots, 0 \text{ or } 1 \text{ for } N = \text{even or odd} \dots\dots\dots(2-32)$$

The expectation value of the $O(6)$ pairing operator, P_6 , can be written in terms of \dagger as [52]:

$$\langle P_6 \rangle = \frac{1}{4} (N - \dagger)(N + \dagger + 4) \dots\dots\dots(2-33)$$

As stated in Ref. [52], the quantum number \ddagger is chosen to characterize the representations of $O(5)$ where

$$\ddagger = \dagger, \dagger - 1, \dots, 0 \dots\dots\dots(2-34)$$

The expectation value of C_5 in the \ddagger representation of $O(5)$ is given by [52]

$$v \langle C_5 \rangle = \frac{1}{6} \ddagger (\ddagger + 3) \dots\dots\dots(2-35)$$

Therefore, the eigenvalues of states corresponding to the Hamiltonian in Eq. (2-29) are [52]:

$$E([N] \ddagger \ddagger \hat{\Delta} JM) = \frac{A}{4} (N - \dagger)(N + \dagger + 4) + B \ddagger (\ddagger + 3) + C J(J+1) \dots\dots\dots(2-36)$$

where the $\frac{1}{6}$ in Eq. (2-35) has been incorporated into the constant B . The quantum number $\hat{\Delta}$ is useful in labelling the states: it is related to n_Δ , which counts the number of boson triplets coupled to angular momentum zero.

The quantum numbers \dagger and ν_{Δ} are related by $\dagger = 3\nu_{\Delta} + \}$ for $\nu_{\Delta} = 0, 1, \dots$. The value of $\}$ determines the angular momentum of states via [52]:

$$J = 2\}, 2\} - 2, 2\} - 3, \dots, \} + 1, \} \dots \dots (2-37)$$

Arima and Iachello have also succeeded in obtaining analytic expressions for transition probabilities [52]. As in the $SU(5)$ and $SU(3)$ symmetries, they require the $E2$ transition operator, $T(E2)$, to be a generator of the underlying group structure, in this case $O(6)$. The form of $T(E2)$ satisfying this requirement is [52]:

$$T(E2) = r (d^{\dagger} s + s^{\dagger} d)^{(2)} \dots \dots \dots (2-38)$$

Since $T(E2)$ is a generator of $O(6)$, it cannot connect states from different representations; therefore, one selection rule is $\Delta\dagger = 0$. Also, due to the $O(5)$ structure contained in $O(6)$, the $O(5)$ selection rule $\Delta\dagger = \pm 1$ still holds.

Within each \dagger grouping itself, the level spacing somewhat resembles that of a vibrational model, as described in subsection (2.1.1), but with an energy spacing proportional to $\dagger(\dagger + 3)$ rather than simply to \dagger . This will give rise to the energy ratio $E(4_1^+)/E(2_1^+) = 2.5$ rather than 2, as expected in the vibrational picture; also, as \dagger increases even larger energy differences will occur between states of different \dagger . Further, the degeneracies of the geometrical vibrational phonon model are explicitly eliminated by the $J(J + 1)$ term and certain states, e.g., the 0^+ state of the two-phonon triplet, do not occur. As described earlier in subsection (2.1.1), the state which would correspond to this 0^+ state is "repelled" by the ground state and is raised in energy due to the repulsive pairing force which characterizes this limit. Branching ratios and absolute $B(E2)$ values also differ significantly from the geometrical prescription.

The $O(6)$ limit (especially for large N) seems to resemble most closely the χ -unstable model described by Wilets and Jean [56].

However, in the $O(6)$ scheme, the level degeneracies are no longer

maintained, and there are spin cutoffs, and a specific number of different \dagger groupings. It is reasonable that the $O(6)$ description may correspond to the χ -unstable geometrical model, in analogy to the $SU(5)$ -vibrator and $SU(3)$ -symmetric rotor correspondences. The Hamiltonian of a χ -unstable oscillator is characterized by a potential energy which is independent of χ , although χ -dependent terms are included in the kinetic energy. A correspondence exists between the coordinates of the Bohr-Mottelson picture and the operators of the IBM. Arima has suggested the result that the χ -unstable potential corresponding to the $O(6)$ limit of the IBM would be of the form [52]: $V = -cs^2 + ds^4$, where s is the deformation parameter and c and d are arbitrary constants. This form of potential arises from the zero d -boson and two d -boson number changing terms of the $O(6)$ Hamiltonian. A χ -dependent term in the potential would be of the form $s^3 \cos 3\chi$, which corresponds to one d -boson number changing terms that are not included in this symmetry. Currently, attempts to understand more explicitly the analogy between the $O(6)$ symmetry and relevant geometrical models are being pursued [52]. A convenient basis in which to describe the $O(6)$ level wave functions is that of the vibrational limit, given by $J^f |n_d n_s n_\Delta\rangle$, where $n_d n_s n_\Delta$ are, as usual, the number of d -bosons, number of d -boson pairs coupled to angular momentum zero, and the number of d -boson triplets coupled to angular momentum zero, respectively. Although the wave functions are not pure in this basis, they can be described in a simple manner as a linear combination of basis states differing in the n_d and n_β quantum numbers. For example, in the vibrational limit, the ground state is a pure $0^+ |000\rangle$ state; in $O(6)$, the ground state, with $\dagger = \dagger_{\max}$ would be characterized by the 0^+ wave function. A convenient basis in which to describe the $O(6)$ level wave functions is that of the vibrational limit, given by $J^f |n_d n_s n_\Delta\rangle$, where $n_d n_s n_\Delta$ are, as usual, the number of d -bosons, number of d -boson pairs coupled to angular momentum zero, and the number of

d-boson triplets coupled to angular momentum zero, respectively. Although the wave functions are not pure in this basis, they can be described in a simple manner as a linear combination of basis states differing in the n_d and n_β quantum numbers. For example, in the vibrational limit, the ground state is a pure $0^+|000\rangle$ state; in $O(6)$, the ground state, with $\dagger = \dagger_{\max}$ would be characterized by the 0^+ wave function $r|000\rangle + s|210\rangle + x|420\rangle + \dots + v|NN/20\rangle$. The relation between \dagger and the more familiar phonon number is given by calculating the expectation value of n_d . Iachello has determined that, for the $\dagger = \dagger_{\max} = N$ states, the expectation value of n_d in the $O(6)$ limit is given by [52]:

$$\langle n_d \rangle = \frac{N(N-1)}{2(N+1)} + \frac{\dagger(\dagger+3)}{2(N+1)} \dots \dots \dots (2-39)$$

Two types of perturbations may be added to the exact results of the $O(6)$ limit: one which does not change the forces of the symmetry, and one which introduces a force from outside the limit. The former type can be accomplished, for example, by changing the boson energy from the value determined by B in Eq. (2-36). This will alter the amplitudes of the non-zero components of all wave- functions, but will not add new components. The result will be to break the selection rule $\Delta\dagger = 0$, but to preserve the $\Delta\dagger = \pm 1$ E2 selection rule. The second type of perturbation can be accomplished, for example, by the introduction of a quadrupole-quadrupole interboson force. Since such an interaction contains one *d*-boson changing terms, all wave function components would be non-zero, though perhaps small, and the effect would be to break both $O(6)$ E2 selection rules, as well as to alter all E2 branching ratios.

The interferences between these three dynamical symmetries give three transitional regions. These regions are as follows:

$SU(3) \rightarrow SU(5)$: This transitional region can be treated by breaking $SU(3)$ symmetry in the direction of $SU(5)$ by adding

$\hat{H} = v(\hat{n}_s + \hat{n}_d) + a_3 \hat{T}_3 \cdot \hat{T}_3 + a_4 \hat{T}_4 \cdot \hat{T}_4$ terms. The Hamiltonian of this region can be written as:

$$\hat{H} = v(\hat{n}_s + \hat{n}_d) + a_1 \hat{L} \cdot \hat{L} + a_2 \hat{Q} \cdot \hat{Q} + a_3 \hat{T}_3 \cdot \hat{T}_3 + a_4 \hat{T}_4 \cdot \hat{T}_4 \dots \dots (2-40)$$

$SU(3) \rightarrow O(6)$: The nuclei in this transitional region can be treated by breaking $SU(3)$ symmetry in the direction of $O(6)$ by adding $\hat{P} \cdot \hat{P}, a_3 \hat{T}_3 \cdot \hat{T}_3$ terms. The Hamiltonian of this region can be written as:

$$\hat{H} = a_0 \hat{P} \cdot \hat{P} + a_1 \hat{L} \cdot \hat{L} + a_2 \hat{Q} \cdot \hat{Q} + a_3 \hat{T}_3 \cdot \hat{T}_3 \dots \dots (2-40a)$$

$O(6) \rightarrow SU(5)$: The nuclei in this transitional region can be treated by a Hamiltonian containing $v(\hat{n}_s + \hat{n}_d)$ and $a_0 \hat{P} \cdot \hat{P}$ terms as :

$$\hat{H} = v(\hat{n}_s + \hat{n}_d) + a_0 \hat{P} \cdot \hat{P} + a_1 \hat{L} \cdot \hat{L} + a_3 \hat{T}_3 \cdot \hat{T}_3 + a_4 \hat{T}_4 \cdot \hat{T}_4 \dots \dots (2-40b)$$

The $O(6)$ limit of the IBM-1 possesses N as a good quantum number together with the conventional $O(6)$ quantum numbers \dagger, \ddagger but n_d is not a good quantum number [55]. The E0 transition operator possesses the selection rules $\Delta \dagger = 0, +2; \Delta \ddagger = 0$. Thus, the E0 matrix elements that connect to the 0^+ ground-state level $[[N], \dagger = N, \ddagger = 0, L = 0\rangle$ originate in the $\dagger = N - 2$ multiplet, i.e.. $[[N], \dagger = N - 2, \ddagger = 0, L = 0\rangle$

2.2- Interacting Boson Model-2 (IBM-2)

In the IBM-2 model the neutrons and protons degrees of freedom are taken into account explicitly. Thus the Hamiltonian [66, 67] can be written as:

$$H = H_f + H_\epsilon + V_{f\epsilon} \dots \dots \dots (2-41)$$

$$H = v_f d_f^\dagger \tilde{d}_f + v_v d_v^\dagger d_\epsilon^\dagger + V_{ff} + V_{vv} + |Q_f \cdot Q_v + M_{fv} \dots \dots \dots (2-42)$$

Here v is the d -boson energy, $|$ is the strength of the quadrupole interaction between neutron and proton bosons.

In the IBM-2 model, the quadrupole moment operator is given by:

$$Q_{\dots} = (s^\dagger \tilde{d} + d^\dagger \tilde{s})_{\dots}^{(2)} + t_{\dots} (d^\dagger \tilde{d})_{\dots}^{(2)} \dots \dots \dots (2-43)$$

where $\dots = f$ or ϵ , Q_{\dots} is the quadrupole deformation parameter for neutrons ($\dots = \epsilon$) and protons ($\dots = f$). Where the terms $V_{\epsilon\epsilon}$ and V_{ff} are the neutron-neutron and proton-proton d-boson interactions only and given by:

$$V_{\dots} = \sum_{J=0,2,4} \frac{1}{2} C_{L\dots} (2J+1)^{1/2} \left[(d^\dagger d^\dagger)_{\dots}^{(2)} (\tilde{d}\tilde{d})_{\dots}^{(2)} \right]^{(0)} \dots \dots \dots (2-44)$$

The last term $M_{f\epsilon}$ is the Majorana interaction, shifts the states with mixed proton-neutron symmetry with respect to the totally symmetric ones. Since little experimental information is known about such states with mixed symmetry, which has the form:

$$M_{f\epsilon} = - \sum_{k=1,3} 2 \langle (d_f^\dagger d_f^\dagger)^{(k)} (\tilde{d}_f \tilde{d}_f)^{(k)} + {}_2 \langle (d_f^\dagger s_\epsilon^\dagger - \tilde{s}_f \tilde{d}_\epsilon)^{(2)} (\tilde{d}_f \tilde{s}_\epsilon - \tilde{s}_f \tilde{d}_\epsilon)^{(2)} \rangle \dots \dots \dots (2-45)$$

2.2.1-Electromagnetic Transitions and Quadrupole Moments in IBM-2

The general one-body E2 transition operator in the IBM-2 is

$$T(l) = T_f(l) + T_v(l) \dots \dots \dots (2-46)$$

$$T(E2) = e_f \left[(s_f^\dagger \tilde{d} + d_f^\dagger \tilde{s})_f^{(2)} + t_f (d_f^\dagger \tilde{d})_f^{(2)} \right]^{(2)} + e_v \left[(s_v^\dagger \tilde{d} + d_v^\dagger \tilde{s})_v^{(2)} + t_v (d_v^\dagger \tilde{d})_v^{(2)} \right]^{(2)}$$

$$T(E2) = e_f Q_f + e_v Q_v \dots \dots \dots (2-47)$$

where Q_{\dots} is in the form of Eq.(2-43). For simplicity, the t_{\dots} has the same value as in the Hamiltonian. This is also suggested by the single j -shell microscopy. In general, the $E2$ transition results are not sensitive to the choice of e_ϵ and e_f , whether $e_f = e_\epsilon$ or not. Thus, the reduced electric quadrupole transition rates between $J_i \rightarrow J_f$ states are given by:

$$B(E2; J_i^+ \rightarrow J_f^+) = \frac{1}{2J_i + 1} \left| \langle J_f^+ \| T(E2) \| J_i^+ \rangle \right|^2 \dots \dots \dots (2-48)$$

The electric quadrupole moment in IBM-2 is given:

$$Q_J = \left[\frac{16f}{5} \right]^{1/2} \begin{bmatrix} J & 2 & J \\ -J & 0 & J \end{bmatrix} \langle J \| T(E2) \| J \rangle \dots \dots \dots (2-49)$$

In the IBM-2, the M1 transition operator up to the one-body term ($l=1$) is

$$T(M1) = \left[\frac{3}{4f} \right]^{1/2} (g_f L_f^{(1)} + g_v L_v^{(2)}) \dots \dots \dots (2-50)$$

where $L_{\dots}^{(1)} = \sqrt{10}(d^\dagger \tilde{d})_{\dots}$ and $L^{(1)} = L_f^{(1)} + L_v^{(1)}$. The g_f and g_ϵ are the boson g-factors (gyromagnetic factors) in unit \sim_N (nuclear magneton) that depends on the nuclear configuration. They should be different for different nuclei.

$$T(M1) = \left[\frac{3}{4f} \right]^{1/2} \left[\frac{1}{2} (g_f + g_v) (L_f^{(1)} + L_\epsilon^{(1)}) + \frac{1}{2} (g_f - g_\epsilon) (L_f^{(1)} + L_\epsilon^{(1)}) \right] \dots \dots \dots (2-51)$$

The magnetic dipole moment operator is given by:

$$T(M1) = 0.77 \left[(d^\dagger \tilde{d})_f - (d^\dagger \tilde{d})_v \right]^{(1)} (g_f - g_v) \dots \dots \dots (2-52)$$

the reduced magnetic dipole transition rates between $J_i \rightarrow J_f$ states are given by:

$$B(M1, J_i^+ \rightarrow J_f^+) = \frac{1}{2J_i + 1} | \langle J_i^+ || T(M1) || J_f^+ \rangle |^2 \dots \dots (2-53)$$

The reduced $E2$ and $M1$ matrix elements were combined in the calculation of the mixing ratio ($E2/M1$) using the relation [68]:

$$u(E2/M1; J_i^+ \rightarrow J_f^+) = 0.835 E_x (MeV) \frac{\langle J_f^+ || T(E2) || J_i^+ \rangle}{\langle J_f^+ || T(M1) || J_i^+ \rangle} \dots \dots \dots (2-54)$$

The $E0$ (electric monopole transition) transition occurs between two states of the same spin and parity by transferring the energy and zero units of angular momentum, and it has no competing gamma ray. The $E0$ transition is present when there is a change in the surface of the nucleus. For example, in nuclear models where the surface is assumed fixed, $E0$ transitions are strictly forbidden, such as in shell and IBM-1 models. Electric monopole transitions are completely under the penetration effect of atomic electrons on the nucleus, and can occur not only in $0^+ \rightarrow 0^+$ transition but also, in competition with gamma multipole transition, and depending on transition selection rules that may compete in any $J = 0$ decay such as a $2^+ \rightarrow 2^+$ or any $J_i = J_f$ states in the scheme. When the

transition energy greater than $2m_0c^2$, monopole pair production is also possible. The $E0$ reduced transition probability is written [69]:

$$B(E0; J_i \rightarrow J_f) = e^2 R_0^4 \dots^2 (E0), J_i = J_f \dots \dots \dots (2-55)$$

where e is the electron effective charge, $R_0 = 1.25A^{1/3} fm$ is the nuclear radius, A is the atomic mass, and $(E0)$ is the monopole transition matrix elements. There are only limited cases of $(E0)$ that can be measured directly. The electric monopole transition operator is:

$$T(E0) = S_{0\dots} (d^\dagger \times \tilde{d})_{\dots}^{(0)} + \chi_{\dots} (s^\dagger \times \tilde{s})_{\dots}^{(0)} \dots \dots \dots (2-56)$$

$$T(E0) = S_{0\dots} (d^\dagger \times \tilde{d})_{\dots}^{(0)} + \chi_{\dots} N_{\dots} \dots \dots \dots (2-57)$$

$$S_{0\dots}' = S_{0\dots} / \sqrt{5} - \chi_{0\dots}$$

$$N_{\dots} = \sqrt{5} (d^\dagger \times \tilde{d})_{\dots}^{(0)} + (s^\dagger \times \tilde{s})_{\dots}^{(0)}.$$

The monopole matrix element is given by:

$$\dots_{if} (E0) = \frac{Z}{R^2} \sum S_{0\dots}' \langle f | d^\dagger \times \tilde{d} | i \rangle \dots \dots \dots (2-58)$$

The two parameters s_{0f} , s_{0e} in Eq. (2-56) must be estimated. In most cases we have to determine the intensity ratio of $E0$ to the competing $E2$ transition, $X(E0/E2)$ [69]:

$$X(E0/E2; J_i^+ \rightarrow J_f^+) = e^2 R_0^4 \dots^2 (E0; J_i^+ \rightarrow J_f^+) / B(E2; J_i^+ \rightarrow J_f^+) \dots \dots \dots (2-59)$$

where $J_f = J_f'$ for $J_i = J_i' = 0$, and $J_f' = 2$ for $J_i = J_i' = 0$. The two parameters s_{0f} and s_{0e} in Eq. (2-57) may be estimated by fitting the isotope shift, which is different in the mean square radius between neighboring isotopes in their ground state. They are given by *Bijker et al.*, [70]:

$$\Delta \langle r^2 \rangle = \langle 0_1 | r^2 | 0_1 \rangle_A - \langle 0_1 | r^2 | 0_1 \rangle_{A+1}$$

$$\begin{aligned} \Delta \langle r^2 \rangle = & \tilde{S}_{0f} [\langle 0_1 | d_f^\dagger \tilde{d}_f | 0_1 \rangle_{N_\epsilon} - \langle 0_1 | d_f^\dagger \tilde{d}_f | 0_1 \rangle_{N_\epsilon}] \\ & + S_{0e} [\langle 0_1 | d_\epsilon^\dagger \tilde{d}_\epsilon | 0_1 \rangle_{N_\epsilon} - \langle 0_1 | d_\epsilon^\dagger \tilde{d}_\epsilon | 0_1 \rangle_{N_\epsilon}] - \chi_{0e} \dots \dots \dots (2-60) \end{aligned}$$

The isomer shift is the difference between the mean square radius $u \langle r^2 \rangle$ of an excited state and the ground state in a given nucleus [70]:

$$\begin{aligned} u \langle r^2 \rangle &= \langle r^2 \rangle_{e.s.} - \langle r^2 \rangle_{g.s.} \\ u \langle r^2 \rangle &= \langle 2_1 | r^2 | 2_1 \rangle - \langle 0_1 | r^2 | 0_1 \rangle \\ u \langle r^2 \rangle &= S_{0f} [\langle 2_1 | d_f^\dagger \tilde{d}_f | 2_1 \rangle - \langle 0_1 | d_f^\dagger \tilde{d}_f | 0_1 \rangle] \\ &+ S_{0\epsilon} [\langle 2_1 | d_\epsilon^\dagger \tilde{d}_\epsilon | 2_1 \rangle - \langle 0_1 | d_\epsilon^\dagger \tilde{d}_\epsilon | 0_1 \rangle] \dots (2-61) \end{aligned}$$

2.2.2- Two-neutron Separation Energy

The binding energy E_B of a nucleus is given by the negative of its ground-state energy. This energy is not just the eigenvalue of 0_1^+ state, since we are looking for an absolute number. We must recall all of the unused constant terms in the Hamiltonian described in Eq. (2-42). These give:

$$E_{g.s.} = -E_B = E_{core} + v_{s\epsilon} N'_\epsilon + v_{sf} N'_f + \frac{1}{2} u_0^\epsilon N'_\epsilon (N'_\epsilon - 1) + \frac{1}{2} u_0^f N'_f (N'_f - 1) + E_{B(def.)} \dots (2-62)$$

where E_{core} is the energy of the closed shells and $E_{def.}$ is the deformation energy (i.e., the 0_1^+ eigenvalue using IBM-2 Hamiltonian). The primes on N_f and N_ϵ again emphasize that they are to represent boson particles.

For constant proton number, the binding energy can thus be written as:

$$E_B = A + B N'_f + \frac{1}{2} C N'_\epsilon (N'_\epsilon - 1) + E_{B(def.)} \dots (2-63)$$

where A and B , and C are constants and $E_{def.} = -E_{def.}$.

Instead of the actual binding energy we will examine the two-neutron separation energy. This is the energy required to remove two neutrons (one neutron boson) from a given isotope and is given by:

$$S_{2\epsilon}(N'_\epsilon) = E_B(N'_\epsilon) - E_B(N'_\epsilon - 1) = B + C(N'_\epsilon - 1) + \Delta E_{B(def.)} \dots (2-64)$$

where $\Delta E_{B(def.)} = E_{B(def.)}(N'_\epsilon) - E_{B(def.)}(N'_\epsilon - 1)$.

2.2.3-The *IBM-2* Basis States

The calculation of *IBM-2* energy eigenvalues and eigenfunctions is usually done numerically using the computer code *NPBOS* [71]. The resulting eigenvectors can then be used to calculate transition rates and related properties using the computer code *NPBTRN* [71]. The relationship between the parameters of Eq. (2-42).

The basis states used in the calculations are the products of neutron and proton basis states. The complete *IBM-2* basis state can be stated as:

$$|\Psi JM\rangle = |[N = N_\epsilon + N_f] n_{d\epsilon}, v_\epsilon, n_{\Delta\epsilon}, L_\epsilon, M_\epsilon; n_{df}, v_f, n_{\Delta f}, L_f, M_f; JM\rangle$$

$$= \left[|[N] n_d, v, n_\Delta, L, M \rangle_\epsilon \left[|[N] n_d, v, n_\Delta, L, M \rangle_f \right]_M \right]$$

The basis states can be found by choosing states that transform as the representations of the chain of algebras that can be derived from the $U(6)$ algebra formed by the bilinear pair of boson creation and annihilation operators. In the *IBM-2*, the bilinear pairs of proton and neutron creation and annihilation operators respectively form the algebras $U_f(6)$ and $U_\epsilon(6)$. There are several ways decompose and combine the two algebras into a chain of subalgebras and each way will determine the basis. As in the *IBM-1*, the requirement for the chain is the inclusion of the $SO_{f+\epsilon}(3)$ algebra as it is related to a good total angular momentum quantum number. The algebra $SO_{f+\epsilon}(3)$ is created from the sum of generators of the algebras $SO_f(3)$ and $SO_\epsilon(3)$.

As an example, one may take the two chains of algebras for protons and neutron,

$$U_f(6) \supset U_f(5) \supset SO_f(5) \supset SO_f(3) \supset SO_f(2)$$

$$U_\epsilon(6) \supset U_\epsilon(5) \supset SO_\epsilon(5) \supset SO_\epsilon(3) \supset SO_\epsilon(2)$$

These two chains can be combined at any point up except at $SO_{f+\epsilon}(2)$ since the combined algebra $SO_{f+\epsilon}(3)$ is needed. One of the possibilities is:

$$\begin{array}{ccccccc}
 U_f(6) \supset U_f(5) \supset SO_f(5) \supset SO_f(3) & \searrow & & & & & \\
 N_f & n_{df} & v_f, n_{f\Delta} & L_f & & & SO_{f+\epsilon}(3) \supset SO_{f+\epsilon}(2) \\
 U_\epsilon(6) \supset U_\epsilon(5) \supset SO_\epsilon(5) \supset SO_\epsilon(3) & \nearrow & & & L & M & \\
 N_\epsilon & n_{d\epsilon} & v_\epsilon, n_{\epsilon\Delta} & L_\epsilon & & &
 \end{array}$$

where the quantum numbers are labelled beneath the corresponding algebra. This is the basis that is used in the *IBM-2* program *NPBOS*.

Another set of bases can be obtained if one combines the algebras at a different point such as:

$$\begin{array}{c}
 U_f(6) \searrow \\
 U_{f+\epsilon}(6) \supset U_{f+\epsilon}(5) \supset SO_{f+\epsilon}(5) \supset SO_{f+\epsilon}(3) \supset SO_{f+\epsilon}(2) \\
 U_\epsilon(6) \nearrow
 \end{array}$$

In general there are three chains that can be combined at $U_{f+\epsilon}(6)$ to give three different bases. In these chains, the proton and neutron bosons exhibit a symmetry and this is the subject of the following section.

2.2.4- Mixed-Symmetry States

The low-energy spectrum of even-even nuclei is dominated by simple collective excitation modes [72]. These correlations in the nucleon motion are induced by the long-range quadrupole component of the nuclear force. In spherical nuclei with few valence nucleons, surface vibrations evolve which can be described as bosons, so-called phonons. In an ideal case, the excitation spectrum of a vibrator nucleus is a harmonic oscillator with equidistant level spacings $\hbar\tilde{S}$, where phonons can couple to multiphonon states with different angular momenta and parities. For large numbers of the valence nucleons, an elliptically deformed equilibrium state becomes energetically more favorable. Its vibrational modes can be divided into vibrations of the deformation parameter s (s -vibrations) and the form parameter χ (χ -vibrations).

Multiphonon excitations of atomic nuclei are interesting collective structures of the nuclear many-body system. Their existence enables us to

judge the capability of the corresponding phonon modes to act as building blocks of nuclear structure. Possible deviations from harmonic phonon coupling occur due to the microscopic structure of the underlying phonon modes and serve as a sensitive source of information on the formation of collectivity in the nuclear many-body system. The proton-neutron interaction in the nuclear valence shell has been known for a long time as the driving force for the evolution of the low-energy nuclear structure. This has been discussed in many ways, e.g. in terms of the evolution of collectivity in heavy nuclei as a function of the product of valence proton and neutron numbers $N_p N_n$ [73]. Otsuka *et al.* (2006) have identified the proton-neutron interaction as being responsible for the evolution of shell structure [74]. Therefore, it is interesting to study those nuclear excitations that are most sensitive to the proton-neutron interaction in the valence shell. One class of states are collective isovector valence shell excitations that are frequently called **Mixed-Symmetry States (MSSs)** in the terminology of the interacting boson model.

The first observation of a nuclear *MSS* was made in electron scattering experiments [75] on the deformed nucleus ^{156}Gd . A strong *M1* excitation to a 1^+ state close to 3 MeV excitation energy, the scissors mode, was observed. The scissors mode has subsequently been studied mainly in electron and photon scattering experiments on deformed nuclei. Data are available for many nuclei in the rare-earth mass region and interpretations of the systematic of the centroid and the total strength as a function of deformation have been put forward [76].

2.2.4.1- *F-Spin*

The *F-spin* formalism is analogous to the isospin formalism of nucleons. Proton bosons and neutron bosons have $F = 1/2$ and the *z*-projection is $F_z = +1/2$ for protons and $F_z = -1/2$ for neutrons. For a system of N_p proton bosons and N_n neutron bosons, the maximum *F-spin* is $F = F_{max} = (N_p + N_n)/2$ and

$$F_z = \frac{|N_f - N_\epsilon|}{2} \leq F_{\max} \leq \frac{N_f + N_\epsilon}{2} \dots\dots\dots(2-65)$$

In the F -spin space, one can also define the creation and annihilation operators F_+ and F_- by

$$F_+ = s_f^\dagger s_\epsilon + \sum_{\tilde{}} d_{f,-}^\dagger d_{\epsilon,-} \dots\dots\dots(2-66)$$

$$F_- = s_\epsilon^\dagger s_f + \sum_{\tilde{}} d_{\epsilon,-}^\dagger d_{f,-} \dots\dots\dots(2-67)$$

The projection operator F_z is given by

$$F_z = \frac{1}{2} \left[s_f^\dagger s_\epsilon + \sum_{\tilde{}} d_{f,-}^\dagger d_{\epsilon,-} + s_\epsilon^\dagger s_f + \sum_{\tilde{}} d_{\epsilon,-}^\dagger d_{f,-} \right] \dots\dots\dots(2-68)$$

A state composed by N proton bosons and N neutron bosons with F -spin quantum number $F = F_{\max}$ can be transformed by the successive action of the F -spin raising operator F_+ into a state that consists of proton bosons only. This state has still a total F -spin quantum number $F = F_{\max}$ since the raising operator does not change the total F -spin quantum number. This new state has only proton bosons and obviously stays unchanged under a pairwise exchange of proton and neutron labels. Therefore, *IBM-2* states with $F = F_{\max}$ are called **Full Symmetry States (FSSs)**. These states correspond actually to the *IBM-1* states which are all symmetric. All others states with F -spin quantum numbers $F < F_{\max}$ contain pairs (at least one) of proton and neutron bosons that are antisymmetric under a pairwise exchange of protons and neutrons labels. They are called **Mixed-Symmetry States (MSSs)**.

A comprehensive review of the F -spin symmetry of the *IBM-2* has been given by Van Isacker *et al.* [77]. One important result of the F -spin formalism is given by the proton-neutron contribution to the matrix elements of any one-body operator between *FSSs*:

$$\langle F_{\max}, r \parallel b_{\dots,S}^+ b_{\dots,S} \parallel F_{\max}, r' \rangle = N_{\dots} c_{rr',SS} \dots\dots\dots(2-69)$$

where r, r', S, S' are additional quantum numbers and $c_{r,r',S,S'}$ is independent of N . This major result tells us that there are no *M1* transition between *FSSs*.

Both operators $E2$ and $M1$ can be divided into F -scalar (denoted by s) and F -vector (denoted by v) parts

$$T(M1)_s = \frac{g_f + g_\epsilon}{2} (L_f + L_\epsilon) \dots \dots \dots (2-70)$$

$$T(M1)_\epsilon = \frac{g_f - g_\epsilon}{2} (L_f - L_\epsilon) \dots \dots \dots (2-71)$$

$$T(E2)_s = \frac{e_f + e_\epsilon}{2} (Q_f^{t_s} + Q_\epsilon^{t_s}) \dots \dots \dots (2-72)$$

$$T(E2)_\epsilon = \frac{e_f - e_\epsilon}{2} (Q_f^{t_\epsilon} - Q_\epsilon^{t_\epsilon}) \dots \dots \dots (2-73)$$

with

$$t^s = \frac{e_f t_f + e_\epsilon t_\epsilon}{e_f + e_\epsilon} \dots \dots \dots (2-74)$$

$$t^\epsilon = \frac{e_f t_f - e_\epsilon t_\epsilon}{e_f - e_\epsilon} \dots \dots \dots (2-75)$$

From the previous discussion concerning the $E2$ and $M1$ decays of full symmetric states and the mixed-symmetry states (here discussed in near vibrational nuclei), we expect following signatures for mixed-symmetry one-phonon and two phonon excitations for vibrational and transitional nuclei:

First: The one-quadrupole-phonon $2_{1,ms}^+$ state is the lowest-lying MSS in vibrational nuclei.

Second: The $2_{1,ms}^+$ state decays to the 2_1^+ state by a strong $M1$ transition $(\langle 2_{1,ms}^+ || T(M1) || 2_1^+ \rangle) \approx 1 \sim \frac{2}{N}$.

Third: A weakly collective $E2$ transition strength of a few $e^2 b^2$ for the $2_{1,ms}^+ \rightarrow 0_1^+$ transition.

In the IBM-1, geometrical shapes can be assigned to the algebras of the three possible chains, which correspond directly to the description of nuclear shapes by Bohr and Mottlesohn's shape variables [78, 79]. In the IBM-2, the mixed-symmetry states correspond to a quadrupole vibration where the protons and neutrons oscillate out of phase. For deformed nuclei, the protons and neutrons oscillate with respect to one another as the

nucleus as a whole rotates. Because of this type of motion, the mixed-symmetry states for deformed nuclei are also known as the scissors mode.

Mixed-symmetry states can be identified by their unique signature, namely a collective M1 decay to a fully-symmetric state. M1 transitions are forbidden between fully-symmetric states and between mixed-symmetry states in the F -spin basis.

2.3-Interacting Boson-Fermion Model

2.3.1. Interacting Boson-Fermion Model-1 (IBFM-1)

The description of collective nuclear states in even-odd nuclei has been proposed in terms of a mixed system of interacting bosons and fermions [51-80]. The corresponding model, which is referred to as the interacting boson-fermion model (IBFM), is an extension of the interacting boson model (IBM) [50-51] introduced a few years ago in order to provide a unified description of collective states in even-even nuclei. In the IBFM, the fermionic degrees of freedom of the single (unpaired) nucleon are coupled to the even-even core nucleus, which is described by the IBM. Whenever the core (IBM) Hamiltonian possesses one of its three possible dynamical symmetries, U(5), SU(3), and O(6) or SO(6) [50-55], the corresponding spectra in odd-even nuclei exhibit simple features, which in the case of the odd nucleon occupying a single j -orbit, are shown to be analogous to the particle-vibrational model, the Nilsson model, and the particle-plus- x – soft-rotor model. Transitional regions between any of these limiting situations can be treated equally well in IBFM.

In addition to providing a framework for the description of collective properties in even-odd nuclei, the IBFM-Hamiltonian has an interesting algebraic structure, which suggests the occurrence of dynamical symmetries. The concept of dynamical symmetries, which is usually used for a system of bosons or fermions separately, has been extended to a mixed system of bosons and fermions [81, 82]. These symmetries are called dynamical boson-fermion symmetries. Boson-fermion symmetries

can be extended to supersymmetries, in which certain states both in even-even and in odd-even nuclei are treated on equal footing. This can be achieved by imbedding the symmetry group of the combined system of bosons and fermions into a supergroup (graded Lie group).

The boson-fermion symmetries, connected with the boson symmetry $SO^B(6)$ have been discussed [81] and in more detail in the preceding publication in this series, for $j = \frac{3}{2}$ and a forthcoming publication [80] for $j = \frac{1}{2}, \frac{3}{2}, \frac{5}{2}$. In this work we will discuss the boson-fermion symmetries, which are related to the boson symmetry $U^B(5)$. These symmetries arise when the fermions occupy a single particle orbit with $j = \frac{1}{2}, j = \frac{3}{2}$ or $j = \frac{3}{2}, j = \frac{5}{2}$ and will be referred to as the Spin(3), Spin(S), and $U^{(B+F)} \otimes U^F(2)$ limit, respectively. Although in reality nuclei will never show properties which are exactly identical to the ideal situations described by the dynamical symmetries, the analytic formulae presented here may provide a tool for understanding the gross features of the properties of collective states in even-odd nuclei.

In order to describe the interplay between collective and single-particle motion in nuclei, one has to introduce explicitly collective and single-particle degrees of freedom. Within the framework of the IBFM the collective degrees of freedom are described by a set of N bosons with angular momentum $L = 0$ (s-bosons) and $L = 2$ (d-bosons). The single-particle degrees of freedom are described by a set of M fermions with angular momentum j, j', \dots , where $M = 0$ for the low-lying collective states in even-even nuclei, $M = 1$ for the one quasi-particle states in odd-even nuclei, $M = 2$ for the two quasi-particle states in even-even nuclei, etc. The most general one- and two-body Hamiltonian for a mixed system of bosons and fermions can be written as [81, 82]:

$$H=H_B+H_F+H_{BF} \dots\dots\dots(2-76)$$

where H_B is the usual IBM-1 Hamiltonian [50] for the even-even core, H_F is the fermion Hamiltonian containing only one-body terms and V_{BF} is the boson-fermion interaction that describes the interaction between the odd quasi-nucleon and the even-even core nucleus. H_F is the fermion Hamiltonian containing only one-body terms [81, 82]:

$$H_F = \sum_{jm} a_{jm}^\dagger \epsilon_{jm} a_{jm} \dots\dots\dots(2-77)$$

where the ϵ_{jm} are the quasiparticle energies and $a_{jm}^\dagger (a_{jm})$ is the creation (annihilation) operator for the quasiparticle in the eigenstate $|jm\rangle$. The boson-fermion interaction V_{BF} that describes the interaction between the odd quasi-nucleon and the even-even core nucleus contains, in general, have many different terms and is rather complicated, but has been shown to be dominated by the following three terms:

$$\begin{aligned} V_{BF} = & \sum_j A_j \left[(d^\dagger \times \tilde{d})^{(0)} \times (a_j^\dagger \times \tilde{a}_j)^{(0)} \right] + \sum_{jj'} \Gamma_{jj'} \left[Q^{(2)} \times (a_j^\dagger \times \tilde{a}_j)^{(2)} \right]_0^{(0)} \\ & + \sum_{jj''} \Lambda_{jj''}^{j''} : \left[(d^\dagger \times \tilde{a}_j)^{(j'')} \times (a_j^\dagger \times \tilde{d}_j)^{(j'')} \right]_0^{(0)} \dots\dots\dots(2-78) \end{aligned}$$

where the core boson quadrupole operator is given by the equation (2-43), and t is a parameter shown by microscopic theory to lie between $\sqrt{7}/2$ and $-\sqrt{7}/2$. V_{BF} is dominated by three terms: a monopole interaction characterized by the parameter A_0 which plays a minor role in actual calculations, the most important arise from the quadrupole interaction [83,84] characterized by Γ_0 , and the exchange of the quasiparticle with one of the two fermions forming a boson [54,82] characterized by Λ_0 .

$A_j = A_0 \sqrt{2j+1}$ $s, d, s^\dagger, d^\dagger$ are boson operators with $u_{jm} = (-1)^{j-m}$ and denotes normal ordering whereby contributions that arise from commuting the operators are neglected. The first term in V_{BF} is a monopole interaction which plays a minor role in actual calculations and the dominant term are

the second and third, which arise from the quadrupole interaction. The third term represents the exchange of the quasiparticle with one of the two fermions forming a boson; Talmi [85] has shown that this exchange force is a consequence of the Pauli principle for the quadrupole interaction between protons and neutrons. The remaining parameters in Equation (2-78) can be related to the BCS occupation probabilities u_j , v_j of the single-particle orbits:

$$\Gamma_{jj'} = \sqrt{5}\Gamma_0 (u_j u_{j'} - \epsilon_j \epsilon_{j'}) Q_{jj'} \dots \dots \dots (2-79)$$

$$A_{jj'}^j = \sqrt{5}\Lambda_0 [u_j \epsilon_{j'} + \epsilon_j u_{j'}] Q_{jj'} S_{jj'} + (u_j \epsilon_{j'} + \epsilon_j u_{j'}) Q_{jj'} S_{jj'} / \sqrt{2j'' + 1} \dots \dots (2-80)$$

where $Q_{jj'}$ are single particle matrix elements of the quadrupole operator and

$$S_{jj'} = (u_j \epsilon_{j'} + \epsilon_j u_{j'}) Q_{jj'} / (v_j + v_{j'} - \hbar \check{S}) \dots \dots \dots (2-81)$$

are the structure coefficients of the d -boson deduced from microscopic considerations, with $\hbar \check{S}$ being the energy of a $|D\rangle$ pair relative to an $\langle S|$ pair [86].

The BCS occupation probability ϵ_j and the quasiparticle energy v_j of each single particle orbital can be obtained by solving the gap equations [54, 82]:

$$v_j = [(E_j - \})^2 + \Delta^2]^{1/2} \dots \dots \dots (2-82)$$

$$\epsilon_j^2 = \frac{1}{2} \left[1 - \frac{(E_j - \})}{v_j} \right] \dots \dots \dots (2-83)$$

where E_j is the single particle energy calculated from the relations in [86], $\}$ is the Fermi level energy, and Δ is the pairing gap energy, which was chosen to be $12A^{-1/2}$ MeV [87].

That leaves the strengths A_0 , Γ_0 , and Λ_0 as free parameters which are varied to give the best fit to the excitation energies.

The IBFM Hamiltonian has been an interesting algebra structure, that suggests the possible occurrence of dynamical symmetries in odd A . In

the single- j case, the value of m is $m=2j+1$. Thus, in general, a chain of algebras:

$$U(2j+1) \supset SU(2j+1) \supset SP(2j+1) \supset SU(2) \supset O(2) \quad \dots\dots(2-84)$$

Since in the IBFM odd A nuclei are described in terms of a mixed system of interacting bosons and fermions, the concept of dynamical symmetries has to be generalized. Under the restriction, that both the boson and fermion states have good angular momentum, the respective group chains should contain the rotation region group (O(3) for boson and SU(2) for fermion) as subgroup.

$$\left\{ \begin{array}{l} U^B(6) \dots\dots\dots O^B(3) \\ U^F(m) \dots\dots\dots SU^F(2) \end{array} \right\} \dots\dots\dots(2-85)$$

If one of subgroups of $U^B(6)$ is isomorphic to one of the subgroups of $U^F(m)$, the boson and fermion group chains can be combined into a common boson-fermion group chain. When the Hamiltonian is written in terms of Casimir invariants of the combined boson-fermion symmetry arises.

Among the many different possibilities, we consider two dynamical boson-fermion symmetries associated with the O(6) limit of the IBM. The first example discussed in the Refs. [88,89] it corresponds to bosons with O(6) symmetry and fermions occupying a state with $j=3/2$. The relevant group chains are:

$$\left\{ \begin{array}{l} U^B(6) \supset O^B(6) \supset O^B(5) \supset O^B(3) \supset O^B(2) \\ U^F(4) \supset SU^F(4) \supset SP^F(4) \supset SU^F(2) \supset SO^{F2}(2) \end{array} \right\} \dots\dots\dots(2-86)$$

The Spinor group spin (n) ($\text{spin}^{\text{BF}}(6)$) are the universal covering groups of the orthogonal groups O(n), with the isomorphism's of the algebras $SU(4) \approx O^B(6) \approx Spin(6)$, $SP(4) \approx O^B(5) \approx Spin(5)$ and $SU(2) \approx O^B(3) \approx Spin(3)$. The boson with one-fermion group chains can be combined into:

$$\begin{aligned}
O^B(6) \otimes U^F(4) & [N = N_B] \{N_F = 1\} \\
\supset O^B(6) \otimes SU^F(4) & \sum \\
\supset Spin^{BF}(6) & (\dagger_1, \dagger_2, \dagger_3) \\
\supset Spin^{BF}(5) & \langle \dagger_1, \dagger_2 \rangle \\
\supset Spin^{BF}(3) & \epsilon_\Delta, J \\
\supset Spin^{BF}(2) & M_J
\end{aligned}$$

The second example discussed of a multi- j case [90,91] is that of a dynamical boson-fermion symmetry associated with the $O(6)$ limit and the odd nucleon occupying single-particle orbits with spin $j = 1/2, 3/2, 5/2$. In this case, the fermion space is decomposed into a pseudo-orbital part with $K = 0, 2$ and pseudo-spin with $s = 1/2$, in general, an algebra $U^F(m_j)$ can be broken into [82]:

$$U^F(m_j) \supset U^F(m_k) \otimes U^F(m_s) \dots \dots \dots (2-87)$$

where

$$m_j = \sum_{j_i} (2j_i + 1), \quad m_k = \sum_{k_i} (2k_i + 1), \quad m_s = \sum_{s_i} (2s_i + 1) \dots \dots \dots (2-88)$$

then

$$U^F(12) \supset U^F(6) \otimes U^F(2) \dots \dots \dots (2-89)$$

Since the pseudo-orbital angular momentum K has the same values as the angular momentum of the s -and d -boson of the IBM, it is clear that the pseudo-orbital part can be combined with all three dynamical symmetries of the IBM.

$$U^B(6) \supset \begin{cases} U^B(5), \\ SU^B(3), \dots \dots \dots (2-90) \\ O^B(6), \end{cases}$$

Recently, a different way to construct dynamical boson-fermion symmetries was introduced [16]. Suppose that the fermion part, which consists of the single-particle orbits j, j', \dots , can be split into a pseudo-orbital part k and a spin part s . The pseudo-orbital part does not necessarily coincide with the actual orbital angular momentum. Suppose that the

bosons can be described by the group chain $G^{(B)} \supset G'^{(B)} \supset \dots$. If the pseudo-orbital angular momentum k or the spin s forms the full angular momentum content of a certain representation of one of the groups in the boson group chain, this representation can be combined with its bosonic counterpart to yield representations of a common boson plus fermion ($B + F$) group (class $BF-2$). An example of this second class is that of bosons with $U^{(B)}(6) \supset SO^B(6)$ symmetry and fermions with angular momenta $j = 1/2, 3/2, 5/2$. The fermion spins can be decomposed into $k = 0, 2$ with which we can associate the $U(6)$ representation and $s = 1/2$. The boson and fermion group chains can then be coupled at the level of the common $U(6)$ group or at one of its subgroups.

2.3.1.1- $U^B(5)$ Plus Particle

In this section we will discuss the symmetries associated with the boson symmetry $U^B(5)$. The group chain for the boson symmetry $U^B(5)$ is given by [54]:

$$U^B(6) \supset U^B(5) \supset SO^B(5) \supset SO^B(3) \supset SO^B(2) \dots \dots \dots (2-91)$$

Since the algebras of $SO(5)$ and $SO(3)$ are isomorphic to those of $SP(4)$ and $SU(2)$, respectively, spinor symmetries are possible whenever m is such that the fermions span an irreducible representation of $SU(2)$ and/or $Sp(4)$.

2.3.1.2- $U^B(5)$ plus $j = 4$: the Spin(3) Limit

The coupling of a $j = 1/2$ nucleon to the quadrupole degrees of freedom of an even-even core nucleus has been discussed in terms of core-excitation model [92], in which states in spherical odd-A nuclei are described by coupling the odd nucleon weakly to core excitations. In this section we will examine the coupling of a $j = 4$ particle to a vibrational core nucleus in the framework of the IBFM. It will be shown that by using the algebraic structure of the IBFM it is possible to obtain closed analytic expressions for the energy eigenvalues, electromagnetic transition rates,

static moments, and one and two nucleon transfer intensities. $U^B(5)$ plus $j = 4$: the Spin(3) Limit .

1- Energy Spectra

In this section we discuss the states built on a $j = 4$ shell model orbit. The matching of boson and fermion group chains gives [82]:

$$U^B(6) \supset U^B(5) \supset SO^B(5) \supset SO^B(3) \supset SO^B(2) \dots \dots \dots (2-92)$$

$$U^F(2) \supset \begin{matrix} \approx \\ \approx \end{matrix} SU^F(2) \supset SO^F(2)$$

The two chains can be combined into

$$\begin{aligned} U^B(6) \otimes U^F(2) &\supset U^B(5) \otimes U^F(2) \supset SO^B(5) \otimes U^F(2) \supset SO^B(3) \otimes \\ U^F(2) &\supset Spin(3) \supset Spin(2) \dots \dots \dots (2-93) \end{aligned}$$

where $Spin(3) \approx SU(2)$ and $Spin(2) \approx N SO(2)$. The boson generators of the groups $U^B(5)$, and $SO^B(5)$, and $SO^B(3)$ can be written as B_{-}^{λ} , $\lambda = 0, \dots, 4$, B_{-}^{λ} , $\lambda = 0, \dots, 3$, and, B_{-}^1 respectively, where

$$B_{-}^{\lambda} = \left(d^{\dagger} \times \tilde{d} \right)_{-}^{\lambda} \dots \dots \dots (2-94).$$

The fermion generators of the groups $U^F(2)$ and $SU^F(2)$ are given by A_{-}^{λ} , $\lambda = 0, 1$, and A_{-}^1 , respectively, with

$$A_{-}^{\lambda} = \left(a_{1/2}^{\dagger} \times \tilde{a}_{1/2} \right)_{-}^{\lambda} \dots \dots \dots (2-95)$$

Note that in Eqs. (2-94) and (2-95) we have used Racah's [93] coupled tensor notation, while in Eqs.(2-76), (2-77) and (2-78), we have used the uncoupled notation. The generators of the Spin(3) group can be obtained by combining those of $SO^B(3)$ and $SU^F(2)$:

$$G_{-}^{(1)} = B_{-}^{(1)} - \frac{1}{2\sqrt{5}} A_{-}^{(1)} \dots \dots \dots (2-96)$$

and are proportional to the total angular momentum operator $J_{-}^{(1)} = \sqrt{10}G_{-}^{(1)}$.

The basis states can be characterized by a complete set of labels which are given by the irreducible representations of the groups appearing in Eq.(2- 94):

$$\begin{aligned} &| U^B(6); U^F(2); U^B(5); SO^B(5); SO^B(3); Spin(3); Spin(2); \rangle \\ &| [N]; \{M\}; n_d; \nu; L; J; M_J; \rangle \dots \dots \dots (2-97) \end{aligned}$$

The total number of bosons N labels the totally symmetric irreducible representations of $U^B(6)$ and the total number of fermions M labels the totally antisymmetric irreducible representations of $U^F(2)$. The values of the number of d-bosons n_d contained in each $[N]$ are $n_d = 0, 1, \dots, N$. The values of the boson seniority ν contained in each n_d are $\nu = n_d, n_d - 2, \dots, 1$ or 0 , depending on whether n_d is odd or even. Since the reduction from $SO^B(5)$ to $SO^B(3)$ is not fully decomposable [92], one has to introduce an additional label n_Δ which counts the number of boson triplets coupled to zero angular momentum, to classify the basis states uniquely. The values of the boson angular momentum L contained in each representation of $SO^B(5)$ are given by:

$$L = 2\nu - 6n_\Delta, 2\nu - 6n_\Delta - 2, 2\nu - 6n_\Delta - 3, \dots, 2\nu - 6n_\Delta + 1, 2\nu - 3n_\Delta \dots (2-98)$$

Finally, the angular momentum L with the fermion angular momentum. For a system of N bosons and $M = 0$ fermions $J = L$, and in the case of N bosons and $M = 1$ fermions $J = L \pm 1/2$. M_J is the z component of the total angular momentum J .

A part from terms which only contribute to binding energies, the most general Hamiltonian, which is diagonal in the basis, Eq. (2-97) is given by:

$$H = v_1 C_{1U^B(5)} + v_2 C_{1U^B(5)} \cdot C_{1U^F(2)} + r C_{2U^B(5)} + s C_{2SO^B(5)} + \chi_1 C_{2SO^B(5)} + \chi_2 C_{2Spin(3)} \dots (2-99)$$

Here C_{1G} and C_{2G} denote the linear and quadratic Casimir operators of the group G . In terms of the generators, Eqs. (2-94) and (2-96) can be written as:

$$\begin{aligned} C_{1U^B(5)} &= n_d^\wedge = \sqrt{5} B_0^{(0)} \\ C_{1U^F(2)} &= M^\wedge = -\sqrt{2} A_0^{(0)} \\ C_{2U^B(5)} &= \sum_{j=0}^4 B^{(j)} \cdot B^{(j)} = n_d^\wedge (n_d^\wedge + 4) \\ C_{2SO^B(5)} &= 4 [B^{(3)} \cdot B^{(3)} + B^{(1)} \cdot B^{(1)}] \\ C_{2SO^B(3)} &= 20 B^{(1)} \cdot B^{(1)} \\ C_{2Spin(3)} &= 20 G^{(1)} \cdot G^{(1)} \end{aligned}$$

The energy eigenvalues of the Hamiltonian Eq.(2-99) are now given by:

$$E(N, M, n_d, v, L, J) = v_1 n_d + v_2 n_d M + r n_d (n_d + 4) + 2Sv(v+3) + 2\chi_1 L(L+1) + 2\chi_2 J(J+1) \dots (2-100)$$

We note that since all three boson chains contain the rotation group $SO^B(3)$ as a subgroup, it is obvious that for any of the three boson symmetries we can construct a Spin(3) limit.

2- Electromagnetic Transition Rates

In the interacting boson-fermion model the most general form of a one-body transition operator with multipolarity } is given by:

$$T_{-}^{(\lambda)} = T_{B,-}^{(\lambda)} + T_{F,-}^{(\lambda)} \dots (2-101)$$

where $T_{B,-}^{(\lambda)}$ is given in Eq. (2-43) and $T_{F,-}^{(\lambda)}$ is given by:

$$T_{F,-}^{(\lambda)} = \sum_{\ddot{j}\ddot{j}'} t_{\ddot{j}\ddot{j}'}^{(\lambda)} (a_j^\dagger \times a_{\ddot{j}'}^\dagger)_{-}^{(\lambda)} \dots (2-102)$$

represents the single-particle part of the transition operator.

E2 Transitions.

In this case where the odd nucleon has spin $j = 1/2$, the E2 transitions are fully determined by the collective part of the E2-operator:

$$T_{-}^{(E2)} = q_2^- (s^+ \times d^- + d^+ \times s^-)^{(2)} + q_2^- (d^+ \times d^-)^{(2)}$$

$$T_{-}^{(E2)} = e_B Q_B^{(2)} = e_F \sum_{\ddot{j}\ddot{j}'} Q_{\ddot{j}\ddot{j}'} (a \times a_{\ddot{j}'}^-)^{(2)} \dots (2-103)$$

Since the second term is a generator of $U^B(5)$, it has selection rule $\Delta n_d = 0$, while the first term can change n_d by one unit, $\Delta n_d = \pm 1$. The reduced matrix elements of $T^{(E2)}$ between the basis states, Eq. (2-97), can simply be related to those between the corresponding core states,

$$\langle [N], \{M=1\}, n_d, \epsilon, L, J \| T^{(E2)} \| [N], \{M=1\}, n_d', \epsilon', L', J' \rangle$$

$$(-1)^{L-1/2+J'} \sqrt{(2J+1)(2J'+1)} \left\{ \begin{matrix} L \dots J \dots 1/2 \\ J' \dots L' \dots 2 \end{matrix} \right\}$$

$$\times \langle [N], n_d, \epsilon, L \| T^{(E2)} \| [N], n_d', \epsilon', L' \rangle \dots (2-104)$$

and quadrupole moments

$$Q_J = \sqrt{16f/5} \sqrt{J(2J+1)} / \sqrt{\{(2J+1)(J+1)(2J+3)\}} \langle r, J \| T^{(E2)} \| r, J \rangle \dots (2-105)$$

with $r = [N], \{M = 1\}, n_d, \epsilon, L$

MI Transitions.

The most general MI operator is given by:

$$T_{\sim}^{(M1)} = g_B \sqrt{10} B_{\sim}^{(1)} - g_F \frac{1}{\sqrt{2}} A_{\sim}^{(1)}$$

$$T_{\sim}^{(M1)} = \sqrt{30/4f} g_B (d^+ \times d^-)^{(1)} - \sum_{jj'} \sqrt{\frac{j(j+1)(2j+1)}{4f}} (a_j \times a_{j'})^{(1)} \dots\dots\dots(2-106)$$

where $B_{\sim}^{(1)}$ and $A_{\sim}^{(1)}$ have been defined in Eqs. (2-94) and (2-95). The operator $T^{(MI)}$ has selection rules $\Delta n_d = \Delta \epsilon = \Delta L = 0$. Therefore, the only nonvanishing MI transitions are those between states with $J = L + 1/2$ and $J' = L - 1/2$.

magnetic moments are simply given by:

$$\mu_{J=L\pm 1/2} = \sqrt{J / \{(2J+1)(J+1)\}} \langle rJ \| T^{(M1)} \| rJ \rangle = g_B L \pm g_F \frac{1}{2} \dots\dots\dots(2-107)$$

Again $r = [N], \{M = 1\}, n_d, \epsilon, L$

2.3.1.3- $U^B(5)$ plus $j = 3/2$: the Spin(S) Limit

The coupling of a $j = 3/2$ orbit to the collective quadrupole degrees of freedom has been studied in the framework of various core-particle coupling models. In Ref. [94] Bayman and Silverberg discuss the coupling of a particle in a $j = 3/2$ shell to the quadrupole oscillations of the nuclear surface. The Hamiltonian:

$$H = \hbar \tilde{S} \sum_{\sim} \left(b_{\sim}^+ b_{\sim} + \frac{1}{2} \right) - k \sum_{\sim} r_{\sim} Y_{\sim}^{(2)}(\nu, \Phi) \dots\dots\dots(2-108)$$

is invariant under transformations of the symplectic group $Sp(4)$. This property provides a convenient basis, spanned by the irreducible representations $(\nu + 1, \nu)$ of $Sp(4)$ in which the matrix elements of this Hamiltonian can be calculated. However, the Hamiltonian is not diagonal in this basis. Both in the weak-coupling limit ($k\hbar\tilde{S} \ll 1$) and in the strong-coupling limit ($k\hbar\tilde{S} \gg 1$), approximate solutions are obtained for the energy

eigenvalues. The transition between the weak- and the strong coupling limit can be studied numerically.

In the framework of the IBFM the Hamiltonian, which describes the coupling of a $j=3/2$ particle to a core nucleus, has the group structure $G = U^B(6) \otimes U^F(4)$. In general, no further symmetry is present and the eigenvalue problem has to be solved numerically. However, whenever the Hamiltonian can be expressed in terms of Casimir invariants of a chain of subgroups of G , a dynamical boson-fermion symmetry arises and the energy eigenvalues can be obtained in closed analytic form. The coupling of a $j=3/2$ particle to an even-even nucleus with $SO^B(6)$ symmetry has recently been discussed by **Iachello and Kuyucak** [95, 96].

1- Energy Spectra.

In this section we discuss the states built on a $j=3/2$ shell model orbit. The matching of boson and fermion group chains gives

$$\begin{aligned} U^B(6) \supset U^B(5) \supset SO^B(5) \supset SO^B(3) \supset SO^B(2) \\ \approx \approx \approx \\ U^F(4) \supset SU^F(4) \supset SP^F(4) \supset SU^F(2) \supset SO^F(2) \end{aligned}$$

Since the algebras of $SO^B(5)$, $SO^B(3)$, and $SO^B(2)$ are isomorphic to those of $Sp^F(4)$, $SU^F(2)$, and $SO^F(2)$, respectively, the boson and fermion group chains can be combined into

$$\begin{aligned} U^B(6) \otimes U^F(4) \supset U^B(5) \otimes SU^F(4) \supset SO^B(5) \\ \otimes SP^F(4) \supset Spin(5) \supset Spin(3) \supset Spin(2) \dots (2-109) \end{aligned}$$

where $Spin(S) \approx Sp(4)$, $Spin(3) \approx SU(2)$, and $Spin(2) \approx SO(2)$ [95, 96].

The generators of the groups $U^B(5)$ again are given by $B_{-}^{(j)}$, $j=0, \dots, 4$, and

those of $SO^B(5)$ by $B_{-}^{(1)}$ and $B_{-}^{(3)}$ with $B_{-}^{(j)} = (d^{\dagger} \times \tilde{d})_{-}^{(j)}$. The generators of

$U^F(4)$ can be written as $A_{-}^{(1)}$ and $A_{-}^{(3)}$ those of $Sp^F(4)$ as $A_{-}^{(1)}$ and $A_{-}^{(3)}$ with:

$$A_{-}^{(j)} = (a_{3/2}^{\dagger} \times \tilde{a}_{3/2})_{-}^{(j)} \quad \dots \dots \dots (2-110)$$

The generators of the combined group $Spin(S)$ can be written as

$$G_{\pm}^{(1)} = B_{\pm}^{(1)} - \frac{1}{\sqrt{2}} A_{\pm}^{(1)} \dots\dots\dots(2-111)$$

$$G_{\pm}^{(1)} = B_{\pm}^{(1)} + \frac{1}{\sqrt{2}} A_{\pm}^{(1)} \dots\dots\dots(2-112)$$

The generators of the Spin(3) group are simply $G_{\pm}^{(1)}$, which are proportional to the total angular momentum operator $J_{\pm}^{(1)} = \sqrt{10}G_{\pm}^{(1)}$.

The basis states can be labelled by a set of quantum numbers which characterize the irreducible representations of the groups appearing in Eq.(2-109).

$$\left| U^B(6); U^F(4); U^B(5); SO^B(5); Spin(3); Spin(3); Spin(2) \right\rangle; \\ \left| [N]; \{M\}; n_d; \nu; (\epsilon_1, \epsilon_2); J; M_J \right\rangle \dots\dots(2-113)$$

The quantum numbers N, M, n_d , and ν are the same in the previous section. The values of (ν_1, ν_2) which characterize the irreducible representations of Spin(S), can be obtained from the branching rules. For the case of N bosons and $M = 0$ fermions the values of (ν_1, ν_2) are given by:

$$\epsilon_1 = \epsilon = n_d, n_d - 2, \dots, 1 \text{ or } 0 \text{ (} n_d = \text{odd or even) } \dots\dots\dots(2-114) \\ \epsilon_2 = 0$$

for the case of N bosons and $M = 1$ fermions by

$$\epsilon_1 = \epsilon + \frac{1}{2}, \epsilon - \frac{1}{2} \\ \epsilon_2 = 0 \dots\dots\dots(2-115)$$

Since the step from Spin(S) to Spin(3) is not fully reducible an additional label n_{Δ} is needed to classify the basis states uniquely:

$$n_{\Delta} = 0, 1, 2, \dots \quad \text{For } M = 0$$

$$n_{\Delta} = 0, 1/2, 1, 3/2, \dots \quad \text{For } M = 1$$

Apart from terms which only contribute to binding energies the most general Hamiltonian which is diagonal in the basis, Eq.(2-113), is given by:

$$H = \nu_1 C_{1U^B(5)} + \nu_2 C_{1U^B(5)} \cdot C_{1U^F(2)} \cdot C_{1U^F(4)} + \nu C_{2U^B(5)} + \nu_1 C_{2SO^B(5)} + \nu_2 C_{2Spin(5)} + \nu C_{2Spin(3)} \dots\dots(2-116)$$

The linear C_1 and quadratic C_2 , Casimir operators appearing in Eq. (2-116) can be expressed in terms of the generators Eqs. (2-110), (2-11) and (2-112) as [82]:

$$\begin{aligned}
 C_{1U^B(5)} &= n_d^\wedge = \sqrt{5}B_0^{(0)} \\
 C_{1U^F(4)} &= M^\wedge = \sqrt{4}A_0^{(0)} \\
 C_{2U^B(5)} &= \sum_{j=0}^4 B^{(j)} \cdot B^{(j)} = n_d^\wedge (n_d^\wedge + 4) \\
 C_{2SO^B(5)} &= 4[B^{(3)} \cdot B^{(3)} + B^{(1)} \cdot B^{(1)}] \\
 C_{2Spin(3)} &= 4[G^{(3)} \cdot G^{(3)} + G^{(1)} \cdot G^{(1)}] \\
 C_{2Spin(3)} &= 20G^{(1)} \cdot G^{(1)} \dots\dots\dots(2-117)
 \end{aligned}$$

The expectation values of the Hamiltonian, Eq.(2-116), are given by the energy formula

$$\begin{aligned}
 E(N, M, n_d, v, L, J) &= v_1 n_d + v_2 n_d M + r n_d (n_d + 4) + 2S_1 v (v + 3) \\
 &+ 2S_2 [\epsilon_1 (\epsilon_1 + 3) + \epsilon_2 (\epsilon_2 + 1)] + 2\chi J (J + 1) \dots\dots\dots(2-118)
 \end{aligned}$$

2- Wave Functions.

In order to calculate matrix elements for electromagnetic transitions and other nuclear properties analytically, one needs to know the wave functions explicitly. It is convenient to expand the wave functions, Eq.(2-113), into wave functions of the product group $SO^B(5) \otimes SP^F(4)$.

$$|[N], n_d, \epsilon, \epsilon_1, J\rangle = \sum_L \sum_{\epsilon_1, L}^{\epsilon, L} |[N], n_d, \epsilon, L\rangle \times \left| \frac{1}{2}, \frac{3}{2} \right\rangle \dots\dots\dots(2-119)$$

where $\epsilon = \epsilon_1 \pm \frac{1}{2}$. The wave function $|[N], n_d, \epsilon, \epsilon_1, J\rangle$ denotes the wave function $\left| [N], \{M = 1\}, n_d, \epsilon, (\epsilon_1, \epsilon_2 = \frac{1}{2}), J \right\rangle$, while $|[N], n_d, \epsilon, L\rangle$ denotes the $U^B(5)$ wave function $\left| [N], \{M = 0\}, n_d, \epsilon, (\epsilon_1 = \epsilon, \epsilon_2 = 0), L \right\rangle$ and $\left| \frac{1}{2}, \frac{3}{2} \right\rangle$ the fundamental spinor representation of $Sp(4)$. The expansion coefficients $\sum_{\epsilon_1, L}^{\epsilon, L}$, can be interpreted as the isoscalar factors [97] for the group reduction $Sp(4) \supset SU(2)$. Next we use Racah's factorization lemma [97], which relates the isoscalar factors $\sum_{N+1/2, \epsilon+1/2, J}^{N, \epsilon', L}$ for the group reduction $SU(4) \supset Sp(4) \supset SU(2)$, which already have been calculated, to those for the reductions $SU(4) \supset Sp(4)$, $y_{N+1/2, \epsilon+1/2}^{N, \epsilon'}$ and $Sp(4) \supset SU(2)$, $y_{\epsilon+1/2, J}^{\epsilon', L}$.

$$\langle \sum_{N+1/2, \epsilon, J}^{N, \epsilon', L} = y_{N+1/2, \epsilon}^{N, \epsilon'} g_{\epsilon, J}^{\epsilon', L} \dots\dots\dots(2-120)$$

where $\epsilon = \epsilon_1 \pm 1/2$. Taking $y_{N+1/2, \epsilon+1/2}^{N, \epsilon} = -((N + \epsilon + 4)/(2N + 4))^{1/2}$ and $y_{N+1/2, \epsilon+1/2}^{N, \epsilon+1} = ((N - \epsilon)/(2N + 4))^{1/2}$, we obtain the following expressions for the $\text{Sp}(4) \supset \text{SU}(2)$ isoscalar factors,

$$g_{N+1/2, J}^{\epsilon, L} = -\left(\frac{2N + 4}{N + \epsilon + 4}\right)^{1/2} \langle \begin{smallmatrix} N, \epsilon, L \\ N+1/2, \epsilon+1/2, J \end{smallmatrix} \rangle \dots \dots \dots (2-121)$$

$$g_{N+1/2, L}^{\epsilon+1, L} = \left(\frac{2N + 4}{N - \epsilon}\right)^{1/2} \langle \begin{smallmatrix} N, \epsilon+1, L \\ N+1/2, \epsilon+1/2, J \end{smallmatrix} \rangle \dots \dots \dots (2-122)$$

The coefficients $g_{\epsilon, J}^{\epsilon, L}$ can also be found by diagonalizing the operator $G^{(3)}$. $G^{(3)}$ between the wave functions given in Eq. (2-117). The matrix elements of $G^{(3)}$. $G^{(3)}$ are given by

$$\langle [N], \{M = 1\}, n_d, \epsilon, \epsilon_1, J | G^{(3)}. G^{(3)} | [N], \{M = 1\}, n'_d, \epsilon', \epsilon'_1, J' \rangle \dots \dots \dots (2-123)$$

$$u_{JJ'} u_{\epsilon \epsilon_1} u_{\epsilon \epsilon'_1} u_{n_d n'_d} \left[\frac{1}{2} \left(\epsilon_1 (\epsilon_1 + 3) + \frac{3}{4} \right) - \frac{1}{10} J(J + 1) \right] \dots \dots \dots (2-124)$$

3- Electromagnetic Transition Rates E2 Transitions.

The most general one-body E2 transition operator can be written as [82]:

$$T_-^{(E2)} = q_2^- (s^\dagger \times \tilde{d} + d^\dagger \times \tilde{s})_-^{(2)} + q_2^- (d^\dagger \times \tilde{d})_-^{(2)} + t_2 (a_{3/2}^\dagger \times \tilde{a}_{3/2})_-^{(2)} \dots \dots \dots (2-125)$$

The first term in Eq. (2-125) has selection rules $\Delta n_d = \pm 1$, while the last two terms have $\Delta n_d = 0$. The reduced matrix elements of $T^{(E2)}$ can be calculated by expanding the wave functions according to Eq. (2-119):

$$\begin{aligned} & \langle [N], \{M = 1\}, n_d, \epsilon, \epsilon_1, J | T^{(E2)} | [N], \{M = 1\}, n'_d, \epsilon', \epsilon'_1, J' \rangle \\ &= \sum_{L, L'} \begin{smallmatrix} \epsilon, L, \epsilon', L' \\ \epsilon_1, J, \epsilon'_1, J' \end{smallmatrix} \sqrt{(2J + 1)(2J' + 1)} \\ & \times \left[(-1)^{L-1/2+J'} \langle [N], n_d, \epsilon, L | T_B^{T(E2)} | [N], n'_d, \epsilon', L' \rangle \left\{ \begin{smallmatrix} L \dots J \dots 3/2 \\ J' \dots L' \dots 2 \end{smallmatrix} \right\} \right] \\ & + (-1)^{L+3/2+J} \left\langle \frac{1}{2}, \frac{3}{2} | T_F^{(E2)} | \frac{1}{2}, \frac{3}{2} \right\rangle \left\{ \begin{smallmatrix} 3 \dots J \dots L \\ J' \dots 3/2 \dots 2 \end{smallmatrix} \right\} u_{n_d n'_d} u_{\epsilon \epsilon_1} u_{L, L'} \dots \dots \dots (2-126) \end{aligned}$$

The isoscalar factors $\begin{smallmatrix} \epsilon, L \\ \epsilon_1, J \end{smallmatrix}$, have been derived in the previous section and the reduced matrix elements of $T_B^{(E2)}$ have been derived in the previous section and the reduced can be taken from Ref. [54]. From the reduced

matrix elements, Eq. (2-126), we can calculate $B(E2)$ values, Eq. (2-103), and quadrupole moments, Eq. (2-105), in the usual way.

M1 Transitions.

The $M1$ operator in the Spin(S) limit can be expressed as:

$$T_{-}^{(M1)} = g_B \sqrt{10} B_{-}^{(1)} - g_F \sqrt{5} A_{-}^{(1)} \dots \dots \dots (2-127)$$

where $B_{-}^{(1)}, A_{-}^{(1)}$ are defined in Eqs. (2-94) and, (2-95). The operator in Eq. (2-127), has selection rules $\Delta n_d = 0, \Delta \epsilon = 0, \Delta \epsilon_1 = \pm 1, \Delta \epsilon_2 = 0$. If $g_B = g_F$, the $M1$ -operator is proportional to the total angular momentum operator $J_{-}^{(1)}$ and therefore in this case all $M1$ transitions are forbidden. We will consider the general case $g_B \neq g_F$. The reduced matrix elements of $T^{(M1)}$ can be obtained by expanding the wave functions according to Eq. (2-119).

$$\begin{aligned} & \langle [N]_p, \{M=1\}, n_d, \epsilon, \epsilon_1, J \| T^{(M1)} \| [N]_p, \{M=1\}, n_d, \epsilon, \epsilon_1', J' \rangle \\ & = u_{\epsilon, \epsilon'} u_{J, J'} g_B \sqrt{(J+1)(2J+1)} \\ & + (g_F - g_B) \sum_L \begin{matrix} \epsilon, L, \epsilon_1, L \\ \epsilon_1, L, \epsilon_1', J' \end{matrix} (-1)^{L+3/2+J+1} \sqrt{(2J+1)(2J'+1)} \left\{ \begin{matrix} 3 & \dots & L & \dots & J \\ 2 & & & & \\ J' & \dots & 3 & \dots & 1 \\ 2 & & & & \end{matrix} \right\} \dots \dots \dots (2-128) \end{aligned}$$

From the reduced matrix elements Eq. (2-128) one can calculate $T(M1)$ matrix element values Eq. (2-106) and magnetic moments Eq. (2-107).

2.3.2-Interacting Boson-Fermion Model-2 (IBFM-2)

The interacting boson-fermion model-1 (IBFM-1) describes properties of even-odd nuclei by coupling collective and single-particle degrees of freedom much in the same way this is done in the collective model [72]. The collective degrees of freedom are described either by shape variables μ ($\mu = 0, \pm 1, \pm 2$) or by boson operators s, d_{μ} ($\mu = 0, \pm 1, \pm 2$), with no direct link to the underlying microscopic structure. A microscopic description of nuclei is provided by the spherical shell model. Collective features in this model can be obtained by introducing the concept of correlated pairs with angular momentum and parity $J^f = 0^+$ and $J^f = 2^+$. A treatment of these pairs as bosons leads to the

interacting boson model (IBM). However, since there are protons and neutrons, one has the possibility of forming proton and neutron pairs. In heavy nuclei, the neutron excess prevents the formation of correlated proton-neutron pairs and one thus is led to consider only proton-proton and neutron-neutron pairs. The corresponding model is the interacting boson model-2 (IBM-2) [98, 99]. The introduction of fermions in this models leads to the interacting boson-fermion model-2 (IBFM-2). In addition to a more direct connection with the spherical shell model, the interacting boson-fermion model-2 (IBFM-2) has features that cannot be obtained in the interacting boson-fermion model-1 (IBFM-1).

The structure of interacting boson fermion model-2 (IBFM-2) is very similar to that of model-1 (IBFM-1). In order to avoid repetitions, the discussion here and in the following section will therefore be kept short and will concentrate mostly on numerical studies [82].

2.3.2.1- Bosons and fermions

Consider an odd-even nucleus in the spherical shell model. Single-particle levels here are denoted by nlj with n being the principal quantum number, l the orbital angular momentum and j the total angular momentum, $j = l \pm \frac{1}{2}$. When many particles occupy the valence shells, the diagonalization of the residual interaction in the shell model space is unmanageable. A truncation can be obtained first by assuming that the closed shells are inert and second by considering only those configurations arising from pairing together particles to states with angular momentum and parity $J^f = 0^+$ and $J^f = 2^+$. In even-odd nuclei at least one particle remains unpaired. In odd-proton nuclei it is a proton, in odd-neutron nuclei it is a neutron. One can also consider situations in which both one proton and one neutron are unpaired or cases in which two neutrons or two protons are unpaired. The former situation will arise in odd-odd nuclei while the latter will correspond to excited states in even-even nuclei. (These excited states are often called two-quasi-particle states.) The general situation is

thus described by proton (neutron) bosons with $J^f = 0^+$, denoted by $s_f (s_v)$ and proton (neutron) bosons with $J^f = 2^+$, denoted by $d_f (d_v)$. This is identical to the situation in even-even nuclei. In addition, there are unpaired protons, denoted by a_f and neutrons, a_v . As in the case of even-even nuclei, in order to take into account the particle-hole conjugation in particle space, the number of proton and neutron bosons, N_{Bf} and N_{Bv} , and of proton and neutron fermions, N_{Ff} and N_{Fv} is counted from the nearest closed shell, i.e., if more than half of the shell is full, $N_{Bf(\epsilon)}$ and $N_{Ff(\epsilon)}$ are taken as holes. Thus, for example, for $^{119}_{54}\text{Xe}_{65}$, $N_{Bf} = (54 - 50)/2 = 2$, $N_{Bv} = (64 - 50)/2 = 7$ and $N_{Fv} = 65 - 64 = 1$ while for $^{127}_{54}\text{Xe}_{73}$, $N_{Bf} = (54 - 50)/2 = 2$, $\tilde{N}_{Bv} = (82 - 74)/2 = \tilde{4}$ and $\tilde{N}_{Fv} = 74 - 73 = \tilde{1}$. A bar is sometimes placed over the numbers $N_{Bf(\epsilon)}$ and $N_{Ff(\epsilon)}$ to indicate that these are hole states. The total number of bosons and fermions is then:

$$\begin{aligned} N_B &= N_{Bf} + N_{Bv}, \\ N_F &= N_{Ff} + N_{Fv}. \end{aligned} \quad (2-129)$$

Properties of this model, with protons and neutrons explicitly introduced, will now be discussed.

1- Boson and fermion operators.

The building blocks of the interacting boson-fermion model-2 (IBFM-2) are boson and fermion operators for protons and neutrons. The boson operators are identical to those in section (2.2) [82]:

$$\begin{aligned} s_f^\dagger, d_{f,\sim}^\dagger, s_v^\dagger, d_{v,\sim}^\dagger, & \quad \sim = 0, \pm 1, \pm 2 \\ s_f, d_{f,\sim}, s_v, d_{v,\sim}, & \quad \sim = 0, \pm 1, \pm 2 \end{aligned} \quad \dots\dots\dots(2-130)$$

or, in a more compact notation,

$$b_{\dots,l,m}^\dagger; b_{\dots,l,m}; \quad (\dots = f, v; l = 0, 2; -1 \leq m \leq l) \quad \dots\dots\dots(2-131)$$

These operators satisfy Bose commutation relations,

$$\begin{aligned} [b_{\dots,l,m}, b_{\dots',l',m'}^\dagger] &= \delta_{\dots, \dots'} \delta_{ll'} \delta_{mm'}, \\ [b_{\dots,l,m}, b_{\dots',l',m'}] &= [b_{\dots,l,m}^\dagger, b_{\dots',l',m'}^\dagger] = 0. \end{aligned} \quad \dots\dots\dots(2-132)$$

In addition, there are now fermion creation and annihilation operators,

$$a_{\dots,j,m}^\dagger; a_{\dots,j,m}; \left(\dots = f, v; j = j_1, j_2, \dots, j_n, m = \pm 1/2, \pm 3/2, \dots, \pm j \right) \dots (2-133)$$

The fermion operators satisfy Fermi anticommutation relations,

$$\begin{aligned} \{a_{\dots,j,m}, a_{\dots',j',m'}^\dagger\} &= u_{\dots} u_{jj'} u_{mm'}, \\ \{a_{\dots,j,m}, a_{\dots',j',m'}\} &= \{a_{\dots,j,m}^\dagger, a_{\dots',j',m'}^\dagger\} = 0. \end{aligned} \dots (2-134)$$

The values over which the index j runs are now determined by the single-particle levels in the valence shell. For example, for ${}_{54}^{127}\text{Xe}_{73}$, the values of J_v are 5/2, 7/2, 11/2, 1/2 and 3/2. The principal quantum number, n , is as usual not written as an index on the fermion operators, unless one considers large spaces in which there are two single-particle states with the same j . If only valence shells are included, this never occurs. Boson and fermion operators are assumed to commute,

$$[b_{\dots,l,m}, a_{\dots',j',m'}^\dagger] = [b_{\dots,l,m}, a_{\dots',j',m'}] = [b_{\dots,l,m}^\dagger, a_{\dots',j',m'}^\dagger] = [b_{\dots,l,m}^\dagger, a_{\dots',j',m'}] = 0 \dots (2-135)$$

2-Isospin

Instead of the label $\dots = f, v$, it is possible, for bosons as well as for fermions, to introduce another, equivalent label. For bosons it is called F -spin and was defined in $U(n|m) \supset OSp(n|m)$ where m is even. For fermions the label is precisely identical to isospin. Protons can be characterized by $T = 1/2$ and projection $T_z = +1/2$, while neutrons are characterized by $T = 1/2$ and $T_z = -1/2$, i.e.

$$\begin{aligned} |f\rangle &= \left| \frac{1}{2}, +\frac{1}{2} \right\rangle, \\ |v\rangle &= \left| \frac{1}{2}, -\frac{1}{2} \right\rangle. \end{aligned} \dots (2-136)$$

Using the isospin label, fermion creation and annihilation operators are denoted by

$$a_{\frac{1}{2},m_i,j,m}^\dagger; a_{\frac{1}{2},m_i,j,m}; \quad (m = \pm 1/2) \dots (2-137)$$

When the isospin label is used, spherical tensors are built from creation and annihilation operators of the type

$$\tilde{a}_{\frac{1}{2},m_i,j,m} = (-)^{\frac{1}{2}-m_i+j-m} a_{\frac{1}{2},-m_i,j,-m}^\dagger. \quad (2-138)$$

Isospin for fermions does not play an important role in the interacting boson-fermion model-2 (IBFM-2) since protons and neutrons occupy

different single-particle states. It plays instead an important role in more elaborate versions of the model.

3-Basis states

Basis states in the interacting boson-fermion model-2 (IBFM-2) are rather complex. Denoting the indices l, m as r and the indices j, m as i , basis states can be written as

$$BF : a_{f,i}^\dagger a_{f,i'}^\dagger \cdots a_{v,i}^\dagger a_{v,i'}^\dagger \cdots b_{f,r}^\dagger b_{f,r'}^\dagger \cdots b_{v,r}^\dagger b_{v,r'}^\dagger \cdots |o\rangle \dots\dots\dots (2-139)$$

If no fermion creation operators are present, Eq. (2-139) describes a state in an even-even nucleus, if one fermion operator is present, Eq. (2-139) describes a state in an even-odd nucleus, if one proton and one neutron creation operator is present, the state is in an odd-odd nucleus, etc. Angular momentum couplings are chosen in such a way that bosons and fermions are first coupled among themselves, followed by the final coupling,

$$BF : \left[\left[a_{f,j}^\dagger \times a_{f,j'}^\dagger \times \cdots \right]^{(J_f)} \times \left[a_{v,j}^\dagger \times a_{v,j'}^\dagger \times \cdots \right]^{(J_v)} \right]^{(J_F)} \left[\left[b_{f,l}^\dagger \times b_{f,l'}^\dagger \times \cdots \right]^{(L_f)} \times \left[b_{v,l}^\dagger \times b_{v,l'}^\dagger \times \cdots \right]^{(L_v)} \right]^{(L_B)} \Big]_M^{(J)} |o\rangle. \dots\dots\dots (2-140)$$

2.3.2.2 The IBFM-2 Hamiltonian operator

The Hamiltonian operator has now the general form [82]:

$$H = H_B + H_F + H_{BF} \dots\dots\dots (2-141)$$

with

$$\begin{aligned} H &= H_{fB} + H_{vB} + H_{fvB}, \\ H &= H_{fF} + H_{vF} + H_{fvF}, \\ H &= H_{ffBF} + H_{fvBF} + H_{vfBF} + H_{vvBF} \dots\dots\dots (2-142) \end{aligned}$$

The various parts have the same structure as those discussed in section(2.2), except that indices f, v appear everywhere.

1-Special forms of the interaction

The most general Hamiltonian (2-141) and (2-142) contains many parameters. A phenomenological study using all the parameters is nearly impossible. In the analysis of experimental data simpler Hamiltonians are quite often used which contain the essential features of the interaction. The

part describing the bosons is usually treated in terms of the Talmi Hamiltonian, which contains the basic features of the effective nucleon-nucleon interaction that emerge from pairing, quadrupole and symmetry energy. In addition, in some calculations a d-boson number-conserving interaction arising from a seniority-conserving nucleon-nucleon interaction between like particles is introduced. The adopted boson Hamiltonian is then [82]:

$$H = E_0 + V_f \hat{n}_{d_f} + V_v \hat{n}_{d_v} + \{ \hat{Q}_f^\dagger \cdot \hat{Q}_v^\dagger + \} \hat{M}_{fv} + V_{ff} + V_{vv} \quad \dots\dots\dots(2-143)$$

The operators $\hat{n}_{d_f}, \hat{n}_{d_v}, \hat{Q}_f^\dagger$ and \hat{Q}_v^\dagger have the same meaning as in section (2.2).

In terms of the boson operators they are given by:

$$\begin{aligned} \hat{n}_{d_{\dots}} &= \sum_{\dots} d_{\dots}^\dagger d_{\dots}, \\ \hat{Q}_{\dots}^\dagger &= [s_{\dots}^\dagger \times \tilde{d}_{\dots} + d_{\dots}^\dagger \times \tilde{s}_{\dots}]^{(2)} + t_{\dots} [d_{\dots}^\dagger \times \tilde{d}_{\dots}]^{(2)}, \quad \dots = f, v \quad \dots\dots\dots(2-144) \end{aligned}$$

The Majorana operator \hat{M}_{fv} is given by:

$$\begin{aligned} \hat{M}_{fv} &= [s_v^\dagger \times d_f^\dagger - s_f^\dagger \times d_v^\dagger]^{(2)} \cdot [\tilde{s}_v \times \tilde{d}_f - \tilde{s}_f \times \tilde{d}_v]^{(2)} \\ &\quad - 2 \sum_{k=1,3} \langle_k [d_v^\dagger \times d_f^\dagger]^{(k)} \cdot [\tilde{d}_v \times \tilde{d}_f]^{(k)}. \quad \dots\dots\dots(2-145) \end{aligned}$$

The coefficients \langle_k have been introduced in Eq. (2-145) relative to Eq. (2-45), in order to allow for different strengths of the last two terms relative to the first one. This result arises from microscopic calculations of the coefficients. The d-boson number-conserving interaction is:

$$V_{\dots} = \sum_{L=0,2,4} \frac{1}{2} c_L^{(\dots)} [d_{\dots}^\dagger \times d_{\dots}^\dagger]^{(L)} \cdot [\tilde{d}_{\dots} \times \tilde{d}_{\dots}]^{(L)}, \quad \dots = f, v \quad \dots\dots\dots(2-146)$$

The part related to the fermions is described in terms of an effective nucleon-nucleon interaction. This interaction can be taken either as a schematic interaction (such as a surface u-function interaction), as often used in shell-model calculations [100], or as the effective interaction arising from the free nucleon-nucleon interaction. In most calculation only one proton or one neutron is unpaired. In these cases, only the one-body part of H_F matters. This is just the single-particle energy [82]:

$$H'_F = E_0 + \sum_{j_f} v_{j_f} \hat{n}_{j_f} + \sum_{j_v} v_{j_v} \hat{n}_{j_v}, \quad \dots \dots \dots (2-147)$$

where

$$\hat{n}_{d_{\dots}} = \sum_{m_{\dots}} a_{\dots, j_{\dots}, m_{\dots}}^{\dagger} a_{\dots, j_{\dots}, m_{\dots}}, \quad \dots = f, v \quad \dots \dots \dots (2-148)$$

In odd-odd nuclei there is one unpaired proton and one unpaired neutron. In these cases, one needs also the proton-neutron interaction. This can be taken in the form of a quadrupole interaction:

$$H''_F = \sum_{j_f j'_f j_v j'_v} \frac{1}{2} v_{j_f j'_f j_v j'_v} \left[\left[a_{j_f}^{\dagger} \times a_{j'_f}^{\dagger} \right]^{(2)} \times \left[\tilde{a}_{j_v} \times \tilde{a}_{j'_v} \right]^{(2)} \right]_0^{(0)}, \quad \dots \dots \dots (2-149)$$

or, alternatively, a surface u -function interaction is used.

The most important part of the Hamiltonian for even-odd nuclei is the boson-fermion interaction. The microscopic theory of the interacting boson-fermion model suggests specific forms for this interaction. The three important terms are, as in section (2.2) the monopole, the quadrupole and the exchange interaction. The monopole and quadrupole terms are written in the same form as in section (2.2):

$$V_{BF}^{MON} = \sum_{j_f} A_{j_f} (\hat{n}_{d_{j_f}} \hat{n}_{j_f}) + \sum_{j_v} A_{j_v} (\hat{n}_{d_{j_v}} \hat{n}_{j_v}) \quad \dots \dots \dots (2-150)$$

$$V_{BF}^{QUAD} = \sum_{j_f j'_f} \Gamma_{j_f j'_f} \hat{Q}_{j_f j'_f}^{\dagger} \hat{q}_{j_f j'_f} + \sum_{j_v j'_v} \Gamma_{j_v j'_v} \hat{Q}_{j_v j'_v}^{\dagger} \hat{q}_{j_v j'_v}, \quad \dots \dots \dots (2-151)$$

where \hat{n}_{j_f} and \hat{n}_{j_v} are defined in Eq. (2-148) and the fermion quadrupole operators $\hat{q}_{j_{\dots} j'_{\dots}}$ are given by:

$$\hat{q}_{j_{\dots} j'_{\dots}} = \left[a_{j_{\dots}}^{\dagger} \times \tilde{a}_{j'_{\dots}} \right]^{(2)}, \quad \dots = f, v \quad \dots \dots \dots (2-152)$$

The microscopic structure of the interacting boson model suggests that the monopole interaction acts predominantly between like particles (proton fermions with proton bosons and neutron fermions with neutron bosons), while the quadrupole interaction acts predominantly between unlike particles (protons with neutrons) [101]. These considerations are built in the special forms (2-150) and (2-151). The last term in the boson-fermion interaction is the exchange term. In the interacting boson-fermion model-2 (IBFM-2) this term has a form somewhat different from the corresponding term in section (2-3):

$$\begin{aligned}
V_{\dots} = & \left[s_f^\dagger \times \tilde{d}_f \right]^{(2)} \cdot \left\{ \sum_{j_v j'_v j''_v} \Lambda_{j_v j'_v j''_v}^{j''_v} : \left[d_v^\dagger \times \tilde{a}_{j''_v} \right]^{(j_v)} \times \left[s_v^\dagger \times a_{j'_v}^\dagger \right]^{(j'_v)} \right\}^{(2)} : \\
& + \left[s_v^\dagger \times \tilde{d}_v \right]^{(2)} \cdot \left\{ \sum_{j_f j'_f j''_f} \Lambda_{j_f j'_f j''_f}^{j''_f} : \left[d_f^\dagger \times \tilde{a}_{j''_f} \right]^{(j_f)} \times \left[s_f^\dagger \times a_{j'_f}^\dagger \right]^{(j'_f)} \right\}^{(2)} : \\
& + \text{Hermitian conjugate.} \qquad \dots\dots\dots (2-153)
\end{aligned}$$

This form again is suggested by the microscopic structure of the model. It should be noted that, if no distinction is made between protons and neutrons, the form (2-153) can approximately be rewritten as by appropriately contracting the s -boson operators.

2-Transition operators

Transition operators can be written in the same way as in section (2-2). There are now four terms describing proton and neutron bosons and fermions [82]:

$$T_{\sim}^{(L)} = T_{fB,\sim}^{(L)} + T_{vB,\sim}^{(L)} + T_{fF,\sim}^{(L)} + T_{vF,\sim}^{(L)} \dots\dots\dots (2-154)$$

The boson terms are given in section (2.2). The fermion terms can, to the lowest order, be written as:

$$\begin{aligned}
T_{fF,\sim}^{(L)} &= f_{f,0}^{(0)} u_{L0} + \sum_{j_f j'_f} f_{j_f j'_f}^{(L)} \left[a_{j_f}^\dagger \times \tilde{a}_{j'_f} \right]_{\sim}^{(L)}, \\
T_{vF,\sim}^{(L)} &= f_{v,0}^{(0)} u_{L0} + \sum_{j_v j'_v} f_{j_v j'_v}^{(L)} \left[a_{j_v}^\dagger \times \tilde{a}_{j'_v} \right]_{\sim}^{(L)} \dots\dots\dots (2-155)
\end{aligned}$$

Particularly important in even-odd nuclei are the transition operators which induce $E2$ and $M1$ transitions. It is customary in the operators to separate the dependence on the angular momenta j_f and j_v from the coefficients that determine the strengths of the transitions. This is done by introducing effective charges and moments. For $E2$ transitions, one has:

$$f_{j_{\dots} j'_{\dots}}^{(2)} = -e^F \langle n_{\dots}, l_{\dots} | r^2 | n'_{\dots}, l'_{\dots} \rangle \langle l_{\dots}, \frac{1}{2}, j_{\dots} | Y^{(2)} | l'_{\dots}, \frac{1}{2}, j'_{\dots} \rangle / \sqrt{5}, \quad \dots = f, v \quad (2-156)$$

where now the single particle indices $n, l, s = \frac{1}{2}, j$ are written explicitly. The quantities e_f^F and e_v^F are the fermion effective charges. The free values of these charges are 1 and 0 respectively, in units of the electron charge. Shell

model calculations indicate that $e_f^F \approx 1.5e$ and $e_v^F \approx 0.5e$ [100]. Following, the boson part is written as:

$$T_{\dots B, \sim}^{(L)} = e_{\dots}^B \hat{Q}_{\dots, \sim}^{\dagger}, \dots = f, v \dots \dots \dots (2-157)$$

A superscript B has been added to e_{\dots} in order to distinguish it from the fermion charges. The units of e_{\dots}^B are different from those of e_{\dots}^F since the radial integral is already included in Eq. (2-157). The boson effective charges e_{\dots}^B have the same units as the product:

$$e_{\dots}^B = e_{\dots}^F \langle n_{\dots}, l_{\dots} | r^2 | n'_{\dots}, l'_{\dots} \rangle, \dots = f, v \dots \dots \dots (2-158)$$

that is the units are eb .

For $M1$ transitions, the fermion part of the operator is written in the form [82]:

$$f_{j_{\dots} j'_{\dots}}^{(1)} = -\sqrt{\frac{3}{4f}} \langle l_{\dots}, \frac{1}{2}, j_{\dots} | g_{l, \dots}^F \vec{l} + g_{s, \dots}^F \vec{s} | l'_{\dots}, \frac{1}{2}, j'_{\dots} \rangle u_{l, l'} / \sqrt{3}, \dots = f, v \dots \dots (2-159)$$

The quantities $g_{l, f}^F, g_{l, v}^F, g_{s, f}^F$ and $g_{s, v}^F$ are the single-particle g -factors. The free values are $g_{l, f}^F = 1, g_{l, v}^F = 0, g_{s, f}^F = 5.58$ and $g_{s, v}^F = -3.82$ in units of nuclear magnetons, \sim_N . In actual calculations, the spin factors g_s are renormalized. Typical values in shell-model calculations are $g_s^{\text{renorm}} \approx 0.7 g_s^{\text{free}}$. Following, the boson part of the $M1$ operator is usually written as:

$$T_{\dots B, \sim}^{(M1)} = \sqrt{\frac{3}{4f}} g_{\dots}^B \hat{L}_{\dots, \sim}, \dots = f, v \dots \dots \dots (2-160)$$

where \hat{L}_{\dots} is the angular momentum operator of the \dots ($\dots = f$ or ϵ) bosons.

The boson g -factors have the same units as the fermion g -factors since no radial integrals are involved in $M1$ transitions.

3-Transfer operators

Transfer operators assume a particularly important role in the interacting boson-fermion model-2 (IBFM-2). This is because the transferred particle is either a proton or a neutron (or a pair of protons or neutrons) and it is thus natural to compute matrix elements of transfer

operators within a framework of a model that explicitly treats proton and neutron degrees of freedom. There are two types of one-nucleon transfer operators, those that change the boson number by one unit and those that do not. When expanded in terms of creation and annihilation operators, the transfer operators of the second kind can be written as [82]:

$$P_{+,m}^{(j)} = p_{j,m} a_{j,m}^\dagger + \sum_{j'} q_{j'}^{(j)} \left[[s^\dagger \times \tilde{d}]_{m}^{(2)} \times a_{j',m}^\dagger \right]_{m}^{(j)} + \sum_{j'} q_{j'}^{(j)} \left[[d^\dagger \times \tilde{s}]_{m}^{(2)} \times a_{j',m}^\dagger \right]_{m}^{(j)} \\ + \sum_{k,j'} q_{k,j'}^{(j)} \left[[d^\dagger \times \tilde{d}]_{m}^{(2)} \times a_{j',m}^\dagger \right]_{m}^{(j)} + \dots \dots \dots (2-161)$$

Those of the first kind can be written as

$$P'_{+,m}^{(j)} = p'_{j,m} [s^\dagger \times \tilde{a}]_{m}^{(j)} + \sum_{j'} q_{j'}^{(j)} [d^\dagger \times \tilde{a}]_{m}^{(j)} + \dots \dots \dots (2-162)$$

The subtraction operators, P_- , are obtained by taking Hermitian conjugate of Eqs. (2-161) and (2-162).

Two-neutron addition and subtraction operators are written terms of boson operators alone, at least if one considers only states with at most one unpaired particle.

4-Algebras: Boson and Fermion Algebras

The algebraic structure of the interacting boson-fermion model-2 (IBFM-2) is a combination of the algebraic structures discussed previously and those of section (2.2). There are now four parts corresponding to proton and neutron bosons and fermions. By combining these four pieces one can obtain a large number of possible couplings. Since these are simple extensions of the couplings described in section (2.2), only a few selected examples will be discussed here.

From the bilinear products of boson and fermion operators one can form now four algebras [82]:

$$g_f^B : B_{f,rs} = b_{f,r}^+ b_{f,s}, \\ g_v^B : B_{v,rs} = b_{v,r}^+ b_{v,s}, \\ g_f^F : B_{f,ik} = b_{f,i}^+ b_{f,k}, \\ g_v^F : B_{v,ik} = b_{v,i}^+ b_{v,k}. \dots \dots \dots (2-163)$$

The algebras in Eq. (2-163) are the unitary algebras discussed previously,

$$g_f^B = u_f^B(6), g_v^B = u_v^B(6),$$

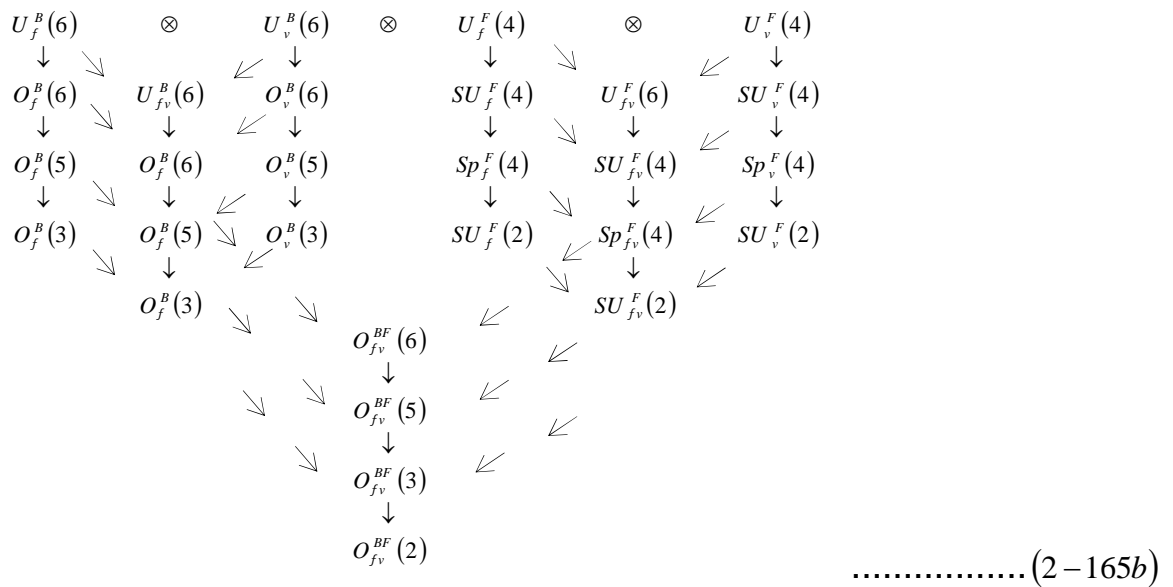
$$g_f^F = u_f^B(\Omega_f), g_v^F = u_v^B(\Omega_v), \dots\dots\dots(2-164)$$

where Ω_f and Ω_v are the dimensions of the fermionic spaces, i.e., $\Omega_f = \sum_{j_f} (2j_f + 1)$ and $\Omega_v = \sum_{j_v} (2j_v + 1)$. The algebraic structure of the model

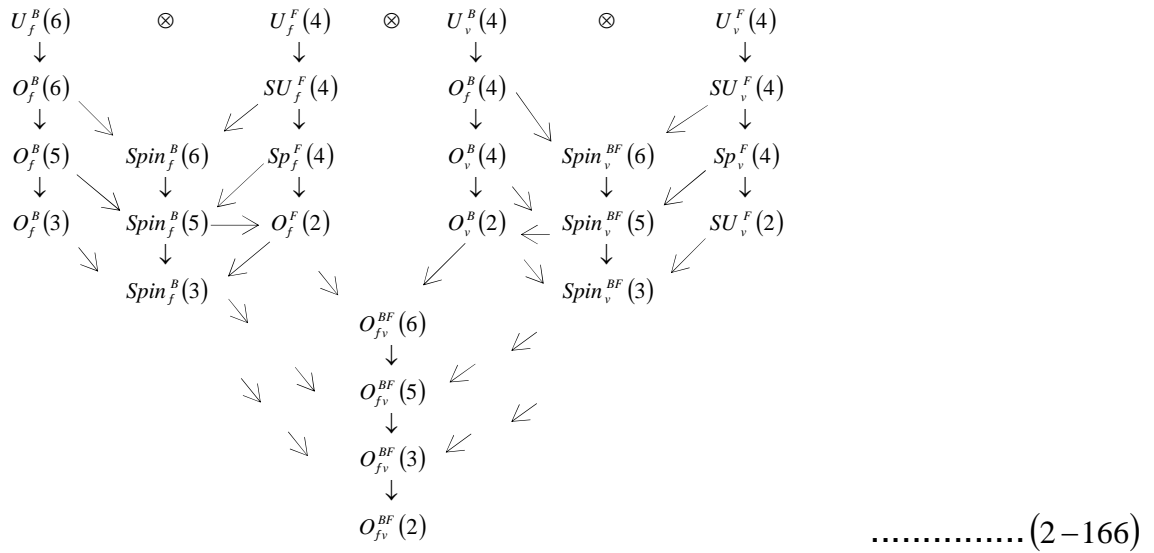
is thus that of the direct sum of all four algebras, or, using the notation appropriate for groups, the product:

$$G = U_f^B(6) \otimes U_v^B(6) \otimes U_f^F(\Omega_f) \otimes U_v^F(\Omega_v), \dots\dots\dots(2-165)$$

This product is reduced to the rotation group O(3). There are two main routes, which will now be illustrated with an example. The first route is that in which bosons are first coupled and so are fermions and subsequently the combinations of bosons and fermions are coupled. The second route is that in which protons first are coupled and so are neutrons and subsequently the combinations of protons and neutrons are coupled. To clarify this, consider the case in which $\Omega_f = \Omega_v = 4$. This case has been extensively investigated [102]. The first route corresponds to the lattice of algebras.



The second route correspond to the lattice of algebras



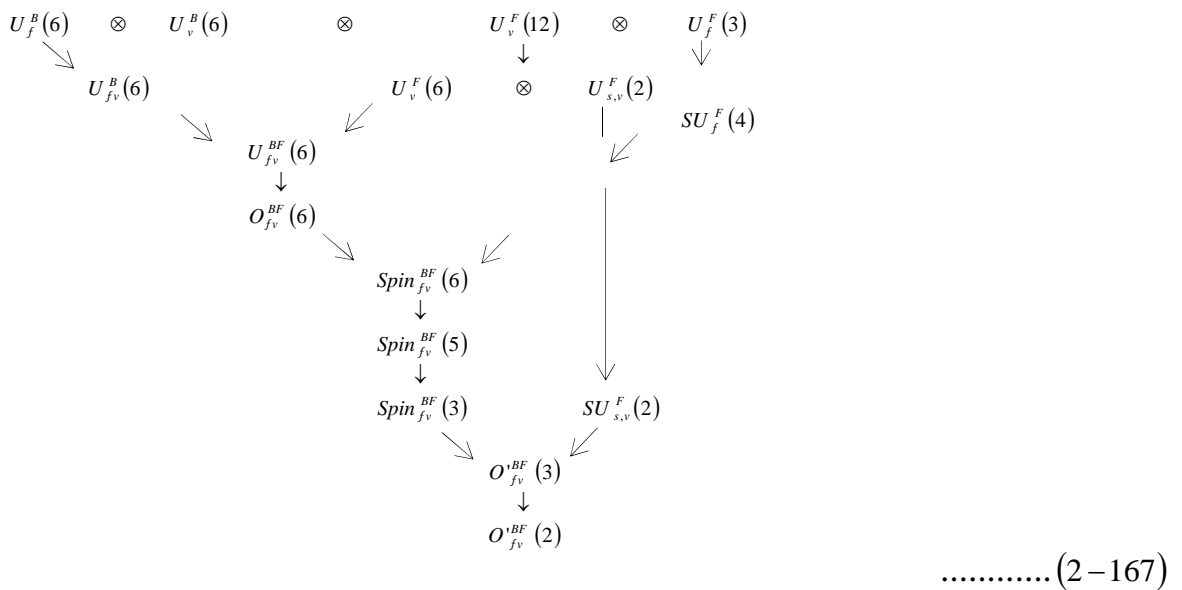
The complexity of the problem is clear from Eqs. (2-165) and (2-166).

2.3.2.3-Dynamic symmetries

The only dynamic symmetry that will be considered here in detail is one that has found useful applications in the description of odd-odd nuclei in the region of the Au isotopes. This symmetry corresponds to bosons described by $O(6)$, protons occupying a single-particle level with $j_f = 3/2, \Omega_f = 4$ and neutrons occupying single-particle levels with $j_v = 1/2, 3/2, 5/2, \Omega_v = 12$.

1-Lattice of algebras

The lattice of algebras considered [103] is intermediate between the two schemes discussed in section (2.3.2).



2-Energy Eigenvalues

The usual procedure of writing the Hamiltonian in terms of Casimir operators gives [82]:

$$\begin{aligned}
 H = & e_0 + e_1 C_1(U_f^B 6) + e_2 C_2(U_f^B 6) + e_3 C_1(U_v^B 6) + e_4 C_2(U_f^B 6) \\
 & + e_5 C_1(U_f^F 4) + e_6 C_2(U_f^F 4) + e_7 C_1(U_v^F 12) + e_8 C_2(U_f^F 12) \\
 & + a C_1(U_{fv}^B 6) + a' C_2(U_{fv}^B 6) + y C_2(U_{fv}^B 6) \\
 & + y' C_2(U_{fv}^{BF} 6) + y'' C_2(Spin_{fv}^{BF} 6) + s C_2(Spin_{fv}^{BF} 5) \\
 & + \chi C_2(Spin_{fv}^{BF} 3) + \chi' C_2(Spin_{s,v}^F 2) + \chi'' C_2(O_{fv}^{BF} 3) \quad \dots\dots\dots (2-168)
 \end{aligned}$$

$$\left. \begin{array}{l}
 U_f^B(6) \otimes U_v^B(6) \otimes U_f^F(4) \otimes U_v^F(12) \\
 \downarrow \qquad \qquad \downarrow \qquad \qquad \downarrow \qquad \qquad \downarrow \\
 [N_{Bf} = N_f] \quad [N_{Bv} = N_v] \quad [N_{Ff} = 1] \quad [N_{Fv} = 1] \\
 \Rightarrow U_{fv}^B(6) \otimes U_f^F(4) \otimes U_v^F(6) \otimes U_{s,v}^F(2) \\
 \downarrow \qquad \qquad \qquad \qquad \qquad \downarrow \\
 [N_1, N_2] \qquad \qquad \qquad [1] \\
 \Rightarrow U_{fv}^{BF}(6) \otimes U_f^F(4) \otimes U_{s,v}^F(2) \Rightarrow U_{fv}^{BF}(6) \otimes SU_f^F(4) \otimes U_{s,v}^F(2) \\
 \downarrow \qquad \qquad \qquad \qquad \qquad \qquad \qquad \downarrow \\
 [N'_1, N'_2, N'_3] \qquad \qquad \qquad (\dagger_1, \dagger_2, \dagger_3) \\
 \Rightarrow Spin_{fv}^{BF}(6) \otimes U_{s,v}^F(2) \Rightarrow Spin_{fv}^{BF}(5) \otimes U_{s,v}^F(2) \\
 \downarrow \qquad \qquad \qquad \qquad \qquad \qquad \qquad \downarrow \\
 (\dagger'_1, \dagger'_2, \dagger'_3) \qquad \qquad \qquad (\ddagger_1, \ddagger_2) \\
 \Rightarrow Spin_{fv}^{BF}(3) \otimes SU_{s,v}^F(2) \Rightarrow O_{fv}^{BF}(3) \Rightarrow O_{fv}^{BF}(2) \\
 \downarrow \qquad \qquad \qquad \downarrow \qquad \qquad \downarrow \qquad \qquad \downarrow \\
 v_\Delta, J \qquad \qquad S=1/2 \qquad \qquad L \qquad \qquad M_L
 \end{array} \right\} \dots\dots\dots (2-169)$$

Taking the expectation value of \mathbf{H} in the basis

one obtains energy eigenvalues appropriate to describe odd-odd nuclei [82]:

$$\begin{aligned}
 E(N_{Bf} = N_f, N_{Bv} = N_v, N_{Ff} = 1, N_{Fv} = 1, [N'_1, N'_2, N'_3]) \\
 (\dagger_1, \dagger_2, \dagger_3), (\dagger'_1, \dagger'_2, \dagger'_3), (\ddagger_1, \ddagger_2), v_\Delta, J, L, M_L) \\
 = e'_0 + a(N_1 + N_2) + a'[N_1(N_1 + 5) + N_2(N_2 + 3)] \\
 + y[N'_1(N'_1 + 5) + N'_2(N'_2 + 3) + N'_3(N'_3 + 1)] \\
 + 2y'[\dagger_1(\dagger_1 + 4) + \dagger_2(\dagger_2) + \dagger_3^2] \\
 + 2y''[\dagger'_1(\dagger'_1 + 4) + \dagger'_2(\dagger'_2) + \dagger_3'^2] \\
 + 2s[\ddagger_1(\ddagger_1 + 3) + \ddagger_2(\ddagger_{2+1})] + 2\chi J(J + 1) + 2\chi'' L(L + 1) \quad \dots\dots\dots (2-170)
 \end{aligned}$$

where the constant terms have been included in e'_0 . Similar formulas can be obtained in the cases where the $U_f^F(4) \otimes U_v^F(12)$ representations are $\{0\} \otimes \{0\}$

(even-even nuclei), $\{1\} \otimes \{0\}$ (odd-proton nuclei) and $\{0\} \otimes \{1\}$ (odd-neutron nuclei) for example ${}_{79}^{198}\text{Au}_{119} (N_{B_f} = 1, N_{B_v} = 3, N_{F_f} = 1, N_{F_v} = 1)$.

Examples of nuclei with $U_f^B(6) \otimes U_\epsilon^B(6) \otimes U_f^F(4) \otimes U_\epsilon^F(12)$ symmetry.

Experimental examples of odd-odd nuclei which can be described by the expression Eq. (2-170) have been found in the Au region. One of these nuclei, ${}_{79}^{198}\text{Au}_{119}$, Recently, this nucleus has been remeasured by [104]. However, due to the complexity of the odd-odd spectrum, it is difficult to establish a one-to-one correspondence between observed and calculated states. Thus, any assignment of quantum numbers to the observed levels in ${}_{79}^{198}\text{Au}_{119}$ can only be viewed as tentative as long as they are not confirmed by nucleon transfer or electromagnetic decay properties. Simple analytic expressions are available for the former [105] and will provide a test of proposed classifications of levels in nuclei in this mass region.

It is worthwhile commenting on the extreme difficulty, both experimental and theoretical, posed by odd-odd nuclei. From the experimental side, the high density of levels makes it very hard to assign spin and parity to individual states. A theoretical analysis of odd-odd nuclei, especially when many single-particle levels are included, is hardly feasible. Dynamic symmetries offer here a unique opportunity. Despite the apparent complexity of the procedure described in section, calculations are still feasible and straightforward. The only complication is in the bookkeeping aspect of the procedure, but this is greatly aided by the use of algebraic methods (group theory). It is in the treatment of these very complex cases that the full power of algebraic methods comes into play[82].

Examples of nuclei with $U_f^B(6) \otimes U_\epsilon^B(6) \otimes U_f^F(4) \otimes U_\epsilon^F(4)$ symmetry.

Although not discussed here in detail, we note that examples of dynamic Bose-Fermi symmetries based on the chain Eq.(2-169) have been found in the spectra of the odd-odd Cu isotopes, in particular of ${}_{29}^{62}\text{Cu}_{33}$.

The odd-even Cu isotopes were discussed in the examples of nuclei with Spin^{BF} (5) symmetry. The odd-odd isotopes provide further examples of Spin^{BF} (5) symmetry in the case in which the odd proton occupies an orbit with $j_f = 3/2$ and the odd neutron one with $j_v = 3/2$.

2.3.2.4-Superalgebras.

Superalgebras can also be used within the context of the interacting boson-fermion model-2 (IBFM-2) [82]. The only difference is that the proton and neutron indices now appear everywhere and that the number of routes possible in the reduction of the superalgebra to the rotation algebra increases considerably. Superalgebras based on the IBFM-2 are particularly useful in the description of odd-odd nuclei, since by fixing the parameters of the Hamiltonian and other operators from a study of even-even and odd-even nuclei, one is able to predict the structure of odd-odd nuclei. These predictions can be compared to the experimental data (when they exist) or used as a guideline for future experiments. In this section, only a few selected cases will be presented.

1- Supersymmetric chains.

Supersymmetric chains can be obtained by embedding the algebras of section (2.3) into superalgebras. There are again two main routes that will be illustrated with an example. Consider the case in which both protons and neutrons occupy a level with $j_f = j_v = 3/2$. The corresponding algebraic structure has been discussed in section (2.3) and can be embedded into the superalgebra [82]:

$$G^* = U_f(6|4) \otimes U_v(6|4) \dots\dots\dots(2-171)$$

When considering the subalgebras of Eq. (2-171), one can either first combines the two subalgebras into their sum:

$$U_f(6|4) \otimes U_v(6|4) \supset U(6|4) \supset U^B(6) \otimes U^F(4) \dots\dots\dots(2-172)$$

where the algebra $U(6|4)$ is obtained by adding the generators of $U_f(6|4)$ to the corresponding generators of $U_v(6|4)$, or one can go

directly from the proton and neutron superalgebras to their maximal Lie subalgebras [82]:

$$U_f(6|4) \otimes U_v(6|4) \supset U_f^B(6) \otimes U_v^B(6) \otimes U_f^F(4) \otimes U_v^F(4) \supset U^B(6) \otimes U^F(4) \quad \dots\dots (2-173)$$

The first alternative only exists if the proton and neutron spaces are identical, $\Omega_f = \Omega_v$. If the first alternative is possible, one can introduce formalism similar to F -spin, but now applied to superalgebras. Proton bosons and fermions can be assigned to a supermultiplet with $F = 1/2$ and F -spin projection $F_z = +1/2$. Similarly, neutron bosons and fermions have $F = 1/2$ and $F_z = -1/2$, i.e.

$$\begin{aligned} |f\rangle &= \left| \frac{1}{2}, +\frac{1}{2} \right\rangle \\ |v\rangle &= \left| \frac{1}{2}, -\frac{1}{2} \right\rangle \quad \dots\dots\dots (2-174) \end{aligned}$$

The supersymmetric multiplets now contain:

$$|f\rangle = \begin{pmatrix} b_{f,r}^\dagger \\ b_{f,i}^\dagger \end{pmatrix}; |v\rangle = \begin{pmatrix} b_{v,r}^\dagger \\ b_{v,i}^\dagger \end{pmatrix}; (r = 1, \dots, 6; i = 1, \dots, 4) \quad \dots\dots\dots (2-175)$$

The F -spin basis can be obtained by constructing the Kronecker products of two $U(6|4)$ representations. The rules for this product, when expressed in terms of Young supertableaux, are identical to those of normal Lie algebras. For example, [82]:

$$\otimes \otimes \otimes \otimes \otimes \quad \dots\dots\dots (2-176)$$

or

$$[1] \otimes [1] = [2] \oplus [1,1] \quad \dots\dots\dots (2-177)$$

One obtains in this case Young supertableaux which are not totally supersymmetric.

2- Dynamic supersymmetries

In heavy nuclei, the situation described in the previous section (the F -spin scheme) seldom occurs. One must therefore use the second possible reduction Eq.(2-172). Some examples of this kind have been found. One such example corresponds to the embedding of the chains discussed in sect. (2.3) into [82]:

$$\left| \begin{array}{cccccc} U_f(6|4) \otimes U_v(6|12) \supset U_f^B(6) \otimes U_v^B(6) \otimes U_f^B(6) \otimes U_v^B(6) \\ \downarrow \qquad \qquad \downarrow \qquad \qquad \downarrow \qquad \qquad \downarrow \qquad \qquad \downarrow \qquad \qquad \downarrow \\ \{N_f\} \qquad \qquad \{N_f\} \qquad \qquad [N_{Bf}] \qquad \qquad [N_{Bv}] \qquad \qquad \{N_{Ff}\} \qquad \qquad N_{Fv} \end{array} \right\rangle \dots\dots(2-178)$$

Use of supersymmetry now allows the construction of supermultiplets obtained by combining the proton supermultiplets with the neutron supermultiplets. The important portion of the supermultiplet that can be accessed easily is that formed by an even-even nucleus, the adjoining odd-even and even-odd nuclei and the neighboring odd-odd nucleus, i.e. the nuclei with 82]:

$$\begin{array}{cccc} N_{Bf} = N_f, & N_{Ff} = 0, & N_{Bv} = N_v, & N_{Fv} = 0, \\ N_{Bf} = N_f - 1, & N_{Ff} = 1, & N_{Bv} = N_v, & N_{Fv} = 0, \\ N_{Bf} = N_f, & N_{Ff} = 0, & N_{Bv} = N_v - 1, & N_{Fv} = 1, \\ N_{Bf} = N_f - 1, & N_{Ff} = 1, & N_{Bv} = N_v - 1, & N_{Fv} = 1. \end{array} \dots\dots(2-179)$$

All these nuclei belong to the supermultiplet $[N_f] \otimes [N_v]$. The set of four nuclei Eq.(2-179) has been termed a magic square. An example of such a magic square is shown in Figure (2.3). If a dynamic supersymmetry is present, all nuclei in the square should be described with the same Hamiltonian. For the nuclei shown in Figure (2.3) the appropriate Hamiltonian is given by Eq. (2-170). One must insert in this formula the appropriate eigenvalues of the Casimir operators corresponding to the four cases in Eq.(2-179). The odd-odd formula is given by Eq. (2-171). The even-even and even-odd formulas are obtained in the manner discussed in sections (2-1) and (2-2). A comparison of the spectra obtained in this way with those experimentally measured is shown in Figure (2.3).

$^{197}_{79}Au_{118}$	$^{198}_{79}Au_{119}$
$^{196}_{78}Au_{118}$	$^{197}_{78}Au_{119}$

Figure (2.3) An example of a magic square in the Pt-Au

Another example of a dynamic supersymmetry including even-even, even-odd, odd-even and odd-odd nuclei has been presented by Hübsch and Paar (1987) [102] in the region of the Cu isotopes.

A further generalization of these studies can be achieved by embedding the direct product of proton and neutron superalgebras into a single, larger superalgebra [82]. This, in general, can be written as Jolie *et al.*, [106]:

$$\left| \begin{array}{ccc} U(12 | \Omega_f + \Omega_v) & \supset & U_f(6 | \Omega_f) \otimes U_v(6 | \Omega_v) \\ \downarrow & & \downarrow \quad \downarrow \\ \{N\} & & \{N_f\} \quad \{N_v\} \end{array} \right\rangle \dots\dots\dots(2-180)$$

with $N_f + N_v = N$. The single representation $[N]$ of $U(12 | \Omega_f + \Omega_v)$ now not only contains all even-even nuclei with $N_{Bf} + N_{Bv} = N$ but also all associated even-odd, odd-even and odd-odd nuclei, as specified in Eq. (2-179). It is clear that, due to the large number of nuclei contained in one multiplied, such schemes have only a very limited applicability.

2.3.2.5-Numerical studies

The degree of complexity when going from even-even to even-odd nuclei increases by at least one order of magnitude. It increases further by another order of magnitude when going from odd-even to odd-odd nuclei. Although the dynamic symmetries discussed in the section (2-2) may give some insight into the structure of specific examples of nuclei, they cannot be used in all cases and one must resort to more realistic, numerical calculations. Many odd-even nuclei have been studied in this way with the interacting boson-fermion model-2 (IBFM-2), using a computer code written by Bijker (1983) [107] and an example will be discussed in next section. Odd-odd nuclei, being more complex, have been studied less accordingly, but nevertheless a few calculations are available. Finally, we

also discuss in this chapter an example of a broken-pair calculations for even-even nuclei.

1- Even-Odd nuclei.

In view of the large number of parameters appearing in the operators of section (2-2), a semi microscopic input is introduced [108]. Here this input is more appropriate, since the (IBM-2) is directly related to the underlying shell model. Coefficients in the operators of sections (2.2) and (2.3) are written in terms of the occupation probabilities obtained through a BCS calculation [86]. This calculation is done separately for protons and neutrons and provides the single-particle energies in the presence of several valence particles (quasi-particle energies, v_{j_f} and v_{j_v}), in terms of the Fermi energies ϵ_f and ϵ_v , the pairing gaps Δ_f and Δ_v and the single-particle energies in the absence of other valence particles, E_{j_f} and E_{j_v} ,

$$v_{j_{\dots}} = \sqrt{(E_{j_{\dots}} - \epsilon_{\dots})^2 + \Delta_{\dots}^2}, \quad \dots = f, v \quad \dots \dots \dots (2-181)$$

The occupation probabilities are then given by

$$v_{j_{\dots}} = \left[\frac{1}{2} \left(1 - \frac{E_{j_{\dots}} - \epsilon_{\dots}}{v_{j_{\dots}}} \right) \right]^{\frac{1}{2}},$$

$$u_{j_{\dots}} = \left(1 - v_{j_{\dots}}^2 \right)^{\frac{1}{2}}, \quad \dots = f, v \quad \dots \dots \dots (2-182)$$

The pairing gaps are usually taken as $\Delta = 12A^{-\frac{1}{2}}$ MeV [72]. The Fermi energies are obtained by solving Eqs. (2-181) and (2-182) with the condition that the number of nucleons be:

$$n_{j_{\dots}} = \sum_{j_{\dots}} v_{j_{\dots}}^2 (2j_{\dots} + 1), \quad \dots = f, v \quad \dots \dots \dots (2-183)$$

For the calculation of energies and wave functions one needs the parameters of the boson-fermion interaction. On the basis of BCS theory one can write them in the form:

$$\Gamma_{j_{\dots}j'_{\dots}} = (u_{j_{\dots}}u_{j'_{\dots}} - v_{j_{\dots}}v_{j'_{\dots}}) Q_{j_{\dots}j'_{\dots}} \Gamma_{\dots},$$

$$Q_{j_{\dots}j'_{\dots}} = \left\langle l_{\dots}, \frac{1}{2}, j_{\dots} \parallel Y^2 \parallel l'_{\dots}, \frac{1}{2}, j'_{\dots} \right\rangle, \quad \dots = f, v \quad \dots \dots \dots (2-184)$$

and

$$\Lambda_{j_{\dots}j'_{\dots}}^{j''_{\dots}} = -S_{j_{\dots}j'_{\dots}} S_{j''_{\dots}j_{\dots}} \left(\frac{10}{N_{\dots} (2j_{\dots} + 1)} \right)^{\frac{1}{2}} \Lambda_{\dots},$$

$$S_{j_{\dots}j'_{\dots}} = (u_{j_{\dots}}v_{j'_{\dots}} + v_{j_{\dots}}u_{j'_{\dots}}) Q_{j_{\dots}j'_{\dots}}, \quad \dots = f, v, \dots \dots \dots (2-185)$$

All energies in odd-even nuclei are then calculated in terms of three coefficients, A_{\dots} , Γ_{\dots} and Λ_{\dots} . The BCS theory also provides a simple parameterization of the coefficients appearing in the one-nucleon transfer operators (2-184) and (2-185):

$$p_{jp} = u_{jp} \frac{1}{K'_{jp}}, \quad q_{j_{\dots}}^{(j_{\dots})} = -\epsilon_{j_{\dots}} S_{j_{\dots}j_{\dots}} \left(\frac{10}{N_{\dots} (2j_{\dots} + 1)} \right)^{1/2} \frac{1}{K_{\dots} K'_{j_{\dots}}}$$

$$p'_{j_{\dots}} = \frac{v_{j_{\dots}}}{\sqrt{N_{\dots}}} \frac{1}{K''_{j_{\dots}}}, \quad q_{j_{\dots}}^{''(j_{\dots})} = u_{j_{\dots}} S_{j_{\dots}j_{\dots}} \left(\frac{10}{(2j_{\dots} + 1)} \right)^{1/2} \frac{1}{K_{\dots} K'_{j_{\dots}}} \quad \dots \dots \dots (2-186)$$

where K_{\dots} , $K'_{j_{\dots}}$ and $K''_{j_{\dots}}$ are obtained from the three conditions:

$$K_{\dots} = \left(\sum_{j_{\dots}j'_{\dots}} S_{j_{\dots}j'_{\dots}}^2 \right)^{\frac{1}{2}}, \quad \dots = f, v \quad \dots \dots \dots (2-187)$$

and

$$\sum_{rJ} \langle odd; rJ \parallel P_+^{(j_{\dots})} \parallel even; 0_1^+ \rangle^2 = (2j_{\dots} + 1) u_{j_{\dots}}^2$$

$$\sum_{rJ} \langle even; 0_1^+ \parallel P_+^{(j_{\dots})} \parallel odd; rJ \rangle^2 = (2j_{\dots} + 1) v_{j_{\dots}}^2, \quad \dots = f, v \quad \dots \dots \dots (2-188)$$

The formulas (2-184) -(2-188) are valid when the odd nucleon is a particle. Corresponding formulas for a hole are obtained by interchanging $u_{j_{\dots}}$ and $v_{j_{\dots}}$. From this parameterization one can obtain that of other operators, since these can be built from one-nucleon operators.

2-Energies

The calculation that will be described here concerns the even-odd isotopes of Hf ($Z=72$) and W ($Z=74$). The single-particle levels included in the calculation and their energies are given in chapter four. In addition, one needs the parameters appearing in the boson part of the Hamiltonian, H_B . These are determined by the energies of nuclei with no unpaired nucleons (even-even nuclei).

In the case discussed here these parameters are taken from the calculation of the even Hf and W isotopes, which are discussed in chapter three. The appropriate parameters are shown in Table (4-1). The only new parameters needed for the calculation of even-odd nuclei, are the strengths of the monopole, quadrupole and exchange interactions, A_{\dots} , Γ_{\dots} and Λ_{\dots} . The calculation separates into two parts, one related to the negative-parity states and another part related to the positive-parity states. The resulting energies are shown in Figs. (4-1) to (4-5) for Hf isotopes and Figs (4-6) to (4-10) for W isotopes.

It is of interest to contrast spectra of even-proton nuclei with those of odd-neutron nuclei with the same mass number. One observes major differences. These differences arise from the fact that the boson-fermion coupling depends on the occupation probabilities which are different for protons and neutrons.

3-Electromagnetic transitions and moments; E2

Matrix elements of electromagnetic transition operators are calculated using the wave functions obtained from the numerical diagonalization of H and the operators discussed in section (2.2). E2 transitions and moments are given in terms of the boson effective charges, e_f^B and e_v^B . The fermion part of the operator requires the fermion effective charges and radial integrals.

The radial integrals are estimated to be $\langle n_{\dots}, l_{\dots} | r^2 | n_{\dots}, l_{\dots} \rangle = 0.0033b$ for the $1h_{11/2}$ level and $\langle n_{\dots}, l_{\dots} | r^2 | n_{\dots}, l_{\dots} \rangle = 0.0027b$ for the positive-parity levels. The fermion effective charges are taken as $e_f^F = 1.5e$ and $e_v^F = 0.5e$.

Without any further parameters, one can then compute all E2 transitions and moments. A portion of these results is shown in chapter 4. The experimental information on electromagnetic transitions and moments in even-odd nuclei in this mass region is rather meager. E2 transitions in odd-even nuclei are still dominated by the collective boson part. The fermion part contributes only 5-10% to the matrix elements. A study of the latter must thus wait more accurate and systematic measurements of E2 transitions.

In contrast to E2 properties, M1 transitions and moments in odd-even nuclei are dominated by the fermion part of the M1 operator. Using the operator of section (2.2), one can compute the corresponding transitions. The boson part of the operator requires a specification of g_f^B and g_v^B . These can be taken from the calculations reported in chapter three for even-even nuclei by Sambataro *et al.*, [109]. The fermion part of the operator requires a specification of the fermion g -factors. The orbital j -factors are $g_{f,l}^F = 1 \sim_N$ and $g_{f,l}^F = 0$. The spin g -factors are taken as the free values quenched by a factor of 0.7, i.e. $g_{S,f}^F = 0.7 \times 5.58 \sim_N$ and $g_{s,f}^F = 0.7 \times 3.82 \sim_N$. Also here the experimental information is rather scarce. For those cases for which experimental data exist, the results of calculations of M1 transitions agree in general less well with the data as compared to the corresponding calculations of E2 transitions. This indicates that while the collective degrees of freedom appear to be well described in even-odd nuclei, the single-particle degrees of freedom still require improvement.

CHAPTER THREE
INTERACTION
BOSON MODEL
RESULTS AND
DISCUSSION

CHAPTER THREE

INTERACTION BOSON MODEL RESULTS AND DISSCUSION

3.1- ¹⁷²⁻¹⁸⁰Hf Isotopes in IBM-1

We investigate the dynamical symmetry of ¹⁷²⁻¹⁸⁰Hf isotopes and energy spectra and the electromagnetic transition probabilities B(E2), B(M1) and mixing ratio u (E2/M1) of these isotopes ($Z = 72$) within the framework of IBM-1.

3.1.1 Hamiltonian Interaction Parameters

According to the Hamiltonian of IBM-1, the energy of ¹⁷²⁻¹⁷⁴Hf isotopes (total numbers of bosons 14 and 15 respectively) lies in the transitional region $SU(3) \rightarrow O(6)$ (Eq.(2-40a)) and the ¹⁷⁶⁻¹⁸⁰Hf isotopes (total number of bosons 16,15 and 14 respectively), lies in the dynamical symmetry $SU(3)$, Eq.(2-22a) have been calculated using the angular momentum, quadrupole and octoupole parameters (a_1 , a_2 t and a_3). The best fit values of these parameters are given in Table (3-1), which show the values of the relevant parameters. These values are obtained by fitting to get results of the energy levels than that the experimental data [110], whereas the first two terms and the last term in Eq.(2-3a)) have now included because they are irrelevant to the case of the fully weakly deformed nuclei (rotational nuclei).

3.1.2 Energy spectra

IBM-1 model has been used in calculating the energy of the positive parity low-lying levels of Hafnium series of isotopes. A comparison between the experimental spectra [110] and our calculations, using the values of the model parameters given in Table (3-1) for the ground beta and gamma bands, is illustrated in Figures (3.1) to (3.5). The agreement between the theoretical and their correspondence experimental values for all the isotopes are in a good agreement but for high spin states are slightly higher but reasonable.

Table (3-1): IBM-1 Hamiltonian parameters for $^{172-180}\text{Hf}$ isotopes.

Isotopes	a_1	a_2	a_3	t
^{172}Hf	0.040	-0.0110	-0.0700	-0.080
^{174}Hf	0.0450	-0.0105	-0.0640	-0.060
^{176}Hf	0.0095	-0.1130	0.000	-0.600
^{178}Hf	0.0960	-0.0146	0.000	-0.110
^{180}Hf	0.0101	-0.0140	0.000	-0.260

Table (3-2) gives the experimental and theoretical energy ratios. It has been found that the $^{172-174}\text{Hf}$ isotopes are in the transitional region $\text{SU}(3) \rightarrow \text{O}(6)$, and the $^{176-178}\text{Hf}$ are deformed isotopes (rotational nuclei) and they have the $\text{SU}(3)$ dynamical symmetry respecting to IBM-1.

The obtained results are given in Figures (3-1) to (3-5), These figures show the ground, s and x –bands of experimental and IBM-1 calculation for $^{172-180}\text{Hf}$ isotopes. They show that there in a good agreement between experimental energy levels and IBM-1 calculations.

Table (3-2): Experimental and theoretical values of energy ratios in $^{172-180}\text{Hf}$ isotopes.

Isotopes	$E(4_1^+ / 2_1^+)$			$E(6_1^+ / 2_1^+)$			$E(8_1^+ / 2_1^+)$		
	Exp.	IBM-1	IBM-2	Exp.	IBM-1	IBM-2	Exp.	IBM-1	IBM-2
^{172}Hf	3.245	3.229	3.249	6.596	6.414	6.614	10.892	10.304	10.536
^{174}Hf	3.3	3.3	3.267	6.67	6.66	6.88	11.21	11.30	11.023
^{176}Hf	3.29	3.29	3.481	6.77	6.72	7.094	11.33	11.41	11.932
^{178}Hf	3.3	3.3	3.290	7	7.2	6.784	11.67	11.8	10.774
^{180}Hf	3.3	3.3	3.3011	6.88	6.82	6.881	11.645	11.7	10.739
SU (5)	2			3			4		
O (6)	2.5			4.5			7		
SU (3)	3.33			7			12		

Experimental data are taken from ref. [110].

The root means square deviation (*rmsd*) [111]:

$$rmsd = \left[\frac{1}{N} \sum (E_{cal.} - E_{exp.})^2 \right]^{1/2} \dots\dots\dots (3-1)$$

(where N is the number of energy levels) is used to compare the experimental and theoretical energy levels. Tale (3-3) gives the *rmsd* between experimental and theoretical energy levels. In this table, we see the ground state levels. The best agreement was found in ^{172}Hf isotope where the smallest value of *rmsd* is equal 0.0039 and equal 0.010 for

gamma band in ^{178}Hf isotope. However, *rmsd* equals 0.0099 for beta band in ^{180}Hf isotope.

Table (3-3): The root means square deviations (*rmsd*) between experimental and calculated energy levels for $^{172-180}\text{Hf}$ isotopes.

Isotopes	root mean square deviations (<i>rmsd</i>)					
	ground state band		s – band		x – band	
	IBM-1	IBM-2	IBM-1	IBM-2	IBM-1	IBM-2
^{172}Hf	0.0039	0.0031	0.059	0.042	0.014	0.018
^{174}Hf	0.0046	0.0029	0.061	0.040	0.013	0.0131
^{176}Hf	0.0360	0.0030	0.054	0.041	0.012	0.001
^{178}Hf	0.0340	0.0025	0.044	0.0038	0.010	0.09
^{180}Hf	0.0140	0.016	0.0099	0.022	0.019	0.012

In general, the experimental and the IBM-1 calculated energy levels in $^{174-180}\text{Hf}$ isotopes increase with angular momentum as $J(J+1)$ because these isotopes are of rotational nuclei (deformed nuclei) [26].

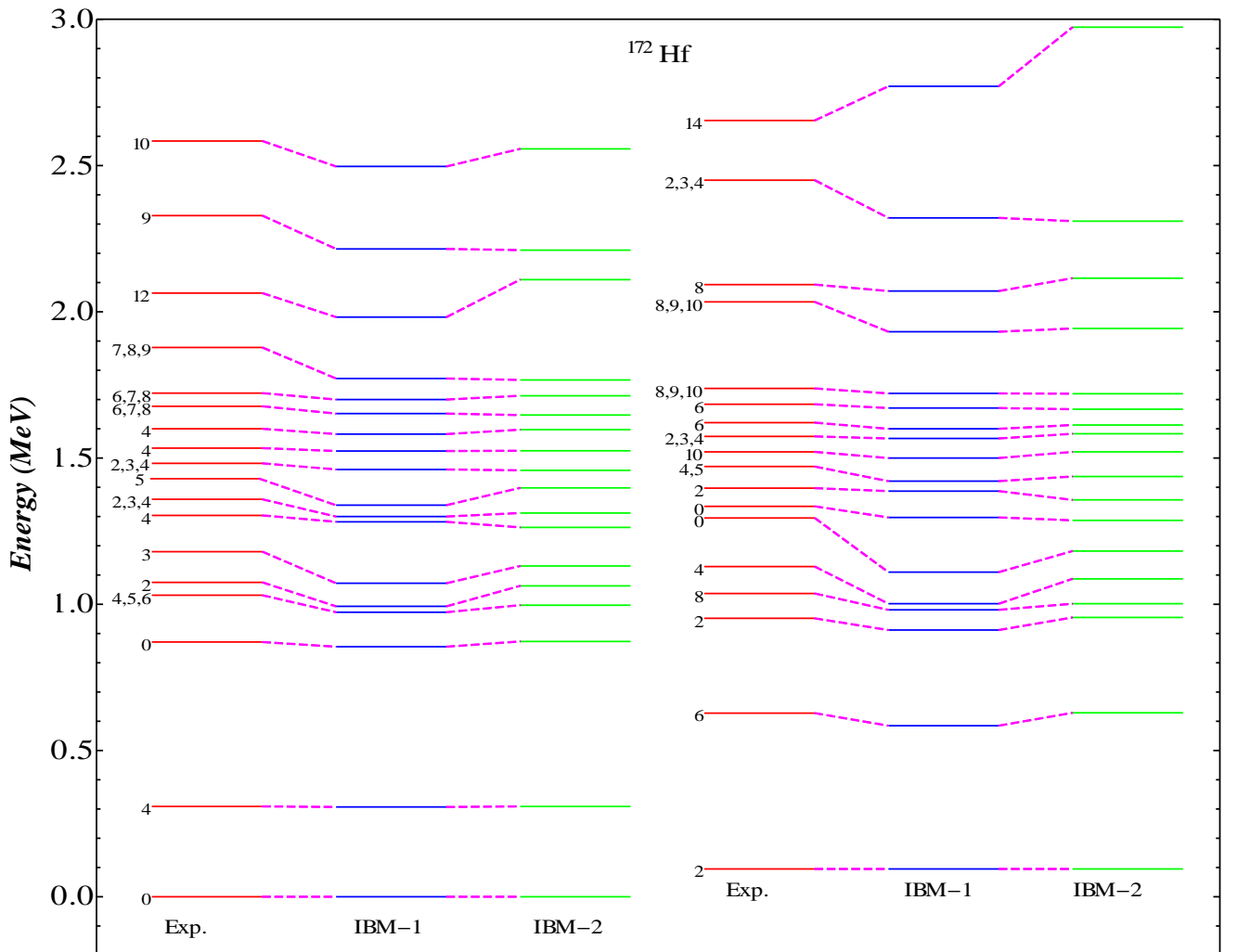


Fig. (3.1): Comparison between experimental data [110], IBM-1 and IBM-2 calculated energy levels for ^{172}Hf .

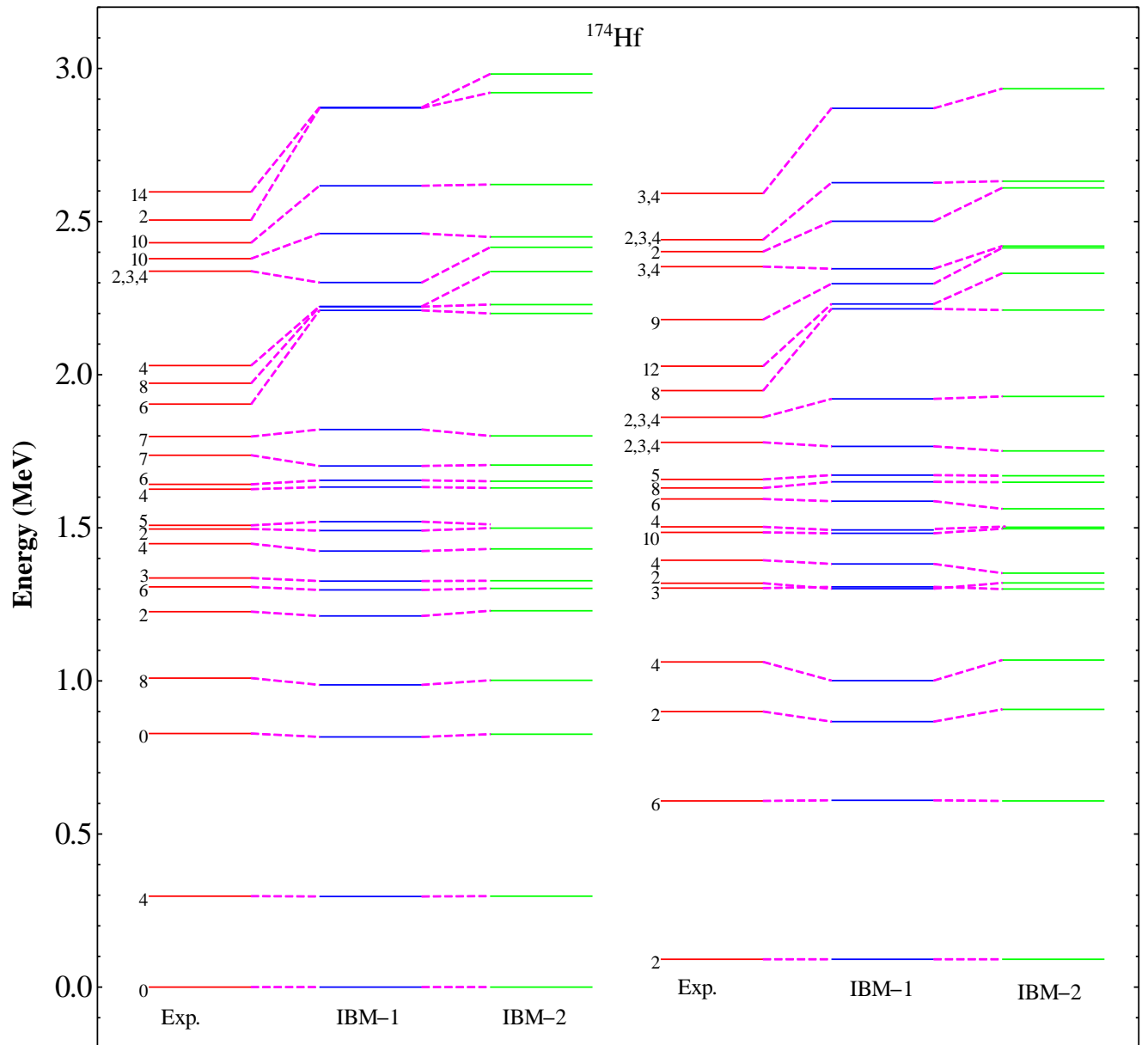


Figure (3.2): Comparison between experimental data [110], IBM-1 and IBM-2 calculated energy levels for ^{174}Hf .

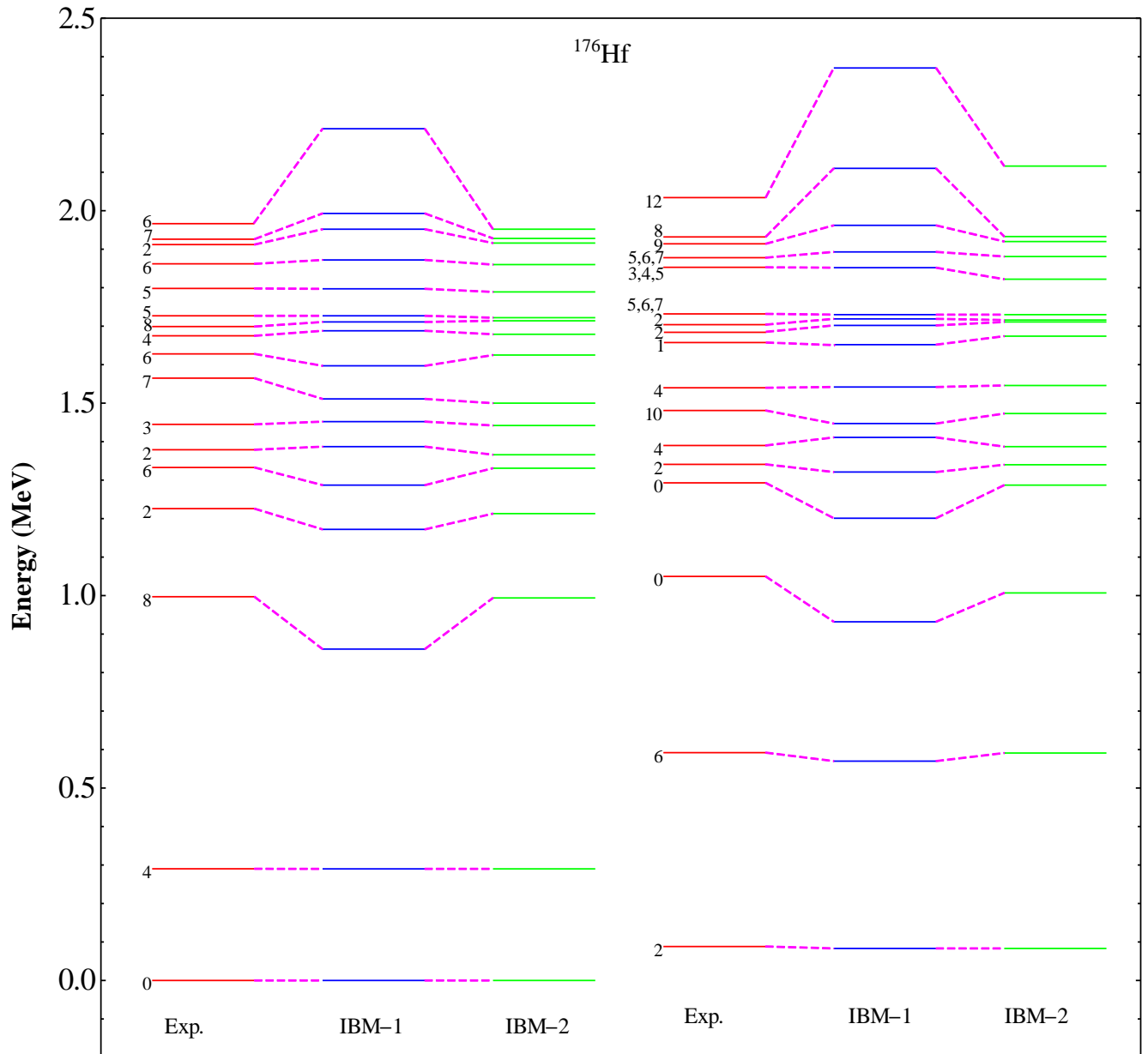


Figure (3.3): Comparison between experimental data [110], IBM-1 and IBM-2 calculated energy levels for ^{176}Hf .

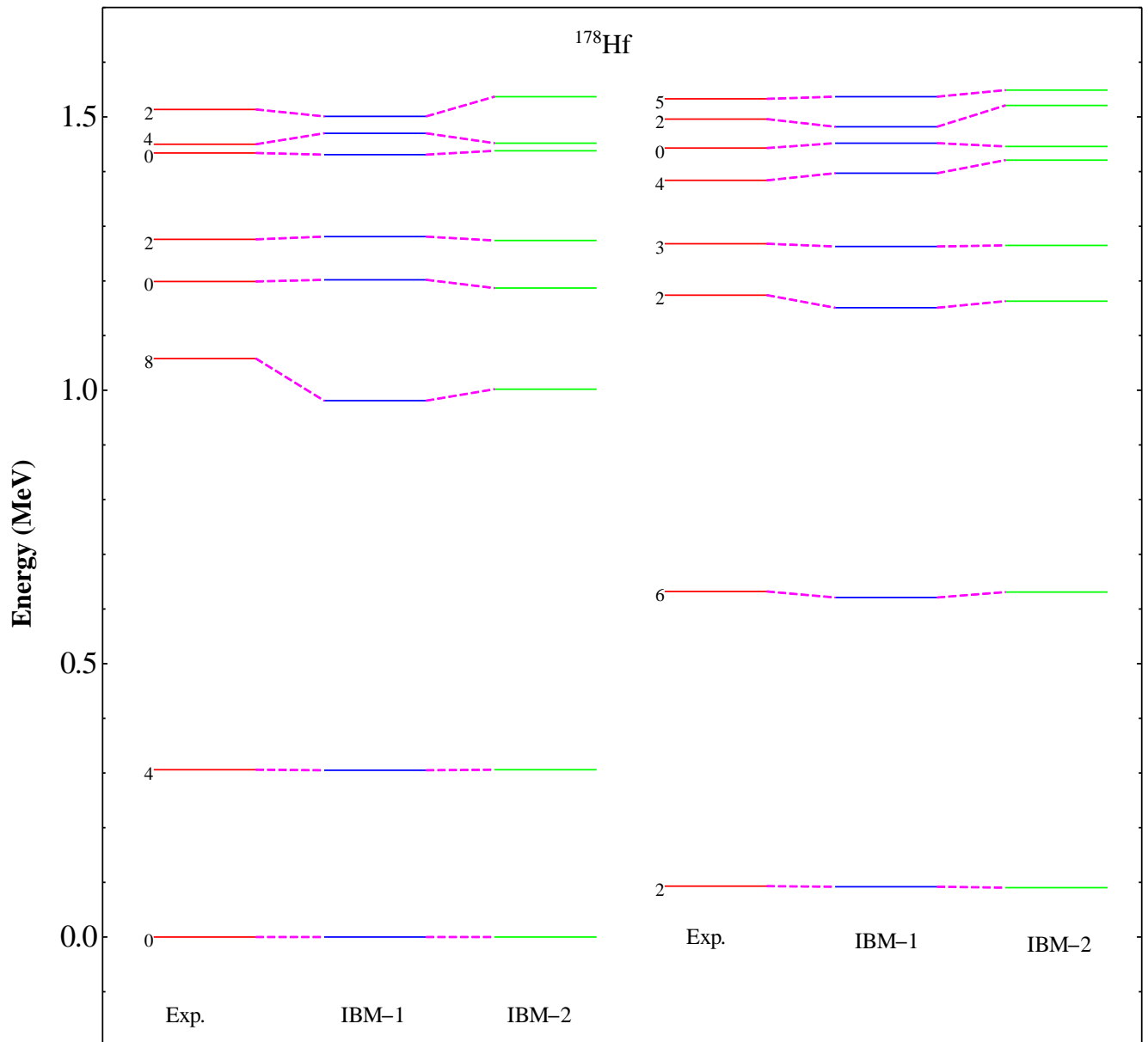


Figure (3.4): Comparison between experimental data [110], IBM-1 and IBM-2 calculated energy levels for ^{178}Hf .

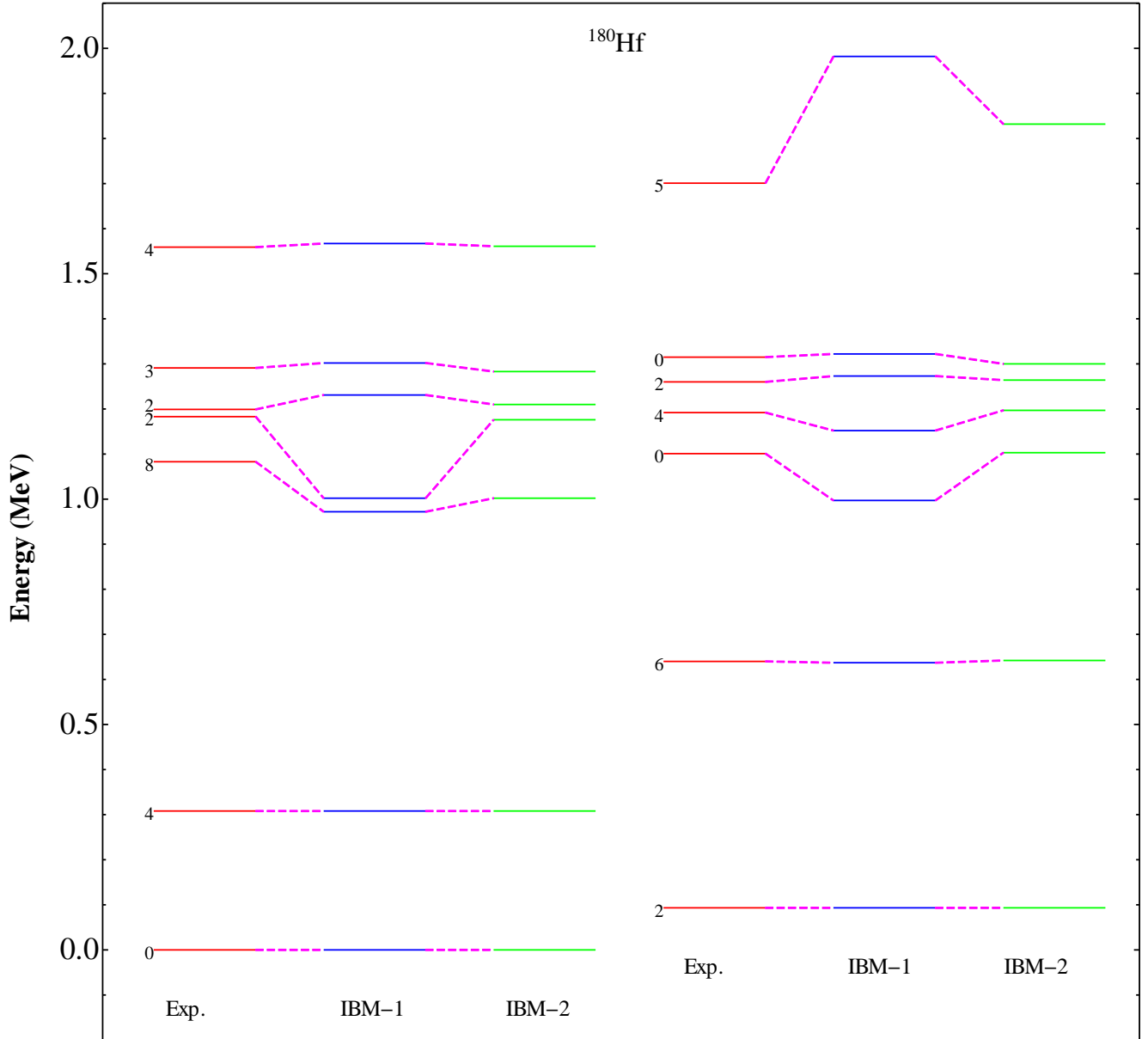


Figure (3.3): Comparison between experimental data [110], IBM-1 and IBM-2 calculated energy levels for ^{180}Hf .

3.1.3 Electric Transition Probability $B(E2)$

The E2 transitions provide a more stringent test of the IBM-1. The general E2 transition operator is given by the Eq. (2-6). The coefficient r_2 called the boson effective charge is an overall scaling factor for all $B(E2)$ values which is determined from the fit to the $B(E2; 2_1^+ \rightarrow 0_1^+)$ value. The coefficient s_2 may be determined from the quadrupole moment $Q(2_1^+)$. The ratio $s_2/r_2 = -1.32$ in the SU(3) limit and is reduced to zero in the O(6) limit. In the “FBEM” program the corresponding parameters are

$r_2 = (E2SD)$ and $s_2 = (1/\sqrt{5})(E2DD)$. The used parameters in T(E2) matrix element of $^{172-180}\text{Hf}$ isotopes are given in Table (3-4).

Table (3-4): The reduced matrix element parameters for $^{172-180}\text{Hf}$ isotopes.

Isotopes	$B(E2; 2_1^+ \rightarrow 0_1^+) (e^2.b^2)$	$r_2(e.b)$	$s_2(e.b)$
^{172}Hf	0.920	0.046	-0.220
^{174}Hf	1.0615	0.042	-0.330
^{176}Hf	1.040	0.125	-0.540
^{178}Hf	0.970	0.127	-0.033
^{180}Hf	0.950	0.139	-0.031

As we noticed in IBM-1 results the B(E2) for $s \rightarrow g$ and $x \rightarrow g$ transitions can vanish when these nuclei are treated as SU (3) symmetric nuclei. This problem was solved by breaking this symmetry in the direction of U (5) and employing the ν parameter. The calculated B(E2) values were improved by this attempt.

Table (3-5) shows that the electric transition probability for $s \rightarrow g$ and $x \rightarrow g$ are smaller than the electric transition probabilities between $g \rightarrow g$ band. This table also shows also that, in general, there is a good agreement between the experimental and theoretical B(E2) values in the ground state band in $^{174-180}\text{Hf}$ isotopes except the transition $6_1^+ \rightarrow 4_1^+$ in $^{174-180}\text{Hf}$, where the experimental and IBM-1 results of this transitions are weak in agreement. The experimental and IBM-1 B(E2) calculations between beta and ground band and between gamma band in general are weak in agreement except the transition $2_2^+ \rightarrow 0_1^+$ in ^{176}Hf isotope and $2_3^+ \rightarrow 0_1^+$ in ^{178}Hf isotope which gave a good agreement.

The weak agreement between experimental and theoretical in some B(E2) values in those isotopes can be explained by the fact that many small component of the initial and final wave functions contribute coherently to the value of the reduced E2 transition probability, since these small components are not stable enough against small changes in the model parameters [114]. There are no available experimental data to many transitions in Table (3-5); therefore, it has been predicted by IBM-1.

Table (3-5): Electric Transition Probability $B(E2; J_i \rightarrow J_f)$ for $^{172-180}\text{Hf}$ in $e^2 \cdot b^2$ units.

$J_i \rightarrow J_f$	^{172}Hf			^{174}Hf			^{176}Hf			^{178}Hf			^{180}Hf		
	Exp.	IBM-1	IBM-2	Exp.	IBM-1	IBM-2	Exp.	IBM-1	IBM-2	Exp.	IBM-1	IBM-2	Exp.	IBM-1	IBM-2
$2_1 \rightarrow 0_1$	0.92	0.982	0.871	1.0615	1.081	1.0592	1.04	1.087	1.0531	0.97	0.953	0.972	0.95	0.93	0.942
$4_1 \rightarrow 2_1$	-	0.0371	0.0831	-	1.426	1.428	-	1.427	1.439	-	1.42	1.426	1.38	1.02	1.43
$2_2 \rightarrow 0_1$	-	7×10^{-4}	0.00228	0.012	0.016	0.015	0.00057	0.0007	0.00033	0.0043	0.0052	0.0047	0.114	0.097	0.1071
$2_3 \rightarrow 0_1$	-	3×10^{-4}	0.0036	0.027	0.029	0.031	0.023	0.072	0.042	0.023	0.033	0.029	0.023	0.031	0.028
$2_3 \rightarrow 2_1$	-	0.072	0.0841	0.0567	0.072	0.0632	-	0.081	0.027	-	0.431	0.0427	-	0.22	0.0428
$2_3 \rightarrow 2_2$	-	0.0073	0.0048	0.042	0.028	5.32×10^{-2}	-	0.0066	0.0032	0.026	0.028	0.03	0.031	0.052	0.047
$2_3 \rightarrow 4_1$	-	-	-	0.00179	0.001	1.1×10^{-2}	-	-	-	0.026	0.031	0.029	0.031	0.044	0.039
$2_4 \rightarrow 4_1$	-	-	-	$> 3.80 \times 10^{-4}$	2.2×10^{-4}	5.6×10^{-4}	-	-	-	-	-	-	-	-	-
$2_4 \rightarrow 0_1$	-	-	-	-	-	-	-	-	-	0.013	0.0157	0.022	-	-	-
$6_1 \rightarrow 4_1$	-	-	-	-	1.269	1.132	-	1.54	1.437	1.3	1.472	1.372	1.32	1.302	1.397
$8_1 \rightarrow 6_1$	-	-	-	-	-	-	-	-	-	1.41	1.627	1.473	1.5	1.672	1.532
$10_1 \rightarrow 8_1$	-	-	-	-	-	-	-	-	-	1.51	1.596	1.632	1.44	1.621	1.543
$0_2 \rightarrow 2_1$	-	-	-	-	-	-	-	-	-	-	0.0022	0.0025	0.0018	0.0022	0.0027
$1 \rightarrow 2_1$	-	0.00044	0.0007	-	0.0066	0.0365	0.0284	0.0007	0.0005	-	0.00088	0.0221	-	-	-
$1 \rightarrow 2_2$	-	0.00023	0.0021	-	0.053	0.071	0.0129	0.0024	0.0023	-	0.00001	0.0001	-	-	-
$1 \rightarrow 2_3$	-	0.0451	0.1861	-	0.128	0.171	0.098	0.096	0.078	-	0.086	0.072	-	-	-
$Q(2_1^+)$	-	-0.431	-0.542	-	-1.872	-1.852	-2.1	-2.21	-2.22	-2	-2.11	-2.07	-2	-1.872	2.2087

Experimental values are taken from Refs. [110, 112, 113]

3.1.4 Magnetic Transition Probability and Mixing Ratio u ($E2/M1$)

To evaluate the magnetic transition probability $B(M1)$, we depend on Eqs. (2-7a) and (2-7b), where the effective boson g -factor is estimated using the fact $g = Z/A$ is. The form of eq. (2-7) of the operator has no off-diagonal matrix elements, implying that in this approximation, $M1$ transitions are forbidden [54,55,58]. Some of the transition probabilities obtained from perturbation theory are further discussed in [54,55].

The results show that the transitions between low-lying collective states are weak. This is because of the increase of antisymmetric component in the wave functions. The magnitude of $M1$ values increase with increasing spin for $x \rightarrow g$ and $x \rightarrow x$ transitions, see Table (3-6).

The $E2/M1$ multiple mixing ratios for $^{172-180}\text{Hf}$ isotopes, ($E2/M1$), were calculated for some selected transitions between states of $J = 0$. The sign of the mixing ratio must be chosen according to the sign of the reduced matrix elements. The equations used are (2-7) for $M1$ transitions and (2-54) for the mixing ratios. The results are listed in Table (3-7). The agreement with available experimental data [110] is more than good especially in the sign of the mixing ratio. However, there is a large disagreement in the mixing ratios of $3^+ \rightarrow 2^+$, due to the small value of $M1$ matrix elements.

The present high-precision measurements indicate some disagreements and these would not change significantly if the u value recommended by Lange *et al.*, [115] were used. The most serious disagreement occurs for the $3^+ \rightarrow 4^+$ transition which has the same initial state as the $3^+ \rightarrow 2^+$ reference transition. A possible conclusion is that one or both of the ground-state band levels contain admixtures. The difference between the measured and deduced u values for the $2^+ \rightarrow 2^+$ transition may be due to mixing in either or both of the levels.

Band mixing, and in particular a $K = 1$ admixture within the $K = 0$ ground state band, has previously been considered necessary in order to

explain the M1 component in transitions linking the x and ground-state bands. An analysis following the **Mikhailov** formulation and involving the lower-spin states indicates a substantial $K = 1$ admixture. The approximately equal value $u(E2/M1)$ obtained for all such transitions suggests that this mixing is uniform within the ground-state band.

The IBM-1 formalism predicts essentially the same spin dependence for M1 transitions in $^{172-180}\text{Hf}$ isotopes as does a geometrical approach, and is thus capable of giving at least an equally good description of the data. In addition, the IBM-1 model yields the simple prediction that $\Delta(E2/M1)$ values of $x \rightarrow x$ and $x \rightarrow g$ transitions should be equal for the same initial and final spins, and this prediction seems to be borne out empirically. It has been shown that different signs for $s \rightarrow g$ and $x \rightarrow g$ $\Delta(E2/M1)$ values can be reproduced by the IBM-1 model.

Table (3-6): Magnetic Transition Probability $B(M1; J_f \rightarrow J_i^*)$ for $^{172-180}\text{Hf}$ isotopes in μ_N^2 .

$J_i \rightarrow J_f$	^{172}Hf		^{174}Hf		^{176}Hf		^{178}Hf		^{180}Hf	
	IBM-1	IBM-2	IBM-1	IBM-2	IBM-1	IBM-2	IBM-1	IBM-2	IBM-1	IBM-2
$2_2 \rightarrow 2_1$	0.0038	0.0031	0.028	0.0236	0.0077	0.00065	0.0035	0.00291	0.0279	0.0295
$2_3 \rightarrow 2_1$	0.0773	0.0883	0.024	0.0026	0.0139	0.0132	0.079	0.0075	0.0732	0.0671
$3_1 \rightarrow 2_1$	0.0034	0.003	0.0091	0.00087	0.0089	0.00099	0.00078	0.0008	0.00039	0.0003
$3_1 \rightarrow 2_2$	0.037	0.0301	0.025	0.0167	0.0022	0.00201	0.0062	0.00078	0.00062	0.00071
$3_2 \rightarrow 2_1$	0.017	0.0159	0.0031	0.0052	0.0065	0.0062	0.0067	0.0079	0.00048	0.00041
$4_2 \rightarrow 4_1$	0.0035	0.0032	0.0037	0.00281	0.006	0.0061	0.0045	0.00432	0.0029	0.0022
$1_1 \rightarrow 0_1$	0.814	0.732	0.822	0.747	0.768	0.824	0.834	0.902	0.88	0.932
$1_1 \rightarrow 2_1$	0.0018	0.0013	0.0037	0.00143	0.0173	0.0172	0.002	0.0002	0.0026	0.0022
$1_1 \rightarrow 2_2$	0.0138	0.0131	0.0271	0.0172	0.00162	0.00145	0.0052	0.004	0.0031	0.00231
$1_1 \rightarrow 2_3$	0.0971	0.0891	0.093	0.084	0.023	0.021	0.0237	0.0221	0.012	0.019
$\mu(2_1^+)$	0.381	0.321	0.420	0.439	0.420	0.501	0.33	0.40	0.783	0.55

Table (3-7): Mixing Ratio $\delta(E2/M1)$ for $^{172-180}\text{Hf}$ in eb/μ_N units.

$J_i \rightarrow J_f$	^{172}Hf			^{176}Hf			^{178}Hf			^{180}Hf					
	Exp.	IBM-1	IBM-2	Exp.	IBM-1	IBM-2	Exp.	IBM-1	IBM-2	Exp.	IBM-1	IBM-2			
$2_2 \rightarrow 2_1$	-	0.0431	0.021	-2_{-2}^{+2}	-3.779	-4.327	$ \delta \geq 4$	6.431	8.201	0.410	0.621	0.521	$9.8_{-3.2}^{+3.6}$	10.761	12.257
$2_3 \rightarrow 2_1$	-	10.227	11.50	-	2.551	3.167	-	10.2	12.21	$\delta < 32$	20	16.7	$6.8_{-3.2}^{+3.6}$	5.257	7.190
$3_1 \rightarrow 2_1$	-	4.762	3.378	-	4.530	0.238	-	2.098	2.098	-	-0.471	2.218	-	1.334	0.097
$3_1 \rightarrow 4_1$	-	-	-	-	1.320	3.761	-	-	-	-	-	-	-	-	-
$4_2 \rightarrow 4_1$	-	0.007	-0.09	$-2.5_{-0.7}^{+13}$	-18.5	-10.25	$ \delta \geq 0.7$	1.22	0.988	-	-	-	$4.5(1.1)$	6.573	8.331
$2_4 \rightarrow 4_1$	-	-	-	0.00039	0.0752	0.00031	0.022	2.87	0.11	$-0.74_{-0.12}^{+0.19}$	-0.931	-	-	-	-
$6_2 \rightarrow 6_1$	-	3.272	2.270	-0.92(8)	-7.420	-1.372	0.04	0.0073	0.088	-	0.761	-	-	32.12	12.90

Experimental data are taken from Refs. [68,110]

3.1.5 Electric Monopole Transition Matrix Element

Strongly-deformed nuclei are easily identified by their rotational behavior. There have been remarkably few such nuclei for which $B(E0)$ data are available. Consequently, we have undertaken a compilation and evaluation of data from which $B(E0)$ values have been extracted for deformed nuclei. We present the data in Table (3-8). Traditionally, strongly-deformed nuclei have been discussed in terms of rotations, ν vibrations and quasiparticle excitations; with an association between E0 transitions and ν vibrations. This association has been based largely on the nuclei ^{174}Hf . This ν -vibrational band picture has probably retained its popularity because E0 transitions are expected with equal strength for all $\Delta J = 0$; ν -band to ground-band transitions. Indeed, $J_s \rightarrow J_g$ E0 transitions are seen in ^{174}Hf up to $J = 8$. However, the identification of ν vibrations has generally been elusive and the current picture is confused.

The strength of the electric monopole transition matrix element, $X_{if} (E0/E2)$ can be calculated using Eqs. (2-58) and (2-59) and presented in Tables (3-8) and (3-9).

As pointed out previously [116], a large $X (E0 / E2)$ value is not necessarily a signature of a ν -vibrational state. For instance, our calculated $X (E0 / E2)$ value for $2_2^+ \rightarrow 2_1^+$ transition. However, it should be kept in mind that a large result from the vanishing B(E2) values, especially in the case of higher bands whose structure may be quite different from that of the lower bands. Because of the possibility of accidental cancellations in the calculation of a sum of terms with different signs, only the correct order of magnitude can be expected from present calculation of a large number of states and matrix element.

In the present $X(E0/E2)$, branching ratios are used to extract the $B(E0; 0_2^+ \rightarrow 0_1^+)$ and $B(E0; 0_2^+ \rightarrow 0_1^+)$ values associated with 0_2^+ states. Our results

are shown in Table (3-9). In to complete the monopole values of $^{172-180}\text{Hf}$ isotopes, the measurements of E0 matrix elements of excited 0_3^+ states in these isotopes are in progress. The ratio of the reduced transition probabilities $B(E0;0_2^+ \rightarrow 0_1^+)/B(E2;0_2^+ \rightarrow 0_1^+)$, is small for some transitions which is close to transitional rotor value. However, the assumed two-phonon 0_2^+ state is strongly pushed too high in energy, which is explained as being due to x -soft.

The most conspicuous features of the 0_3^+ states in $^{172-180}\text{Hf}$ is strongly enhanced $E2$ decay to the 0_1^+ state. This may be connected with the intriguing question of the possible deformation of the excited 0^+ state: the large $B(E2)$ values could alternatively be interoperated to imply a vibrational structure associated e.g., with mixed bands.

The measurement of E0 components in $\Delta J = 0$ transitions are also sensitive to the model predictions and using the IBM-1. An excellent agreement for ... (E0) of the 0.692 MeV $2_2^+ \rightarrow 2_1^+$ transition for which we are also able to deduce the sign of E2 reduced matrix element, that is the relative phase of the E0:E2 matrix elements.

From Table (3-9), the $X(E0/E2)$ values for 2^+ states are taken when the large M1 admixtures in the $2^+ \rightarrow 2^+$ transitions are included. These large differences emphasize the need for knowledge of the M1 admixture before a theoretical analysis of 2^+ state.

The ratio $X(E0/E2)$ does increase with nuclear deformation because the E2 matrix element goes to zero at a slower rate than E0. Hence, a larger $X(E0/E2)$ value, especially a larger ... (E0) value, should be noted regarded as firm evidence of more collectively. In ^{178}Hf , it is the lower 2^+ state which has a smaller $B(E2)$ to the ground state but higher $X(E0/E2)$ value.

Table (3- 8): Monopole transition matrix element $\rho^{(E0)}$ for $^{172-178}\text{Hf}$ isotopes

$J_i \rightarrow J_f$	^{172}Hf		Exp.	^{174}Hf		^{176}Hf		^{178}Hf	
	IBM-1	IBM-2		IBM-1	IBM-2	IBM-1	IBM-2	IBM-1	IBM-2
$0_2 \rightarrow 0_1$	0.132	0.187	0.22[115]	0.2	0.287	0.046	0.078	0.052	0.086
$0_3 \rightarrow 0_1$	4.62×10^{-2}	3.16×10^{-3}	-	0.097	0.0072	0.053	0.0073	0.0073	0.0084
$0_3 \rightarrow 0_2$	0.063	0.087	-	0.0044	0.00035	-	0.00065	0.0011	0.00093
$2_2 \rightarrow 2_1$	0.022	0.0034	-	0.089	0.066	0.0031	0.0035	0.0034	0.0087

Table (3-9) Mixing Ratio $X(E0/E2)$ for $^{172-180}\text{Hf}$ isotopes

$J_i \rightarrow J_f$	^{172}Hf			^{174}Hf			^{176}Hf			^{178}Hf			^{180}Hf		
	Exp.	IBM-1	IBM-2	Exp.	IBM-1	IBM-2	Exp.	IBM-1	IBM-2	Exp.	IBM-1	IBM-2	Exp.	IBM-1	IBM-2
$0_2 \rightarrow 0_1$	0.121	0.197	0.146	-	16.3	15.32	-	5.447	6.872	0.18	0.101	0.21	-	7.221	4.562
$2_2 \rightarrow 2_1$	0.156	0.143	0.187	-	2.251	23.2	0.9	1.227	0.873	0.14	0.197	0.182	-	2.621	4.62
$0_3 \rightarrow 0_1$	19	12.22	10.2	-	0.0073	0.0089	-	0.0032	0.0086	0.1	0.19	0.231	-	5.20×10^{-2}	3.32×10^{-2}
$0_3 \rightarrow 0_2$	-	0.211	0.642	-	9.65	12.26	-	3.729	5.327	1.38	1.671	2.61	-	1.778	3.372
$0_4 \rightarrow 0_1$	6	7.307	8	-	10.2	7.8	-	2.076	3.098	-	-	-	-	-	-
$2_3 \rightarrow 2_2$	-	0.0112	0.0123	-	0.0231	0.08	0.097	0.0731	0.0772	0.12	0.253	0.187	-	-	-

experimental data are taken from ref. [115].

3.2 - $^{180-190}\text{W}$ Isotopes in IBM-1

The present study attempts a unitary IBM-1 treatment of positive parity states in even-even $^{182-188}\text{W}$ isotopes. IBM-1 is a powerful tool for studying the low-lying excited states and electromagnetic transition rates.

3.2.1 Hamiltonian Parameters and Energy Spectra

The best fit for the Hamiltonian Parameters Eq. (2-3a) used in the present work is presented in Table (3-10) which gives the best agreement between the calculated energy levels in the present work and their corresponding experimental data taken from [117] as shown in Figures (3.6) to (3-11).

The best fit values for the Hamiltonian parameters for $^{180-190}\text{W}$ isotopes are given in Table (3-10). The boson-boson interaction parameter was fixed by the calculations on the boson core nuclei.

Table (3 - 10): IBM-1 Hamiltonian parameters for $^{180-190}\text{W}$ Isotopes

Isotopes	N	a_1	a_2	a_3	t
^{180}W	14	0.0553	0.01150	-0.0140	-1.3228
^{182}W	13	0.0597	0.0120	-0.0150	-1.3228
^{184}W	12	0.0460	0.01423	-0.0115	-1.3228
^{186}W	11	0.0401	0.0168	-0.0080	-1.3228
^{188}W	10	0.3420	0.02063	-0.0085	-1.3228
^{190}W	9	0.0206	0.0326	-0.0052	-1.3228

The examination of the experimental and theoretical energy levels ratios (Table (3-11)) for the nuclei $^{180-190}\text{W}$ shows that they lie in the transitional region $\text{SU}(3) \rightarrow \text{O}(6)$, therefore the Hamiltonian of the transition region $\text{SU}(3) \rightarrow \text{O}(6)$ has been employed in the calculation by using the program *PHINT* [60].

Good global agreement was obtained in comparison with the most recent experimental data and the model with the best fitted parameters

proves that the isotopes ^{188}W and ^{190}W have high deformation and tend to be near O(6) limit than to SU(3) limit.

The results indicate that the energy spectra of all different quasi-band of $^{180-190}\text{W}$ isotopes can be presented quite well. It is noticed; however, that the results agree with the experimental data.

Table (3-11): Energy ratios for $^{180-190}\text{W}$ isotopes in IBM-1 and its dynamical symmetries

Isotopes	$E(4_1^+ / 2_1^+)$			$E(6_1^+ / 2_1^+)$			$E(8_1^+ / 2_1^+)$		
	Exp.	IBM-1	IBM-2	Exp.	IBM-1	IBM-2	Exp.	IBM-1	IBM-2
^{180}W	3.260	3.278	3.175	6.647	5.726	6.166	10.999	12.344	10.958
^{182}W	3.290	3.096	2.375	6.797	6.693	6.786	11.431	11.324	11.393
^{184}W	3.273	3.190	3.194	6.726	6.330	6.637	11.258	10.654	11.734
^{186}W	3.245	3.256	3.196	6.631	6.880	6.557	7.065	7.188	7.008
^{188}W	3.096	2.835	3.090	6.090	6.264	6.034	9.965	9.864	9.769
^{190}W	2.724	2.219	2.661	5.067	4.795	4.685	7.922	7.247	7.666
SU (5)	2			3			4		
O (6)	2.5			4.5			7		
SU (3)	3.33			7			12		

Experimental data are taken from ref. [117].

The root means square deviation (*rmsd*) (Eq. (3-1)) is used to compare the experimental and theoretical energy levels (see Tale (3-12)). In this table we see the ground state levels. The best agreement was found in ^{180}W isotope where the smallest value of *rmsd* is equal 0.0028 and equal 0.011 for gamma band in ^{188}W isotope. However, *rmsd* equals 0.0078 for beta band in ^{182}W isotope.

Table (3-12): The root means square deviations (*rmsd*) between experimental and calculated energy levels for $^{180-190}\text{W}$ isotopes.

Isotopes	root mean square deviations (<i>rmsd</i>)					
	ground state band		s – band		x – band	
	IBM-1	IBM-2	IBM-1	IBM-2	IBM-1	IBM-2
^{180}W	0.0028	0.0024	0.055	0.044	0.017	0.015
^{182}W	0.0044	0.0040	0.060	0.053	0.015	0.013
^{184}W	0.0350	0.032	0.054	0.050	0.013	0.011
^{186}W	0.0320	0.030	0.043	0.041	0.011	0.010
^{188}W	0.0300	0.023	0.0078	0.030	0.015	0.012
^{190}W	0.0290	0.020	0.0088	0.0062	0.015	0.013

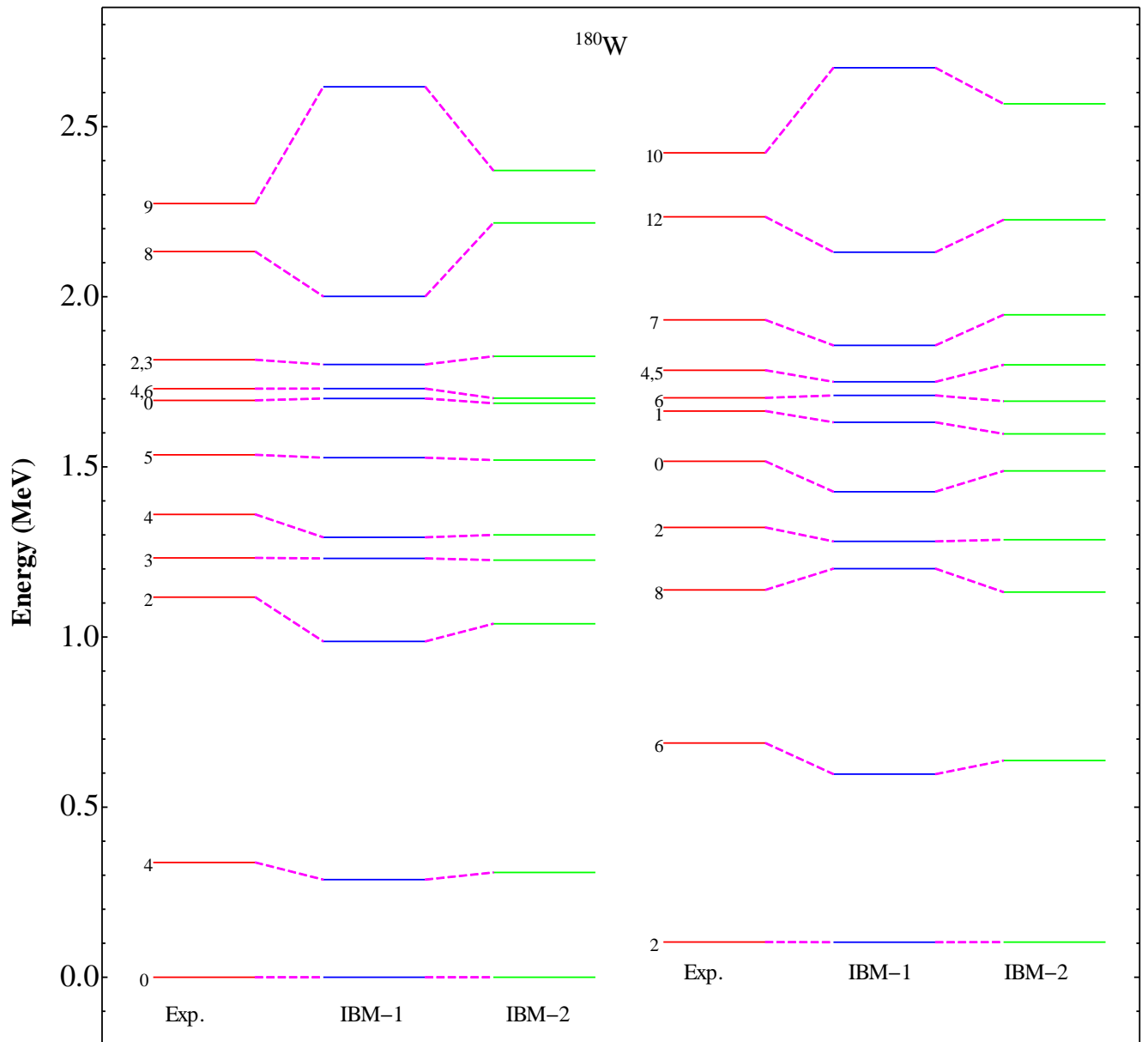


Figure (3.6): Comparison between experimental data [110], IBM-1 and IBM-2 calculated energy levels for ^{180}W .

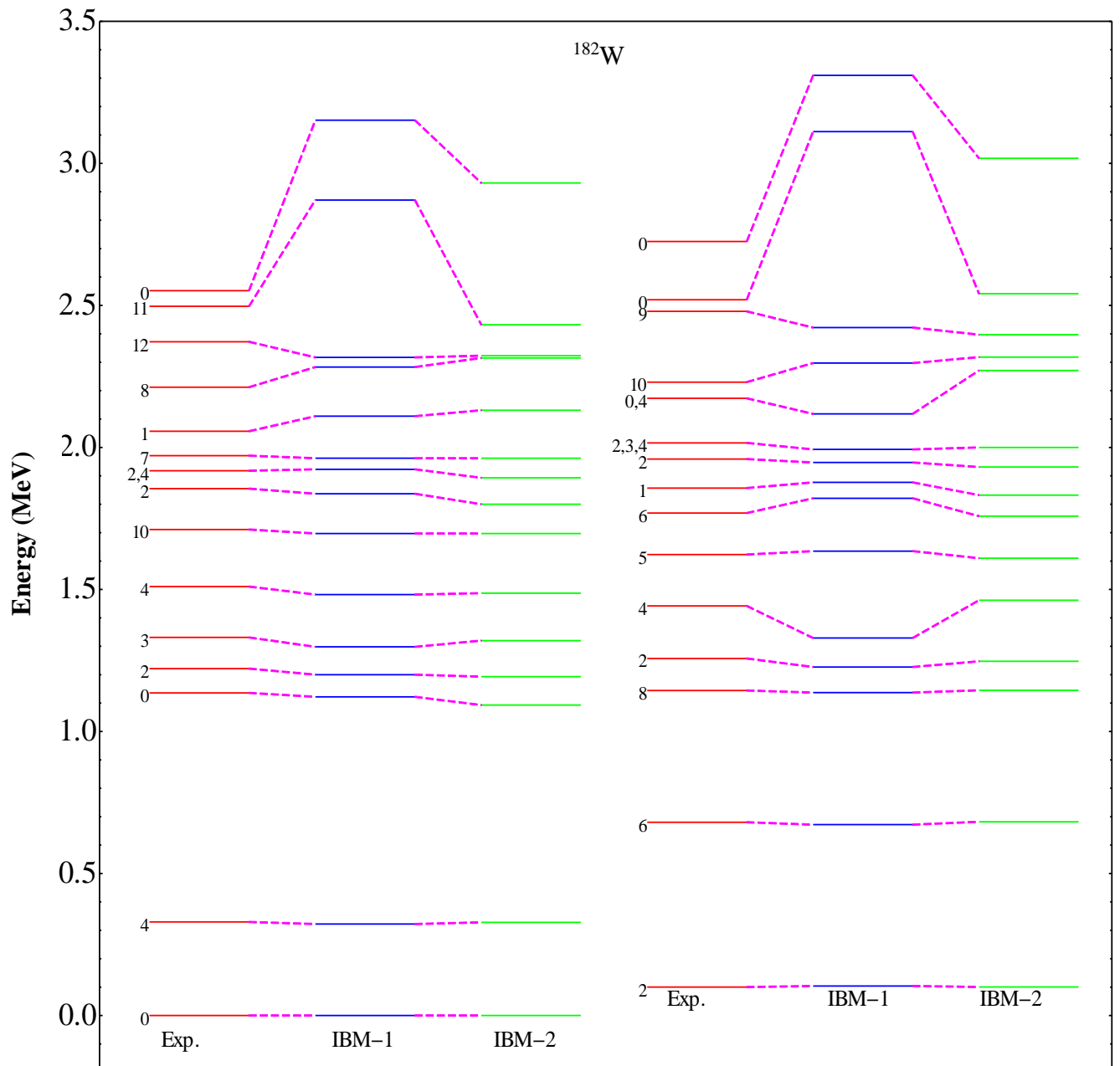


Figure (3.7): Comparison between experimental data [110], IBM-1 and IBM-2 calculated energy levels for ^{182}W .

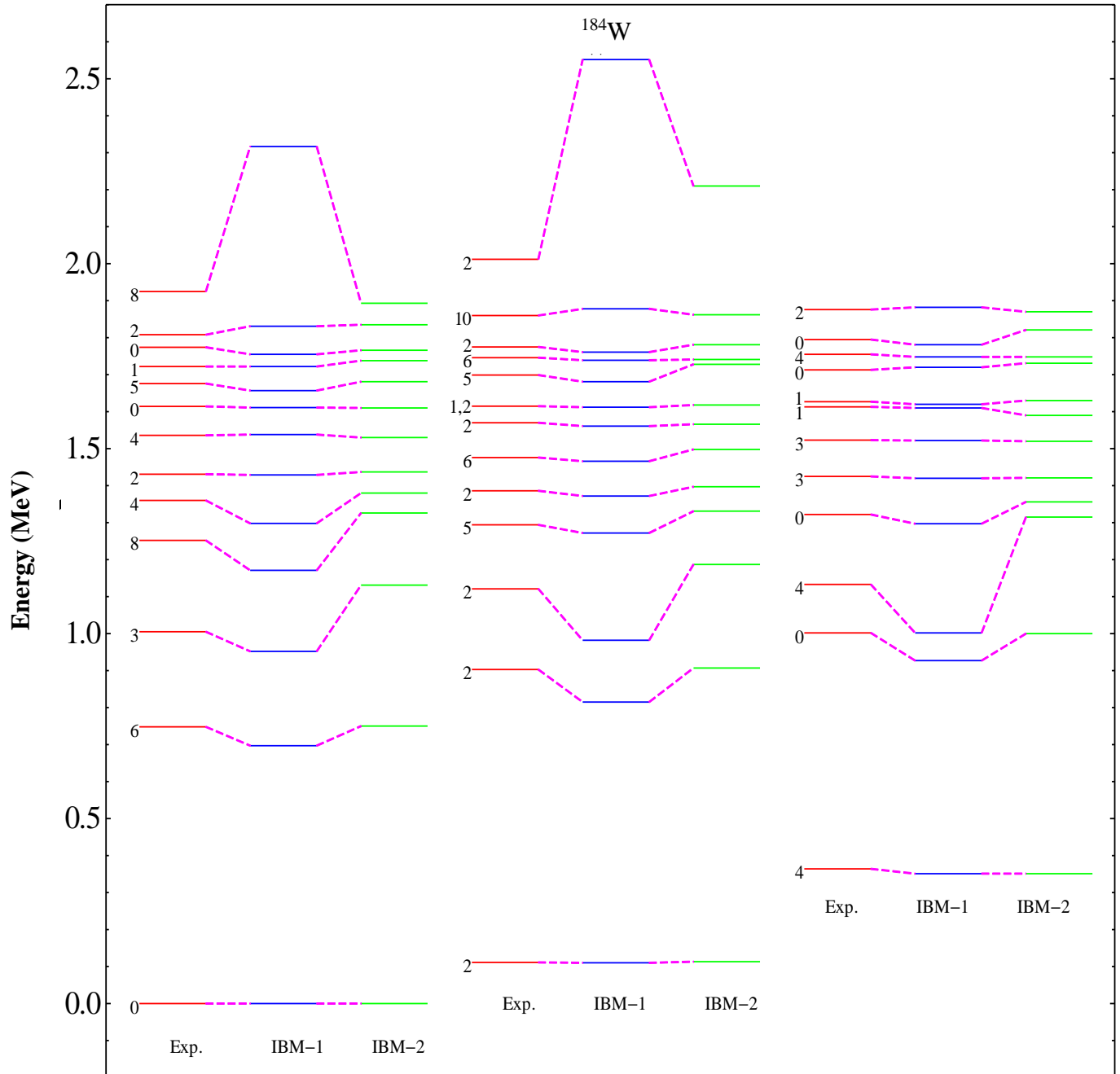


Figure (3.8): Comparison between experimental data [110], IBM-1 and IBM-2 calculated energy levels for ^{184}W .

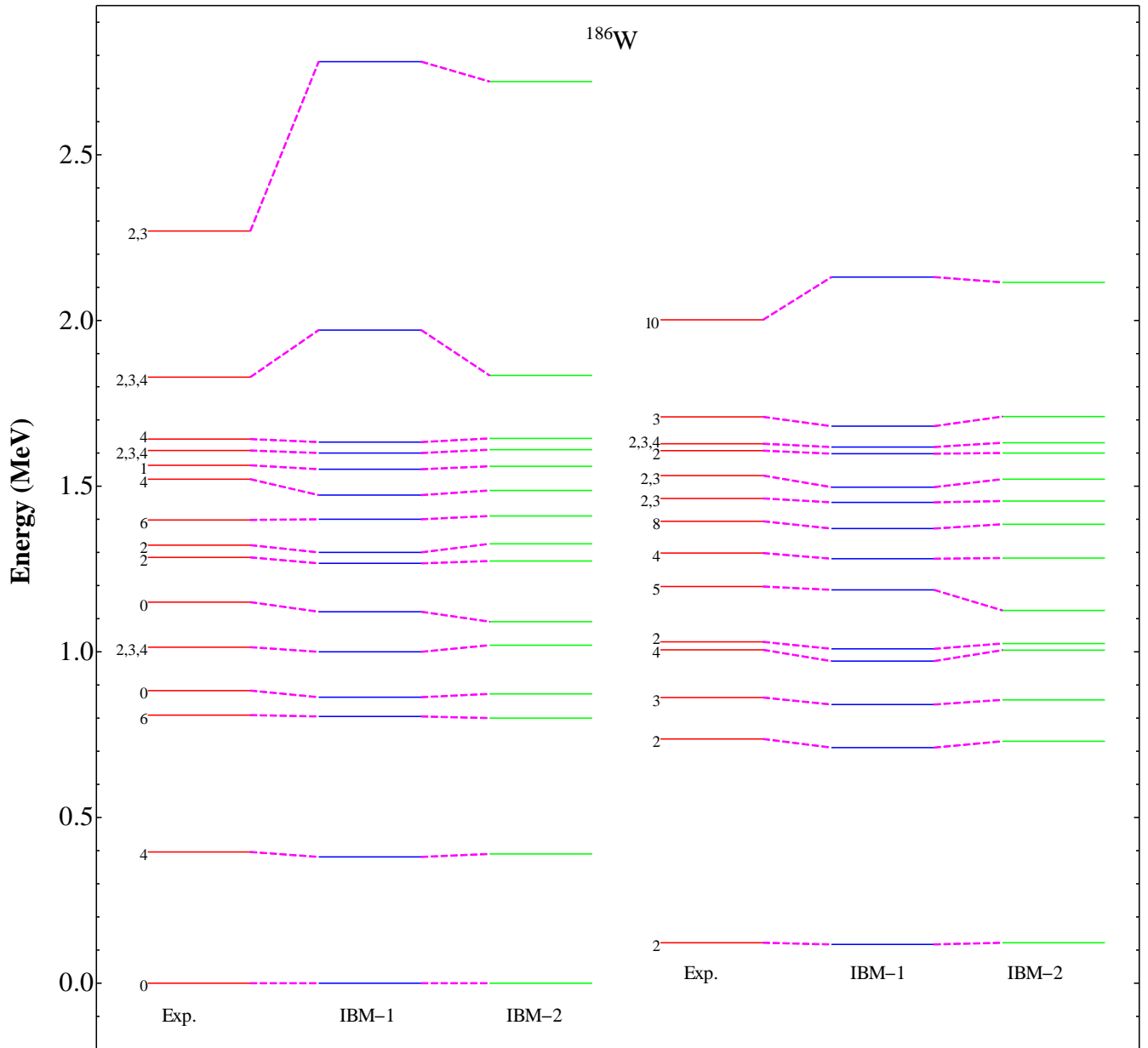


Figure (3.9): Comparison between experimental data [110], IBM-1 and IBM-2 calculated energy levels for ^{186}W .

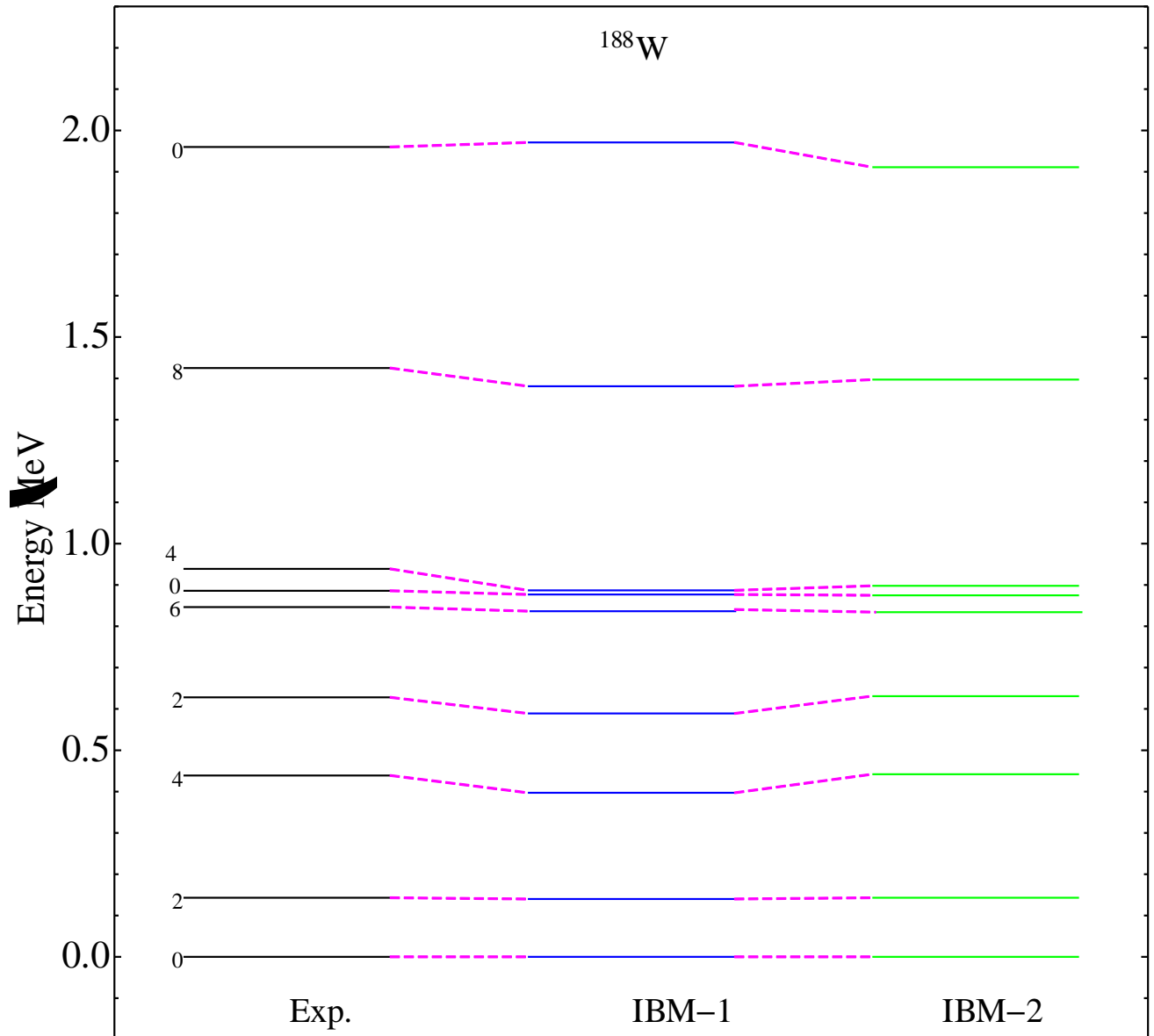


Figure (3.10): Comparison between experimental data [110], IBM-1 and IBM-2 calculated energy levels for ^{188}W .

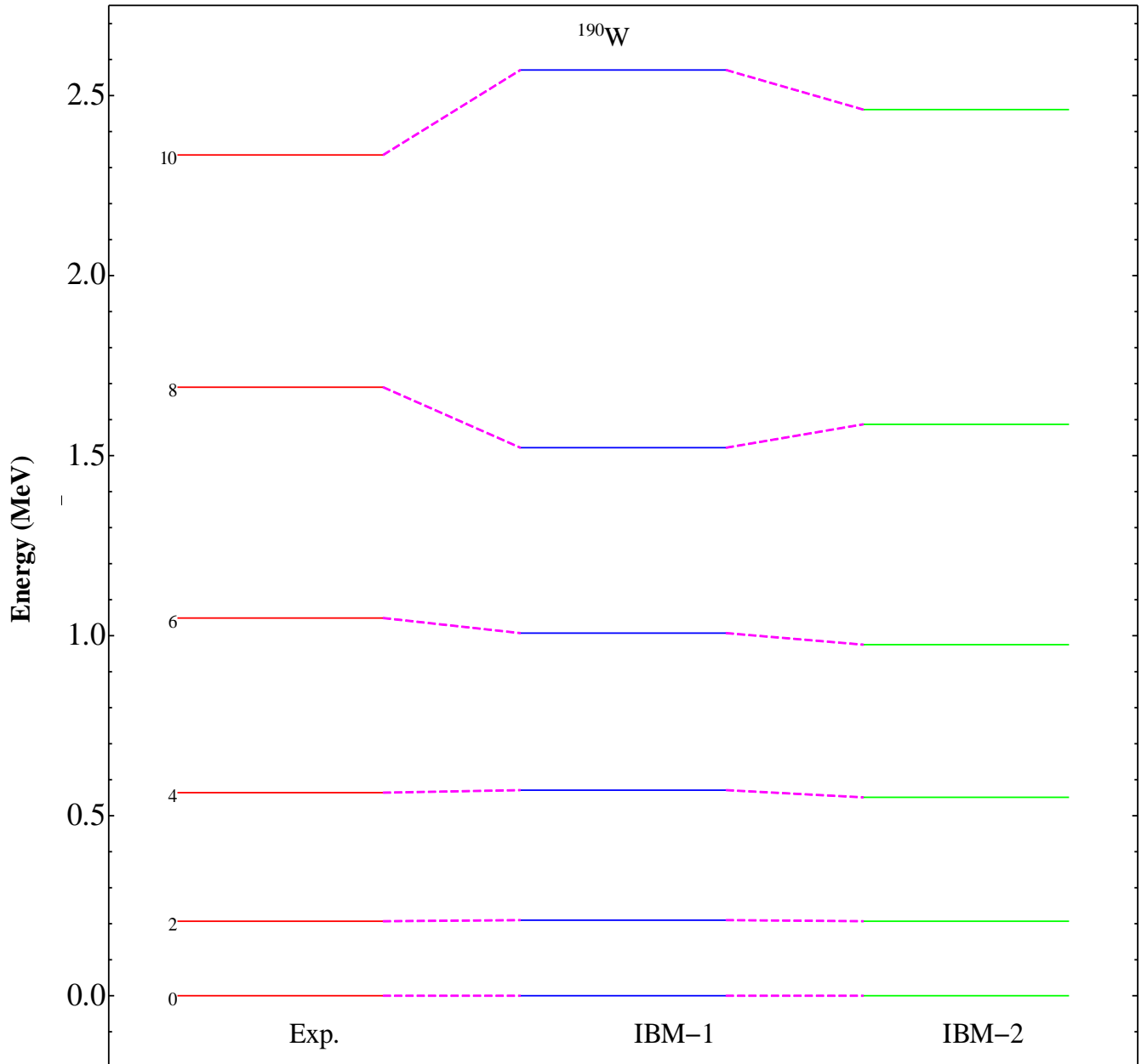


Figure (3.11): Comparison between experimental data [110], IBM-1 and IBM-2 calculated energy levels for ^{190}W .

3.2.2 Electric Transition Probability $B(E2)$

The even-even nuclei in $^{182-188}\text{W}$ isotopic chains represent a good opportunity for studying the behavior of the total low-lying E2 strengths in the transitional region from $SU(3) \rightarrow O(6)$ nuclei. After having obtained wave functions of the states, we can calculate the electromagnetic transition rates between low-lying states of all chain for $^{182-186}\text{W}$ isotopes. Calculation of electromagnetic transitions is a sign of good test for the nuclear model wave functions. To determine the boson effective charges $r_2 = \mathbf{E2SD}$ and

$s_2 = \mathbf{E2DD}$, we perform a fit to the experimental $B(E2)$ values in such isotopes (see Table (3-13)). The matrix elements of the $E2$ operator of Eq. (2-6) have been calculated by using the following values of effective charge parameters.

More information can be obtained by studying the reduced transition probabilities $B(E2)$. The **FBEM** program were employed and the values of r_2 and s_2 , were estimated to reproduce the experimental $B(E2; 2_1^+ \rightarrow 0_1^+)$ values. The parameters **E2SD** and **E2DD** used in the present calculations were determined by normalizing the calculated values to the experimentally known ones and displayed in Table (3-13).

Table (3-13): The reduced matrix element parameters for $^{180-190}\text{W}$ Isotopes.

Isotopes	$B(E2; 2_1^+ \rightarrow 0_1^+) [117,118]$	$r_2 (e.b)$	$s_2 (e.b)$
^{180}W	0.850	0.0990	-0.3001
^{182}W	0.840	0.10555	-0.312214
^{184}W	0.756	0.108013	-0.3201
^{186}W	0.7001	0.11310	-0.3341
^{188}W	0.6001	0.1141	-0.3061
^{190}W	0.414	0.1050	-0.3099

$B(E2)$ values of $^{180-186}\text{W}$ isotopes have been studied within the framework of IBM-1. It is shown that there is a good agreement between the results found, especially with the experimental once [117, 118].

The calculated values of the electric transition probability which has shown the transition connect the levels with the same parity and $E2$ transitions are predominant. As seen from Table (3-14), the theoretical $B(E2)$ values agree with the experimental data within the indicated errors in the experimental values. Moreover, the theoretical $B(E2)$ values for the transition seem to be systematically too small. This can be explained by the fact that many small components of the initial and final wavefunctions contribute coherently to the value of the reduced matrix element $E2$ transition probability [119]. Since the small components are not stable enough against small changes in the model parameters, a quantitative comparison with the experimental data is not possible.

However, the calculated values in Table (3-14) are in agreement with the experimental results. There are some differences between the $B(E2)$ values of $2_2^+ \rightarrow 0_2^+$ transition. Because there is no enough data and certain result for this transition. The experimental $B(E2)$ values of $2_3^+ \rightarrow 0_2^+$, $2_3^+ \rightarrow 2_2^+$ transitions are little and the experimental $B(E2)$ values of $6_1^+ \rightarrow 4_1^+$ for $^{184-186}\text{W}$ isotopes do not exist. The calculated $B(E2)$ value of $2_2^+ \rightarrow 2_1^+$ transition is between the error limits. For $4_1^+ \rightarrow 2_1^+$ transition, the difference between the experimental and theoretical values is seen very small.

The quadrupole moment for the first excited state $Q(2_1^+)$ and the second excited state $Q(2_2^+)$ is an important property for nuclei and is defined as the deviation from the spherical charge distribution inside the nucleus and from the quadrupole moment we can determine if the nucleus is spherical, deformed oblate or prolate shapes. From the results in Table (3-14), the shape of $^{182-186}\text{W}$ isotopes is prolate in the first excited state, and oblate shape in the second excited state.

In the quadrupole moment, qualitatively, with for the ground state band, a negative $Q(2_1^+)$ means a positive intrinsic quadrupole moment Q_0 . For the gamma band, a negative $Q(2_1^+)$ means a negative Q_0 . The negative Q_0 implies that the nucleus has an oblate shape. The overall agreement is surprisingly good in view of the interacting boson model-1 (IBM-1).

Table (3-14): Electric transition probability $B(E2; J_i^+ \rightarrow J_f^+)$ for $^{180-186}\text{W}$ in $e^2 \cdot b^2$ units.

$J_i^+ \rightarrow J_f^+$	^{180}W			^{182}W			^{184}W			^{186}W		
	EXP.	IBM-1	IBM-2	EXP.	IBM-1	IBM-2	EXP.	IBM-1	IBM-2	EXP.	IBM-1	IBM-2
$2_1 \rightarrow 0_1$	0.850(5)	0.852	0.850	0.839(18)	0.624	0.846	0.72	0.673	0.731	0.51	0.531	0.517
$2_1 \rightarrow 0_2$	-	0.0077	0.085	-	0.009	0.11	-	-	-	-	-	-
$2_2 \rightarrow 0_1$	-	0.0073	0.0062	0.021(1)	0.028	0.025	0.025	0.0331	0.0255	0.03	0.032	0.033
$2_2 \rightarrow 0_2$	-	0.352	0.273	-	-	-	-	-	-	-	-	-
$2_2 \rightarrow 2_1$	0.109	0.137	0.109	0.041(1)	0.059	0.043	0.05	0.0731	0.062	0.064	0.0621	0.068
$2_3 \rightarrow 0_1$	-	0.0088	0.0072	0.0056	0.0057	0.0061	0.002	0.0019	0.0025	0.0016	0.019	0.0018
$4_1 \rightarrow 2_1$	-	0.573	0.232	1.201(61)	1.197	1.371	1.03	0.987	1.21	0.905	0.643	0.873
$2_2 \rightarrow 4_1$	-	0.0055	0.0057	0.0002(1)	0.006	0.0021	0.0030(2)	0.098	0.0033	-	0.0078	0.0045
$6_1 \rightarrow 4_1$	-	0.373	0.221	1.225(135)	1.371	1.375	1.138(62)	1.08	1.239	1.123(82)	2.13	1.650
$2_3 \rightarrow 0_2$	-	0.0078	0.1054	1.225(368)	1.561	1.414	-	0.574	0.577	-	0.754	0.468
$2_3 \rightarrow 2_1$	-	0.043	0.0041	0.0039(5)	0.0024	0.0044	0.050	0.069	0.061	-	0.0031	0.0047
$2_4 \rightarrow 0_3$	-	-	-	-	1.413	1.622	-	-	-	-	-	-
$4_2 \rightarrow 2_1$	-	-	-	-	0.0731	0.0321	-	-	-	-	-	-
$Q(2_1^+)$	$-1.966_{-0.04}^{+0.04}$	-1.737	-1.821	-2.13	-1.920	-2.270	-1.87(20)	-1.631	-1.791	-1.57(30)	-1.48	-1.521
$Q(2_2^+)$	-	-	-	$1.94_{-0.04}^{+0.1}$	1.371	1.873	0.1_{-3}^{+4}	0.352	0.181	1.3(3)	1.371	1.432

Experimental taken from ref. [117,118]

3.2.3- Magnetic Transition Probability and Mixing Ratio $\mu(E2/M1)$

In order to examine $B(M1)$ and the magnetic dipole moment μ of 2_1^+ and 2_2^+ state, we employed the relation [72]:

$$\mu = gI \dots \dots \dots (3-2)$$

where g is the boson gyromagnetic factor and I is the nuclear angular momentum, where g estimated using the fact that Eq. (3-2), and the experimental value $\mu(2_1^+) = 0.25 (8) \mu_N$ [117] for ^{184}W , we obtained $g = 0.2605 \mu_N$. For the parameter in the M1 operator the value of $g = 0.7 \mu_N$ is used in Eq. (2-7a). The $B(M1)$ results are shown in Table (3-15). It is seen that there is a good agreement between experimental and calculated ones in IBM-1. The magnetic dipole moment of the first excited $\mu(2_1^+)$ and second excited state $\mu(2_2^+)$ for the $^{182-188}\text{W}$ isotopes are given in Table (3-15). It is seen that a very good agreement among the values is obtained.

Magnetic dipole moment for first excited state $\mu(2_1^+)$, second excited state $\mu(2_2^+)$ and for $\mu(4_1^+)$ are given in Table (3-15). It has been shown that the data on $\mu(2_1^+)$ in $^{182-188}\text{W}$ isotopes provides a sensitive test of the effective proton boson number in the IBM-1 framework. $^{182-188}\text{W}$ isotopes, conform the validity of assuming a drastic change in number of bosons N when the number of neutron increased.

Table (3-15): Magnetic transition probability B(M1) in μ_N^2 units for $^{182-188}\text{W}$ isotopes.

$J_i^+ \rightarrow J_f^+$	^{182}W			^{184}W			^{186}W			^{188}W		
	EXP.	IBM -1	IBM -2	EXP.	IBM -1	IBM -2	EXP.	IBM -1	IBM -2	EXP.	IBM -1	IBM -2
$2_2 \rightarrow 2_1$	0.0001	0.362	0.00323	0.0001	0.311	0.0005	0.11	0.201	0.121	0.0002	0.333	0.328
$2_3 \rightarrow 2_1$	2.2	1.971	2.414	0.58	0.6001	0.621	-	0.462	0.432	-	0.108	0.102
$2_3 \rightarrow 2_1$	-	0.021	0.016	0.004(1)	0.0022	0.0034	-	0.031	0.037	-	0.361	0.238
$3_1 \rightarrow 2_1$	-	0.052	0.046	0.00428(2)	0.0029	0.0039	-	0.063	0.075	-	0.211	0.171
$3_1 \rightarrow 2_2$	-	0.008	0.009	-	0.0091	0.0085	-	0.241	0.237	-	0.228	0.22
$2_3 \rightarrow 3_1$	-	0.362	0.246	-	0.328	0.31	-	0.229	0.236	-	0.317	0.216
$3_1 \rightarrow 4_1$	-	0.0421	0.035	0.00457(3)	0.0054	0.0057	-	0.119	0.116	-	0.251	0.211
$4_2 \rightarrow 4_1$	-	0.0071	0.0046	0.00333(3)	0.0042	0.0031	-	0.0031	0.0029	-	0.004	0.0031
$1_1 \rightarrow 2_1$	-	0.003	0.0021	-	0.032	0.212	-	0.065	0.098	-	0.66	0.876
$1_1 \rightarrow 2_2$	-	0.00012	0.00022	-	0.0021	0.0025	-	0.0055	0.00043	-	0.0011	0.0014
$1_1 \rightarrow 0_1$	-	0.11	0.177	-	0.10	0.194	-	0.11	0.172	-	0.201	0.163
$\mu(2_1^+) \mu_N$	0.521(16)	0.550	0.5223	0.578(14)	0.610	0.591	0.615(24)	0.622	0.621	-	0.642	0.631
$\mu(4_1^+) \mu_N$	0.88(17)	0.85	0.83	1.17(9)	1.09	1.10	1.28(10)	1.33	1.31	-	1.47	1.38
$\mu(2_2^+) \mu_N$	-	0.23	0.21	0.25(8)	0.21	0.23	0.39(8)	0.42	0.38	-	0.51	0.46

Experimental data are taken from ref. [117]

The direct measurement of $B(M1)$ matrix elements is difficult normally, so the $M1$ strength of gamma transition may be expressed in terms of the multipole mixing ratio which can be written in Eq. (2-54) as [68]. The multipole mixing ratio, $u(E2/M1)$, of $^{180-190}\text{W}$ isotopes was calculated. The comparison between experimental and calculated values for this quantity is given in Table (3-16). The results highly agreed with the experimental data.

In this work, we have also examined the mixing ratio $u(E2/M1)$ of transitions linking the x -band and g -state bands. The transitions which link low spin states and those obtained in the present work are in a good agreement and show a little bit of irregularities.

The results of the $u(E2/M1)$ calculations are listed in Table (3-16). These results exhibit disagreement in some cases, with one case showing disagreement in sign. However, it is a ratio between very small quantities and any change in the dominator that will have a great influence on the ratio. The large calculated value for $3_1^+ \rightarrow 2_1^+$ in $^{184-186}\text{W}$ is not due to dominate $E2$ transition, but may be under the effect of very small $M1$ component in the transition. Moreover, the large predicted value for some transitions compared to experimental value may be related to the highly predicted energy level values of the IBM-1. We are unable to bring the energy value of this state close to the experimental value simply by changing the parameters.

Table (3-16) Mixing ratio $\delta(E2/M1)$ for $^{182-186}\text{W}$ Isotopes in eb/μ_N units.

$J_i^* \rightarrow J_f^*$	^{182}W			^{184}W			^{186}W		
	EXP.	IBM -1	IBM -2	EXP.	IBM -1	IBM -2	EXP.	IBM -1	IBM -2
$2_2 \rightarrow 2_1$	$16.7^{+4.1}_{-2.7}$	24	18.001	-16.7(5)	-11.2	-14.77	-11^{+3}_{-1}	-2.215	-13.201
$2_3 \rightarrow 2_1$	$(-8.7)^{+5.5}_{-2.5}$	-19.51	-10.227	$2.3^{+0.7}_{-0.3}$	2.678	4.671	13^{+7}_{-6}	18.702	14.622
$3_1 \rightarrow 2_1$	-60^{+100}_{-30}	0.2	-10.51	$ 8 \geq 12$	20.11	11.56	-16.9(9)	6.221	7.310
$3_1 \rightarrow 4_1$	$-8.9^{+2.3}_{-1.8}$	-7.77	-5.218	-8.3(6)	1.51	-2.587	-	-5.471	-8.716
$4_2 \rightarrow 4_1$	$(-20)^{+8}_{-15}$	-28	0.115	$ 8 \geq 14$	28	16.875	-	2.681	18.66
$1 \rightarrow 2_1$	-	0.291	0.517	-	5.51	8.661	-	-	-
$1 \rightarrow 2_2$	-	2.251	4.521	-	-	-	-	-	-
$1 \rightarrow 2_3$	-	6.731	7.807	-	-	-	-	-	-
$1 \rightarrow 3_1$	-	18.22	20.781	-	-	-	-	-	-
$3_1 \rightarrow 4_1$	$5.6^{+1.3}_{-1}$	6.67	4.589	$-7.93^{+2.36}_{-3.6}$	-2.	-5.372	-	4.98	0.325
$2_3 \rightarrow 2_1$	$-7^{+4}_{-\infty}$	0.061	0.731	$3^{+0.6}_{-0.05}$	12.0	5.43	1.7(4)	2.98	1.88
$2_4 \rightarrow 2_1$	-	-	-	28^{+8}_{-1}	14	25.903	11.1(5)	2.51	5.225

Experimental data are taken from [68,117]

3.2.4 Electric Monopole Transition Matrix Element

The monopole matrix element is important for nuclear structure and the model predictions due to their sensitivity for the nuclear shape. We conclude that more experimental work is needed to clarify the band structure and investigate an acceptable degree of agreement between the predictions of the IBM-1 and the experimental data.

The calculation of the matrix elements of the E0 transition operator (2-8a) requires the knowledge of the parameters s_0 and x_0 . We calculate these parameters

by fitting procedure into two experimental values of reduced E0 matrix element for transition $2_2^+ \rightarrow 2_1^+$, in $^{182-184}\text{W}$ isotopes. The parameters which were subsequently used to evaluate the ... (E0) -values were; $s_0 = 0.064 \text{ fm}^2$ and $x_0 = 0.032 \text{ fm}^2$. From Table (3-17), there is no enough experimental data to compare with the IBM-1 calculations.

The forbiddenness of E0 transitions in the U (5) limit of IBM-1 and their allowed character in the harmonic quadrupole vibrator needs some comment. Primarily, the model operators are quite different. For the geometric model, the $\Delta N = 0, +2$ selection rules follow directly. For the interacting boson model, the operator is the simplest monopole operator that can be constructed from the boson operators. It is fair to say that the IBM-1 E0 operator is too simplistic. There are other concerns with the interacting boson model: the bosons of the model are regarded as superposition's of pair-correlated configurations restricted to the valence shell. This has been formalized in the *OAI* mapping procedure [120]. Restriction to a valence shell within a harmonic oscillator-based shell model, as noted earlier, would result in vanishing E0 matrix elements. Thus, we infer that the description of E0 transitions within the IBM-1 is probably seriously deficient.

Table (3-17): Monopole Matrix Element ...($E0$) for $^{182-186}\text{W}$ isotopes.

$J_i^+ \rightarrow J_f^+$	^{182}W			^{184}W			^{186}W		
	EXP.	IBM -1	IBM -2	EXP.	IBM -1	IBM -2	EXP.	IBM -1	IBM -2
$2_2 \rightarrow 2_1$	$4^{+0.6}_{-0.6} \times 10^{-2}$	0.0093	0.005	$2.9^{+1.5}_{-2.9} \times 10^{-2}$	0.109	2.87	0.11	0.0621	0.083
$0_2 \rightarrow 0_1$	-	0.187	0.173	-	0.0161	0.172	-	0.151	0.164
$0_3 \rightarrow 0_1$	-	0.317	0.126	-	0.0372	0.153	-	0.0171	0.169
$0_3 \rightarrow 0_2$	-	0.0931	0.083	-	0.0810	0.108	-	0.143	0.136

Experimental data are taken from ref. [121]

We notice that the theoretical values for the ratio $X(E0/E2)$ are small for some transitions (see Table (3-18)) which means that there is a small contribution of E0 transition on the life time of 0^+ states. There are two high values of $X(E0/E2)$ in transition from 0_2^+ to 0_1^+ in ^{182}W isotope means that this state decay mostly by E0 and according to this one could say that the study of this state gives information about the shape of the nucleus, because the E0 transitions matrix elements are connected strongly with the penetration of the atomic electron to the nucleus. So, combination of the wave function of atomic electron, which is well known, and the nuclear surface give good information of the nuclear shape.

Table (3-18) shows that the IBM-1 predicts well the monopole matrix elements compare to the quadrupole transition from the same states. However, it is not easy to estimate the ratio because of the smallness on the monopole matrix element and it is one of the reasons not getting the exact ratio. A small $X(E0/E2)$ value for transition from 0_3^+ to 0_2^+ agrees well with the experimental despite the band crossing transition, which means that the 0_3^+ has a collective structure.

The large value of $X(E0/E2)$ interpreted for several 0^+ states in terms of pair vibrations, s-band vibration and spin quadrupole excitations. However, the nature of 2^+ states is not clear. Also, there is no available experimental data for ^{186}W isotopes.

Table (3-18): $X(E0/E2)$ for $^{182-186}\text{W}$ Isotopes.

$J_j^+ \rightarrow J_f^+$	^{182}W			^{184}W			^{186}W		
	EXP.	IBM -1	IBM -2	EXP.	IBM -1	IBM -2	EXP.	IBM -1	IBM -2
$0_2 \rightarrow 0_1$	1.28(2)	0.0031	0.0027	0.0020_{-8}^{+12}	0.0038	0.0028	-	0.0034	0.004
$2_2 \rightarrow 2_1$	0.0120(4)	0.022	0.015	-	0.0281	0.018	-	0.0221	0.022
$0_3 \rightarrow 0_1$	0.0020(10)	0.0037	0.0023	-	0.0047	0.0054	-	0.057	0.006
$2_3 \rightarrow 2_1$	0.0022(14)	2.11	0.33	-	2.317	1.38	-	2.471	2.414

Experimental are taken from ref. [68].

There is a good agreement between the calculated values and the available experimental results for both the E0 transitions and the isotope shifts. However, rather different sets of the E0 parameters can be found which give similar isotope shifts but different isomer shifts. Therefore, in the absence of any experimental isomer shift data, it is not possible to tell whether it represents the "best" possible set of E0 parameters. Besides a good agreement was found between the calculated and experimental values for Isomeric and isotopic shifts for all $^{182-186}\text{W}$ isotopes (Tables (3-19) and (3-20)).

Table (3-19): Isomer Shift $u \langle r^2 \rangle$ in fm^2 for $^{182-186}\text{W}$ Isotopes.

Isomer Shift	EXP.	IBM -1	IBM -2
W-182	-0.2×10^{-3}	-0.25×10^{-2}	-0.28×10^{-3}
	-0.37×10^{-3}		
	0.0×10^{-3}		
W-184	0.16×10^{-3}	0.13×10^{-3}	0.169×10^{-3}
	0.12×10^{-3}		
	0.0×10^{-3}		
W-186	0.14×10^{-3}	0.21×10^{-3}	0.172×10^{-3}
	0.12×10^{-3}		
	-0.49×10^{-3}		
W-188	-	0.14×10^{-3}	0.121×10^{-3}
W-190	-	0.12×10^{-3}	0.111×10^{-3}

Experimental data are taken from refs. [117,122,123,124].

Table (3-20): Isotopic shifts $\Delta\langle r^2 \rangle$ in fm² for ¹⁸²⁻¹⁸⁶W Isotopes.

Isomer shift	EXP.	IBM -1	IBM -2
¹⁸⁰ W- ¹⁸² W	0.074 0.068(4)	0.066	0.072
¹⁸² W- ¹⁸⁴ W	0.120 0.099(5)	0.140	0.150
¹⁸⁴ W- ¹⁸⁶ W	0.092 0.085(4)	0.068	0.087
¹⁸⁶ W- ¹⁸⁸ W	-	0.088	0.0873
¹⁸⁸ W- ¹⁹⁰ W	-	0.092	0.097

Experimental data are taken from refs. [117,122,123,124].

3.3- ¹⁷²⁻¹⁸⁰Hf Isotopes in IBM-2

3.3.1 Hamiltonian Interaction Parameters

Since the Hamiltonian contains many parameters, it is unpractical and not very meaningful to vary all parameters freely. Instead, it is convenient to use the behavior of the parameters predicted by a microscopic point of view as a zeroth-order approximation. In a simple shell-model picture based upon degenerate single nucleon levels [120], the expected dependence of $v, |, t_\epsilon$ and t_f on neutron (N_ϵ) and proton (N_f) boson numbers can be expressed as:

$$v = \text{constant}, | = |_f |_\epsilon, |_\dots = \sqrt{\frac{\Omega_\dots - N_\dots}{\Omega_\dots - 1}} |_\dots^{(0)}, t_\dots = \frac{\Omega_\dots - 2N_\dots}{\sqrt{\Omega_\dots - N_\dots}} t_\dots^{(0)} \dots\dots(3-3)$$

Here $|_\dots^{(0)}$ and $t_\dots^{(0)}$ are constants, and Ω_\dots is the pair degeneracy of the shell. We see that while $|_\dots$ has always the same sign, t_\dots changes the sign in the middle of the shell.

In realistic cases, the estimates of Eq. (3-3) are expected to be valid only approximately. In this work, somewhat weaker constraints we have imposed on the parameters: **(i)** it is assumed that within a series of isotones (isotopes) (t_f) does not vary at all isotopes; **(ii)** the parameters $v, |$ and t_ϵ are assumed to be smooth functions of (N_ϵ).

Concerning the sign of t_ϵ and t_f , a complication arises. From very simple microscopic consideration it follows that the t 's (which also

determined to a large extent the sign of the quadrupole moment of the first excited state 2_1^+) are negative in the region where the valence shell is less than half filled (particle-boson) and positive in the region where the valence shell is more than half filled (hole-boson). Quantitatively, such a behavior was confirmed in other phenomenological calculations with IBM-2. For example, in a study of the Hf isotopes with $100 < N < 108$ good fit to the energy levels was obtained with $t_\epsilon \approx -0.90$ to -1.0 (see Table (3-21)). Since in the native shell-model picture in this region both neutrons and protons are hole-like and therefore both t_s would be positive, there would be no way to obtain an $SU(5)$ type spectrum, which requires opposite signs of t_ϵ and t_f . This indicates that the situation is not so simple and that more complicated effects play a role, such as a possible nonclosedness of the $Z = 82$ or $N = 126$ core. Although the Hamiltonian invariant under simultaneous change in sign of both t_f , t_ϵ and thus equally good, fits to energy spectra can be obtained for both combinations $t_f < 0$ and $t_\epsilon < 0$. Namely, only with this choice the observed sign of the mass quadrupole moment of the 2_1^+ state in $^{170-180}\text{Hf}$ can be reproduced.

The remaining parameters play a less important role and are used mainly to improve the fit with experiment. In this work only $C_{0...}$, $C_{2...}$ and $C_{4...}$, representing part of the d-boson conserving interaction between neutron bosons, were used as free parameters independent of N_ϵ (N_f). Finally, the values of $\langle_1 = \langle_3$ were constant for all isotopes. The parameters used for the various isotopes are shown in Table (3-21).

It is seen that parameters are constant or vary smoothly: within a series of isotopes t_f does not vary and the values of t_f and t_ϵ are close to the values calculated by Pittle *et al.*, [125]. The variation in v is small and there is a slight decrease of the value of $|$ for the $^{170-180}\text{Hf}$ isotopes. The change in character of the spectra through a series of isotopes is essentially

due to two effects: **(i)** the increase of the value of t_ϵ for $^{172-174}\text{Hf}$ and decreases for ^{176}Hf , and **(ii)** the increased of the number of neutron bosons N_ϵ for $^{172-174-176}\text{Hf}$ ($N_\epsilon=9,10$ and 11 respectively) and decrease for $^{178-180}\text{Hf}$ ($N_\epsilon=10$ and 9). We note that the behaviors of $v, |, t_\epsilon$ and t_f is a qualitative agreement with microscopic considerations (see Eq. (3-3)). It was found that $C_{0...}$, $C_{2...}$ and $C_{4...}$ constant for the isotopes. Such a behavior agrees with the trend found in other regions. The positive value of \langle_2 guarantees that no low-lying anti-symmetric multiplets occur for which there is no experimental evidence.

This was determination from fitting the first excited state without effecting the ground band energy spacing. The overview of the parameters indicates that there is good continuity without a marked change, and at the same a good fit to the experimental energies of the ground state band and of beta and gamma bands was obtained.

3.3.2 Energy spectra

The calculated excitation energies of positive parity levels to $^{172-180}\text{Hf}$ are given in Table (3-21) and displayed in Figures (3.1) to (3.5). The agreement between the calculated and experimental values is satisfactory.

Using the parameters in Table (3-21), the estimated energy levels are shown in the Figures (3.1) to (3.5), along with experimental energy levels. As can be seen, the agreement between experiment and IBM-2 is quite good and the general features are reproduced well. We observe the discrepancy between IBM-2 and experimental for high spin states. But one must be careful in comparing theoretical with experimental, since all calculated states have a collective nature, whereas some of the experimental states may have a particle-like structure. Behavior of the ratio $R_{4/2} = E(4_1^+)/E(2_1^+)$ of the energies of the first 4_1^+ and 2_1^+ states are good criteria for the shape transition. The value of $R_{4/2}$ ratio has the limiting value 2.0 for a quadrupole vibrator, 2.5 for a non-axial gamma-soft rotor

and 3.33 for an ideally symmetric rotor. $R_{4/2}$ remain nearly constant at increase with neutron number. The estimated values change from isotope to another (see Table (3-2)), this meaning that their structure seems to be varying from deformed (rotational nuclei) to gamma soft $SU(3) \rightarrow O(6)$. Since Hf nucleus has a rather vibrational-like character, taking into account of the dynamic symmetry location of the even-even Hf isotopes at the IBM phase Casten triangle, where their parameter sets are at the $SU(3) \rightarrow O(6)$ transition region and closer to $SU(3)$ character and we used the multiple expansion form of the Hamiltonian for our approximation. The shape transition predicted by this study is consistent with the spectroscopic data for these isotopes.

$^{172-180}\text{Hf}$ are typical examples of isotopes that exhibit a smooth phase transition from rotational (deformed) nuclei ($SU(3)$) to gamma soft ($O(6)$).

In the Figures (3-1) to (3-5) the results of calculations for the energies are shown the ground state band ($2_1^+, 4_1^+, 6_1^+$ and 8_1^+) in the $^{172-180}\text{Hf}$ isotopes. We observe the small discrepancy between theory and experiment for $J^f = 6_1^+$ and $J^f = 8_1^+$ in $^{170-180}\text{Hf}$ isotopes. However, one must be careful when comparing theory to experiment, since all calculated low-lying states have a collective nature.

The order of the 0_2^+ and 3_1^+ is correctly predicted in $^{170-180}\text{Hf}$ isotopes and we remark that the energy of the 3_1^+ state is predicted systematically too high. This is a consequence of the presence of a Majorana term $M_{f\epsilon}$ in the Hamiltonian (Eq. (2-45)). We have chosen the parameters of the Majorana force in such a way that it pushes up states which are not completely symmetric with respect to proton and neutron bosons, since there is no experimental evidence for such states. However, experimental information becomes available about these states with mixed symmetry. This situation could possibly be improved. In the present case, it would

have been possible to further higher its energy by constant the value of $\langle_1 = \langle_3$.

Table (3-21): IBM-2 Parameters of $^{172-180}\text{Hf}$, all parameters in MeV units except the parameters t_f and t_v are dimensionless.

Isotopes	v	$ $	t_ϵ	t_f	$\langle_1 = \langle_3$	\langle_2	$C_{0\dots}$	$C_{2\dots}$	$C_{4\dots}$
^{172}Hf	0.522	-0.029	-0.9	-0.9	-0.422	-0.033	-0.151	0.08	0.0
^{174}Hf	0.525	-0.035	-0.85	-0.9	-0.422	-0.025	-0.151	0.072	0.0
^{176}Hf	0.528	-0.031	-1.02	-0.9	-0.422	-0.023	-0.151	0.075	0.0
^{178}Hf	0.530	-0.033	-0.8	-0.9	-0.422	-0.020	-0.151	0.09	0.0
^{180}Hf	0.532	-0.035	-1.0	-0.9	-0.422	-0.190	-0.151	0.09	0.0

The position of the 2_3^+ state is relative to the 0_2^+ state especially in $^{176-178-180}\text{Hf}$ isotopes. The moment of inertia of the ground state band increases, the quasi γ -band is pushed up, and also 0_2^+ state becomes a member of a $K = 0$ γ -band. The energy spectra show the first criterion for identifying the collective 0_2^+ states. For instance, in $^{170-180}\text{Hf}$ isotopes, the experimental energies of the 0_2^+ states are close to those of the calculated 0_2^+ states. As a consequence, we suspect that these states are collective. However, no final conclusion can be drawn from the energies alone, since it is very likely that collective 0_2^+ states will occur in the same energy region.

It is found that the present calculations fit very well most states in the scheme, except the case of γ -band members (2_3^+ , 3_1^+ and 4_2^+ states), which were pushed higher. In Table (3-3), the root mean square deviation (*rmsd*) is used to compare the experimental and calculated IBM-2 energy levels. In this table (3-3), we see the ground state levels the best agreement was found in ^{178}Hf isotope where the smallest value of *rmsd* is equal 0.0025 and equal 0.0038 for beta band in ^{178}Hf isotope. However, *rmsd* equals 0.001 for γ -band in ^{176}Hf isotope.

From the results of energy levels, the experimental and IBM-2 calculation increased with increasing the angular momentum because the Hf nuclei are deformed nuclei (rotational nuclei).

3.3.3 Electric Transition Probability B(E2)

Calculations of electromagnetic properties give us a good test of the nuclear models prediction. The electromagnetic matrix elements between eigenstates were calculated using the programs *NPBTRN* for IBM-2 model.

From Eq. (2-47), we note that an E2 transition mainly depends on identifying proton and neutron bosons effective charges e_f and e_ϵ . The relationship between (e_f, e_ϵ) and the reduced transition probability B(E2) for rotational limit $SU(3)$ is given in the form [77]:

$$B(E2; 2_1^+ \rightarrow 0_1^+) = \frac{(2N + 3)(e_f N_f + e_\epsilon N_\epsilon)}{5N} \dots\dots\dots (3-4)$$

This relation was used to estimate the effective boson charges for proton and neutron bosons (e_f, e_ϵ) . In these calculations, we use the following criteria to determine the effective charges. $e_f = 0.1165 e.b$ is constant throughout the whole isotopic chain and the e_ϵ changes with the neutron number. This is true if the neutron (proton) interaction does not depend on the proton (neutron) configurations. The values of e_f and e_ϵ are determined by fitting to the five $B(E2; 2_1^+ \rightarrow 0_1^+)$ and $B(E2; 2_2^+ \rightarrow 2_1^+)$ in ^{174}Hf . They are given in Table (3-22).

Table (3-22): Effective charge used in E2 transition calculations ($e_f = 0.1165 e.b$).

Isotopes	^{172}Hf	^{174}Hf	^{176}Hf	^{178}Hf	^{180}Hf
e_ϵ (eb)	0.266	0.319	0.301	0.330	0.350

It is well known that absolute gamma ray transition probabilities offer the possibility of a very sensitive test of nuclear models and the majority of the information on the nature of the ground state has come from studies of the energy level spacing. The transition probability values of the excited state in the ground state band constitute another source of nuclear information. Yrast levels of even-even nuclei ($J_i = 2, 4, 6, \dots$) usually decay by E2 transition to the lower lying yrast level with $J_f = J_i - 2$.

In Table (3-5), we show the $B(E2;2_1^+ \rightarrow 0_1^+)$ and $B(E2;4_1^+ \rightarrow 2_1^+)$ values, which are of the same order of magnitude and display a typical decrease towards the middle of the shell.

As a consequence of possible $M1$ admixture, the $B(E2;2_2^+ \rightarrow 2_1^+)$ quantity is rather difficult to measure. For $^{170-180}\text{Hf}$ isotopes, we give the different, conflicting experimental results and we see that no general feature be derived from them, from these values seems to decrease for $^{172-174}\text{Hf}$ and increase for $^{176-180}\text{Hf}$.

In the same table, we show $B(E2;2_2^+ \rightarrow 0_1^+)$ values. Experimentally, the results are radically different for the Hf isotopes. In the some Hf isotopes, the value seems to increase towards the middle of the shell, whereas in another Hf isotopes, is decreased. Our calculations could not reproduce these contradictory features simultaneously.

The quantity $B(E2;0_2^+ \rightarrow 2_1^+)$, which is shown in Table (3-5), provides a second clue for identifying intruder 0_2^+ states. If the experimental $B(E2;0_2^+ \rightarrow 2_1^+)$ value is small, it largely deviates from the results of our calculation. It is very likely that the observed 0_2^+ states do not correspond to the collective state, but it is rather an intruder state.

In ^{180}Hf isotope, there is a good agreement between experimental and calculated $B(E2;0_2^+ \rightarrow 2_1^+)$ value. This confirm, our earlier statement about the nature of the lowest 0_2^+ state in this isotope. Other transitions are small values because these transitions are between different bands (cross over transitions).

The electric transition probabilities from the mixed-symmetry state $J^f = 1^+$ to the symmetric states $(2_1^+, 2_2^+)$ is a weak collective $E2$ transition. The $E2$ transition between the 1^+ and the 2^+ ground state is small, whereas $E2$ transitions are large between fully-symmetric states and between mixed-symmetry states.

To conclude this section on the $E2$ properties, we give the results for the quadrupole moments $Q(2_1^+)$ of the first excited Table (3-5) (see equation (2-49)). We show complication of theoretical results. The general features of these results are clear, namely an increase in the negative quadrupole moment with the increasing neutron number.

3.3.4 Magnetic Transition Probability and Mixing Ratio u ($E2/M1$)

The M1 transition operator is given in Eq. (2-52), where the gyromagnetic factors for bosons g_f and g_ϵ are estimated. The reduced E2 and M1 matrix elements were combined in a calculation of mixing ratio $u(E2/M1)$ using the relation which is given by Eq. (2-54).

Sambatora *et al.*, [109] suggested a total g -factor which is given in the following equation:

$$g = g_f \frac{N_f}{N_f + N_\epsilon} + g_\epsilon \frac{N_\epsilon}{N_f + N_\epsilon} \dots\dots\dots(3-5)$$

it is used to compute the 2_1^+ state g -factor. The value of the measured magnetic moment for ^{178}Hf isotope, $\sim 2g = 0.48(3)\sim_N$ [110], and the experimental mixing ratio $u(E2/M1; 2_2^+ \rightarrow 2_1^+) = 0.410eb/\sim_N$ [68] for ^{178}Hf isotope were used to produce suitable estimation for the boson gyromagnetic factors. The values are $g_f = 0.70\sim_N$ and $g_\epsilon = 0.05\sim_N$. The results of the calculations are listed in Table (3-6).

From the results of $B(M1)$, the transitions between low-lying collective states in IBM-1 and IBM-2 vanish is not necessarily a consequence of F -spin symmetry, but may be related to the existence of other symmetries, like SU (3). The M1 excitation strength for the $B(M1; 1_1^+ \rightarrow 0_1^+)$ transition is proportional to the factor g_ϵ^2 and depends only weakly on the strength of Majorana force.

The magnetic dipole moment for the first excited state in even-even $^{172-180}\text{Hf}$ isotopes in Table (3-6) provides a sensitive test of the effective boson number in the IBM-2 framework. In $^{172-180}\text{Hf}$ isotopes with $N = 100-$

108, it confirms the validity of assuming a drastic change in number of proton boson when the number of neutron boson increased from 106 to 108.

The E2/M1 multipole mixing ratios for $^{172-180}\text{Hf}$ isotopes, $u(E2/M1)$, were calculated for some selected transitions between states. The sign of the mixing ratios must be chosen according to the sign of the reduced matrix elements. The equations used are (2-52) for M1 transitions and (2-54) for the mixing ratios. The results are listed in Table (3-7). The agreement with available experimental data [68,110] is more than good especially in the sign of the mixing ratio. However, there is a large disagreement in the mixing ratios of some transitions. It is not due to a dominant E2 transition, but may be under the effect of a very small value of M1 matrix element. However, it is a ratio between very small quantities and may change in the denominator that will have a great influence on the ratio.

For $\chi \rightarrow \chi$ transitions, the intraband $B(E2)$ values have been estimated by assuming that the intrinsic E2 matrix elements in the ground and gamma bands are equal. Then, combining these $B(E2)$ values with the measured E2/M1 mixing ratios leads to the tabulated $B(M1)$. We note that in IBM, the intrinsic E2 matrix element of the gamma band is *smaller* than that of the ground band due to the finite dimensionality of the boson space. Using the IBM intrinsic E2 matrix elements instead of the pure rotational ones would thus lead to smaller *experimental* $\chi \rightarrow \chi$ M1 matrix elements, which would improve the agreement with the calculation.

The results for the $\chi \rightarrow g$ and $\chi \rightarrow \chi$ mixing ratios, the sign of the mixing ratios is not arbitrary. For large majority of the $\chi \rightarrow g$ transitions considered in Table (3-7) the experimentally known u 's are negative; the sign is not known for $\chi \rightarrow \chi$. According, we have assumed that all $u(\chi \rightarrow g)$

values are negative in some transitions and used then as a constraint on the parameters t_f and t_ϵ . Specially, it implies that $t_\epsilon - t_f > 0$.

The calculated $x \rightarrow g$ M1 transition probability in Table (3-6) has been obtained by a recourse to the IBM-2: the $u(E2/M1)$ mixing ratios from the complication of Lang *et al.*, [68] from this work are combined with the $B(E2; 2_3^+ \rightarrow 0_1^+)$ values and the conventional band mixing parameters. Note that in a few cases the asymmetric errors on the measured mixing ratio values have been incorporated in the M1 matrix elements by shifting the central value slightly to ensure that the overall error range denoted is correct.

These results exhibit disagreement in some cases, with one case showing disagreement in sign. However, it is a ratio between very small quantities and any change in the dominator that will have a great influence on the ratio. The large calculated value for $2_2^+ \rightarrow 2_1^+$ is not due to a dominant E2 transition, but may be under the effect of very small M1 component in the transition. Moreover, the large predicted value for transition $2_2^+ \rightarrow 2_1^+$ in ^{180}Hf compared to the experimental value may be related to the high predicted energy level value of the IBM-2; $E(2_2^+) = 1.162$ MeV, while the experimental value is 1.174 MeV. We are unable to bring the energy value of this state close to the experimental value simply by changing the Majorana parameters.

Most experimentally observed low-spin levels, apart from 1^+ states below 2.5 MeV; have their counterpart in the **IBM-2** level spectrum although the energy match is not good in every case. It also appears that we may identify the members of the family of mixed-symmetry states corresponding to the $[N-1, 1]$ representation [77]. The small E2/M1 mixing ratios are consistent with this interpretation but level lifetimes are required for a firmer identification.

3.3.5 Electric Monopole Transition Matrix element

The $E0$ monopole matrix element is given in Eq. (2-58). The parameters in Eq. (2-57) can be predicted from the isotope shift [110], $\Delta \langle r^2 \rangle = 0.098 \text{ fm}^2$ for ^{178}Hf - ^{180}Hf and $\Delta \langle r^2 \rangle = 0.048(4) \text{ fm}^2$ for ^{180}Hf - ^{182}Hf , since such data are not available for Hf isotopes. These parameters are calculated by fitting procedure into two experimental values of isotopic shifts (Eq. (2-60)). The parameters which were subsequently used to evaluate the $\dots(E0)$ -values were; $s_{of} = 0.056 \text{ fm}^2$, $s_{oe} = 0.028 \text{ fm}^2$ and $x_{oe} = 0.032 \text{ fm}^2$. From Table (3-8), there is no enough experimental data to compare with the IBM-2 calculations.

The monopole matrix element is important for nuclear structure and the model predictions due to their sensitivity for the nuclear shape. We conclude that more experimental work is needed to clarify the band structure and investigate an acceptable degree of agreement between the predictions of the models and the experimental data.

Table (3-9) contains the experimental and calculated $X(E0/E2)$ values. In general there is good agreement except for the $0_3^+ \rightarrow 0_1^+$ and $0_4^+ \rightarrow 0_1^+$, transitions but it is not possible to say if these disagreements are attributed to the $E0$ or $E2$ component in the ratio. The disagreement in the results for some transitions could be removed by interchanging the ordering since for the higher lying states, the correspondence between the experimental and theoretical levels is uncertain.

It must also be remarked that the comparatively large X -values for transitions from the 2_3^+ mixed-symmetry state and from the 2_2^+ states indicate that substantial $E0$ components occur in these decays from mixed-symmetry states. The $E0$ matrix element describing such decay is proportional to $s_{oe} - s_{of}$ and, although the $s_{0\dots}$ values are small, their sign difference results in $E0$ matrix being greatest.

In making this comparison, we have assumed that all the identified 0^+ levels correspond to **IBM** states and that the experimental level ordering is the same as the calculated order. Some previous work, attempted to fit levels in several $^{170-180}\text{Hf}$ isotopes [20] with a single set of regularly varying parameters, has not been successful for $^{176-178}\text{Hf}$. These isotopes are distinctly different from their neighbors; the 2_2^+ lies well above the 4_1^+ level at the two phonon energies.

3.3.6 Mixed Symmetry States in $^{172-180}\text{Hf}$ Isotopes

One of the advantage of the IBM-2 is the ability to reproduce the mixed symmetry states. These states are created by a mixture of the wave function of protons and neutrons that are observed in most even-even nuclei. These mixed symmetry states (*MSSs*) have been observed in many nuclei. In more vibrational and χ - *soft* nuclei these mixed symmetry states (*MSSs*) have been observed in many nuclei. In more vibrational and gamma soft nuclei. We expect the lowest MSS with $J^f = 2^+$ state, while in rotational nuclei observed as the $J^f = 1^+$ state. In $^{170-180}\text{Hf}$ isotopes, we see that when the states $J^f = 2_2^+, 2_4^+$ and 3_1^+ are strongly dominated by the $F=F_{max}$, the strongest contribution to the $J^f = 2_3^+, 3_2^+$ states is the one with $F=F_{max-1}$. We can see the $J^f = 2_3^+, 3_2^+$ states as mixed symmetry states in $^{170-180}\text{Hf}$ isotopes.

In this work, we proposed that the 2_3^+ state decays to the first excited state with an energy 1.226 MeV in ^{174}Hf with a mixing ratio $u(E2/M1) = 2.467 \text{ eb} / \sim_N$ which means it is dominated by the M1 transition, with $B(M1)$ equal to $0.0026 \sim_N$. In ^{178}Hf isotope, for the third $J = 2^+$ state at energy 1.274 MeV excitation is close to the experimental data for 1.276 MeV. The energy is well reproduced by the calculation, where the choice of the Majorana parameters plays a crucial role. This state is quite pure F_{max-1} with $R = \langle J | F^2 | J \rangle / F_{max} (F_{max} + 1) = 50\%$. The excitation energy of 3_2^+ state is 2.109 MeV with mixing ratio

$u(E2/M1; 3_2^+ \rightarrow 2_1^+) = 0.0231eb/\sim_N$, $B(M1; 3_2^+ \rightarrow 2_1^+) = 0.0054\sim_N^2$. In the ^{178}Hf , the calculation predicted the 2_3^+ state at 1.274 MeV with $R = 83\%$.

In other isotopes, the states 2_3^+ and 3_2^+ are mixed symmetry states, their excitation energies are close to available experimental data and the values of $R = 73\%, 75\%, 72\%$ and 80% respectively.

The energy that fits to several levels is very sensitive to the parameters in the Majorana term which also strongly influences the magnitude and sign of the multipole mixing ratios of many transitions. In particular, we find that the calculated energies of a number of states are affected in a very similar way and these might be considered to have a mixed-symmetry origin, or contain substantial mixed-symmetry components. Those with a mixed-symmetry origin have no counterpart in IBM-1. The energy dependence of the 2_2^+ and 2_4^+ levels is consistent with the mixed-symmetry character of the 2_3^+ level being shared with neighboring states.

The influence of the different parameters (see Table (3- 23)) on these states is shown in Figure (3.12). The \langle_2 term strongly affects the energies of all of the levels considered to have a mixed-symmetry character or to contain mixed-symmetry components. In obtaining this plot, the \langle_1 and \langle_3 terms were maintained at their best-fit values.

Table (3-23): IBM-2 Parameters of $^{172-180}\text{Hf}$, all parameters in MeV units except the parameters t_f and t_v are dimensionless used in mixed symmetry states.

Isotopes	v	$ $	t_ϵ	t_f	\langle_1	\langle_3	\langle_2	$C_{0\dots}$	$C_{2\dots}$	$C_{4\dots}$
^{172}Hf	0.522	-0.029	-0.9	-0.9	0.07	0.02	0.120	-0.151	0.08	0.0
^{174}Hf	0.525	-0.035	-0.85	-0.9	0.08	0.022	0.121	-0.151	0.072	0.0
^{176}Hf	0.528	-0.031	-1.02	-0.9	0.083	0.22	0.130	-0.151	0.075	0.0
^{178}Hf	0.530	-0.033	-0.8	-0.9	0.09	0.23	0.160	-0.151	0.09	0.0
^{180}Hf	0.532	-0.035	-1.0	-0.9	0.11	0.026	0.20	-0.151	0.09	0.0

The mixing ratio data have a strong dependence on \langle_2 and it has been shown that \langle_2 cannot be zero in our fit. The 1^+ level is strongly affected by changing \langle_1 , Figure (3-12), while the 3_1^+ level energy depends on the \langle_3

value as shown in Figure (3-12). The 2_3^+ mixed-symmetry state and the predominantly symmetric 2_2^+ and 2_4^+ levels are largely unaffected by changing κ_1 , or κ_3 in contrast to their dependence on κ_2 , see Table (3-24).

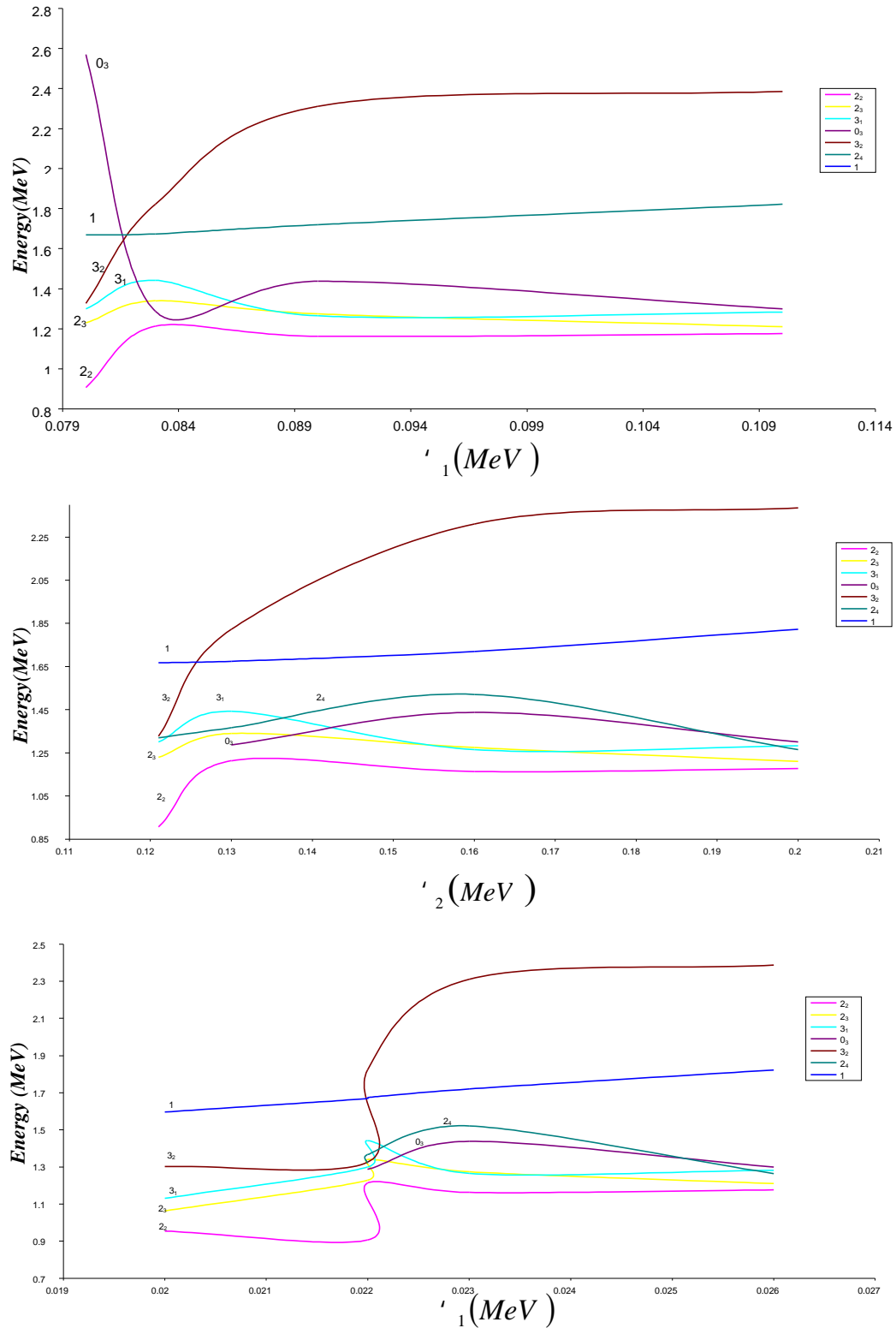


Fig. (3-12): The change in level energy as $\kappa_1, \kappa_2, \kappa_3$.

The F -spin components in the 2_2^+ , 2_3^+ , 2_4^+ and 0_3^+ levels as a function of \langle_2 are shown in Figure (3-13). Our \langle_i parameters, of Table (3-23), obtained from the level energy fit disagree with those obtained by Subber [20]. He found \langle_1 and \langle_3 to be large and negative and \langle_2 small and negative.

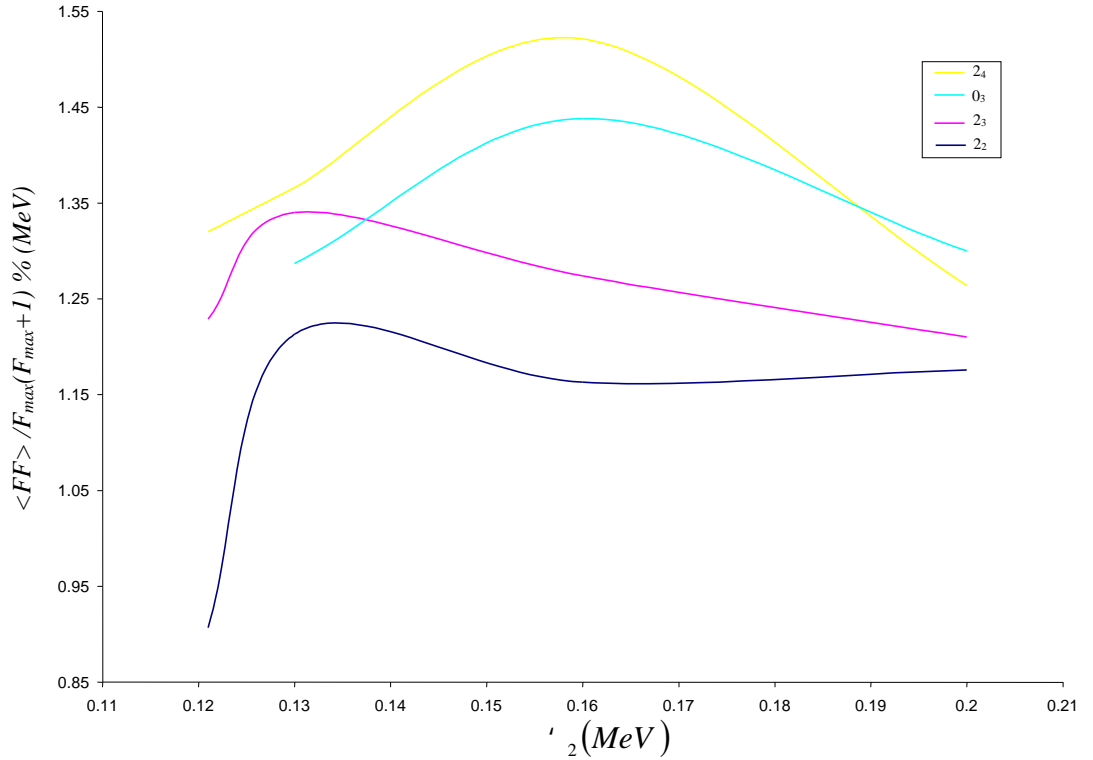


Fig. (3-13): F-spin components in the 2_2 , 2_3 , 2_4 and 0_3 levels as a function of \langle_2 when all other parameters are as in Table (3-22).

Table (3-24): Mixing Ratio $u(E2/M1)$ for $^{172-180}\text{Hf}$ in eb/\sim_N units.

$J_i^+ \rightarrow J_f^+$	^{172}Hf		^{174}Hf		^{176}Hf		^{178}Hf		^{180}Hf	
	Exp.	IBM-2	Exp.	IBM-2	Exp.	IBM-2	Exp.	IBM-2	Exp.	IBM-2
$2_2 \rightarrow 2_1$	-	0.031	-2_{-2}^{+2}	-6.377	$ u \geq 4$	12.701	0.410	0.731	$9.8_{-3.2}^{+3.6}$	14.257
$2_3 \rightarrow 2_1$	-	12.60	-	2.467	-	12.0	$u < 32$	20.71	$6.8_{-3.2}^{+3.6}$	8.190
$3_1 \rightarrow 2_1$	-	5.510	-	20.238	-	3.098	-	2.818	-	0.045
$3_1 \rightarrow 4_1$	-	0.044	-	5.261	-	-	-	10.97	-	-
$4_2 \rightarrow 4_1$	-	-0.09	$-2.5_{-0.7}^{+13}$	-4.980	$ u \geq 0.7$	0.781	-	0.0981	4.5(1.1)	10.981
$2_4 \rightarrow 4_1$	-	0.123	0.00039	0.0051	0.022	0.0424	$-0.74_{-0.12}^{+0.19}$	-0.561	-	-
$2_5 \rightarrow 2_1$	0.022	0.90	-	0.098	-	0.123	-	-0.76	-	0.87
$2_6 \rightarrow 2_1$	-	1.56	-	2.780	-	3.907	-	-0.84	-	3.09
$2_4 \rightarrow 4_1$	-	11.5	-	8.97	-	12.87	-	0.098	-	1.134
$1 \rightarrow 2_1$	-	0.0887	-	1.605	-	0.5674	-	22.701	-	1.3559
$1 \rightarrow 2_2$	-	0.0492	-	2.104	-	0.0614	-	3.617	-	0.0492
$1 \rightarrow 2_3$	-	2.227	-	0.855	-	3.560	-	0.527	-	2.227

In $^{172-180}\text{Hf}$ isotopes, all hitherto discovered *MSSs* have been reviewed in [126]. It has been shown that the lowest lying *MSSs* is the one quadrupole phonon *MSS* labeled as $2_{1,M_s}^+$, $3_{1,M_s}^+$ and characterized by a weakly-collective *E2* transition probability to the ground state and a large *M1* transition to the 2_1^+ state.

The reduced transition probability $B(E2;0_1^+ \rightarrow 2_M^+) = 0.064e^2b^2$, in the two cases the $B(E2;0_1^+ \rightarrow 2_M^+)$ value is smaller than $B(E2;0_1^+ \rightarrow 2_1^+)$ by a factor of ~ 100 , making the identification of the 2_M^+ state in electron scattering experiment difficult. In addition, the mixing with background two-quasi-particle states will render the observation of the 2_M^+ state even more complicated. In $^{172-180}\text{Hf}$ isotopes the 2_M^+ level belonging to a $K^f = 1^+$ band, a second mixed symmetry 2^+ state occurs, which is the head of a $K^f = 2^+$ band.

The information of 1_M^+ decay became available on the decay intensities from 1_M^+ level toward the 0_1^+ and 2_1^+ ground band members. The ratio $B(M1;1_M^+ \rightarrow 0_1^+)/B(M1;1_M^+ \rightarrow 2_1^+) = 2$. The same result from the Alaga rule (which predicts it as the ratio of two Clebsch- Gordan coefficients, i.e., $(11\ 1-1|00)^2 / (11\ 1-1|20)^2 = 2$) and, hence, the result does not constitute a good test of the IBM-2. In the IBM-2 exact ratio [120]:

$$\frac{B(M1;1_M^+ \rightarrow 0_1^+)}{B(M1;1_M^+ \rightarrow 2_1^+)} < 2$$

Thus, this predicted ratio is slightly less than the corresponding ratio derived from the Alaga rule, due to the Finite- N character of the IBM. It would be interesting to know whether this deviation from the Alaga rule is confirmed experimentally.

Most characteristics and measurable quantities of *MSS* states is the electromagnetic decay by allowing *F*-vector any *M1* transition to symmetric states. This is an important feature because the *M1* transitions between *FSS* are prohibited and therefore *M1* transition is a distinct of *MSS*

states. The M1 transitions between *MSS* and *FSS* are proportional to the quantity $[(g_f - g_\epsilon)^2 N_f N_\epsilon]$, while, E2 transitions between *FSS* are proportional to the quantity $(e_f N_f + e_\epsilon N_\epsilon)^2$ and E2 transition between *MSS* and *FSS* are proportional to the quantity $(e_f - e_\epsilon)^2 N_f N_\epsilon$. The proportionality factors that depend on the structures of the wave functions are included.

3.4- ¹⁸⁰⁻¹⁹⁰W Isotopes in IBM-2

3.4.1 Hamiltonian Interaction Parameters

The program *NPBOS* [71] was used to diagonalize the Hamiltonian. The electromagnetic matrix elements between eigenstates were calculated using the program *NPBTRN*. The isotopes ¹⁸⁰⁻¹⁹⁰W have $N_f = 4$, and N_ϵ varies from 5 to 10, while the parameters v , $|$, and t_ϵ , as well as the Majorana parameters $\langle_1 = \langle_3$ and \langle_2 , were treated as free parameters and their values were estimated by fitting to the measured level energies. This procedure was made by selecting the ‘traditional’ values of the parameters and then allowing one parameter to vary while the parameter t_f keeping constant until the best fit was obtained. The IBM-2 parameters obtained for ¹⁸⁰⁻¹⁹⁰W are summarized in Table (3-25).

The Hamiltonian parameters are fitted to obtain the excitation energies and the electromagnetic properties in the following way. The least-squares that fit the excitation energies of each isotope was attempted in the full IBM-2 calculation. Only six parameters, however, were varied in the fit, namely [43]:

$$v = \frac{N_f}{N} v_f + \frac{N_\epsilon}{N} v_\epsilon \dots \dots \dots (3-6a)$$

$$t = \frac{N_f}{N} t_f + \frac{N_\epsilon}{N} t_\epsilon \dots \dots \dots (3-6b)$$

$$| = |_f |_\epsilon \dots \dots \dots (3-6c)$$

$$C_L = [N_f(N_f - 1)C_{Lf} + N_\epsilon(N_\epsilon - 1)C_{L\epsilon}] / N(N - 1) \dots \dots \dots (3-6d)$$

where $L = 0, 2, 4$

while the differences

$$\Delta V = V_f - V_\epsilon \dots\dots\dots(3-7a)$$

$$\Delta t = t_f - t_\epsilon \dots\dots\dots(3-7b)$$

$$\Delta C_L = C_{Lf} - C_{L\epsilon} \dots\dots\dots(3-7c)$$

The earlier results of Duval and Barrett [38] for the W isotopes, and those of Bijker *et al.*, [127] for the Os and Pt isotopes are characterized by sharply rising values of t_ϵ , with change of sign over the neutron number in the range 108-112. In the present work t_ϵ rises, but less sharply, and it does not become positive for $^{186-190}\text{W}$ isotopes. In contrast to this, references [38,127] have fixed values of the Majorana parameters, while we find them to rise sharply as the neutron number increases. The reason for these significant differences is that we have included the u mixing ratios in the fits to obtain the best parameters.

The structure of the energy spectra is determined mainly by the first three terms on the right-hand side of Eq. (2-42) (the pairing plus quadrupole terms), while the remaining terms have minor, but non-negligible contributions. This is borne out by our calculations for the $^{180-190}\text{W}$ isotopes. We expect the importance of V_{ff} term (or the $V_{\epsilon\epsilon}$ term) to be manifest when there are many more proton bosons than neutron bosons (or vice-versa). We also assume that those parameters in the Hamiltonian labeled with a f depend only on proton number and those labeled with a ϵ depend only on neutron number. Those left un-subscripted may depend on both proton and neutron numbers.

We now apply the IBM-2 model to the calculation of the energy spectra of the tungsten isotopes ($Z=74$, $N_f = 4$ and $82 < N < 126$). To reduce this number of free parameters, the following simplifications are made.

First: we set $v_f = v_\epsilon = v$, which is the usual assumption. This might seem an oversimplification, especially since the proton bosons and neutron bosons are in different shells. However, calculations using

this assumption have led to reasonable results, not only for $^{180-190}\text{W}$, but also for other nuclides.

Second: we include the $C_{L\dots}$ terms in the V_{\dots} interaction since for most of all region fitted, $N_{\epsilon} > N_f$ and we do not expect the V_{ff} term to be very important.

Third: in the Majorana term, we set κ_2 and $\kappa_1 = \kappa_3$ values in Table (3-25) for the entire isotopic chain. The Majorana term is used primarily to push up the energy of those states with large anti-symmetric parts. Since the low-lying collective states are largely asymmetric, we then expect the influence of the Majorana term on these states to be minimal.

The experimentally determined energy levels for the even-even $^{180-190}\text{W}$ isotopes span the range in neutron number from $N = 106$ to $N = 116$. We can make predictions beyond this region by smooth extrapolation of the above parameters.

3.4.2 Energy Spectra

The IBM-2 parameters obtained for $^{190-180}\text{W}$ are summarized in Table (3-25). The boson numbers used $N_f = 4$ and N_{ϵ} vary from 5 to 10 respectively. The corresponding calculated and experimental energy spectra are shown in Figures (3-6) to (3-11). It is apparent that the calculated spectra are in a good agreement with the experimental ones. A characteristic feature of the present calculation is the appearance of nonzero C_L terms. Excluding those terms from the fit and setting them to zero would lead to a substantially worse description of the spectra. From Table (3-25) we observe that t_f remains almost constant for all the isotopes, while v and t_{ϵ} increase from ^{186}W to ^{190}W . The C_L parameters get reduced on average with increasing N_{ϵ} .

Table (3-25): IBM-2 Parameters for $^{180-190}\text{W}$ Isotopes, all parameters in MeV units except t_f and t_ϵ are dimensionless.

Parameter	^{180}W	^{182}W	^{184}W	^{186}W	^{188}W	^{190}W
v	0.51	0.52	0.52	0.53	0.54	0.54
K	-0.122	-0.121	-0.22	-0.23	-0.123	-0.11
t_f	-1.6	-1.6	-1.6	-1.6	-1.6	-1.6
t_ϵ	-0.089	-0.09	-0.095	0.001	0.02	0.04
\langle_2	0.021	0.039	0.04	0.136	0.161	0.161
$\langle_1 = \langle_3$	0.092	0.1	0.1	0.4	0.4	0.41
C_{of}	-0.521	-0.487	-0.437	-0.383	-0.289	-0.277
C_{2f}	-0.321	-0.295	-0.260	-0.225	-0.201	-0.190
C_{4f}	0.185	0.132	0.105	0.049	-0.060	-0.070
C_{o^-}	-0.523	-0.420	-0.357	-0.343	-0.287	-0.278
C_{2^-}	-0.165	-0.172	-0.180	-0.185	-0.202	-0.221
$C_{4\epsilon}$	0.011	0.019	0.025	0.089	-0.060	-0.070

The examination of the experimental and IBM-2 energy levels ratios (Table (3-11)) for the $^{180-190}\text{W}$ isotopes shows that they lie in the transitional region $SU(3) \rightarrow O(6)$, therefore the Hamiltonian of the transition region $SU(3) \rightarrow O(6)$ has been employed in the calculation by using the program *NPBOS* [71].

Our calculated energy spectrum is shown in Figures (3-6) to (3-11). The root means square deviation (*rmsd*) for the ground, beta and gamma bands totaling levels are 0.109, 0.82 and 0.80 MeV for Duval and Barrett [38] and the present work respectively. (Since the values obtained by Duval and Barrett [38], were interpolated from their level energy plot, small errors may arise and a figures representing their goodness of fit could not be determined accurately). In all four cases, the overall agreement with the experimental energy levels is quite good and shows a strong dominance of the rotational $SU(3)$ symmetry. A comparison of the parameters used to obtain these energy spectra reveals some important points.

These calculations depend on two parameters obtained from a fit of the 2_1^+ and 4_1^+ levels in nuclei in the region. The relative spacing of the

levels is satisfactory although the overall energy fit is not nearly as good as for the IBM-2 results.

In Figures (3.6) to (3.11), we present the results of our calculation of the energy levels for the isotopes chain ^{180}W to ^{190}W , and in figures we give a detailed comparison with the experimental data according to the quasi-ground state rotational band and the quasi gamma and beta vibrational bands.

Perhaps the most striking feature of the energy spectra is the sharp rise in the beta and gamma bands at neutron number $N = 108$, which may be due to a sub-shell in the $i_{13/2}$ Nilsson level and/or a reversal in the deformation. This is supported by such effects as a large change in the two neutron separation energy after $N = 108$. The same rise also occurs in the gamma band of the neighboring Os isotopes ($Z=76$). Fitting this has led to a dip in the value of t_ϵ at $N=108$. Note that the IBM-2 predicts a dramatic increase in the 0_3^+ state at this neutron number [38].

Another interesting feature is a relatively sharp increase in the ground state band at $N=104$. Once again, this same feature shows up in the Os data. When the ground state band is fitted for ^{180}W , the IBM-2 predicts even larger increases in the higher energy levels of the gamma and beta bands. In general, the agreement with experimental for the ground state band and gamma and beta bands energy levels is quite good. The agreement with the high spin states energies, however, is not successful, notably in ^{186}W and ^{188}W isotopes.

The root means square deviation (*rmsd*) (Eq. (3-1)) is used to compare the experimental and IBM-2 energy levels (see Tale (3-12)). In this table we see the ground state levels, the best agreement was found in ^{180}W isotope where the smallest value of *rmsd* equals 0.0024 and equals 0.010 for gamma band in ^{186}W isotope. However, *rmsd* equals 0.0062 for beta band in ^{190}W isotope.

3.4.3- Electric Transition Probability B(E2)

Having obtained the wavefunctions for the energy states in the $^{180-190}\text{W}$ isotopes by fitting to the experimental energy levels, we can determine the electromagnetic transition rates between these states. The most general single-boson transition probability of angular momentum $J = 2$ given in Eq. (2-47).

In principle, the parameters t_f and t_ϵ may be different from those in the quadrupole operators in the Hamiltonian (Eq. (2-42)), however, we have taken to be the different in our calculations so as to reduce the number of free parameters.

From Eq. (2-47), it can be noted that, the reduced transition probability B(E2) is dependent on e_f and e_ϵ . The relationship between (e_f, e_ϵ) and the reduced transition probability B(E2) for rotational limit SU (3) is given in Eq. (3-4) [77]. This relation was used to estimate the effective boson charges for proton and neutron bosons (e_f, e_ϵ) . In this calculation, we use the following criteria to determine the effective charges. $e_f = 0.151$ e.b is constant throughout the whole isotopic chain and the e_ϵ changes with neutron number. This is true if the neutron (proton) interaction does not depend on the proton (neutron) configurations. The values of e_f and e_ϵ are determined by fitting to the five $B(E2; 2_1^+ \rightarrow 0_1^+)$ and $B(E2; 2_2^+ \rightarrow 2_1^+)$ in ^{186}W . They are given in Table (3-26).

Table (3-26): Effective charge used in E2 transition calculations ($e_f = 0.151$ e.b).

Isotopes	^{180}W	^{182}W	^{184}W	^{186}W	^{188}W	^{190}W
e_ϵ (eb)	0.100	0.110	0.120	0.130	0.140	0.150

The boson effective charges (e_f, e_ϵ) have the same dependence on proton number and neutron number as do $|_f$ and $|\epsilon$ however, as an even further simplification Duval and Barrett [38] used $e_f \neq e_\epsilon$ equals a constant for all isotopes.

The results of the calculations are presented in Table (3-14). Looking through the table, one can easily recognize that our calculations reproduce the experimental data quite well.

The $B(E2;2_1^+ \rightarrow 0_1^+)$ and $B(E2;4_1^+ \rightarrow 2_1^+)$ values decrease as the neutron number increases toward the middle of the shell as the value of $B(E2;2_2^+ \rightarrow 2_1^+)$ has a small value because it contains admixture of M1. As a consequence of possible M1 admixture, this quantity is rather difficult to measure. The value of $B(E2;2_2^+ \rightarrow 0_1^+)$ is small because this has a transition from a quasi-beta band to a ground state band (cross over transition).

In Table (3-14), the $B(E2)$'s obtained between the ground state band agrees almost perfectly with the experiment. The agreement of the IBM-2 $B(E2)$'s with the experiment, for transitions from beta and gamma bands states to the ground band states is also rather good, though not as good as it is for transitions within the ground band states.

The results for $B(E2;2_2^+ \rightarrow 0_1^+)$ and $B(E2;2_3^+ \rightarrow 0_1^+)$ values are rather small since this transition is forbidden in all three limits of IBM [54]. Our agreement with the available data is generally quite good. It should be noted that no attempt was made to fit any of the $B(E2)$ values while determining the parameters in the Hamiltonian.

One of the important properties which can be calculated is the branching ratios, through which one can identify the position for the nuclei studied in Casten triangle, and hence to identify the dynamic symmetry for the nuclei by using the Alaga rule. Table (3-27) shows the branching ratios for $^{182-186}\text{W}$. These are compared to the experimental data. Our agreement with available data is generally quite good, but it must be noted that in the $B(E2;2_2^+ \rightarrow 2_1^+)/B(E2;2_2^+ \rightarrow 0_1^+)$ branching ratio the denominator is small and hence the ratio is very sensitive to experimental errors and/or precision in the numerical calculation.

Table (3-27): Branching ratios for $^{182-186}\text{W}$ Isotopes.

Isotopes	$B(E2;2_2^+ \rightarrow 2_1^+)/B(E2;2_2^+ \rightarrow 0_1^+)$			$B(E2;2_3^+ \rightarrow 2_1^+)/B(E2;2_3^+ \rightarrow 0_1^+)$		
	EXP.	IBM -1	IBM -2	EXP	IBM-1	IBM-2
^{180}W	-	1.414	1.654	-	2.541	2.561
^{182}W	1.95	1.561	1.930	-	2.877	2.570
^{184}W	1.88	1.971	1.837	3.60	3.158	3.871
^{186}W	2.37	3.872	20572	-	3.647	4.100
^{188}W	-	3.881	2.120	-	3.771	4.210
^{190}W	-	3.921	2.223	-	3.821	4.228

Experimental data taken from ref. [128]

The E2 transition operators is, in fact, a quadrupole operator moments for a nucleus in state characterized by angular momentum $J = 2$, is given by the Eq. (2-49). Using the IBM-2 wavefunction and E2 transition operator given by Eq. (2-47), we obtain the results shown in Table (3-14) for $J = 2_1^+$ and $J = 2_2^+$. Note that the parameters e_f and e_ϵ in the $T(E2)$ operator have already determined from fitting experimental $B(E2;2_1^+ \rightarrow 0_1^+)$ data and as before t_f and t_ϵ are the same numbers used in the Hamiltonian (Eq.(2-47)), so that we fit no new parameters in determining the quadrupole moments. The IBM-2 predicts the correct sign in both of the above cases, and the agreement with the experimental is very good for quadrupole moment for first excited state $Q(2_1^+)$. But, in the case of quadrupole moment for second excited state $Q(2_2^+)$, the IBM-2 values differ dramatically from the experimental data for ^{184}W . The experiment indicates a sharp decrease in $Q(2_2^+)$, for this isotope, which is not predicted by the IBM-2, but for other properties associated with the 2_2^+ state (i.e., energy levels and E2 transition), the IBM-2 agrees much better with the experiment.

3.4.4- Magnetic Transition Probability and Mixing Ratio u (E2/M1)

The magnetic dipole moment operator $T(M1)$ were calculated using Eq.(2-53), and the boson gyromagnetic factors g_f and g_ϵ were estimated using the fact that $g = Z/A$ and the relation (3-5), and one of the experimental $B(M1;2_2^+ \rightarrow 2_1^+) = 0.11 \sim \frac{2}{N}$ [117] for ^{186}W isotope, was used to

produce a suitable estimation for the boson gyromagnetic factors. These values are $g_f = 0.71 \sim_N$ and $g_\epsilon = 0.051 \sim_N$. They are different from those of the rare-earth nuclei, ($g_\epsilon - g_f = 0.65 \sim_N$), suggested by Van Isacker *et al.*, [129] also used $g_f = 1 \sim_N$ and $g_\epsilon = 0 \sim_N$ to reduce the number of the model parameters in their calculation of $M1$ properties in deformed nuclei. The results of our calculation are listed in Table (3-15). A good agreement between the theory and the available experimental data is achieved. As can be seen from the table, yields to a simple prediction that $M1$ matrix elements values for gamma to ground band and transitions should be equal for the same initial and final spin. Also the size of gamma to ground band matrix elements seems to decrease as the mass number increases.

The results show that the transitions between low-lying collective states are relatively weak. This is because of the increase of the anti-symmetric component in the wave functions introduced by F -spin breaking in the Hamiltonian. The magnitude of $M1$ values increases with increasing spin for $\chi \rightarrow g$ and $\chi \tilde{E} \chi$ transitions and we see:

1- By fitting $B(M1)$ from 2_2^+ to 2_1^+ we always get a small value for

$g_\epsilon - g_f$ compared to the value basis on the microscopic calculations

$$g_\epsilon - g_f = 1 \sim_N.$$

2- There are evidences that $M1$ small mode exists in all spectra.

3- One cannot make decisive conclusions related to the agreement between theoretical and experimental data from the above table due to the lack of experimental data. However, both experiments and IBM-2 predicts small $M1$ component which is due to symmetry and forbiddances of band crossing gamma transitions.

4- The $\chi \tilde{E} \chi$ $M1$ matrix elements are larger than the $\chi \tilde{E} g$ $M1$ matrix elements by a factor of 2 to 3. Again, this agrees qualitatively with the perturbation expressions derived in ref. [130].

5- The size of the $\chi \tilde{E} g$ M1 matrix elements seems to decrease with the increasing mass, specially, a change in $\chi \tilde{E} g$ M1 strengths occurs when the gamma band crosses the beta band.

These three aspects of M1 data shown in Table (3-15) are reproduced by the calculation through a smooth variation of the parameters ν and Δt , and with a few exceptions (e.g., some $\chi \tilde{E} g$ transitions in ^{186}W and $3_1^+ \rightarrow 2_1^+$ transition in ^{184}W). A good agreement between the theory and the experimental data is achieved.

The calculated values for B(M1) are acceptable to some extent as compared to the available experimental data, where some of B(M1) values are small compared to the values of the quadrupole transition probabilities because the wavelength of the gamma ray transitions is greater than it is in the magnetic transitions according to the following the relationship: $\} (ML) = 0.3A^{-2/3} \} (EL)$. This relation shows that the B(M1) transition probability is less than B(E2) transition probability and our results confirm this.

The *M1* properties of collective nuclei are certainly very sensitive to various, even small, components in the wave functions either of collective or non-collective character. In the $^{182-184}\text{W}$ isotopes it was shown that the inclusion of excitations across the major shell and two quasi-particle states is important. One expects that also for ^{188}W isotopes (which are near to closed shell for neutron) similar effects come into play. As the above analysis suggests, they can manifest in a considerable renormalization of IBM-2 boson *g*-factors from their slandered values. The magnetic dipole moment for first excited state is given by:

$$\sim = g_f L_f + g_\epsilon L_\epsilon \dots\dots\dots(3-8)$$

where g_f (g_ϵ) is the *g*-factor for the correlated proton (neutron) boson and L_f (L_ϵ) is the corresponding angular momentum operator. According to the microscopic foundation of the model, g_f (g_ϵ) is expected to depend, in the

first approximation, on proton (neutron) number N_f (N_ϵ) only, $g_f(N_f)$ and $g_\epsilon(N_\epsilon)$. The IBM-2 calculations for $\sim(2_1^+)$, $\sim(4_1^+)$ and $\sim(2_2^+)$ are listed in Table (3-15), where we see a good agreement with the experimental data.

It is clear that the two effects contribute to the dependence of the magnetic moments on proton and neutron number: the dependence of g_f and g_ϵ on proton and neutron number and the variation of the matrix elements of the operator $L_f(L_\epsilon)$ with N_f and N_ϵ . As will be better shown below, the former effect is related to the shell structure of the orbits, while the latter is related to the average number of proton and neutron boson taking part in the collective motion.

The characteristic of $M1$ of deformed nuclei is the summed $M1$ strength measured for rare-earth nuclei [131]. When calculated in the IBM-2, it is found to be proportional to $(g_f - g_\epsilon)^2$. If the Hamiltonian is F -spin invariant, the summed $M1$ strength is given by the Ginocchio sum rule [132] and is proportional to the average number of d bosons in the ground state. On the other hand, F -spin breaking may affect the summed $M1$ strength. Therefore, once one decides to study $M1$ properties using the IBM-2, as many characteristics as possible should be considered simultaneously [43].

Table (3-28) gives the g -factor in \sim_N units for $^{182-186}\text{W}$ isotopes for the first excited state (2_1^+) and second excited state (2_2^+) and compares it with the experimental data. The g -factor of a state $|k\rangle$ is given by [43]:

$$g_k = \frac{\langle k || T(M1) || k \rangle}{\langle || (\sqrt{3/4f})(L_f + L_\epsilon) || K \rangle} \dots\dots\dots(3-9)$$

Table (3-28): Experimental and IBM-2 calculations for g -factors for $^{182-186}\text{W}$ in \sim_N units.

g-factor	^{182}W		^{184}W		^{186}W		^{188}W	
	Exp.	IBM-2	Exp.	IBM-2	Exp.	IBM-2	Exp.	IBM-2
$g(2_1^+) \sim_N$	0.263(7)	0.266	0.288(7)	0.32	0.308(2)	0.43	-	0.49
$g(2_2^+) \sim_N$	-	0.099	0.12(4)	0.18	0.20(4)	0.33	-	0.36

Experimental data are taken from ref. [133].

We evaluate the mixing ratio $u(E2/M1)$ for $^{182-186}\text{W}$ isotopes depending on the Eq.(2-54). The results of IBM-2 calculation for $u(E2/M1)$ together with the experimental values are shown in Table (3-16). The g factors together with the experimental data are presented in Table (3-28). For this calculation we used the standard boson g - factors $g_f = 0.71 \sim_N$ and $g_\epsilon = 0.051 \sim_N$.

We were able to reproduce the 2_1^+ g -factors as well as most of the $u(E2/M1)$ mixing ratios. In particular, all the signs are reproduced correctly. It should be noted that a sign change appears in both the $u(2_2^+ \rightarrow 2_1^+)$ and $u(2_3^+ \rightarrow 2_1^+)$ transition mixing ratios, when going from ^{184}W to ^{182}W . Moreover, in ^{186}W there is an opposite sign between the $u(2_2^+ \rightarrow 2_1^+)$ mixing ratio and the $u(3_1^+ \rightarrow 2_1^+)$ mixing ratio. We were able to reproduce all of these features in the calculation. Mainly, the sign change of Δv and Δv for ^{182}W in comparison to $^{184-186}\text{W}$ is responsible for this effect. We also calculated the admixtures of lower F -spin states in the ground state. They are 1.6%, 2.2%, 1.3% for $^{186-184-182}\text{W}$, respectively.

The properties of low-lying levels in the $^{180-190}\text{W}$ isotopes have also been calculated within the context of the dynamic deformation model (**DDM**) [134]. In Ref. [134], the authors have mainly focused on an analysis of quadrupole moments, for which reasonable agreement is also obtained in the present IBM-2 calculations. Unfortunately, only one $u(E2/M1)$ mixing ratio is given in Ref.[134] ($-43 \text{ eb} / \sim_N$) for the $u(2_2^+ \rightarrow 2_1^+)$ transition in ^{186}W to be compared with the experimental value ($-11 \frac{+3}{-1} \text{ eb} / \sim_N$) and the IBM-2 result ($-13.201 \text{ eb} / \sim_N$). One should, however, keep in mind that the **DDM** approach is more microscopically motivated than the present phenomenologically oriented IBM-2 analysis.

The sign of the mixing ratio must be chosen according to the sign of the reduced matrix elements. The equations used are (2-52) for M1 transitions and (2-54) for the mixing ratios. The results are listed in Table

(3-16). The agreement with available experimental data [68,117] is more than good especially in the sign of the mixing ratio. However, there is a large disagreement in the mixing ratios of some transitions, is not due to a dominant E2 transition, but may be under the effect of very small value of M1 matrix element. However, it is a ratio between very small quantities and may change in the dominator that will have a great influence on the ratio.

3.4.5 Electric Monopole Transition Matrix element

Electric monopole (E0) transitions between nuclear levels proceed mainly by internal conversion with no transfer of angular momentum to the ejected electron. For transition energies greater than $2m_0c^2$, electron-positron pair creation is also possible; two-photon emission is possible at all energies but extremely improbable. The E0 transition also occurs in cases where the levels have the same spin and parity. This means that the E0 transition competes with E2 and M1 components in these transitions.

The reduced matrix monopole transition is given in Eq.(2-58), the necessary parameters of the monopole matrix element $...(E0)$ are derived from fitting the isotope and isomer shifts ($s_{of} = 0.078 fm^2$, $s_{oe} = -0.043 fm^2$). There is a good agreement with the experimental data (see Table (3-17)) for the transition $...(E0, 2_2^+ \rightarrow 2_1^+)$. Other IBM-2 results of $...(E0)$ values are available upon request.

In $^{182-186}W$ isotopes E0 values increased with the increasing neutron numbers and they go up to the highest value at ^{186}W isotope. This means that all the isotopes are deformed because they possess the amount of excess energy and that they are trying to get rid of this by lessen the E0 transitions to the state of stability. This is an additional evidence of the deformation of these isotopes.

We notice that the theoretical values for the X ($E0/E2$) ratio are small, for some transitions (see Table (3-18)) which means that there is a

small contribution of E0 transition on the life time of the 0^+ states. There are two high values of X ($E0/E2$) in transitions from $0_2^+ \rightarrow 0_1^+$ in $^{182-186}\text{W}$ isotopes means that this state decay mostly by the E0 and according to this one could say that the study of this state gives information about the shape of the nucleus, because the E0 transitions matrix elements are connected strongly with the penetration of the atomic electron to the nucleus. So combination of the wavefunction of atomic electron, which is well known, and the nuclear surface give good information of the nuclear shape.

Tables (3-19) and (3-20) shows theoretical versus experimental isomer and isotopic shifts. The values of the parameters were determined to be $S_{of} = 0.169 \times 10^{-3} \text{ fm}^2$ and $\chi_{oe} = -0.119 \text{ fm}^2$ by fitting to isomer shift $u < r^2 > = 0.16 \text{ fm}^2$ for ^{184}W and the value of isotopic shifts $\Delta < r^2 > = 0.150 \text{ fm}^2$ and 0.087 fm^2 for the $^{182}\text{W}-^{184}\text{W}$ and $^{184}\text{W}-^{186}\text{W}$ respectively. These same values were used in determining the monopole matrix element.

The agreement is good with the experimental data, although the IBM-2 does predict the experimentally observed sign not to change in the isomer shift. It should be noted that the certainties in isomer shift data are roughly an order of magnitude. Clearly more experimental results on the isomer and isotopic shifts for the $^{180-190}\text{W}$ isotopes would be very useful to compare with the predictions possible using IBM-2.

3.4.6 Two Neutron Separation Energy

Instead of the actual binding energy we will examine the two neutron separation energies. This is to say that the energy required to remove two neutrons (one neutron boson) from a $^{180-190}\text{W}$ isotopes and is given by Eq. (2-64). The parameters $B=23.2 \text{ MeV}$ and $C=-0.71 \text{ MeV}$ are determined by fitting Eq. (2-64) to the experimental data [117] to obtain the results shown in Table (3-29) for $^{180-190}\text{W}$ isotopes. The agreement with experimental is good.

Table (3-29): Two neutron bosons separation energies S_{2n} in MeV units.

Isotopes	Exp. [117]	IBM-2
W-180	16.6	16.01
W-182	15.2	16.0
W-184	14.8	15.4
W-186	13.6	14.23
W-188	12.8	13.21
W-190	11.5	11.4

3.4.7 Mixed Symmetry States in $^{180-190}\text{W}$ Isotopes

The existence of the mixed symmetry states is recognized as a manifestation of a new nuclear mode consisting of oscillations of the angle between symmetry axes of the deformed valance neutron and valance proton. The occurrence of the mixed symmetry state in even-even nuclei is a well-established fact [135], and they lie usually high in energy. In even-even nuclei, the identification is based on the measurement of $M1$ and $E2$ transitions to symmetry states, and strong from these states, weakly collective $E2$ transitions to symmetric states, and strong $M1$ transitions can take place via the bosons.

In rotational nuclei the lowest-energy mixed-symmetry state is a 1^+ level at about 3 MeV, while in vibrational and x -unstable nuclei the M_s level is a 2^+ and occurs at about 2 MeV. The mixed-symmetry states can be excited from, or decay to, normal symmetric states by magnetic dipole transitions ($M1$) which are usually strong. The energy dependence of the mixed-symmetry states and the sharing of mixed-symmetry features with the symmetric states are governed by the parameters of the Majorana term which shifts the energy of the states with mixed proton-neutron symmetry with respect to the totally symmetric ones [42].

The IBM-2 is able to describe mixed-symmetry states because it distinguishes between neutron and proton bosons. The F -spin quantum number [67,77,98] has been introduced in order to classify these states in the model. For a single boson, $F = 1/2$ with $F_z = 1/2$ for a **proton** boson and $F_z = -1/2$ for a **neutron** boson. Two bosons may be combined into a trio of symmetric states with $F = 1$, $F_z = 1, 0, -1$, for the combinations $f f$, $f \bar{f}$

and $\epsilon\epsilon$, respectively. For the $f\epsilon$ system there is also an antisymmetric state with $F = F_Z = 0$. Because the boson wavefunction must be symmetric overall, the orbital wavefunction in the sd space must be symmetric for $F=1$ and antisymmetric for $F=0$. The scheme is readily extended to higher boson numbers. The fully symmetric states of N bosons, containing no antisymmetric boson pairs, have $F = N/2$. These are equivalent to the states described by IBM-1. All other states in IBM-2 are states of mixed symmetry. States containing one antisymmetric boson pair have $F = \frac{N}{2} - 1$, and include the 1^+ and 2^+ states observed experimentally. The Majorana term, $M_{f\epsilon}$, provides a repulsive interaction between the bosons in an antisymmetric pair, and therefore raises the energy of a state containing such a pair. However, the $Q_f \cdot Q_\epsilon$ interaction also contributes to the energy difference between symmetric and mixed-symmetry states. In principle, IBM-2 predicts the existence of further mixed-symmetry states with $F = N/2 - p$, where $p = 2, 3, 4, \dots, [N/2]$ is the number of antisymmetric boson pairs. These are expected to lie at much higher energy [42].

The best fit values for the Hamiltonian parameters are given in Table (3-25). The κ_2 component is of a completely different nature from the other two terms in the Majorana interaction. The term containing κ_2 corresponds to the matrix element in which the seniority of protons and neutrons changes while the other two terms belong to the seniority-conserving matrix elements. Consequently, in some cases κ_2 and κ_3 are taken equal while κ_2 is set to zero. In the fitting procedures described in this work we set, as a starting point, the three κ_k ($k=1,2,3$) parameters equal and obtained a best-fit value. The best fit was judged on the basis of the level energies of the lower-lying states, ignoring for the moment any that might have a mixed-symmetry character, electric transition probability $B(E2)$ values and the static moments. Now with $\kappa_1 = \kappa_3$ at their best fit

value, we allowed κ_2 to vary. We see that the energy dependence of all 2^+_S symmetric states reaches saturation very quickly with increasing κ_2 , while the energy of the state 2 increases rapidly with increasing κ_2 and becomes constant at about 2.5 MeV. The energy of the 1^+_M shows a linear increase with κ_2 . These features are illustrated in Figures (3.14) and (3.15). It is obvious that the change in energy levels as κ_2 is varied is a good indicator for the lowest 2^+ and 1^+ mixed-symmetry states, and we recommend this method for searching for mixed symmetry states.

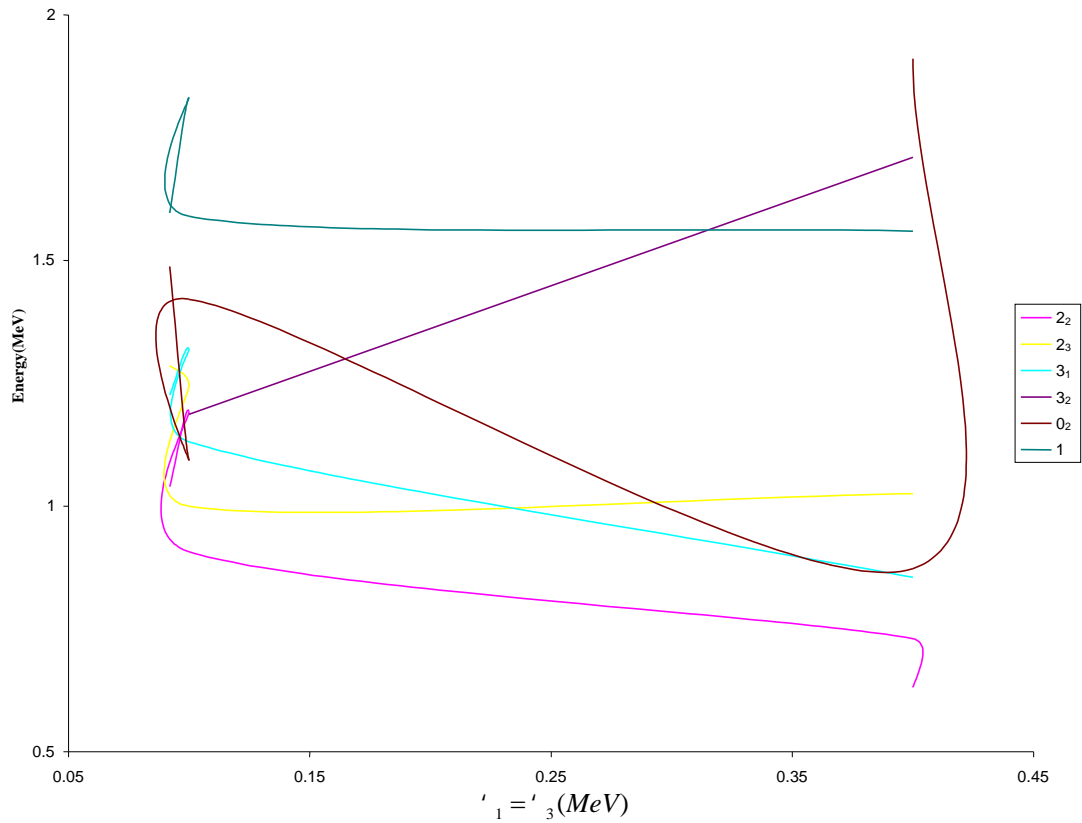


Figure (3.14): The change in energy of low-lying positive parity states as a function of the Majorana term with $\kappa_1 = \kappa_3$

The values of the Majorana parameters will depress κ_2 with respect first scissor mode state. The aim was to minimize the position of 2^+ mixed symmetry states in the $^{180-190}\text{W}$ isotopes, and to monitor the effects of such a change on the calculated energy spectrum. On the other hand, we fixed the value of κ_k for all isotopes.

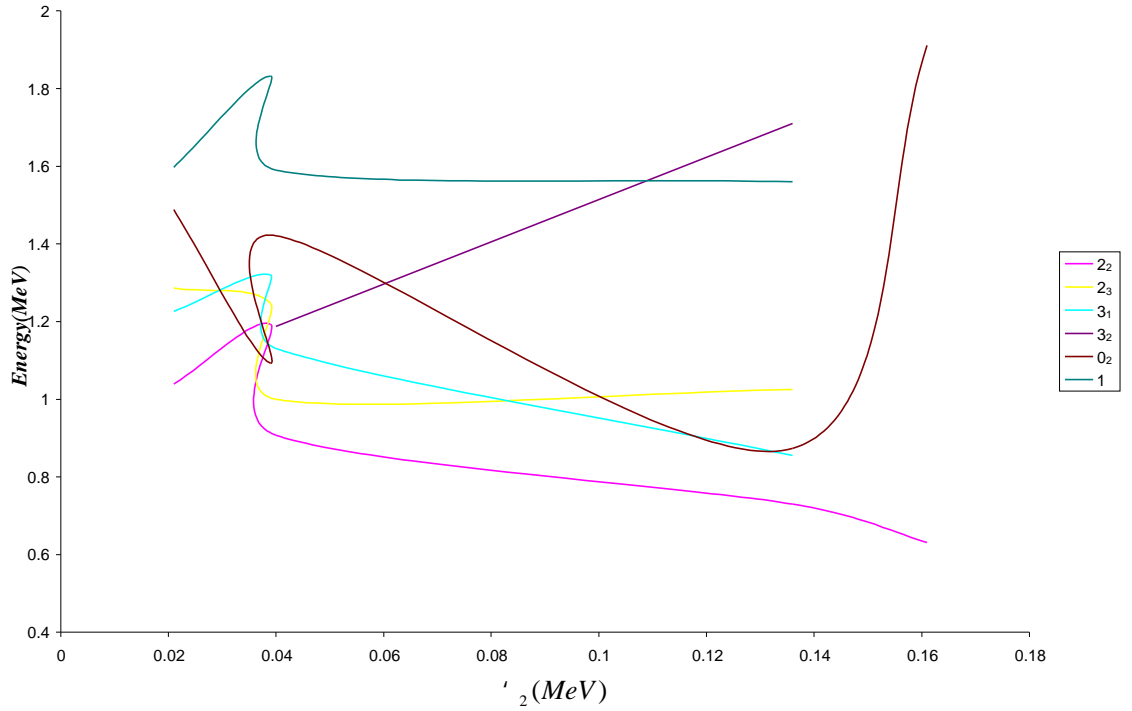


Figure (3.15): The variation in level energy as a function of $\langle \alpha_2 \rangle$.

The calculated energy spectrums of the $^{180-190}\text{W}$ nuclei are shown in Figures (3-6) to (3-11). Reproduction of the trend in the experimental data[117] can be seen, the energy states have been grouped according to bands and F -spin values, and they provide an opportunity to study possible collective band structures that are predicted in these nuclei. As can be seen, our results agree well with the available experimental data. In particular, all symmetry states in different band are reproduced correctly, all second 0_2^+ and 2_2^+ states, except the 0_2^+ in the ^{180}W isotope where the deviation is 0.028 MeV upper than the experimental value. The IBM-2 predictions of the γ -band of the selected set of $^{180-190}\text{W}$ isotopes are also satisfactory. Though the calculated 0_2^+ state at 1.093 MeV in the ^{182}W isotope has been observed, while the 0_2^+ states in the $^{180,184,186}\text{W}$ isotopes are very close to the experimental ones. All 3_1^+ states are fully symmetric states, i.e., belong to γ -collective band. The deviations between theoretical and experimental data may be attributed to the mixing of the collective excitation with quasiparticle excitations.

The parameter κ_2 component of Majorana interaction should have an extreme effect on the energy of the MSS . We set, as starting point, the three parameters κ_1 , κ_2 and κ_3 which obtained the best fit to experimental data and then allow κ_2 to vary. The completely symmetric 2^+ states are not affected by changing κ_2 , or reach the saturation value very quickly, while the energy of the MSS increase (decrease) rapidly by changing the κ_2 value and becomes constant at a certain energy as shown in Figure(3.15). The energy of the (F^*F/\max) shows a linear increase with κ_2 . The 3_M^+ and 4_M^+ behave in the same manner of the 2_M^+ . The F -spin projection calculation confirms these criteria. In other word, we recommend the two methods in searching for the mixed symmetry states.

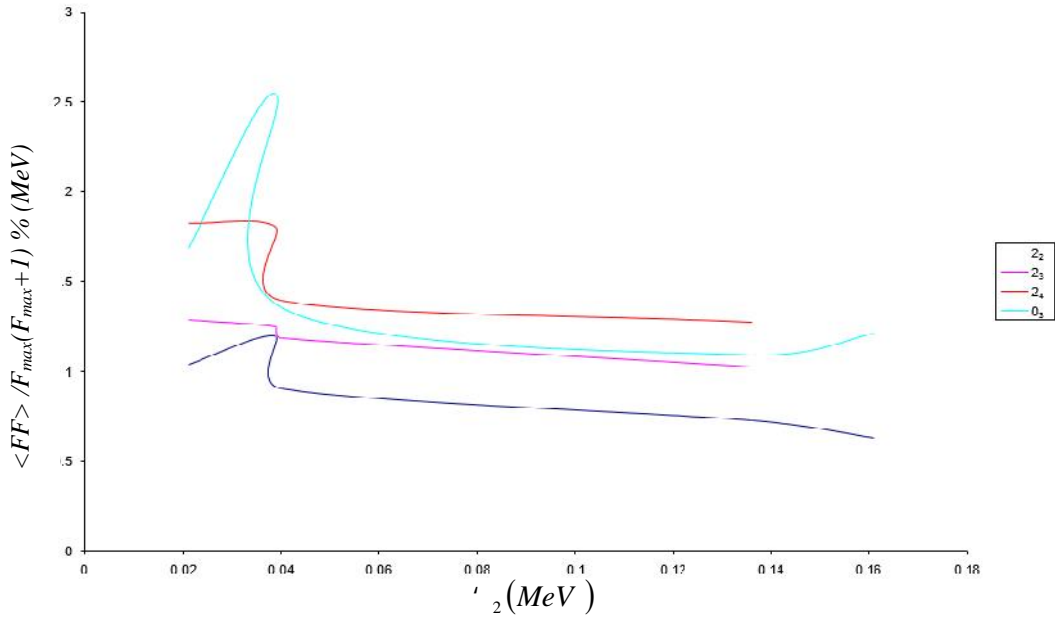


Figure (3.16): F-spin components in the 2_2 , 2_3 , 2_4 and 0_3 levels as a function of κ_2 .

According to the above discussion, it is found that the 2_5^+ and 2_6^+ at calculated energy around 2.1 MeV in $^{180-190}\text{W}$ isotope are mixed symmetry states, plus the 1_1^+ and 1_2^+ at 2.0 MeV and 2.3 MeV respectively. The same states in ^{182}W isotopes are mixed symmetry states. In ^{184}W isotope, it is found that the 2_4^+ and 2_5^+ states at experimental and theoretical energies (1.386, 1.431) MeV and (1.397, 1.437) MeV respectively are the mixed

symmetry states. In ^{186}W has the similar behavior as previous isotope, i.e., the 2_4^+ and 2_5^+ states at experimental and theoretical energies (1.285, 1.322) MeV and (1.274, 1.326) MeV respectively are mixed symmetry states.

The magnitude and sign of the multipole mixing ratios are found to depend sensitively on $\langle \kappa_2 \rangle$. In IBM-2, the E2 transition operator is given by the Eq.(2-42) and the M1 transition operator can be written in Eq.(2-52). The reduced E2 and M1 matrix elements have been evaluated for a selection of transitions in $^{180-190}\text{W}$ isotopes $^{180-190}\text{W}$ isotopes; their dependence on $\langle \kappa_2 \rangle$ is striking. A sudden change in sign is sometimes observed in M1; it occurs when the E2 matrix element is small. It may be attributed to a very low value of the E2 reduced matrix element; even though the program has an arbitrary sign choice, the sign is consistent for all results within a calculation, and the sign of the ratio of the matrix elements which determine the sign of the multipole mixing ratio is not arbitrary.

In Table (2-16), it should be noted that a sign change appears in both the $2_2^+ \rightarrow 2_1^+$ and $2_3^+ \rightarrow 2_1^+$ transition mixing ratios, when going from ^{182}W to ^{184}W . Moreover, in ^{182}W there is an opposite sign between the $2_2^+ \rightarrow 2_1^+$ mixing ratio and the $3_1^+ \rightarrow 2_1^+$ and $3_1^+ \rightarrow 4_1^+$ mixing ratios. We were able to reproduce all of these features in the calculation. Mainly, the sign change of Δv and Δt for ^{182}W in comparison to ^{184}W which is responsible for this effect. We also calculated the admixtures of lower F -spin states in the ground state. They are 1.6%, 2.2%, 1.3% for $^{186-184-182}\text{W}$, respectively. They are 1.5%, 2.10%, 1.2% for $^{186,184,182}\text{W}$, respectively.

From the calculated values for the transition probability $B(E2)$ and $B(M1)$ in $^{182-186}\text{W}$ in Tables (3-14) and (3-15), it has been found that the state 2_4^+ is a mixed symmetry state and represents 2_M^+ because the electric transition probability $B(E2)$ is smaller than the magnetic transition probability $B(M1)$ as well as the 2_4^+ state which represents the mixed

symmetry for the same reason. Whereas 2_4^+ state is a totally symmetric state because of $B(M1) < B(E2)$. While, in the case of $^{184-186}\text{W}$, the 2_4^+ represent the 2_M^+ according to the values of $B(E2)$ and $B(M1)$ [49].

The branching ratios of $B(M1)$ are very helpful in nuclear shape coexistence. Normally the value of $B(M1; 1_1^+ \rightarrow 0_1^+)$ is the largest value in the M1 transition probability between states, so we applied the $B(M1)$ ratio normalized to the value of this transition, according to the following relations;

$$R_1 = B(M1; 1_1^+ \rightarrow 0_1^+) / B(M1; 2_i^+ \rightarrow 2_f^+)$$

$$i = 4, 5, 6, 7, f = 1, 2$$

The ratio R_1 depends on the $B(M1; 2_i^+ \rightarrow 2_f^+)$. The large value of R_1 , means that the 2_i^+ state is a totally symmetric state and this is consistent with the values calculated in the program and with the F -spin values. For small R_1 values the $B(M1; 2_i^+ \rightarrow 2_1^+) = 11 \sim \frac{2}{N}$ is large, in other words, the state, $2_{4,5,6,7}^+$ is a mixed symmetry state and it has the strong $M1$ decay to the 2_1^+ state and one must take into account that the states in which the $M1$ decay are one-phonon or two-phonon differences. It can be seen that $R_1 = 0.00001$ is small when $N_\epsilon = 12$, because this isotope has a larger value of $B(M1)$ than the other isotopes.

The analyses demonstrate the sensitivity of the mixed symmetry states energy to the model parameters F -spin and the Majorana term κ_2 . The comparison with the experimental data shows that, we still lack the experimental data on the $B(M1; 1_1^+ \rightarrow 0_1^+)$ in order to focus on these aspects.

CHAPTER FOUR
INTERACTION
BOSON-FERMION
MODEL RESULTS
AND DISCUSSION

CHAPTER FOUR

INTERACTION BOSON-FERMION MODEL RESULTS AND DISCUSSION

4.1- ¹⁷¹⁻¹⁷⁹Hf Isotopes in IBFM-1

In recent years, many negative and positive parity states of the even-odd nuclei, such even-odd Hf isotopes have been found experimentally. Over the major shell $N = 82$, there are available negative parity single-particle levels, the $2f_{5/2}, 3p_{3/2}$ and $3p_{1/2}$. The basic algebraic structure associated with the **IBFM** model Hamiltonian of the Hf isotopes, whose last unpaired nucleon occupied single-particle orbits with $j = 1/2, 3/2$ and $5/2$, is the direct product $U^B(6) \otimes U^F(12)$, where $U^B(6)$ is the boson group describing the collective properties of the even-even core and $U^F(12)$ is the fermion group associated the single-particle degree of freedom.

4.1.1 Energy Spectra for ¹⁷¹⁻¹⁷⁹Hf isotopes

The even-odd ¹⁷¹⁻¹⁷⁹Hf isotopes consists of 72 protons and 99-107 neutrons, hence the numbers of bosons (12-16), it could be calculated by hole protons that are 5. The **IBFM-1** Hamiltonian (Eq. (2-76)) was diagonalized by means of the **ODDA** program [136]. The **IBFM-1** parameters used in the **ODDA** code are given in Table(4-1) for all isotopes under study ($A_0 = BEM$, $\Gamma_0 = BFQ$, $\Lambda_0 = BFE$)

Table (4-1): Adopted Parameters used for IBFM-1 calculation; all parameters are given in MeV units.

Isotopes	BFE	BFQ	BFM	N_f	$N_{\bar{}}$	N_B	N_F	N
¹⁷¹ Hf	0.071	0.031	-0.011	5	7	12	1	13
¹⁷³ Hf	0.252	0.031	-0.072	5	8	13	1	14
¹⁷⁵ Hf	0.181	0.07	0	5	9	14	1	15
¹⁷⁷ Hf	0.501	0.161	0.131	5	10	15	1	16
¹⁷⁹ Hf	0.9	0.02	-0.25	5	11	16	1	17

In the framework of the **IBFM-1**, we performed the BCS (Barden-Cooper-Schrieffer) calculation, which provide the quasi particle energies v_i

and the shell occupation ϵ_j^2 using in the Eqs. (2-82) and (2-83) which are presented in Table (4-2).

Table (4-2): Adopted values for the parameters used for IBFM calculation.

Parameters	^{171}Hf			^{173}Hf			^{175}Hf		
	$2f_{5/2}$	$3p_{3/2}$	$3p_{1/2}$	$2f_{5/2}$	$3p_{3/2}$	$3p_{1/2}$	$2f_{5/2}$	$3p_{3/2}$	$3p_{1/2}$
v_j (MeV)	2.030	1.7020	2.570	2.0530	1.6970	2.5940	2.0330	1.730	2.0340
ϵ_j^2	0.0510	0.0716	0.0301	0.0480	0.0691	0.0474	0.0690	0.030	0.0471
Parameters	^{177}Hf			^{179}Hf					
	v_j (MeV)								
v_j (MeV)	1.7230	2.5740	2.0349	2.0640	1.7260	2.570			
ϵ_j^2	0.0674	0.0290	0.0471	0.0460	0.0670	0.030			

The IBFM-1 results and experimental data [110] of low-lying negative parity levels were plotted in Figures (4.1) to (4.5) for the $^{171-179}\text{Hf}$ isotopes. In these figures, the IBFM-1 calculations are in good agreement with the experimental data [110].

Because of the discrepancies between experimental results in both energy levels and their assignments, the IBFM-1 parameters used are those which give the same energy value for the first energy level ($1/2^-$) (see Figure (4-1)). Hence, a normalization to the level ($1/2^-$) at 0.021 MeV was made.

The average percentage deviation between experimental levels and the IBFM predictions was calculated to be less than 2% only. The energy levels compared are those below 2 MeV, since most of the levels at higher energy are not assigned and there are a lot of discrepancies in their excitation energy.

The whole Hamiltonian was then diagonalized in the model space spanned by the basis states $|n_s, n_d \in L; J\rangle_{JM}$ where $j = (7/2^+)$ in $^{171-173-175-177}\text{Hf}$ isotopes and $j = (9/2^+)$ in ^{179}Hf isotope. The interaction parameters were determined by fittings to the experimental energy spectra of the $^{171-179}\text{Hf}$ isotopes. In the fittings, all interaction parameters were treated on equal footing. The strength of $L.L$ term can be determined from the relative level spacing's of different L states. From the general level spacing's of even-

even core nuclei in the isotope the parameter a_2 was chosen to be (-0.011 to -0.014) for all nuclei in the isotope string. Also, it was found that the exchange force term has the effect to be complementary with the a_0V_d term and could be unified for all isotopes in the string. Therefore, the value of Λ was chosen in Table (4-1) and the a_0V_d term was renormalized to absorb the relative effects of exchange force for different isotopes.

The best fitted interaction parameters are shown in Table (4-1). It is worth noting that the free varying parameters are very smoothly versus the change of the boson number.

The calculated and experimental energy spectra of positive parity states are shown in Figures (4-6) to (4-10). In general, the agreement is very good. The root mean-square deviation for 64 states is only 0.021MeV. There are several interesting features that are worthy of mentioning.

- 1- High spin states can be reproduced quite well but some high spin states cannot be fitted well. If want to fit these states well by adjusting the interaction parameters, the fittings in the lower spin states will be affected significantly. Therefore, these states were excited in the least-squares fittings and were marked by an asterisk on the energy levels. It seems that these cannot be explained in this one fermion orbit IBFM-1 model.
- 2- The observed order reverse of the $5/2^+$, $7/2^+$, $3/2^+$, $9/2^+$, $11/2^+$. $13/2^+$, doublets in the energy spectra can be reproduced. It was found that the quadrupole-quadrupole interaction is crucial for this order reverse. Note that the sign of this term changes from isotope to another.
- 3- The unflavored high spin states that currently do not have experimental counterparts are not shown in the figures.

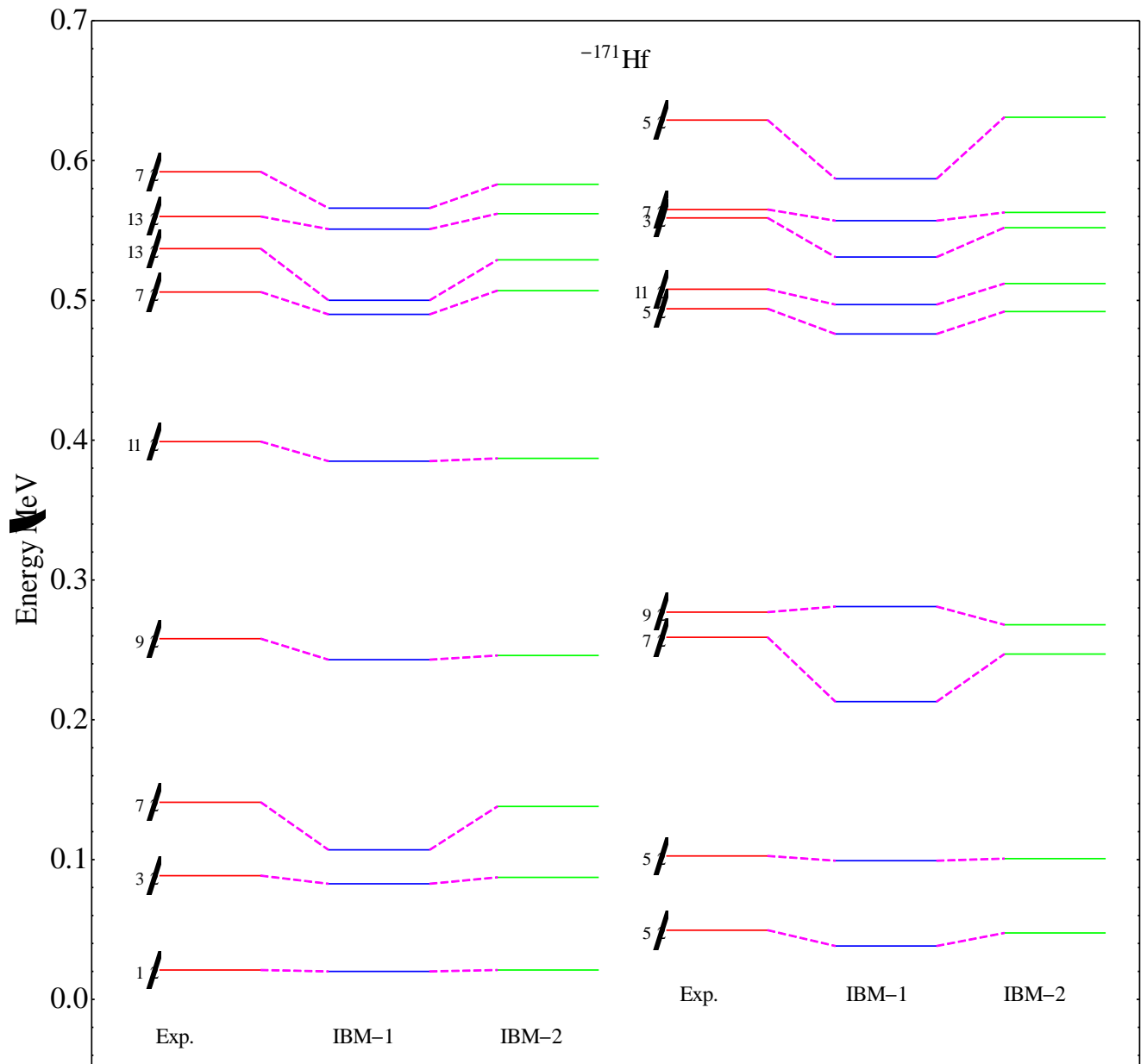


Figure (4.1): Comparison between experimental negative parity states data [110], IBFM-1 and IBFM-2 calculated energy levels for ^{171}Hf .

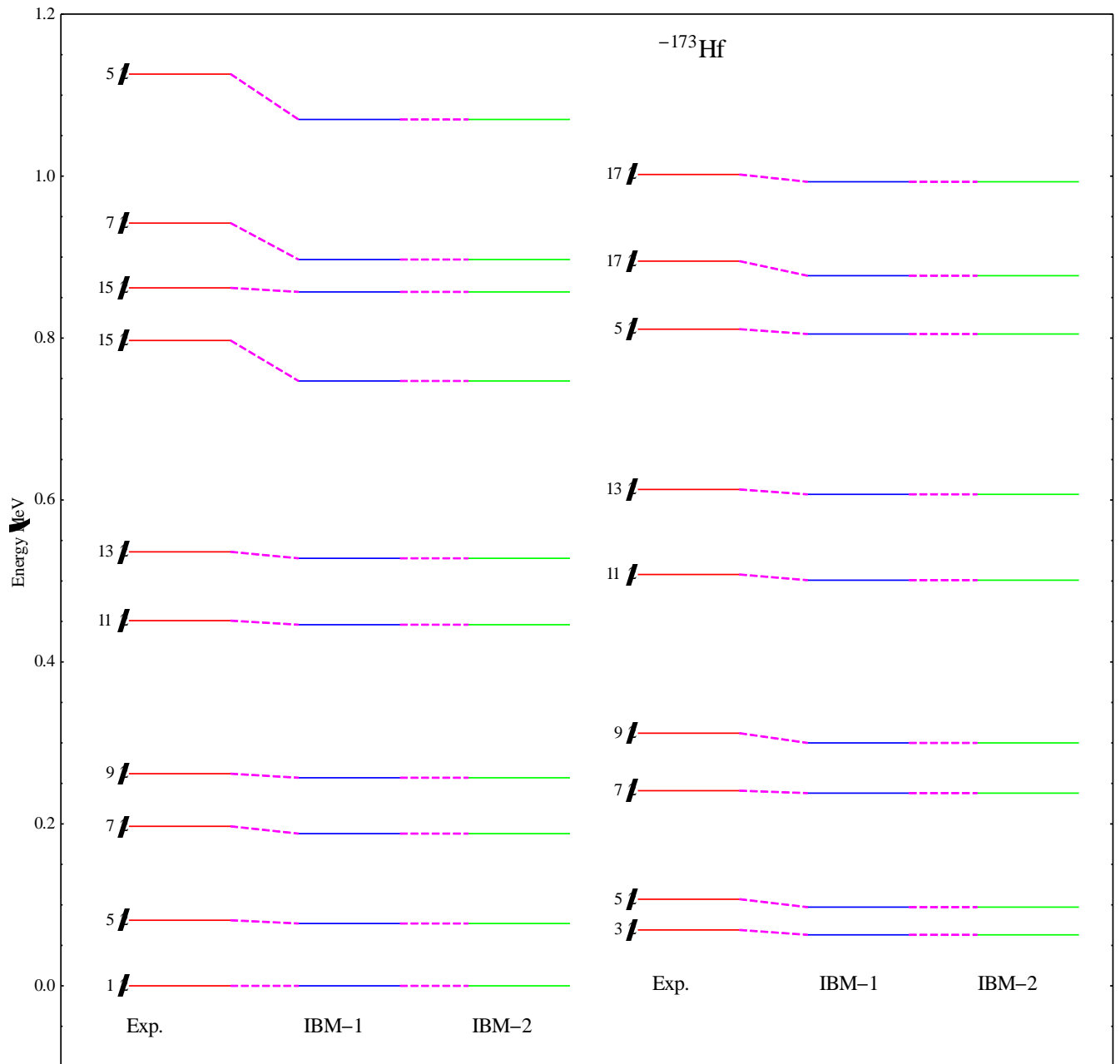


Figure (4.2): Comparison between experimental negative parity states data [110], IBFM-1 and IBFM-2 calculated energy levels for ^{173}Hf .

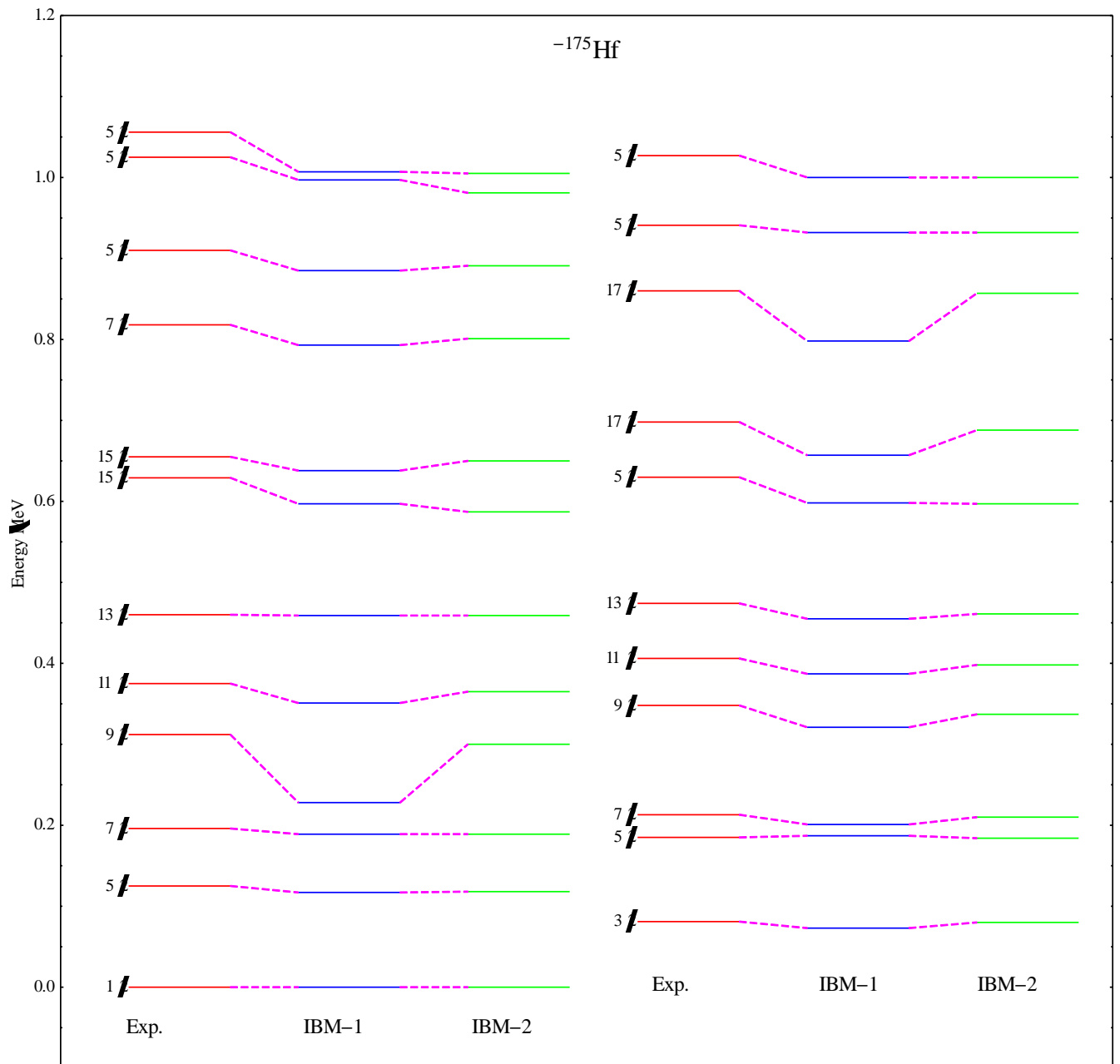


Figure (4.3): Comparison between experimental negative parity states data [110], IBFM-1 and IBFM-2 calculated energy levels for ^{175}Hf .

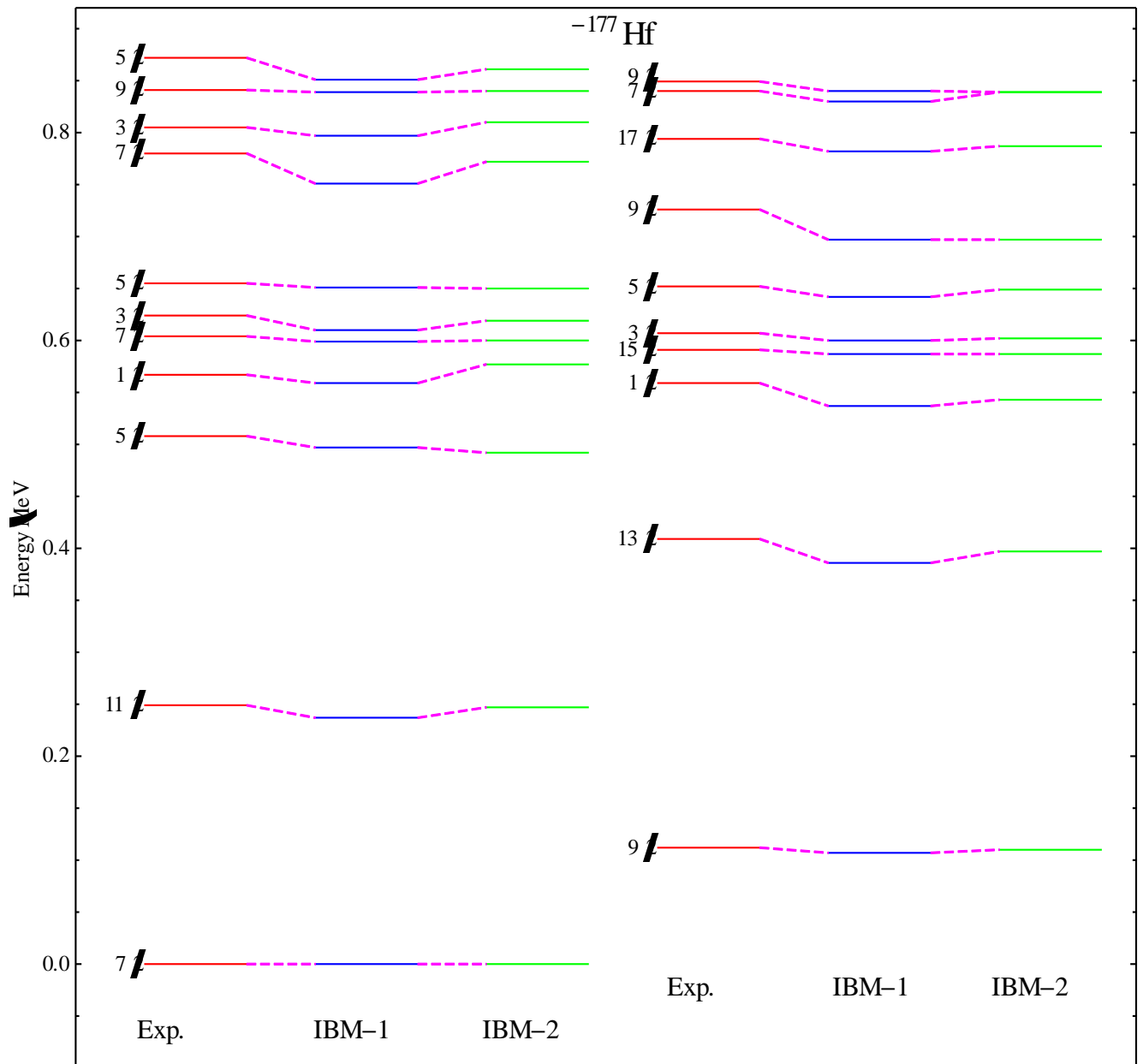


Figure (4.4): Comparison between experimental negative parity states data [110], IBFM-1 and IBFM-2 calculated energy levels for ^{177}Hf .

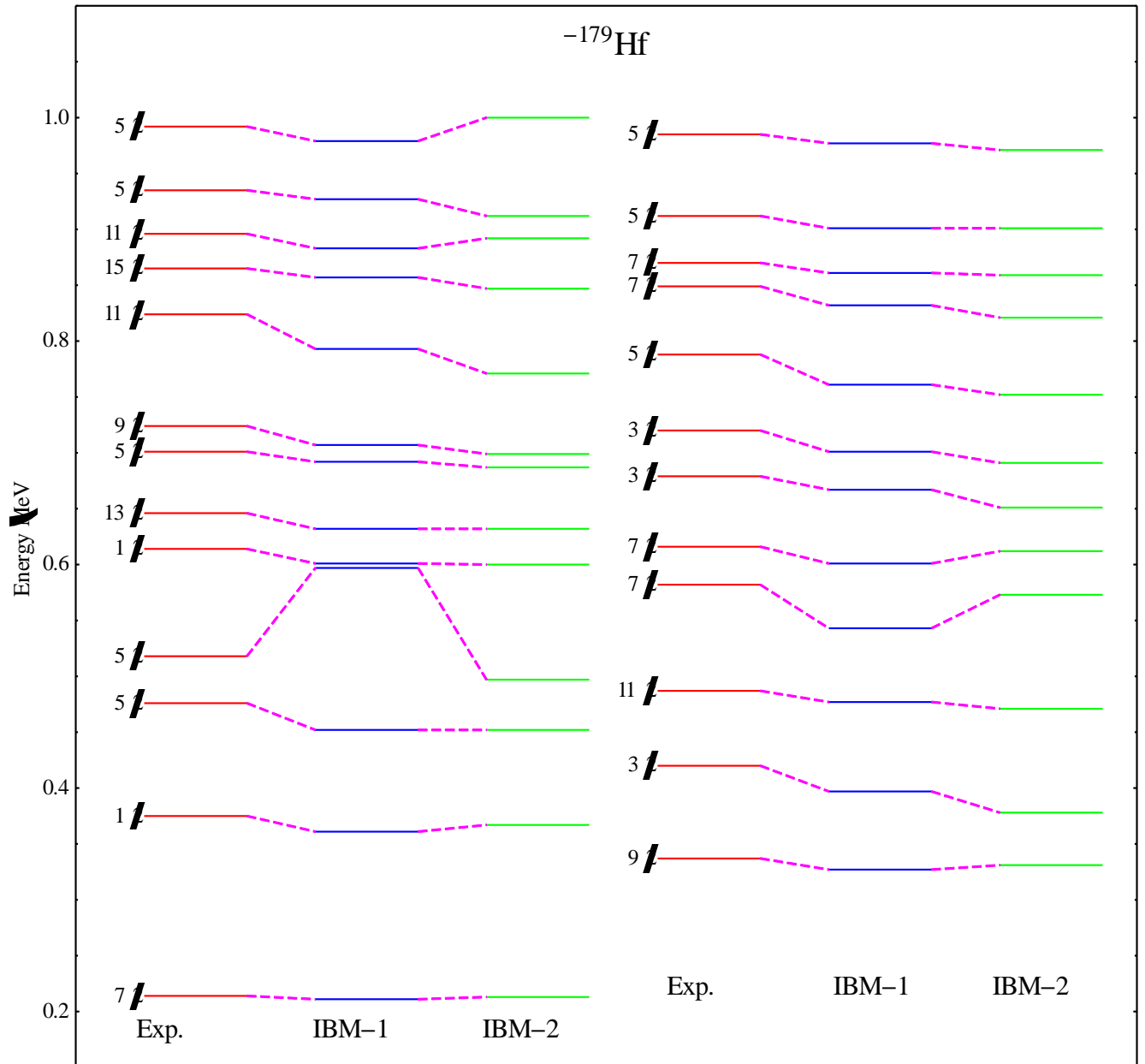


Figure (4.5): Comparison between experimental negative parity states data [110], IBFM-1 and IBFM-2 calculated energy levels for ^{179}Hf .

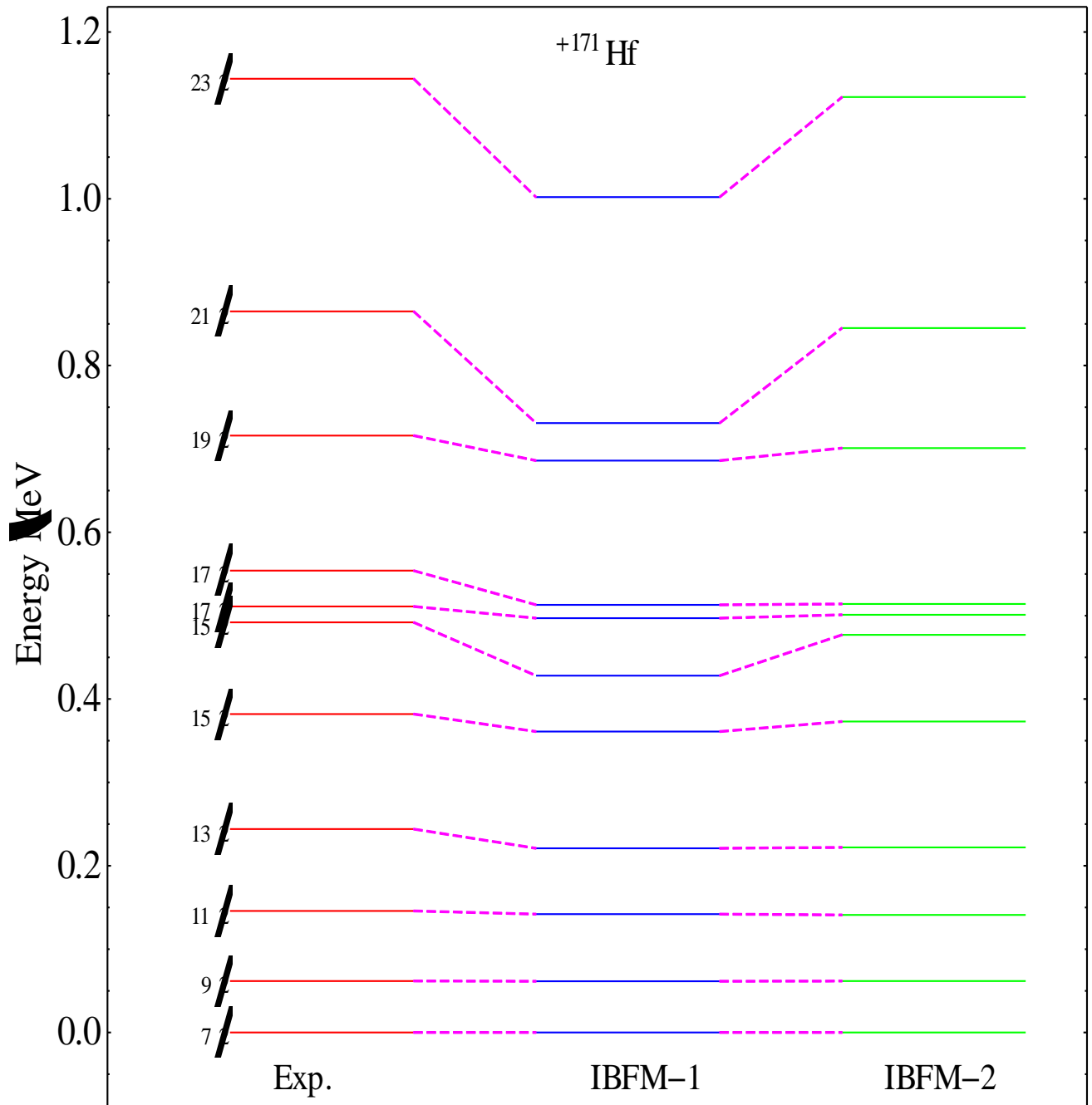


Figure (4.6): Comparison between experimental positive parity states data [110], IBFM-1 and IBFM-2 calculated energy levels for ^{171}Hf .

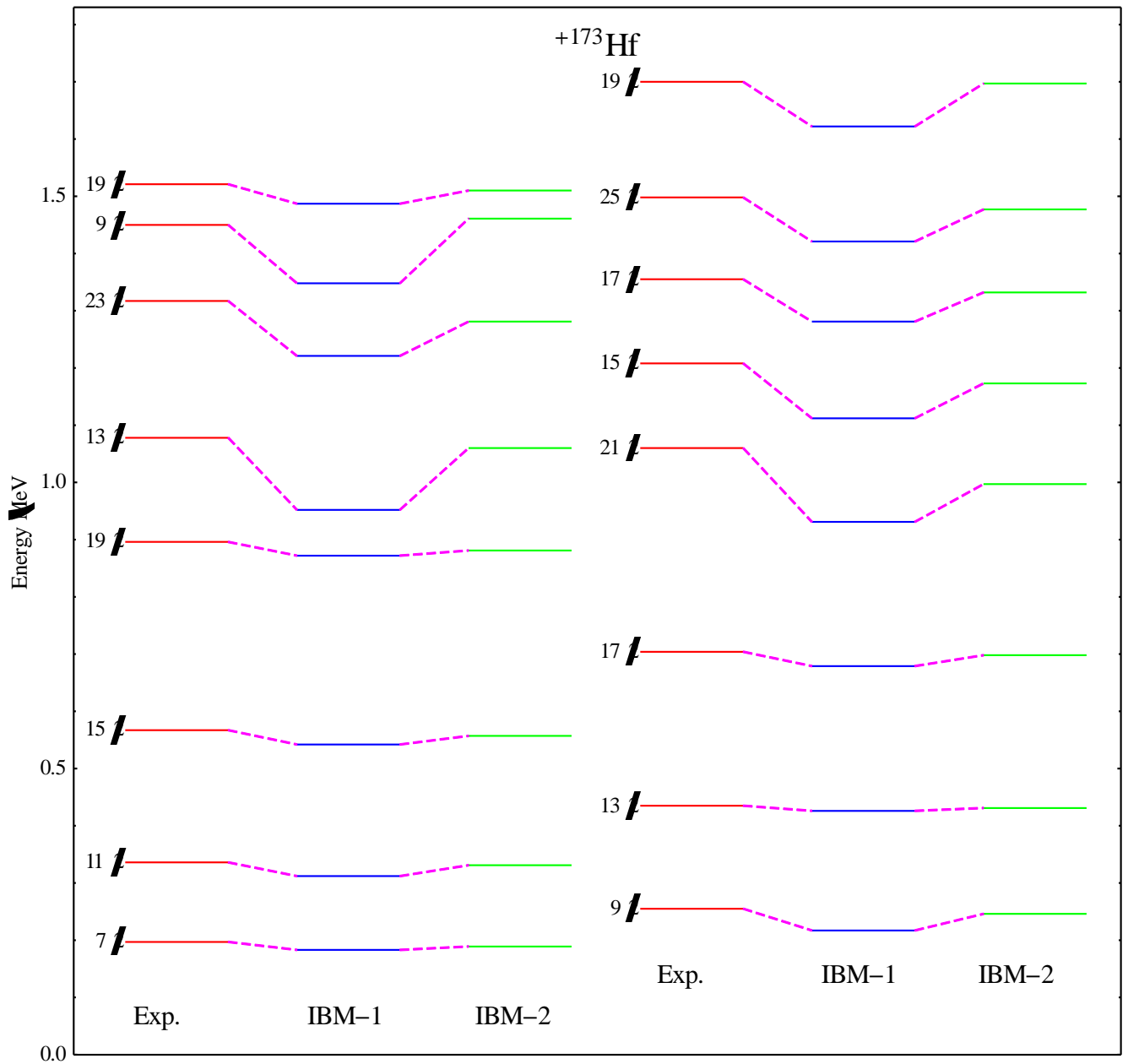


Figure (4.7): Comparison between experimental positive parity states data [110], IBM-1 and IBM-2 calculated energy levels for ^{173}Hf .

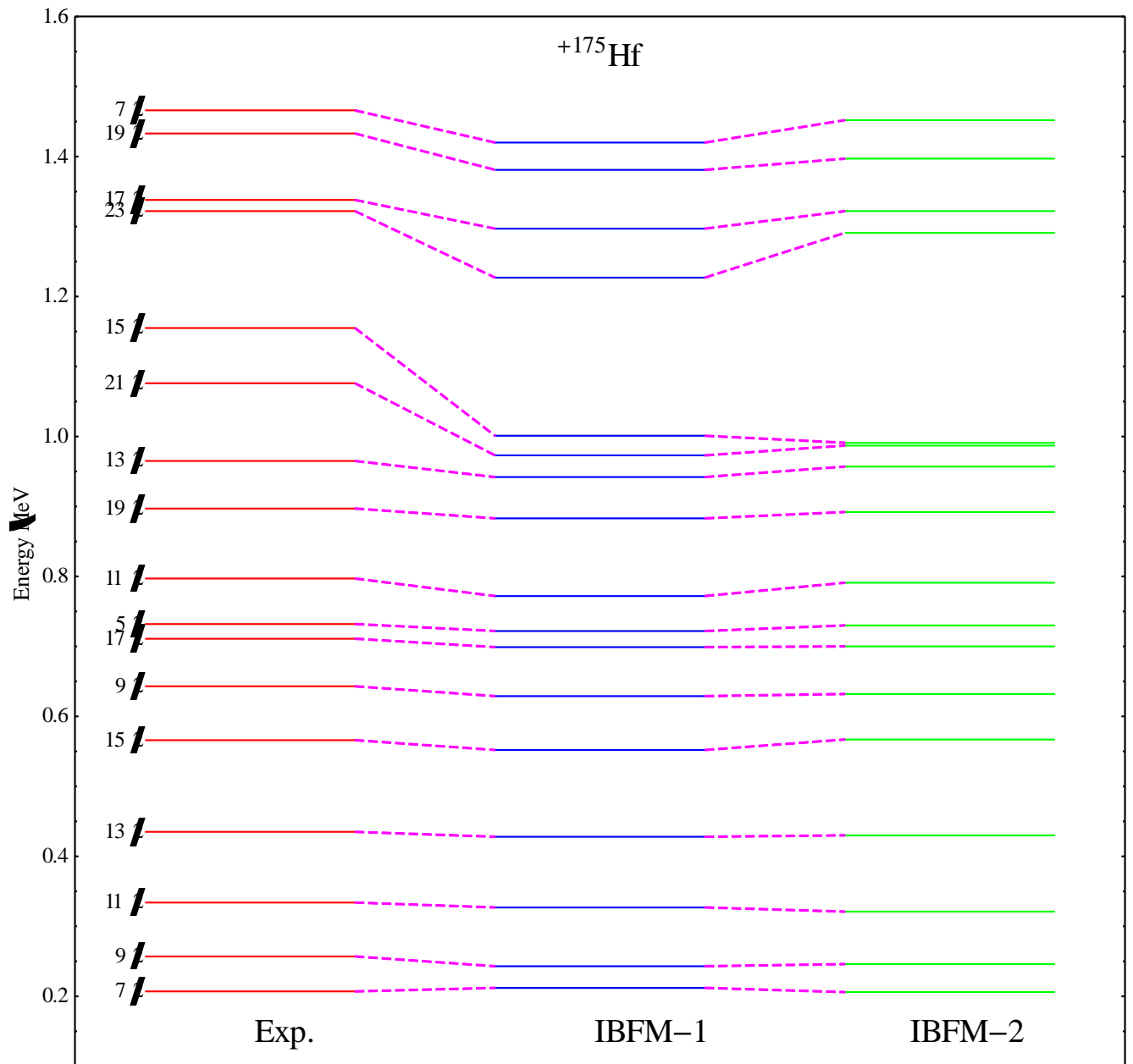


Figure (4.8): Comparison between experimental positive parity states data [110], IBFM-1 and IBFM-2 calculated energy levels for ^{175}Hf .

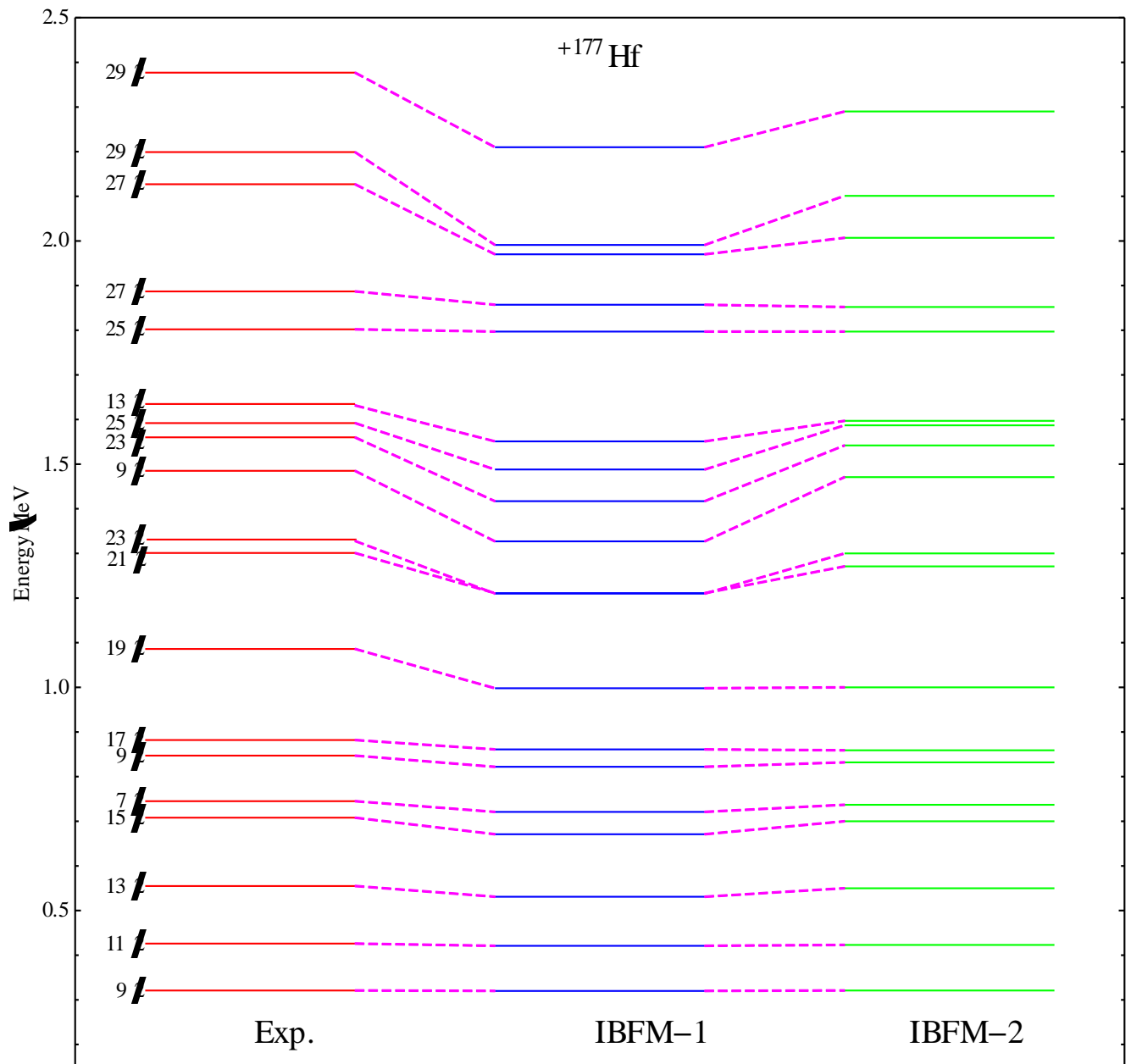


Figure (4.9): Comparison between experimental positive parity states data [110], IBFM-1 and IBFM-2 calculated energy levels for ^{177}Hf .

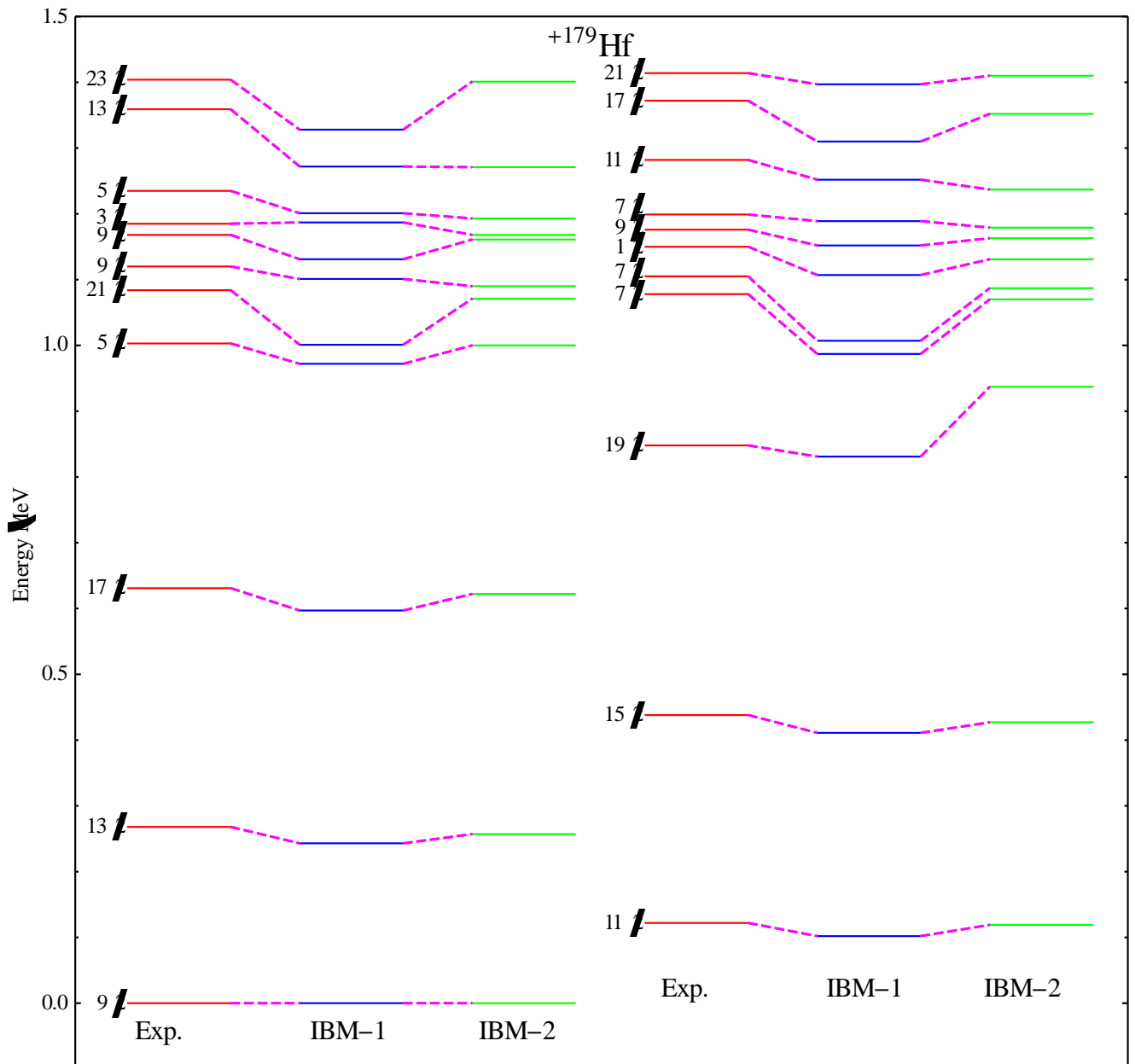


Figure (4.10): Comparison between experimental positive parity states data [110], IBFM-1 and IBFM-2 calculated energy levels for ^{179}Hf .

4.1.2- E2 Transitions for $^{171-179}\text{Hf}$ Isotopes

The IBFM-1 model wavefunctions can be further tested by electromagnetic transition probabilities. Unfortunately, in this region the lack of experimental data prevents any significant theory-experiment comparison.

The calculation of electromagnetic transitions gives a good test of the nuclear model wave functions. In this section, the calculation of the E2 transition strengths and results with the available experimental data are

discussed. In general, the electromagnetic transition operators can be written as a sum of two terms, the first of which acts only on the boson part of the wave function and second only on the fermion part.

In the IBFM-1 the E2 operator is given in Eq. (2-103), where e_B and e_F are the boson and fermion effective charges. The electric quadrupole moments for a state with spin J can be calculated from the E2 operator. Eq. (2-103) contains the E2 boson and the fermion effective charges as adjustable parameters. Experimental B(E2) values were used to find the best fit with **PBEM** [60] and determine the boson effective charges e_b and e_f . The fermion effective charge e_F is taken to be equal to e_B . Fermion effected charge can be reproduced from the experimental $B(E2; J_i \rightarrow J_f)$ and can be written as [82]:

$$B(E2 : J_i \rightarrow J_f) = (r_2 - f_2)^2 \frac{2N(N+3)}{5(N+1)(N+2)} \dots\dots\dots (4-1)$$

and it is tabulated in Table (4-3) together with boson effective charges. The theoretical B(E2) s for $^{171-179}\text{Hf}$ are given in Table (4-4) because there is no experimental data to be comparable to. But we can calculate the B(E2) values depending on the case when $r_2(e_B) = f_2(e_F)$. From Table (4-4) and Table (4-5), some B(E2) transitions for positive and negative parity states are strong because these transitions have selection rules.

Table (4-3): effective fermions charge for Hafnium isotopes.

Isotopes	$e_B (e.b)$	$e_F (e.b)$
^{171}Hf	0.1165	-0.135
^{173}Hf	0.121	-0.419
^{175}Hf	0.123	-0.270
^{177}Hf	0.113	-0.141
^{179}Hf	0.132	-0.162

E2 transitions do not show a clear pattern that allows for the arrangement of the levels into bands. This is partly due to the fact that there are several single-particle levels important for the low-lying states and

partly due to the fact that the even-even cores do not show strong collectivity.

Table (4-4): Electric Transition Probability for $^{171-179}\text{Hf}$ $B(E2; J_i^+ \rightarrow J_f^+)$ in $e^2 \cdot b^2$ units for Positive Parity States.

$J_i^+ \rightarrow J_f^+$	^{171}Hf		^{173}Hf		^{175}Hf		^{177}Hf		^{179}Hf	
	IBFM-1	IBFM-2	IBFM-1	IBFM-2	IBFM-1	IBFM-2	IBFM-1	IBFM-2	IBFM-1	IBFM-2
$\frac{9}{2_1} \rightarrow \frac{7}{2_1}$	0.130	0.221	0.51	0.617	0.023	0.073	-	-	-	-
$\frac{11}{2_1} \rightarrow \frac{9}{2_1}$	0.64	0.622	0.721	0.832	0.011	0.014	0.0414	0.031	0.0621	0.0633
$\frac{11}{2_1} \rightarrow \frac{7}{2_1}$	0.293	0.419	0.0021	0.0027	0.003	0.007	0.0521	0.0547	-	-
$\frac{13}{2_1} \rightarrow \frac{11}{2_1}$	0.073	0.087	0.682	0.672	0.037	0.055	-	-	0.0533	0.0557
$\frac{13}{2_1} \rightarrow \frac{9}{2_1}$	-	-	0.0009	0.008	-	-	0.0007	0.00081	0.0067	0.0071
$\frac{13}{2_1} \rightarrow \frac{7}{2_1}$	-	-	0.0029	0.003	-	-	-	-	-	-
$\frac{17}{2_1} \rightarrow \frac{9}{2_1}$	0.056	0.068	0.131	0.153	-	-	-	-	-	-
$\frac{17}{2_1} \rightarrow \frac{13}{2_1}$	0.375	0.432	0.352	0.427	-	-	-	-	-	-
$\frac{15}{2_1} \rightarrow \frac{13}{2_1}$	-	-	-	-	-	-	-	-	0.0918	0.0816

Table (4-5): Electric Transition Probability for $^{171-179}\text{Hf}$ $B(E2; J_i^+ \rightarrow J_f^+)$ in $e^2 \cdot b^2$ units for negative Parity States

$J_i^+ \rightarrow J_f^+$	^{171}Hf		^{173}Hf		^{175}Hf		^{177}Hf		^{179}Hf	
	IBFM-1	IBFM-2	IBFM-1	IBFM-2	IBFM-1	IBFM-2	IBFM-1	IBFM-2	IBFM-1	IBFM-2
$\frac{5}{2}_1 \rightarrow \frac{1}{2}_1$	0.478	0.621	0.0021	0.0027	-	-	-	-	-	-
$\frac{3}{2}_1 \rightarrow \frac{5}{2}_1$	0.046	0.0321	-	-	-	-	-	-	-	-
$\frac{5}{2}_1 \rightarrow \frac{1}{2}_1$	0.259	0.571	-	-	-	-	-	-	-	-
$\frac{5}{2}_2 \rightarrow \frac{1}{2}_1$	0.622	0.731	-	-	-	-	-	-	-	-
$\frac{5}{2}_2 \rightarrow \frac{3}{2}_1$	0.01	0.011	0.589	0.674	-	-	-	-	-	-
$\frac{3}{2}_1 \rightarrow \frac{1}{2}_1$	0.488	0.377	0.013	0.0021	-	-	-	-	0.051	0.041
$\frac{7}{2}_1 \rightarrow \frac{5}{2}_1$	0.362	0.475	0.19	0.188	0.0321	0.0616	-	-	-	-
$\frac{7}{2}_1 \rightarrow \frac{5}{2}_2$	1.381	2.615	0.47	0.522	-	-	-	-	-	-
$\frac{7}{2}_2 \rightarrow \frac{7}{2}_1$	0.478	0.513	0.419	0.522	-	-	-	-	-	-
$\frac{9}{2}_1 \rightarrow \frac{7}{2}_2$	0.0072	0.0081	0.038	0.0521	-	-	0.0371	0.0351	0.0717	0.0619
$\frac{11}{2}_1 \rightarrow \frac{9}{2}_1$	0.626	0.731	0.0132	0.0122	-	-	0.0472	0.0481	-	-
$\frac{5}{2}_2 \rightarrow \frac{5}{2}_1$	-	-	0.0014	0.0018	-	-	-	-	-	-
$\frac{7}{2}_1 \rightarrow \frac{5}{2}_2$	-	-	0.008	0.0078	-	-	-	-	-	-
$\frac{9}{2}_2 \rightarrow \frac{9}{2}_1$	-	-	0.066	0.061	-	-	-	-	-	-

4.1.3 - M1 Transitions and $^{171-179}\text{Hf}$ Isotopes

The M1 transition operator is given by the Eq. (2-106), where, $g_B = 0.31 \sim_N$ is the boson g-factor determined by the magnetic moment of levels in the even-even core and, g_{jj} is the single particle contribution which depends on g_l and g_s of the odd nucleon. In the actual calculations, the computer program **PBEM** [60] has been used. For the odd $^{171-179}\text{Hf}$ neutron, we use $g_l = 0 \sim_N$ and $g_s = -1.5 \sim_N$. The spin g-factor indicates some quenching from that of a free neutron. It should be noted that there is a

wide range of g_l and g_s values that give a reasonable fit to the data. In considering the M1 operator one should keep in mind that for the special choice $g_B = g_l = g_s$ the operator Eq. (2-106) reduces to the operator for a total angular momentum. Since this corresponds to a good quantum number, the calculated B(M1) values vanish exactly for this choice. The relatively large B(M1) values thus requires a significant deviation from $g_B = g_l = g_s$ however the data do not allow an accurate determination of these parameters and a variation of the parameters with 30% is possible without significantly spoiling the agreement.

The Calculated B(M1) values are only available for some transitions in Tables (4-6) and (4-7). The calculation shows some large discrepancies for $^{175-177}\text{Hf}$. The M1-operator in IBFM-1 higher-order terms are more important than for the E2-operator due to the fact that the M1 transitions are not collective.

Table (4-6): Magnetic Transition Probability $B(M1; J_i \rightarrow J_f)$ in $\sim \frac{2}{N}$ units for $^{171-179}\text{Hf}$ for positive Parity State

$J_i \rightarrow J_f$	^{171}Hf		^{173}Hf		Hf^{175}		Hf^{177}		Hf^{179}	
	IBFM-1	IBFM-2	IBFM-1	IBFM-2	IBFM-1	IBFM-2	IBFM-1	IBFM-2	IBFM-1	IBFM-2
$\frac{9}{2_1} \rightarrow \frac{7}{2_1}$	0.023	0.0461	0.478	0.537	0.0632	0.787	-	-	-	-
$\frac{11}{2_1} \rightarrow \frac{9}{2_1}$	0.011	0.263	0.046	0.0391	0.357	0.0272	0.697	0.532	0.271	0.472
$\frac{11}{2_1} \rightarrow \frac{7}{2_1}$	0.00028	2.5×10^{-3}	0.0488	0.0526	0.0031	0.0004	-	-	-	-
$\frac{13}{2_1} \rightarrow \frac{11}{2_1}$	0.326	0.527	-	-	0.732	0.543	0.521	0.431	0.334	0.437
$\frac{13}{2_1} \rightarrow \frac{9}{2_1}$	-	0.00071	-	-	-	-	0.0072	0.0083	0.007	0.00089
$\frac{13}{2_1} \rightarrow \frac{7}{2_1}$	-	-	2×10^{-5}	3×10^{-5}	-	-	-	-	-	-

Table (4-7): Magnetic Transition Probability $B(M1; J_i \rightarrow J_f)$ in $\sim \frac{2}{N}$ for $^{171-179}\text{Hf}$ for negative Party State

$J_i \rightarrow J_f$	^{171}Hf	^{173}Hf	^{175}Hf		^{177}Hf		^{179}Hf	
	IBFM-1	IBFM-2	IBFM-1	IBFM-2	IBFM-1	IBFM-2	IBFM-1	IBFM-2
$\frac{5}{2_1} \rightarrow \frac{1}{2_1}$	0.34	0.442	0.0024	0.0063	--	0.732	--	--
$\frac{3}{2_1} \rightarrow \frac{5}{2_1}$	0.16	0.264	0.053	0.067	--	0.087	--	--
$\frac{5}{2_1} \rightarrow \frac{1}{2_1}$	-	2×10^{-5}	--	--	--	0.00631	--	--
$\frac{5}{2_2} \rightarrow \frac{1}{2_1}$	0.0025	0.00033	--	--	--	0.468	--	--
$\frac{5}{2_2} \rightarrow \frac{3}{2_1}$	0.1901	0.0156	--	--	--	--	--	--
$\frac{3}{2_1} \rightarrow \frac{1}{2_1}$	--	--	0.243	0.327	--	--	--	--
$\frac{5}{2_2} \rightarrow \frac{5}{2_1}$	--	--	0.00031	0.0077	--	--	--	--
$\frac{7}{2_1} \rightarrow \frac{5}{2_2}$	--	--	0.001	2×10^{-3}	--	--	--	--
$\frac{9}{2_1} \rightarrow \frac{7}{2_1}$	--	--	--	--	--	--	0.732	0.622
$\frac{11}{2_1} \rightarrow \frac{9}{2_1}$	--	--	--	--	--	--	0.872	0.413
$\frac{11}{2_1} \rightarrow \frac{7}{2_1}$	--	--	--	--	--	--	0.0043	0.0007
$\frac{13}{2_1} \rightarrow \frac{11}{2_1}$	--	--	--	--	--	--	0.0006	4×10^{-4}

4.2- $^{181-187}\text{W}$ Isotopes in IBFM-1

4.2.1- Energy Levels for $^{181-189}\text{W}$ Isotopes

The present study, concentrated on the odd-mass $^{181-189}\text{W}$ isotopes. Since in the IBFM-1 no distinction is made between neutron and proton bosons, the IBM-1 parameters were obtained by projecting the IBM-2 Hamiltonian onto the IBM-1 space and equating the matrix elements of the Hamiltonian between states that are fully symmetric in the neutron-proton degree of freedom. The remaining parameters, appearing in the boson-fermion interaction $V_{BF}(A_0, \Gamma_0, \Lambda_0)$, were determined starting from the values obtained in studying the odd-mass $^{171-179}\text{Hf}$ isotopes in this work.

They were subsequently adjusted in order to obtain a good description of both positive-parity and negative-parity states at the same time. Thereby, one finally obtains the values of the interaction parameters $A_0 = -0.25\text{MeV}$, $\Gamma_0 = 0.3\text{MeV}$ and $\Lambda_0 = 2.130\text{MeV}$. The value of $\hbar\tilde{S} = 1.5\text{MeV}$ which is consistent with the excitation energy for the $J_i^+ = 2_1^+$ states in the even-even $^{180-190}\text{W}$ isotopes.

The levels calculation is used to fit experimental energy levels with the boson-fermion parameters for $^{181-187}\text{W}$ isotopes. These parameters have not been changed along the isotopic chain. The dependence of V_{BF} on the specificity of each nucleus is counted for in the occupation probabilities appearing in the exchange term Λ_0 and in the quadrupole term Γ_0 . The best agreement with experiment for the level calculations of $^{181-187}\text{W}$ isotopes is found by slightly varying the occupation probabilities to ϵ_j^2 to allow a better fit with the experiment (see Figs. (4.11) to (4.15) for negative parity states and Figures (3-16) to (3-20) for positive parity states). The Hamiltonian (Eq. (2-76)) was diagonalised by means of the computer program **ODDA** [136] in which the IBFM-1 parameters. The parameters for the $^{180-190}\text{W}$ core are derived in the present work and given in Chapter Three, while the quasi-particle energies and occupation probabilities used in this work are given in Table (4-8).

Table (4-8): Adopted values for the parameters used for IBFM calculation.

Parameters	^{181}W			^{183}W			^{185}W		
	$2f_{5/2}$	$3p_{3/2}$	$3p_{1/2}$	$2f_{5/2}$	$3p_{3/2}$	$3p_{1/2}$	$2f_{5/2}$	$3p_{3/2}$	$3p_{1/2}$
V_j (MeV)	2.0281	1.097	2.419	2.052	1.714	2.584	2.032	1.72	2.576
ϵ_j^2	0.049	0.0715	0.03	0.0477	0.0687	0.0293	0.0462	0.0691	0.0289
Parameters	^{187}W								
V_j (MeV)	2.033	1.722	2.573						
ϵ_j^2	0.0469	0.0672	0.0287						

As an example we discuss ^{185}W isotope. The low lying negative parity states in this nucleus are built upon the negative parity orbits in the 82-126 neutron shell with angular momenta $1h_{9/2}$, $2f_{7/2}$, $2f_{5/2}$, $3p_{3/2}$ and $3p_{1/2}$.

In the $SU(3) \otimes U(2)$ limit these orbits all belong to the pseudo-orbital oscillator shell with $n = 4$.

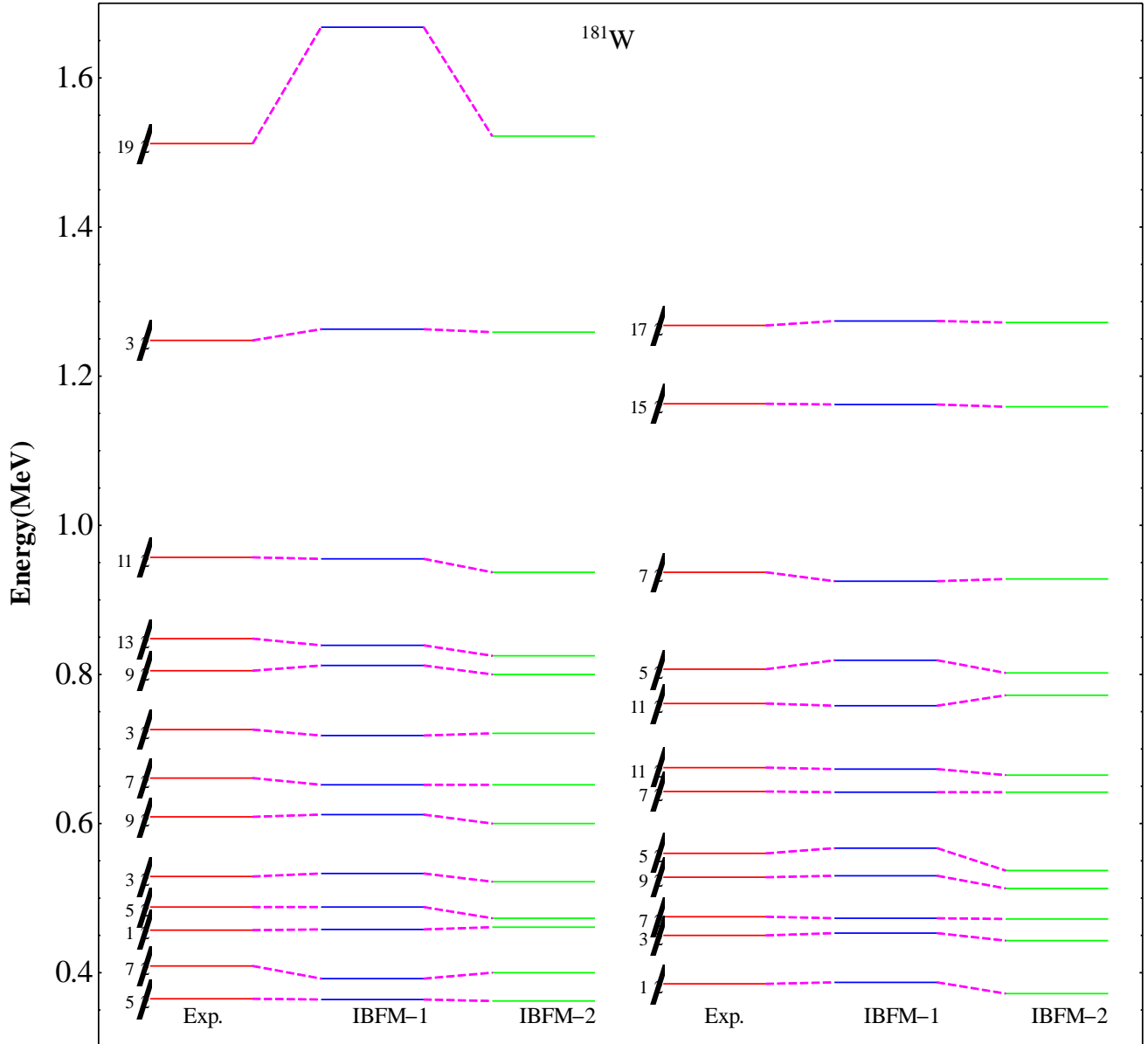


Figure (4.11): Comparison between experimental negative parity states data [110], IBFM-1 and IBFM-2 calculated energy levels for ^{181}W .

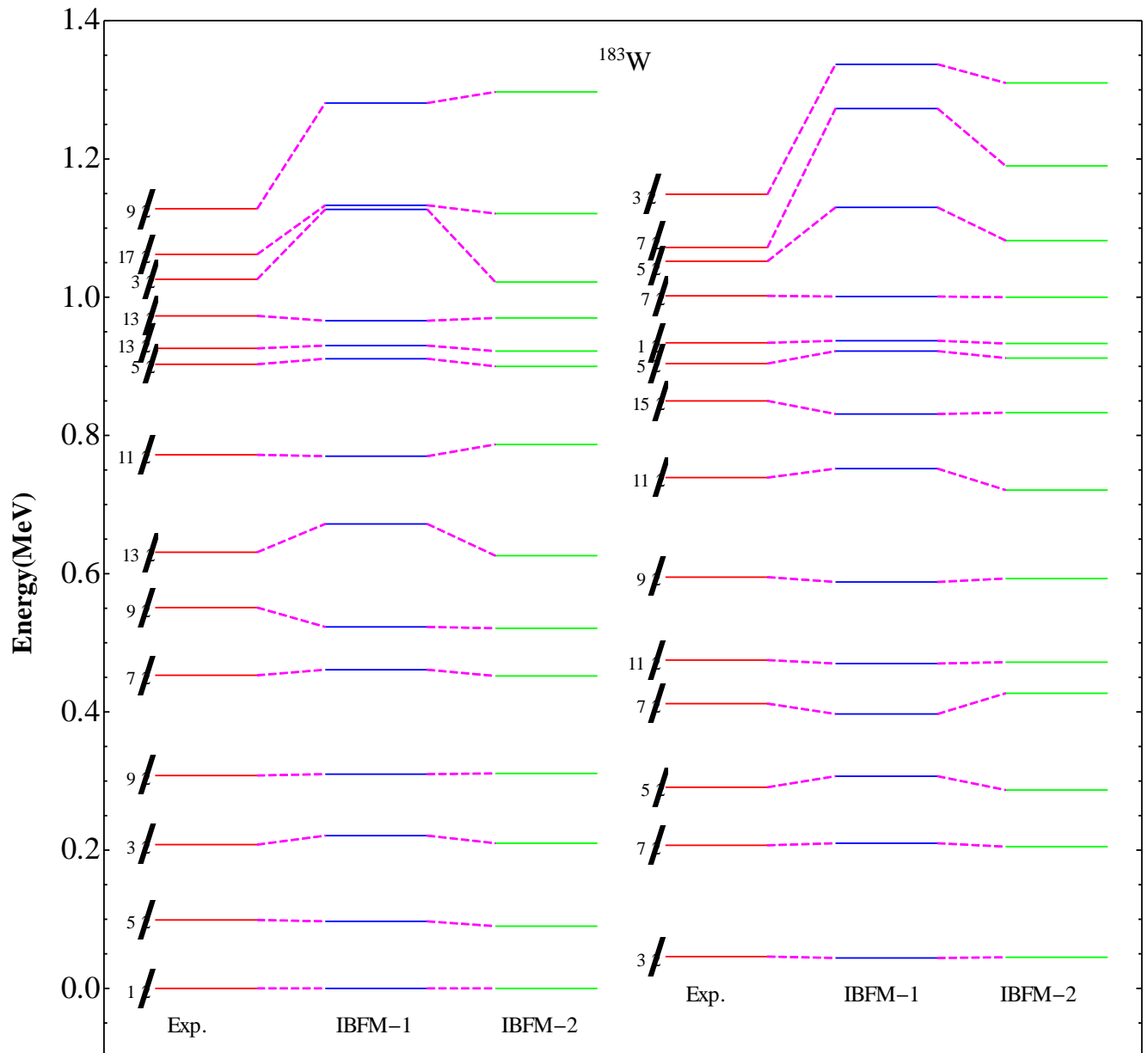


Figure (4.12): Comparison between experimental negative parity states data [110], IBFM-1 and IBFM-2 calculated energy levels for ^{183}W .

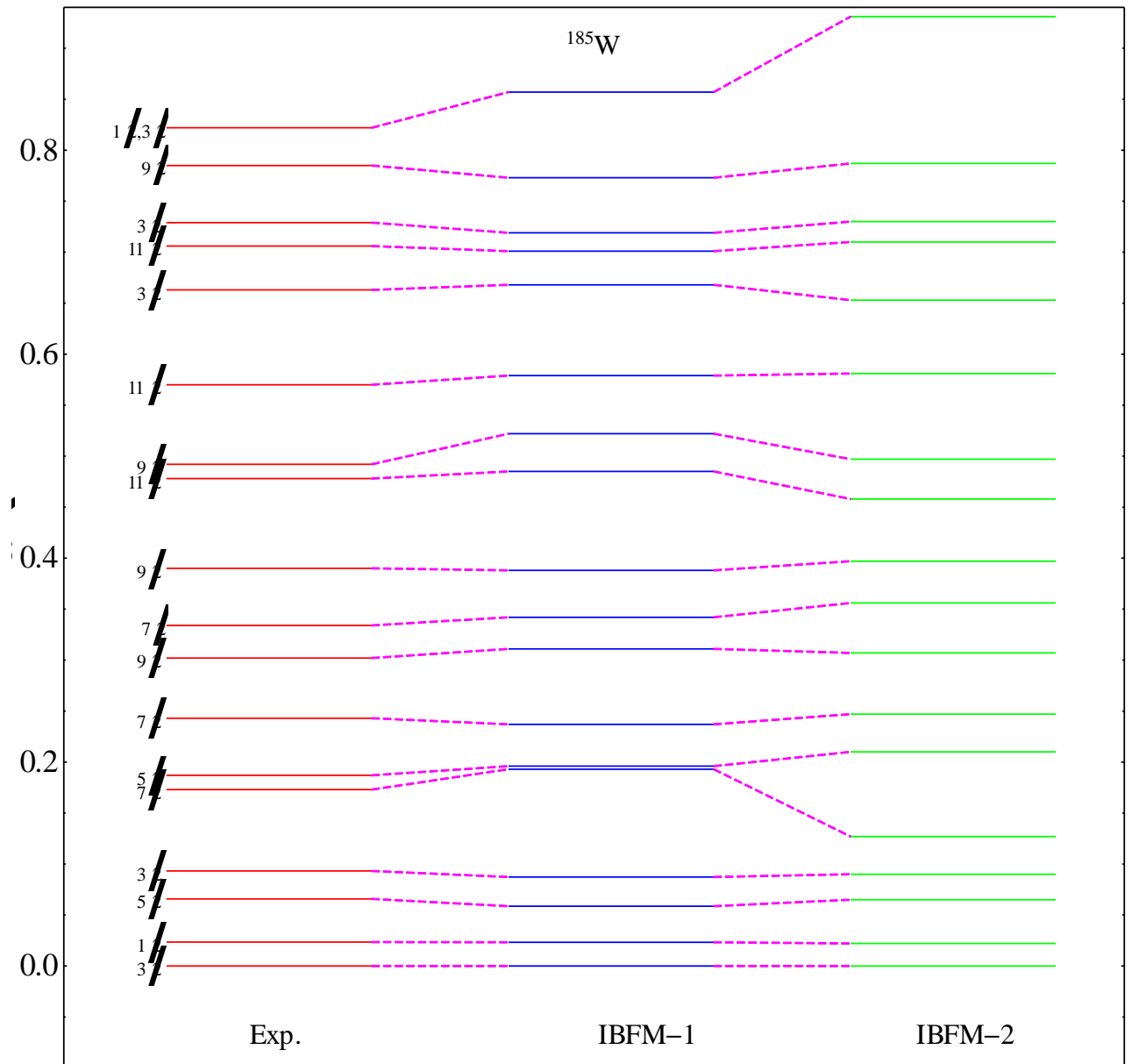


Figure (4.13): Comparison between experimental negative parity states data [110], IBFM-1 and IBFM-2 calculated energy levels for ^{185}W .

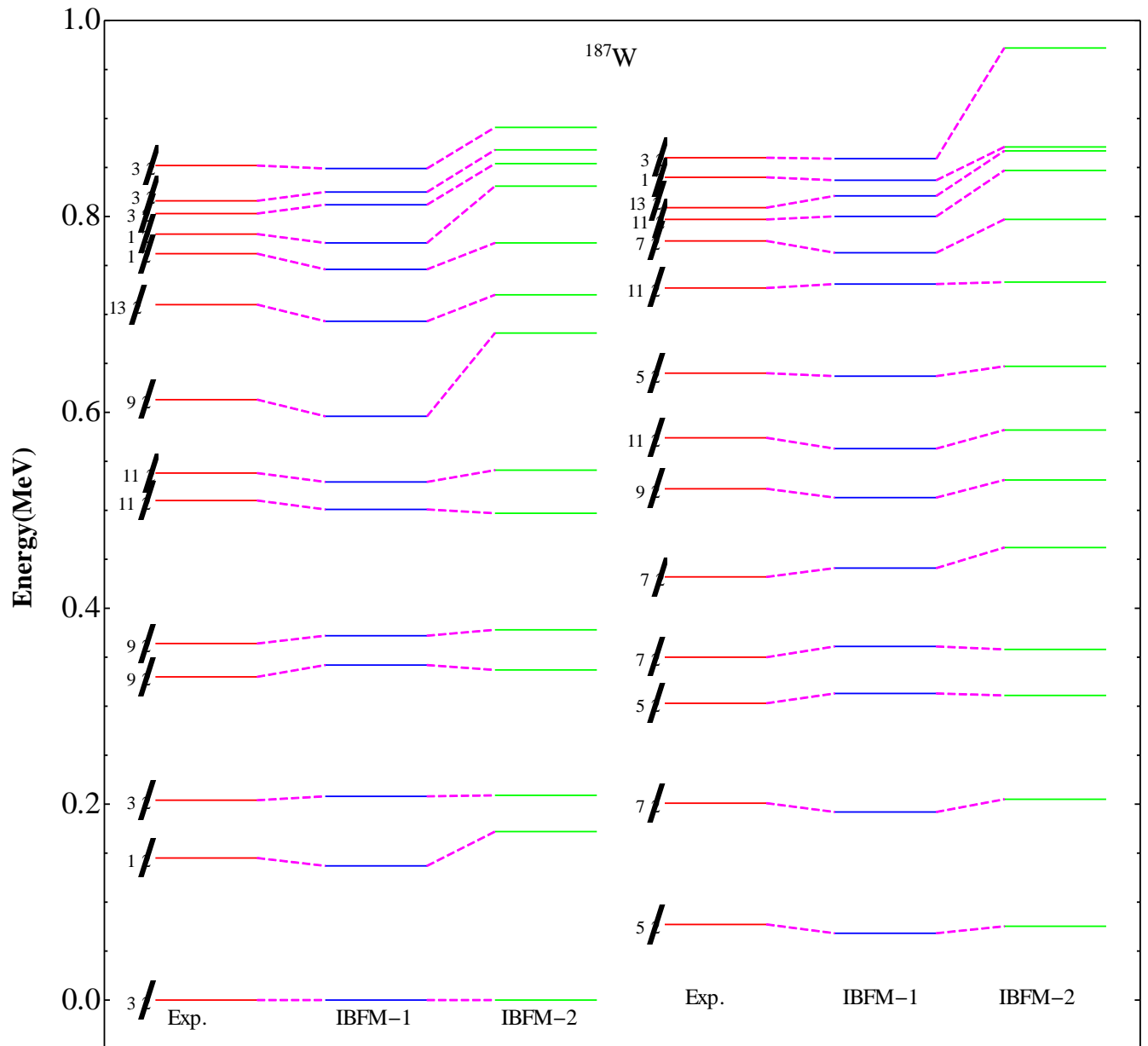


Figure (4.14): Comparison between experimental negative parity states data [110], IBFM-1 and IBFM-2 calculated energy levels for ^{187}W

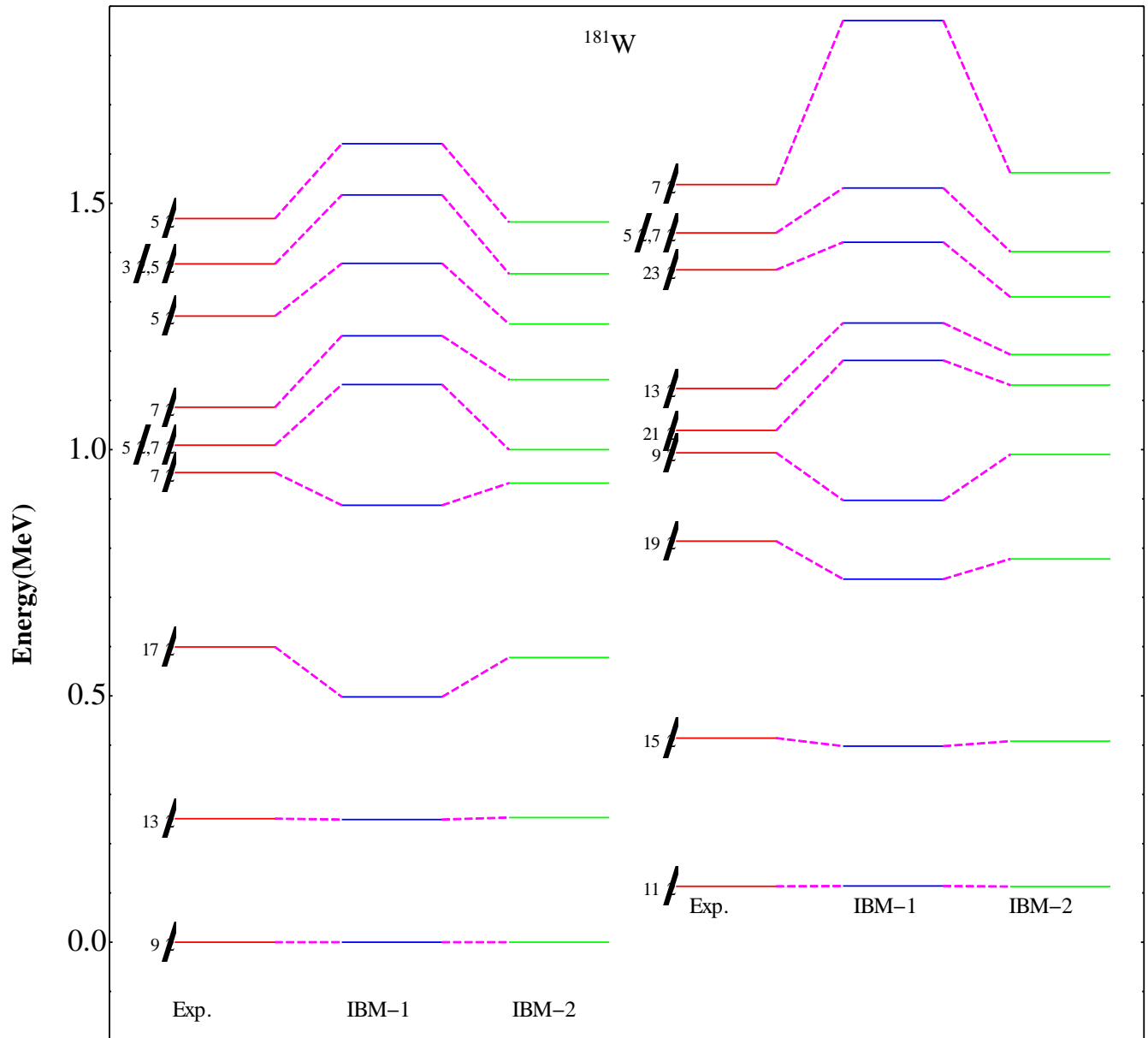


Figure (4.15): Comparison between experimental positive parity states data [110], IBFM- 1 and IBFM-2 calculated energy levels for ^{181}W .

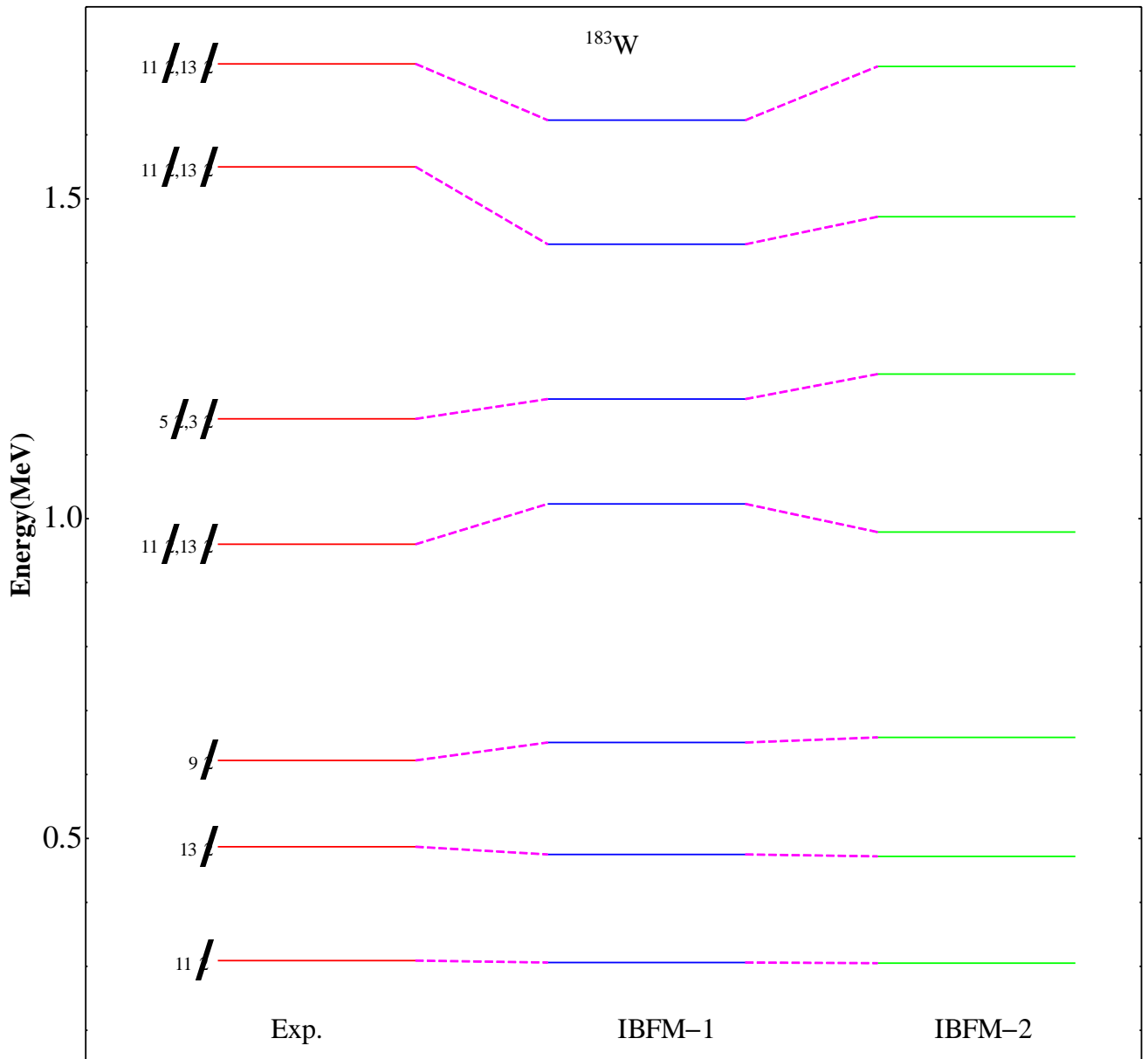


Figure (4.16): Comparison between experimental positive parity states data [110], IBFM-1 and IBFM-2 calculated energy levels for ^{183}W .

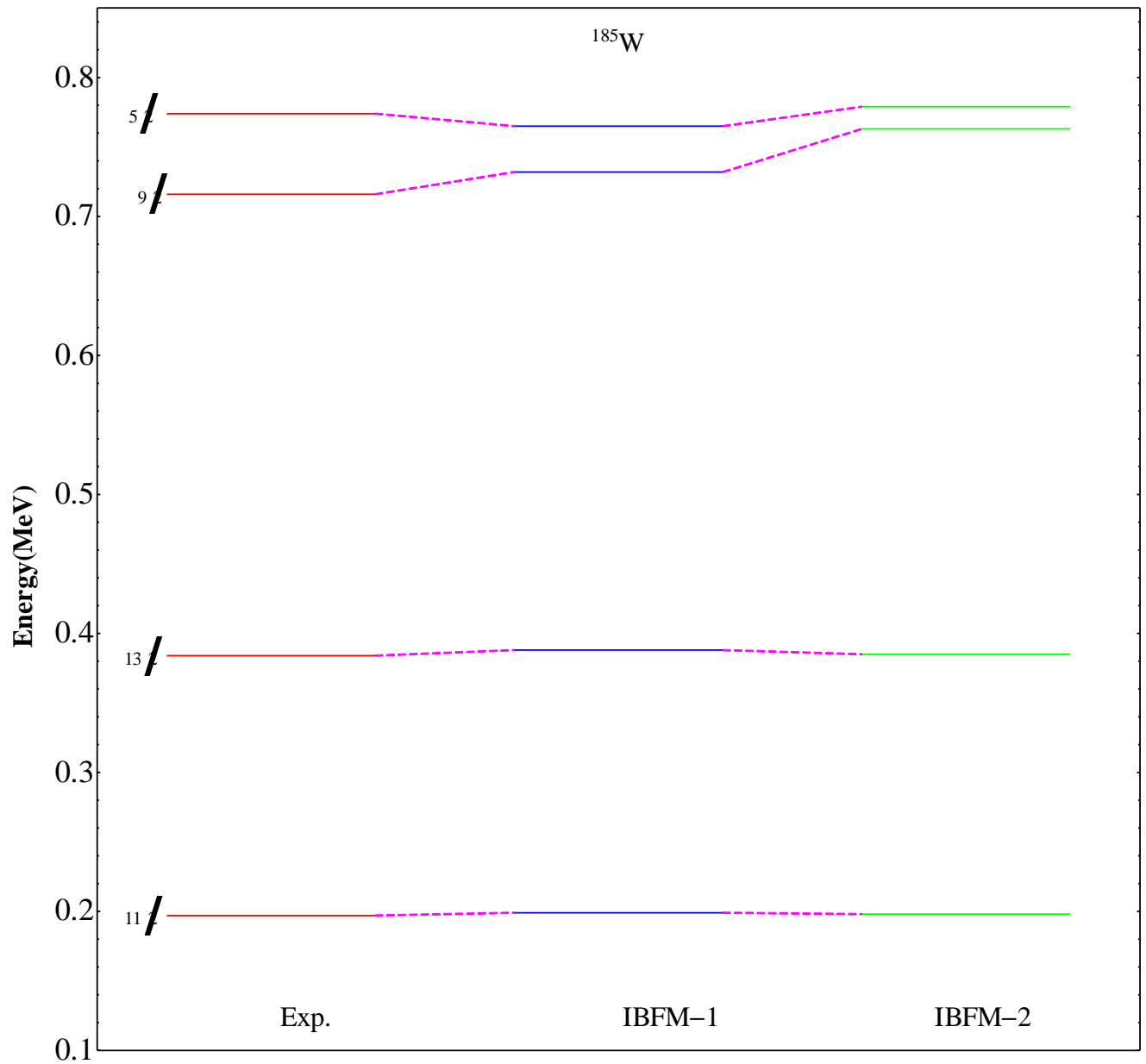


Figure (4.17): Comparison between experimental positive parity states data [110], IBFM-1 and IBFM-2 calculated energy levels for ^{185}W .

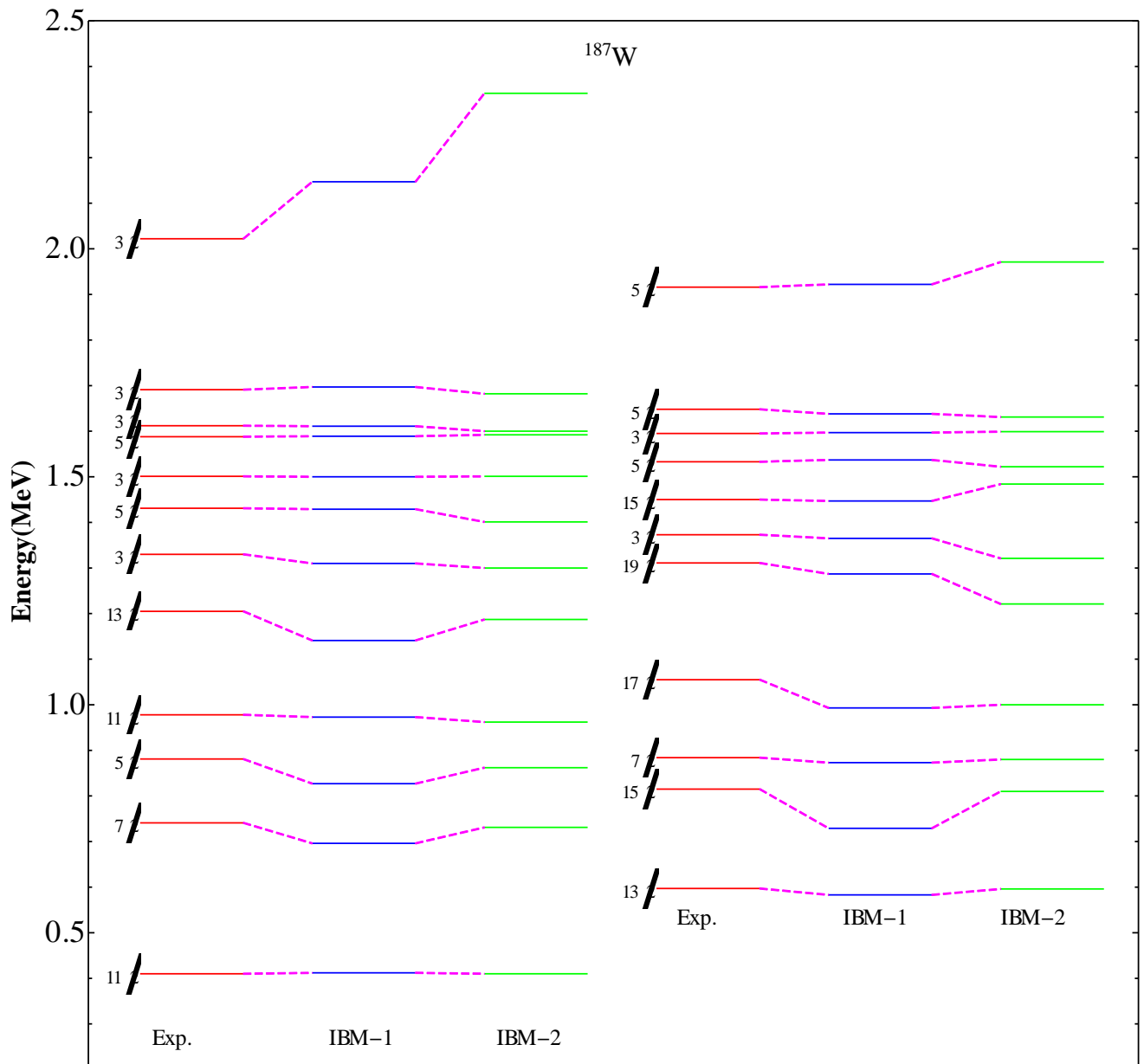


Figure (4.18): Comparison between experimental positive parity states data [110], IBFM-1 and IBFM-2 calculated energy levels for ^{187}W .

4.2.2- E2 Transitions for $^{181-187}\text{W}$ Isotopes

Electromagnetic transitions give a good test of the model wave functions where in particular the extent to which two wave functions have similar single particle components. In general, the electromagnetic transition operators are written as the sum of two terms, the first of which acts only on the boson part of the wave function and second only on the fermion part (see Eq. (2-103)), where Q_B has been defined in Eq. (2-43),

Q_{jj} are single particle matrix elements of the quadruple operator, e_B and e_F are the boson and fermion effective charges respectively. In the calculations, the boson effective charge e_B was chosen such that it reproduces the experimental values for the even mass W isotopes reasonably well with one value taken constant over the entire isotopic chain. This resulted in $e_B = 0.151 eb$ for $^{180-190}\text{W}$ isotopes. The fermion effective charge for W isotopes is taken as $e_F = 0.15 eb$. It should be noted that the fermion effective charge has only a minor influence on the collective E2 transition strengths. Tables (4-9) and (4-10) give $B(E2)$'s for positive and negative parity states in W isotopes.

Table (4-9): Electric Transition Probability $B(E2; J_i^+ \rightarrow J_f^+)$ for $^{181-187}\text{W}$ in $e^2 \cdot b^2$ units for Positive Parity States.

$J_i^+ \rightarrow J_f^+$	^{181}W		^{183}W		^{185}W		^{187}W	
	IBFM-1	IBFM-2	IBFM-1	IBFM-2	IBFM-1	IBFM-2	IBFM-1	IBFM-2
$\frac{11}{2_1} \rightarrow \frac{9}{2_1}$	4.33×10^{-3}	8.6×10^{-3}	-	-	-	-	-	-
$\frac{13}{2_1} \rightarrow \frac{11}{2_1}$	3.72×10^{-3}	3.20×10^{-3}	3.11×10^{-4}	3.27×10^{-4}	0.0008	0.0037	2.50×10^{-4}	0.0055
$\frac{15}{2_1} \rightarrow \frac{13}{2_1}$	6.91×10^{-3}	4.29×10^{-4}	-	-	-	-	-	-
$\frac{13}{2_1} \rightarrow \frac{9}{2_1}$	5.93×10^{-4}	5.30×10^{-4}	-	-	-	-	-	-
$\frac{9}{2_1} \rightarrow \frac{13}{2_1}$	-	-	6.72×10^{-4}	4.61×10^{-4}	0.00078	0.0008	-	-
$\frac{9}{2_1} \rightarrow \frac{11}{2_1}$	-	-	4.33×10^{-3}	5.03×10^{-4}	-	-	-	-
$\frac{7}{2_1} \rightarrow \frac{9}{2_1}$	-	-	-	-	0.048	0.097	-	-
$\frac{9}{2_2} \rightarrow \frac{7}{2_1}$	-	-	-	-	2.92×10^{-4}	3.00×10^{-4}	0.00087	0.087
$\frac{7}{2_1} \rightarrow \frac{13}{2_1}$	-	-	-	-	-	-	7.7×10^{-4}	0.00073

Table (4-10): Electric Transition Probability $B(E2; J_i^- \rightarrow J_f^-)$ for $^{181-187}\text{W}$ in $e^2 \cdot b^2$ units for negative Parity States.

$J_i^- \rightarrow J_f^-$	^{181}W		^{183}W		^{185}W		^{187}W	
	IBFM-1	IBFM-2	IBFM-1	IBFM-2	IBFM-1	IBFM-2	IBFM-1	IBFM-2
$\frac{5}{2}^- \rightarrow \frac{1}{2}^-$	2.28×10^{-2}	3.20×10^{-3}	-	-	3.30×10^{-3}	2.31×10^{-3}	-	-
$\frac{7}{2}^- \rightarrow \frac{1}{2}^-$	1.32×10^{-3}	3.20×10^{-4}	-	-	-	-	-	-
$\frac{3}{2}^- \rightarrow \frac{7}{2}^-$	4.40×10^{-2}	3.20×10^{-2}	-	-	-	-	-	-
$\frac{3}{2}^- \rightarrow \frac{1}{2}^-$	-	-	8.30×10^{-4}	7.32×10^{-4}	-	-	-	-
$\frac{5}{2}^- \rightarrow \frac{3}{2}^-$	-	-	6.50×10^{-3}	8.90×10^{-3}	-	-	3.31×10^{-3}	3.30×10^{-2}
$\frac{7}{2}^- \rightarrow \frac{5}{2}^-$	-	-	9.70×10^{-4}	5.50×10^{-4}	-	-	-	-
$\frac{1}{2}^- \rightarrow \frac{3}{2}^-$	-	-	-	-	5.60×10^{-3}	4.21×10^{-1}	-	-
$\frac{3}{2}_1^- \rightarrow \frac{5}{2}_1^-$	-	-	-	-	4.40×10^{-3}	4.20×10^{-3}	3.70×10^{-4}	4.90×10^{-4}
$\frac{1}{2}^- \rightarrow \frac{5}{2}^-$	-	-	-	-	-	-	4.50×10^{-3}	2.54×10^{-3}

4.2.3- M1 Transitions for $^{181-187}\text{W}$ Isotopes

The M1 operator is given in Eq. (2-106), Where g_B is the boson g-factor determined by the even-even core, and g_{jj} is the single particle contribution which depends on gland ground state band (orbital and spin g-factor) of the odd nucleon, where $g_{jj} = 0.32 \sim_N$ is the boson g-factor determined by the magnetic moment of levels in the even-even core. In the actual calculations the computer program *PBEM* [60] has been used. Tables (4-11) and (4-12) gives the B(M1) for positive and negative parity states for $^{181-187}\text{W}$ isotopes.

Table (4-11): Magnetic Transition Probability $B(M1; J_i^+ \rightarrow J_f^+)$ for $^{181-187}\text{W}$ in $\sim \frac{2}{N}$ units for Positive Party States.

$J_i^+ \rightarrow J_f^+$	^{181}W		^{183}W		^{185}W		^{187}W	
	IBFM-1	IBFM-2	IBFM-1	IBFM-2	IBFM-1	IBFM-2	IBFM-1	IBFM-2
$\frac{3}{2} \rightarrow \frac{5}{2}$	2.28×10^{-2}	3.20×10^{-3}	-	-	-	-	-	-
$\frac{13}{2} \rightarrow \frac{11}{2}$	1.32×10^{-3}	3.20×10^{-4}	8.30×10^{-4}	7.32×10^{-4}	5.60×10^{-3}	4.21×10^{-1}	3.31×10^{-3}	3.30×10^{-2}
$\frac{15}{2} \rightarrow \frac{13}{2}$	4.40×10^{-2}	3.20×10^{-2}	-	-	-	-	-	-
$\frac{9}{2} \rightarrow \frac{13}{2}$	-	-	6.50×10^{-3}	8.90×10^{-3}	3.30×10^{-3}	2.31×10^{-3}	-	-
$\frac{9}{2} \rightarrow \frac{11}{2}$	-	-	9.70×10^{-4}	5.50×10^{-4}	-	-	-	-
$\frac{7}{2} \rightarrow \frac{9}{2}$	-	-	-	-	4.40×10^{-3}	4.20×10^{-3}	-	-
$\frac{7}{2} \rightarrow \frac{13}{2}$	-	-	-	-	-	-	4.50×10^{-3}	2.54×10^{-3}
$\frac{9}{2} \rightarrow \frac{7}{2}$	-	-	-	-	-	-	3.70×10^{-4}	4.90×10^{-4}

Table (4-12): Magnetic Transition Probability $B(M1; J_i^- \rightarrow J_f^-)$ for $^{181-187}\text{W}$ in $\sim \frac{2}{N}$ units for negative Party States.

$J_i^- \rightarrow J_f^-$	^{181}W		^{183}W		^{185}W		^{187}W	
	IBFM-1	IBFM-2	IBFM-1	IBFM-2	IBFM-1	IBFM-2	IBFM-1	IBFM-2
$\frac{5}{2} \rightarrow \frac{1}{2}$	5.0×10^{-5}	4.8×10^{-5}	-	-	-	-	-	-
$\frac{7}{2} \rightarrow \frac{1}{2}$	3.7×10^{-4}	4.57×10^{-5}	-	-	-	-	7.80×10^{-4}	6.70×10^{-5}
$\frac{3}{2} \rightarrow \frac{7}{2}$	4.1×10^{-5}	7.30×10^{-5}	-	-	-	-	-	-
$\frac{3}{2} \rightarrow \frac{1}{2}$	-	-	4.30×10^{-5}	3.80×10^{-5}	-	-	-	-
$\frac{5}{2} \rightarrow \frac{3}{2}$	-	-	5.97×10^{-5}	6.20×10^{-5}	-	-	4.50×10^{-5}	8.00×10^{-5}
$\frac{7}{2} \rightarrow \frac{5}{2}$	-	-	4.48×10^{-5}	5.70×10^{-4}	-	-	-	-
$\frac{1}{2} \rightarrow \frac{3}{2}$	-	-	-	-	3.70×10^{-5}	4.00×10^{-5}	-	-
$\frac{3}{2} \rightarrow \frac{5}{2}$	-	-	-	-	5.20×10^{-5}	6.00×10^{-6}	-	-
$\frac{1}{2} \rightarrow \frac{5}{2}$	-	-	-	-	4.60×10^{-4}	3.40×10^{-5}	3.70×10^{-5}	3.70×10^{-5}

4.3 ¹⁷¹⁻¹⁷⁹Hf Isotopes in IBFM-2

An even-odd Hf isotope is described in IBFM-2 by coupling a neutron to its ⁷²Hf isotope, described in terms of the IBM-2, with the Hamiltonian of Eq. (2-42). Consequently, the first step to describe the even-odd nucleus is a compelling description of the even-even core. In the case of the Hf isotopes, we start pointing for the description of the Hf even-even cores. Afterward, the parameters were slightly changed to take into account later experimental information on mixed symmetry states 1^+ . The resulting values of the parameters used in the description of the Hf cores can be found in Table (3-21). The strength of the Majorana interaction, M , was obtained by fitting the excitation energy of the first 1^+ level, mixed symmetry state allowed in IBM-2, but not in IBM-1. With those parameters, both energy spectra and electromagnetic properties were calculated in a good agreement with the available experimental data for even-even Hf isotopes. Thus, we are confident that the wave functions of the even-even Hf core nuclei provided by the IBM-2 model are good. Once the wave functions for the states in the even-even core have been obtained, the odd-neutron has to be coupled to it in order to calculate excitation energies, electromagnetic properties.

4.3.1- Energy Spectra

The coupling of the neutron to the even-even core is governed by the boson-fermion interaction, where the more important terms are those between the odd fermion and the bosons with the alternative flavor. This interaction, Eq. (2-154), is decomposed into three terms: quadrupole ($V_{\epsilon_f}^Q$), exchange ($V_{\epsilon_f}^E$), and monopole ($V_{\epsilon_f}^M$). Since the Hamiltonian is invariant under parity, positive and negative parity states are studied separately. The parameters in V_{BF} are different for each parity accordingly and are shown in Table (4-13). It is important to emphasize that Γ_f, Λ_f and A_f are phenomenological parameters for the entire chain of isotopes, in contrast to

the above-mentioned IBFM-1 calculation, where these parameters were fitted for each isotope separately. The IBFM-2 Hamiltonian (Eq. (2-142)) was diagonalized by means of the *ODDPAR* program [107] in which the IBFM-2 parameters which used in the *ODDPAR* code are given in Table (4-2) for all isotopes under study ($A = BEM$, $\Gamma = BFQ$, $\Lambda = BFE$)

Table (4-13): Parameters (in MeV) of the boson-fermion interaction used in this work for positive (+) and negative (-) parity states for $^{171-179}\text{Hf}$ isotopes.

Parity	Γ	Λ	A
+	0.455	0.033	-0.095
-	0.879	4.871	-0.864

The single-particle energies E_j^{sp} appear in Eqs. (2-82) and (2-83) are listed in Table (4-2), but we changed the relative position of the $2f_{5/2}$, $3p_{3/2}$ and $3p_{1/2}$ orbits to account for the sequence in the low-lying levels $J^f = 5/2^+$ and $J^f = 3/2^+$ along the chain of isotopes. Table (4-2) shows the quasiparticle energies and the occupation probabilities obtained from the *BCS* calculation. One important feature to note is that the positive parity levels as well as the negative parity levels have high quasiparticle energies and small occupation probabilities when we compare them with the rest of the levels of the same parity.

In Figs. (4-1) to (4-5), experimental and calculated excitation energies of the negative parity levels in $^{171-179}\text{Hf}$ isotopes are shown. The correspondence between experimental and calculated levels was done using the electromagnetic properties discussed below. It can be seen that the structure of the spectrum of ^{171}Hf corresponds to a particle coupled to a deformed core. The first two states come from the coupling of the single-particle states included in the calculation with the ground state of ^{170}Hf . Then there is a gap and, around the energy of the first 2^+ of ^{170}Hf (0.10080 MeV), a set of levels, which comes from the coupling of the single-particle levels to this state, appears. The spectrum of ^{173}Hf corresponds to a transitional situation where the forbidden zone (gap) is absent. Our

calculations reproduce well this structure, although they show a certain tendency to structures of the particle-rotation type in both isotopes. The origin of this effect can be found in the low values of the boson-fermion parameters, which supply weak coupling schemes.

Experimental and calculated excitation energies of the negative parity levels in $^{171-179}\text{Hf}$ isotopes are compared in Figs. (4.1) to (4.5). The correspondence in this case is difficult for some levels in $^{171-179}\text{Hf}$ isotopes, due to the lack of electromagnetic information which would allow for their correct identification. This fact was also observed in the IBFM-1 calculation, where it was suggested that this level could be reproduced when the $7/2^-$ level of Hf is included, which is beyond the scope of this work. The calculation for the ^{173}Hf isotope shows a sequence of levels distributed almost uniformly up to 0.7 MeV, while there is a set of experimental levels grouped together around 0.3 MeV. However, there is an almost 1:1 correspondence between experimental and calculated levels below 0.5 MeV.

Finally, as it can be seen in Figures (4-6) to (4-10) for positive parity states that in $^{177-179}\text{Hf}$ there is an excellent agreement between the calculated and the experimental energies for the positive parity levels. Again, the calculation predicts a first excited band led by a $7/2^+$ state at around 0.4 MeV. In the case of the negative parity levels, experimental data are only available for the ground-state band, well described in the calculation, but with a slightly higher moment of inertia. A first excited band, led by a $7/2^-$ state at 0.2 MeV, appears in our calculations, as in ^{179}Hf .

4.3.2- E2 Transitions for $^{171-179}\text{Hf}$ Isotopes

In addition to spectra, we have calculated $B(E2)$'s. This electric quadrupole transition operator $T(E2)$ consists of a bosonic and a fermionic part, $T_B^{(E2)}$ given in Eq. (2-47) and $T_f^{(E2)}$ taken in Eq. (2-155). The

quadrupole operators present in $T_B^{(E2)}$ correspond to those appearing in the Hamiltonian (2-142). The value used for the bosonic effective charges e and e is $0.191 e b$. For the fermionic effective charge e_F , we adopt the value $1.5 e b$. Tables (4-4) and (4-5). These tables show the trend of the calculated values of $B(E2)$ for some low-lying positive parity states in the Hf isotopes. The calculation reproduces well the trend, except some transitions for $A = 171$. These could be due to the existence of a low energy state 0^+ at 0.915.4 MeV in the even-even core, ^{172}Hf , which the IBM is unable to reproduce without including octupole degrees of freedom. The coupling of this state with the fermionic single-particle degrees of freedom may have a relatively high influence on the low-lying states in ^{172}Hf .

Tables (4-4) and (4-5) show the calculated values of $B(E2)$ for this $^{171-179}\text{Hf}$ isotopes. It can be seen that, even when the calculation does not describe fine details of the experimental data, general trends are reproduced. Again the inclusion of octupole degrees of freedom could improve the description of these isotopes. Some calculated values of the reduced transition probabilities $B(E2)$ in ^{175}Hf are quoted in tables.

4.3.3 - M1 Transitions and Mixing Ratio $(E2/M1)$ for $^{171-179}\text{Hf}$ Isotopes

In contrast to E2 properties, M1 transitions and moments in even-odd isotopes are dominated by the fermion part of the M1 operator. Using the operator of Eq. (2-159), one can compute the corresponding transitions. The boson part of the operator requires a specification of g_f^B and g_F^B . These can be taken from the calculations reported for even-even nuclei for Sambataro *et al.*, 1984 [109]. The fermion part of the operator requires a specification of the fermion g-factors. The orbital g-factors are $g_{l,f}^F = 1 - N$ and $g_{l,\epsilon}^F = 0 - N$. The spin g-factors are taken as the free values quenched by a factor of 0.7, i.e. $g_{s,f}^F = 0.7 \times 5.58 - N$. A portion of the results is shown in Tables (4-6) and (4-7). Also here there is no experimental information. For those cases for the results of calculations of M1 transitions agree in general

less well with the data as compared to the corresponding calculations of E2 transitions. This indicates that while the collective degrees of freedom appear to be well described in odd-even nuclei, the single-particle degrees of freedom still require improvement.

Calculations of electromagnetic transitions give a good test of nuclear model wave functions. In this section discussed the calculation of M1 and E2 transition strengths and compare them with the available experimental information.

With $T^{(E2)}$ and $T^{(M1)}$ operators completely specified it is possible to calculate $u(E2/M1)$ mixing ratios for transitions between states of spin as in Eq. (2-54).

From the reduced E2 and M1 matrix elements, the multipole mixing ratios for transitions in $^{171-179}\text{Hf}$ were calculated and compared with the experimental data. Results are shown in Tables (4 - 13) and (4 - 14) respectively. One can see that there is a good agreement for the sign and the magnitude of the mixing ratios of most transitions, as calculated from the IBFM-1 and IBFM-2, and that obtained from experiment results. The expectation is for some transitions which the calculated sign of mixing ratio is opposite to experiment results. However, this could be attributed to the use of a different sign convention for the definition of mixing ratio, used in the experimental work.

Table (4- 14): Mixing Ratio $\delta(E2/M1)$ for $^{171-179}\text{Hf}$ isotopes for positive Parity States in eb/μ_N units. Exp. are taken fro, ref. [110]

$J_i \rightarrow J_f$	171Hf			173Hf			175Hf			179Hf			
	Exp.	IBFM-1	IBFM-2	Exp.	IBFM-1	IBFM-2	Exp.	IBFM-1	IBFM-2	Exp.	IBFM-1	IBFM-2	
$\frac{9}{2} \rightarrow \frac{7}{2}$	$-0.11\mathcal{Z}_1^{11}$	-0.21	1.2	-	-	-	0.23	0.762	0.442	4.4(4)	1.758	-2.11	
$\frac{11}{2} \rightarrow \frac{9}{2}$	-0.04	2.11	-0.08	0.09(2)	0.621	0.0931	-	-	-	-3.07	2.87	-5.414	
$\frac{3}{2} \rightarrow \frac{1}{2}$	$-0.19\mathcal{Z}_1^{14}$	-0.317	2.2	0.88(20)	0.771	0.932	0.92	0.632	0.851	-2.4	-1.33	0.00047	
$\frac{5}{2} \rightarrow \frac{3}{2}$	$-0.07\mathcal{Z}_1^{12}$	2.611	-0.07	0.029 \mathcal{Z}_1^{11}	0.082	0.031	-	-	-	-	-	-	
$\frac{7}{2} \rightarrow \frac{5}{2}$	-	-	-	0.69 \mathcal{Z}_2^{10}	2.171	0.687	1.08	1.153	2.251	-	-	-	-
$\frac{13}{2} \rightarrow \frac{11}{2}$	-	-	-	-0.05(11)	-2.71	-0.087	-	-	-	-	-	-	
$\frac{7}{2} \rightarrow \frac{7}{2}$	-	-	-	1.9 \mathcal{Z}_1^{11}	2.617	2.271	0.89	1.307	1.414	-	-	-	
$\frac{7}{2} \rightarrow \frac{7}{2}$	-	-	-	1.9 \mathcal{Z}_1^{14}	4.671	3.652	-	-	-	-	-	-	
$\frac{19}{2} \rightarrow \frac{17}{2}$	-	-	-	-0.2	-0.852	-0.652	-	-	-	-	-	-	
$\frac{7}{2} \rightarrow \frac{3}{2}$	-	-	-	-	-	-	0.26	1.321	0.372	-	-	-	
$\frac{13}{2} \rightarrow \frac{9}{2}$	-	-	-	-	-	-	0.4	2.471	0.387	0.3(3)	1.478	2.414	
$\frac{5}{2} \rightarrow \frac{3}{2}$	-	-	-	-	-	-	-	-	-	0.82	4.527	0.772	
$\frac{7}{2} \rightarrow \frac{5}{2}$	-	-	-	-	-	-	-	-	-	0.7(3)	0.951	1.37	
$\frac{7}{2} \rightarrow \frac{9}{2}$	-	-	-	-	-	-	-	-	-	0.23	0.337	0.522	
$\frac{9}{2} \rightarrow \frac{5}{2}$	-	-	-	-	-	-	-	-	-	1.2 \mathcal{Z}_1^{11}	3.459	2.2	
$\frac{11}{2} \rightarrow \frac{7}{2}$	-	-	-	-	-	-	-	-	-	0.5(3)	0.852	0.897	

Table (4- 15): Mixing Ratio $\delta(E2/M1)$ for $^{171-179}\text{Hf}$ isotopes for Negative Parity States in eb/μ_N units.

$J_i \rightarrow J_f$	^{171}Hf			^{173}Hf			^{175}Hf			^{179}Hf		
	Exp.	IBFM-1	IBFM-2	Exp.	IBFM-1	IBFM-2	Exp.	IBFM-1	IBFM-2	Exp.	IBFM-1	IBFM-2
$\frac{9}{2_1} \rightarrow \frac{7}{2_1}$	≈ 0.2	0.827	0.467	0.21	0.317	0.317	0.36	0.362	0.65	-	-	-
$\frac{11}{2_1} \rightarrow \frac{9}{2_1}$	-0.18^{+16}_{-2}	1.171	-2.116	-	-	-	-	2.261	2.141	-	0.754	0.598
$\frac{13}{2_1} \rightarrow \frac{11}{2_1}$	-0.28^{+16}_{-2}	-0.372	0.0096	-0.49	-0.472	-0.52	0.32	0.872	0.672	-	-0.273	0.313
$\frac{15}{2_1} \rightarrow \frac{13}{2_1}$	-0.35^{+15}_{-2}	-0.412	-0.38	-	-	-	1.331	1.331	0.031	-	0.002	-0.02
$\frac{17}{2_1} \rightarrow \frac{15}{2_1}$	-0.9^{+7}_{-19}	1.816	-0.761	-0.25^{+23}_{-1}	0.0721	-0.37	-	-	-	-	-	-
$\frac{19}{2_1} \rightarrow \frac{17}{2_1}$	-0.13^{+10}_{-1}	-1.971	0.0007	-0.9^{+10}_{-5}	-0.731	-0.84	-	-	-	-	-	-
$\frac{21}{2_1} \rightarrow \frac{19}{2_1}$	-0.04^{+12}_{-1}	0.0071	-0.09	0.17^{+12}_{-1}	1.22	1.627	-	-	-	-	-	-
$\frac{23}{2_1} \rightarrow \frac{21}{2_1}$	-0.01^{+18}_{-9}	-0.06	0.007	-	-	-	-	-	-	-	-	-
$\frac{15}{2_1} \rightarrow \frac{11}{2_1}$	-	-	-	-0.21^{+29}_{-1}	0.002	-21.3	-	-	-	-	-	-
$\frac{9}{2_2} \rightarrow \frac{7}{2_1}$	-	-	-	-	-	-	-	0.061	2.121	-	-	-

4.4 $^{181-187}\text{W}$ Isotopes in IBFM-2

4.4.1- Energy Spectra

The Hamiltonian, Eq. (2-142) was diagonalized using the computer program *ODDPAR* [107] in which the IBFM parameters are identified as $A_0 = -0.25\text{MeV}$, $\Gamma_0 = 0.3\text{MeV}$ and $\Lambda_0 = 2.130\text{MeV}$ for negative and positive parity states. The value of $\hbar\tilde{S} = 1.5\text{MeV}$ is consistent with the excitation energy for the $J_i^+ = 2_1^+$ states in the even-even W isotopes. In the present study of the $^{181-189}\text{W}$ isotopes we have used the complete 82-126 major shell, the $2f_{5/2}$, $3p_{3/2}$ and $3p_{1/2}$ single particle orbits, for the odd-neutron quasi particle. The quasi particle for these calculations is the fermion degree of freedom, describing a neutron hole, that is coupled to the bosons of the even-even may occupy. For the description of the even-even cores we have used the parameters as given in Table (3-25). The use of the complete model space allows us, for the first time, to perform a comprehensive and unified calculations for the positive and negative parity states of the neutron-poor even-odd isotopes.

As part of our strategy to have a unified description we have tried, and succeeded, to keep the same values for all isotopes for the interaction strength of the quadrupole, exchange and monopole forces, see Eq. (2-142). We have been able to obtain good results for positive and negative parity states for all isotopes (shown in figures (4-6) to (4-10)).

By performing an overall fit to a larger series of isotopes and by including positive as well as negative parity states the freedom in the choice of the interaction strength is strongly limited. The strength of the Monopole force does not have a very large effect on the results. The quasi-particle energies and occupation probabilities were allowed to vary across the isotopes to get an optimal to excitation energies. At the same time, we

have kept an eye on single-particle transfer amplitudes as these are very sensitive to the occupation probabilities. The used single-particle parameters are given in Table (4-8). Since only on the relative quasi-particle energies enter in the calculation of excitation energies we have set the lowest energy to zero. For $^{181-189}\text{W}$ one observes that the energies as well as the occupation probabilities vary gradually over the mass range, with a minimum in the quasi-particle energies.

4.4.2- E2 Transitions for $^{181-189}\text{W}$ Isotopes

It is very well known that electric quadrupole transitions are dominant in nuclear physics. Striking evidence is given by strong enhancements in the measured E2 strength in even-even nuclei. The large deviations from single particle estimates, expressed in e^2b^2 units, indicate the presence of collective features. Since the transition rate $T(E2)$ has a pronounced energy (E_x) dependence it is desirable to extract it from the other structure effects.

In the IBFM-2 formalism, the operator $T^{(E2)}$ is constructed starting from the boson and fermion contributions is given in Eq. (2-154) The boson effective charges are taken in Table (3-26) for both neutron and proton bosons, whereas in estimating the fermion coefficients the radial integrals $\langle r^2 \rangle$ in Eq. (2-156) are approximated by the harmonic oscillator value $(N + 3/2)\hbar / M\tilde{S}$, which turns out to be the same (0.27 b) for all the positive parity orbits $N = 6$ shell. Furthermore, a renormalization, leading to $e_{F,\epsilon} = 0.136eb$, $e_{F,f} = 0.399eb$ is adopted to account for the effects of the strong interaction among the nuclear constituents.

Even though the ability of accurately describing the observed transitions depends in a crucial way upon details in the structure of the wave functions, it is useful to illustrate how the essential features can be understood by dealing with a specific example in transitions for positive and negative parity states.

From the results presented in Tables (4-9) and (4-10), it appears that the strong collective quadrupole transitions (large $B(E2)$ values) are reproduced quite well by the IBFM-2 model, especially for the ^{185}W isotopes, whereas some disagreement emerges in relation to those transitions which are observed to be weak and in the intermediate cases. The explanation of such a trend can be found by studying the specific nature of the states involved in a de-excitation process.

4.4.3- M1 Transitions and Mixing Ratio $\mu(E2/M1)$ for $^{181-189}\text{W}$ Isotopes

For even-odd nuclei, other electromagnetic transitions, such as the $M1$'s, deserve particular attention, because they carry information about the unpaired nucleon and the delicate coupling to the core. Therefore, they are complementary to the role played by the $E2$'s, where, as we have seen the collective features are prevailing.

The appropriate one-body operator in our language is given in Eq. (2-155). The bosonic g -factors g_f and g_ϵ have been taken from previous studies [109]. The coefficients of the fermionic contribution are given in Eq. (2-159). and the single-particle g -factors of the free nucleons are explicitly: $g_{l,f} = 1 \sim_N$, $g_{s,f} = 5.5857 \sim_N$, $g_{l,\epsilon} = 0 \sim_N$, $g_{s,\epsilon} = -3.8268 \sim_N$. Throughout the applications considered here the spin components need to be modified to the following values: $g_{s,f} = 3.910 \sim_N$ and $g_{s,\epsilon} = -2.678 \sim_N$.

The calculated $B(M1)$ values are given in Eq. (2-53), and presented in Tables (4-11) and (4-12) shows IBFM results for reduced transition probabilities $B(M1)$, and their IBFM prediction for some of the lowest levels. The present IBFM results are more reasonable for positive and negative parity states.

Like the $E2$ transitions, there is no experimental data to compare the theoretical results, the magnetic case is characterized by the occurrence, of relatively strong de-excitations, which are predicted to be weak and vice-versa. Such a behavior can be the result of having neglected higher order

terms in the expression for the operator, or can reflect small configuration admixtures, responsible for large variations in the matrix elements, without appreciably affecting the energies of the corresponding states.

Using the operator of Eq. (2-159), one can compute the corresponding transitions. The boson part of the operator requires a specification of g_f^B and g_F^B . These can be taken from the calculations reported for even-even nuclei for Sambataro *et al.*, 1984 [109]. The fermion part of the operator requires a specification of the fermion g-factors. The orbital g-factors are $g_{l,f}^F = 1 \sim_N$ and $g_{l,\xi}^F = 0 \sim_N$. The spin g-factors are taken as the free values quenched by a factor of 0.66, i.e. $g_{s,f}^F = 0.66 \times 5.58 \sim_N$. A portion of the results is shown in Tables (4-11) and (4-12). Also here there is no experimental information.

Tables of the $u(E2/M1)$ mixing ratios for some selected transitions in the $^{181-187}\text{W}$ isotopes are calculated from the useful equations above and with the help of B(E2) and B(M1) values, which are obtained from *NPBTRAN* (a computer code which is a subroutine of the *NPBOS* package program) [71]; the results are given in Tables (4-15) and (4-16). In general, the calculated electromagnetic properties of the Tungsten isotopes do not differ significantly from those calculated in experimental and theoretical work.

We have also examined the mixing ratio $u(E2/M1)$ of transitions linking the ground state bands. The transitions which link low spin states obtained in the present work are in good agreement and show little irregularities. We find that the transitions which link low-spin states obtained in the present work are largely consistent with this requirement, although some may be considered to show irregularities.

In general, the calculated electromagnetic properties of the tungsten isotopes do not differ significantly from those calculated in experimental and previous theoretical work. The calculated values in this study show that

the transitions connect the levels with the same parity and the E2 transitions are predominant. The later includes transitions originating from the beta and gamma bands, which supports the idea that the beta and bands may be quadrupole excitations of the perturbed ground state, but the existence of M1 indicates that the beta and gamma bands cannot be pure quadrupole excitations of the ground state band.

Table (4- 16): Mixing Ratio $u(E2/M1)$ for $^{181-187}\text{W}$ for Positive Parity States in eb/\sim_N units.

$J_i \rightarrow J_f$	^{181}W		^{183}W		^{185}W		W^{187}	
	IBFM-1	IBFM-2	IBFM-1	IBFM-2	IBFM-1	IBFM-2	IBFM-1	IBFM-2
$\frac{11}{2} \rightarrow \frac{9}{2}$	0.0089	0.007	-	-	-	-	-	-
$\frac{13}{2} \rightarrow \frac{11}{2}$	5.22	2.31	4.32	5.37	2.1×10^{-2}	3.71×10^{-1}	0.981	0.431
$\frac{15}{2} \rightarrow \frac{13}{2}$	0.873	0.271	-	-	-	-	-	-
$\frac{9}{2} \rightarrow \frac{13}{2}$	-	-	8.7×10^{-4}	6.0×10^{-3}	2.12	1.1×10^{-4}	-	-
$\frac{9}{2} \rightarrow \frac{11}{2}$	-	-	2.2×10^{-4}	8.0×10^{-4}	-	-	-	-
$\frac{7}{2} \rightarrow \frac{9}{2}$	-	-	-	-	0.731	5.39	-	-
$\frac{7}{2} \rightarrow \frac{13}{2}$	-	-	-	-	-	-	2.1×10^{-4}	3.5×10^{-4}
$\frac{9}{2} \rightarrow \frac{7}{2}$	-	-	-	-	-	-	4.31	2.21

Table (4- 17): Mixing Ratio $\delta(E2/M1)$ for $^{181-187}\text{W}$ for Negative Parity States in eb/μ_N units.

$J_i \rightarrow J_f$	^{181}W		^{183}W		^{185}W		^{187}W	
	IBFM-1	IBFM-2	IBFM-1	IBFM-2	IBFM-1	IBFM-2	IBFM-1	IBFM-2
$\frac{5}{2} \rightarrow \frac{1}{2}$	2.97	5.57	-	-	7.0×10^{-4}	9.7×10^{-3}	-	-
$\frac{7}{2} \rightarrow \frac{1}{2}$	3.2×10^{-3}	3.71	-	-	-	-	12.5	26.7
$\frac{3}{2} \rightarrow \frac{7}{2}$	2.0×10^{-4}	1.33	-	-	-	-	-	-
$\frac{3}{2} \rightarrow \frac{1}{2}$	-	-	7.2×10^{-1}	6.51×10^{-1}	-	-	-	-
$\frac{5}{2} \rightarrow \frac{3}{2}$	-	-	2.93	2.57	-	-	1.32	2.25
$\frac{7}{2} \rightarrow \frac{5}{2}$	-	-	1.12	5.67	-	-	-	-
$\frac{1}{2} \rightarrow \frac{3}{2}$	-	-	-	-	7.14	12	-	-
$\frac{3}{2} \rightarrow \frac{5}{2}$	-	-	-	-	22.1	27	-	-
$\frac{1}{2} \rightarrow \frac{5}{2}$	-	-	-	-	-	-	6.6×10^{-3}	9.0×10^{-4}

CHAPTER FIVE
CONCLUSIONS AND
SUGGESTIONS FOR
FUTURE WORK

CHAPTER FIVE

CONCLUSIONS AND SUGGESTIONS FOR FUTURE WORK

5-1 Concluding Remarks

In this work we have described various properties and shape evolution of the *Hf* and *W* isotopes in the framework of the IBM and IBFM, we conclude the following points.

Hf Isotopes

- 1- Theoretical calculations of $^{170-180}\text{Hf}$ (with $Z=72$) were performed by using IBM-1 and IBM-2. The $^{172-174}\text{Hf}$ total numbers of bosons 14,15 respectively (weakly deformed) lies in the transitional region $\text{SU}(3)\rightarrow\text{O}(6)$ and the $^{176-180}\text{Hf}$ isotopes (total number of bosons 16,15 and 14 respectively), lies in the dynamical symmetry $\text{SU}(3)$ (deformed nuclei).
- 2- In Hf isotopes see that when the states $J^f = 2_2^+, 2_4^+$ and 3_1^+ are strongly dominated by the $F=F_{max}$, the strongest contribution to the $J^f = 2_3^+, 3_2^+$ states is the one with $F=F_{max-1}$. The $J^f = 2_3^+, 3_2^+$ and 1^+ states as a mixed symmetry states in Hf isotopes.
- 3- The reduced electric transition probability $B(E2)$ values are required in order to identify the strength of E2 transitions within the $g \rightarrow g$ band and from beta band to ground state band and from gamma band to beta and ground band.
- 4- The root mean square deviation (*rmsd*) is used to compare the experimental and calculated IBM-2 energy levels. The ground state levels the best agreement was found.
- 5- The yrast levels of even-even nuclei ($J_i = 2,4,6,\dots$) usually decay by $E2$ transition to the lower lying yrast level with $J_f = J_i - 2$.
- 6- As a consequence of possible $M1$ admixture the $B(E2; 2_2^+ \rightarrow 2_1^+)$ quantity is rather difficult to measure. For Hf isotopes, give the different,

conflicting experimental results and we see that no general feature be derived from them, from these values seems to decrease for $^{172-174}\text{Hf}$ and increased for $^{176-180}\text{Hf}$.

- 7- The electric transition probabilities from the mixed-symmetry state $J^f = 1^+$ to symmetric states ($2_1^+, 2_2^+$) is weak collective $E2$ transition.
- 8- The $E2$ transition between the 1^+ and the 2^+ ground state is small, whereas $E2$ transitions are large between fully-symmetric states and between mixed-symmetry states.
- 9- The general features of the quadrupole moment for first excited state (2_1^+) results is clear, namely an increased in the negative quadrupole moment with increasing neutron number.
- 10- The $B(M1; 1_1^+ \rightarrow 0_1^+)$ transition probability is proportional to the factor g_ϵ^2 and weakly depends only on the strength of Majorana force.
- 11- The magnetic dipole moment for first excited state (2_1^+) in even-even $^{172-180}\text{Hf}$ isotopes provide a sensitive test of the effective boson number in the IBM-2 framework, in $^{172-180}\text{Hf}$ isotopes with $N = 100-108$, confirm the validity of assuming a drastic change in number of proton boson when the number of neutron boson is increased from 106 to 108.
- 12- The theoretical and experimental $X(E0/E2)$ values are in general in a good agreement except for the $0_3^+ \rightarrow 0_1^+$ and $0_4^+ \rightarrow 0_1^+$, transitions but it is not possible to say if these disagreements may be attributed to the $E0$ or $E2$ component in the ratio. The disagreement in the results for some transitions could be removed by interchanging the ordering since for the higher lying states the correspondence between the experimental and theoretical levels is uncertain.
- 13- The possibility of obtaining a description of both positive and negative-parity levels, starting from a single Hamiltonian is probably due to the following two factors. (i) The IBM-2 Hamiltonian was obtained from detailed study of spectra and $E2$ electromagnetic properties of the even-even Hf nuclei. (ii) The single-particle properties (quasi-particle energy

E_j and occupation probabilities ϵ_j^2) have been determined from a BCS calculation for the $3p_{3/2}$, $3p_{1/2}$ and $2f_{5/2}$ orbital's.

W Isotopes

- 1- The structure of the energy spectra is determined mainly by the first three terms on the right-hand side of the Hamiltonian in Eq. (2-42) (the pairing plus quadrupole terms), while the remaining terms have minor, but non-negligible contributions.
- 2- The examination of the experimental and IBM-2 energy levels ratios for the $^{180-190}\text{W}$ isotopes shows that they lie in the transitional region SU (3) O (6), therefore the Hamiltonian of the transition region SU (3) O (6) has been employed in the calculation by using the program *NPBOS*.
- 3- Our calculated energy spectrum is shown in Figs. (3-6) to (3-11). The root mean square deviation (*rmsd*) for the ground, beta and gamma bands totaling 19 levels are 0.109, 0.82 and 0.80 MeV for Duval and Barrett [38] and the present work respectively. (Since the values obtained by Duval and Barrett [38], were interpolated from their level energy plot, small errors may arise and a figures representing their goodness of fit could not be determined accurately.)
- 4- The boson effective charges (e_f, e_ϵ) have the same dependence on proton number and neutron number as do $|_f$ and $|\epsilon$ however, as even a further simplification Duval and Barrett [38] used $e_f \neq e_\epsilon$ equals constant for all nuclei.
- 5- The electric transition probabilities from the mixed-symmetry state $J^f = 1^+$ to the symmetric states 2_1^+ and 2_2^+ is weak collective *E2* transition. The *E2* transition between the 1^+ and the 2^+ ground state is small, whereas *E2* transitions are large between fully-symmetric states and between mixed-symmetry states.

- 6- The energy of the 1_{ms}^+ shows a linear increase with κ_2 . It is obvious that the change in energy levels as κ_2 is varied to be a good indicator for the lowest 2^+ and 1^+ mixed-symmetry states, and we recommend this method for searching for mixed symmetry states.
- 7- The states 2_5^+ and 2_6^+ at calculated energy around 2.1 MeV in $^{180-190}\text{W}$ isotope are mixed symmetry states, plus the 1_1^+ and 1_2^+ at 2.0 MeV and 2.3 MeV respectively. The same states in ^{182}W isotopes are mixed symmetry states.
- 8- The analyses demonstrate the sensitivity of the mixed symmetry states energy to the model parameters F-spin and the Majorana term κ_2 . The comparison with experimental data shows that, we are still lacking of experimental data on the $B(M1; 1_1^+ \rightarrow 0_1^+)$ in order to focus on these aspect.
- 9- The values of gyromagnetic factors of boson used to evaluate the B(M1) and mixing ratios are $g_f = 0.71 \sim_N$ and $g_\epsilon = 0.051 \sim_N$. The results of the calculations are listed in Table (3-15).
- 10- The size of the $\chi \rightarrow g$ M1 matrix elements seems to decrease with increasing mass, specially, a change in $\chi \rightarrow g$ M1 strengths occurs when the gamma band crosses the beta band.
- 11- The B(M1) transition probability values are small compared to the values of the B(E2) transition probabilities because the wavelength of the gamma ray transitions is greater than it is in the magnetic transitions according to the following the relationship: $\} (ML) = 0.3A^{-2/3} \} (EL)$.
- 12- The magnetic transition probability B(M1) in the IBM-2, it is found to be proportional to $(g_f - g_\epsilon)^2$.
- 13- We reproduce the 2_1^+ g-factors as well as most of the u ($E2/M1$) mixing ratios. In particular, all the signs are reproduced correctly.
- 14- In W isotopes E0 values increased with increasing neutron numbers and they go up to the highest value at ^{186}W isotope. This means that all

the nuclei are deformed because they possess the amount of excess energy and that they are trying to get rid of this by lessen the E0 transitions to the state of stability. This is an additional evidence of the deformation of these isotopes.

- 15- The theoretical values for the X ($E0/E2$) ratio are small, for some transitions which means that there is a small contribution of E0 transition on the life time of the 0^+ states.
- 16- The energy of the 1_{ms}^+ shows a linear increase with $\langle \kappa_2 \rangle$. These features are illustrated in figures (3.14) and (3.15). It is obvious that the change in energy levels as $\langle \kappa_2 \rangle$ is varied is a good indicator for the lowest 2^+ and 1^+ mixed-symmetry states, and we recommend this method for searching for mixed symmetry states.
- 17- The branching ratios of B(M1) are very helpful in nuclear shape coexistence. Normally the value of $B(M1; 1_1^+ \rightarrow 0_1^+)$ is the largest value in the M1 transition probability between states, so we applied the B(M1) ratio normalized to the value of this transition.
- 18- The possibility of obtaining a description of both positive and negative-parity levels, starting from a single Hamiltonian is probably due to the following two factors. (i) The IBM-2 Hamiltonian was obtained from detailed study of spectra and E2 electromagnetic properties of the even-even W nuclei. (ii) The single-particle properties (quasi-particle energy E_j and occupation probabilities ϵ_j^2) have been determined from a BCS calculation for the $2f_{5/2}$, $3p_{3/2}$ and $3p_{1/2}$ orbital's.

5-2 Suggestions for Future Work

Several suggested projects remain for the future, which can be abbreviated by the following possible works:

1. One of the most significant recent developments in nuclear structure physics is the prediction that a Supersymmetry Model (SSM) may be realized in nuclei. The recognition of dynamical symmetries in

even-even nuclei via the introduction of bosons has reoriented our directions nuclear spectroscopy. Therefore, this suggests to use this model to study the level schemes in odd-even mass nuclei, and study the non-collective motion in transitional and deformed nuclei.

2. This work can be extended to calculate E4 (hexadecupole degree of freedom) in transitional nuclei, by addition of a g-boson ($L = 4$), to test the important $K^f = 4^+$ band in this region.
3. The 2^+_{M} states found so far in the $A = 140$ mass region give us an interesting glimpse into the behavior of mixed-symmetry states. The extent of the existence of these states and also their purity would test the limits of the validity of describing them as states of mixed proton-neutron symmetry. Efforts are continuing in the search of mixed-symmetry states in this mass region.
4. Using other collective models, i.e., Dynamic Deformation Model (DDM) to study the Nuclear structure and electromagnetic transitions for this region.
5. Studying the two-neutrino double- decay within the framework of the interacting boson model (IBM-2) and its extensions (IBFM-2 and IBFFM-2) models.

REFERENCES

References

- [1] E. Rutherford. Philosophical Magazine, 21 (1911),661.
- [2] J. Chadwick. Nature,129 (1932), 312.
- [3] P. A. M. Dirac, Proc. R. Soc. A, 117(1928), 610.
- [4] P. A. M. Dirac, Proc. R. Soc. A, 118 (1928),351.
- [5] C. Anderson, Phys. Rev., 43 (1933),491.
- [6] G. Gamow, Proc. R. Soc. A, 126 (803) (1930),632–644.
- [7] C. F. von Weizsäcker, Zeits. f. Physik, 96 (1935),431.
- [8] M. Goeppert-Mayer, Phys. Rev., 75(1969), 1949.
- [9] O. Haxel, J. H. D. Jensen, and H. E. Suess, Zeits. f. Physik, 128 (1950),295.
- [10] J. Rainwater, Phys. Rev. 79 (1950) 432.
- [11] A. Bohr. Kgl. Danske Videnskab. Selskab, Mat.fys. Medd. 26 (1952) 14.
- [12] A. Bohr and B. Mottelson, Kgl. Danske Videnskab. Selskab, Mat.fys. Medd. 27 (1953) 16.
- [13] D. L. Hill and J. A. Wheeler, Phys. Rev. 89 (1953) 1102.
- [14] S. G. Nilsson, Dan. Mat. Fys. Medd., 29 (1955),16.
- [15] A. Arima and F. Iachello, Phys. Rev. Lett., 35 (1975),1069.
- [16] L. Eisenbud and E. P. Wigner, *Nuclear Structure*, Princeton University Press, Princeton, New Jersey, 1958.
- [17] K. S. Krane, Phys. Rev. C 8 (1973) 1494.
- [18] J. H. Hamilton, K. Kumar, L. Varnell, A. V. Ramayya and P. E. Little, Phys C 10 (1974) 2540.
- [19] L. M. Chen, S. T. Hsien and C. Chiang, IL Nuovo Cimento Vol. 104, No.12 (1991) 1713.
- [20] A. R. Subber, J. Basrah researchs (sciences) Vol. 31 (2005) 1.
- [21] L. I. Abuo-Salem and K. E. Abd-Elmageed, Acta Phys. Polonica B No.6(2005) 2105.

References

- [22] Yu Shao-Ying, LI Yan-Xin and SHEN Cai-Wan, Commun. Theor. Phys. 50 (2008) 459.
- [23] N. Mansour and A. F. Saad, Bulg. J. Phys. 36 (2009) 244.
- [24] P. N. Usmanov, A. A. Okhunov, U. S. Salikhbaev and A. I. Vdovin , Physics of particles and Nuclei Letters Vol. 7 No. 3 (2010) 185.
- [25] H. Olsson, Nuclear Physics and Radiation Physics A3400 (2010).
- [26] K. A. AL-Maqtary, M. H. AL-Zuhairy, M. N. AL-Sharaby and N. A. Shamlan, Jordan Journal of Physics Vol. 4, No. 1 (2011) 51.
- [27] K. Nomura, T. Otsuka, R. Rodriguez, L. M. Robledo and P. Sarriguren, Phs. Rev. C84 (2011) 1.
- [28] C. R. Praharaj, S. K. Patra, R. K. Bhowmik and Z. Naik, Journal of Physics: Conference Series 312 (2011) 1.
- [29] J. H. Gupta, The European Physical Journal A 40 (2013) 126.
- [30] Wenchao Ma, EPJ Web of Conference 66 (2014) 2115.
- [31] K. Kumar and M. Baranger, Nucl. Phys. A122 (1968) 273.
- [32] E. Glenn and J. X. Saladin, Phys. Rev. Lett. 20 (1968) 1298.
- [33] K. Sprinkle, D. Cline, P. Russo, R. P. Scharenberg and P. B. Vild, Bull. Am. Phys. Soc. 22 (1977) 545.
- [34] W. T. Milner, F. K. McGowan, R. L. Robinson, P. H. Stelson and R. O. Sayer, Nucl. Phys. A177(1971) 1.
- [35] J. J. O'Brien, J. X. Saladin , C. Baktash, and J. G. Alessi, Phys. Rev. Lett. 38 (1977) 324.
- [36] C. Gunther, P. Kleinheinz, R. F. Casten and B. Elbek, Nucl. Phys. A172 (1971) 273.
- [37] P. O. Hess, J. Maruhn and W. Greiner, J. Phys. G 72(1981) 737.
- [38] P. D. Duval and B. R. Barrett, Phys. Rev. C23 (1981) 492.
- [39] D. D. Warner, Phys. Rev. Lett. 52 (1984) 259, D. D. Warner, and M. A. Bruce, Phys. Rev. C 26 (1984) 1066.
- [40] P. Van Isacker, J. P. Elliott, and D. D. Warner, Phys. Rev. C 36 (1987) 1229.

References

- [41] C. Y. Wu, D. Cline, E. G. Voget, W. J. Kernan, T. Czosnyka, A. Kavak, R. M. Diamond Phys. Rev. C40 (1989) 40.
- [42] D. S. Mosbah, J. A. Evans and W. D. Hamilton, J. Phys. G: Nucl. Part. Phys. 20 (1994) 787.
- [43] P. Navratil, B. R. Barrett and J. Dobes, Phys. Rev. C53 (1996) 2794.
- [44] M. A. Ameer and M. A. H. AL-Shimmary, Armenian Journal of Physics, 4 (2011) 146.
- [45] A. A. Abojasseem and F. A. AL-Temeame, Journal of Kufa-Physics 3 (2011) 44.
- [46] F. I. Sharrad, H. Y. Abdulla, N. AL-Dahan, N. M. Urman, A. A. Okhunov and H. Abu Kaasim, Chinese Physics C 37 (2013) 34101.
- [47] M. A. AL-Ameer and M. A. Hussain, Journal of Babylon Univ. /Pure and Applied Sciences No. 4 Vol. 21 (2013) 1431.
- [48] S. Mohmmadi and Banafsheh Nemati Giv, Asian Journal of Eng. and Tech. Innovation 02 (03) (2014) 14.
- [49] A. Mahdi, F. H AL-Khudair and A. R. Subber, nternational Journal of Physics, and Research (IJPR)Vol. 4, Issue 5 (2014) 1-12.
- [50] F. Iachello and A. Arima, Phys. Lett. 53B (1974) 309.
- [51] A. Arima and F. Iachello, Phys. Rev. Lett. 35 (1975) 1069.
- [52] A. Arima and F. Iachello, Phys. Rev. Lett. 40 (1978) 111.
- [53] A. Arima, Lectures Fall 1977, SUNY, Stony Brook, New York.
- [54] A. Arima and F. Iachello, Ann. Phys. (N.Y). 99 (1976) 253.
- [55] A. Arima and F. Iachello, Ann. Phys. (N.Y). 111 (1978) 201.
- [56] L. Wilets and M. Jean, Phys. Rev. 102 (1956) 788.
- [57] F. Iachello *Informal Lectures*, July 1977, Brookhaven National Laboratory, Upton, New York.
- [58] F. Iachello, Nukleonika 22 (1977) 107.
- [59] A. Arima and F. Iachello, Phys. Rev. Lett. 40 (1978) 385.
- [60] O. Scholten, *computer code PHINT*, K. V. I., Groningen, Holand.
- [61] K. T. Hacht in *Selected Topics in Nuclear Spectroscopy* ob. cit. p.51.

References

- [62] J. P. Elliott, Proc. Roy. Soc. A245, 128 (1958) 562.
- [63] J. Millener, *Lectures at Brookhaven National Laboratory, Upton, New York* 1977.
- [64] J. Larysz, Thesis, University of Manchester, Manchester, U.K. (unpublished).
- [65] O. Scholten, F. Iachello and A. Arima, Ann. Phys. (N.Y).1978.
- [66] G. Puddu, O. Scholten, T. Otsuka, Nucl. Phys. A348, (1980) 109.
- [67] F. Iachello and A.Arima, *The Interacting Boson Model*, Cambridge University Press, Cambridge, 1987.
- [68] J. Lang, K. Kumar and J. H. Hamilton, Rev. Mod. Phys. Vol.54 No. 1 (1982).
- [69] E. L. Church and J. Weneser, *Phys. Rev.*, 103 (1956), 1035.
- [70] R. Bijker, A. E. L. Dieperink and O. Scholten, Nucl. Phys. A 344 (1980) 207.
- [71] T. Otsulta and N. Yosbida *The IBM-2 compurer program NPBOS* Universiry of Tokyo (1985), T. Otsuka, and O. Soholten, KVI Internal Report No. 253, 1979.
- [72] A. Bohr and B. Mottelson, *Nuclear Structure II*, (Benjamin, Reading, 1975).
- [73] R. F. Casten, Nucl. Phys. A443 (1985) 1.
- [74] T. Otsuka, T. Matsuo, and D. Abe, Phys. Rev. Lett. 97 (2006) 162501.
- [75] D. Bohle, A. Richter, W. Steffen, A. E. L. Dieperink, N. Lo Iudice, F. Palumbo, and O. Scholten, Phys. Lett. 137B (1984) 27.
- [76] J. Enders, P. von Neumann-Cosel, C. Rangacharyulu, and A. Richter, Phys. Rev. C71 (2005) 014306.
- [77] P. Van Isacker, K. Heyde, J. Jolie, and A. Sevrin, Ann. Phys. (NY) 171, (1986) 253.
- [78] A. Bohr. Kgl. Danske Videnskab. Selskab, Mat.fys. Medd. 26 (1952) 14.
- [79] A. Bohr and B. Mottelson. Kgl. Danske Videnskab. Selskab, Mat. fys. Medd. 27 (1953) 16.
- [80] F. Iachello and O. Scholten, Phys. Rev. Lett. 43 (1979) 679.
- [81] R. Bijker, A. E. L. Dieperink, Nucl. Phys. A379 (1982) 221.

References

- [82] F. Iachello and P. Van Isacker, *Interacting Boson-Fermion Model* Cambridge University Press, Cambridge (1991).
- [83] M. J. A. de Voigt, J. Duedk and Z. Szymanski, Rev. Mod. Phys. 55 (1983) 949.
- [84] D.D. Warner, R. F. Casten and W. F. Davidson, Phys. Rev. Lett. 47 (1981) 1819.
- [85] I. Talmi, in *Interacting Bose-Fermi System in Nuclei*, ed. F. Iachello (New York, Plenum Press, (1981) p. 329).
- [86] J. Bardeen, L. N. Cooper and J. R. Schrieffer, Phys. Rev. 106 (1957) 1175.
- [87] B. S. Reehal and R. A. Sorensen, Phys. Rev. C2 (1970) 819.
- [88] F. Iachello, Phys. Rev. Lett., 44 (1980) 772.
- [89] F. Iachello and S. Kuyucak, Ann. Phys. (N.Y) 136 (1981) 19.
- [90] R. Bijker, and F. Iachello, Ann. Phys. (N.Y) 161 (1985) 360.
- [91] A. M. Burce , W. Gelletly, J. Lukasiak, W. R. Philips and D. D. Warner, Phys. Lett. B 65 (1985) 43.
- [92] A. De Shalit, Phys. Rev. 122 (1961) 1530.
- [93] G. Racah, Phys. Rev. 62 (1942) 438.
- [94] B. F. Bayman and L. Silverberg, Nucl. Phys. 16 (1960), 625.
- [95] D. Murnaghan, “*The Theory of Group Representations*,” John Hopkins Press, Baltimore, 1938.
- [96] R. Gilmore, “*Lie Groups, Lie Algebras, and Some of Their Applications*,” Wiley, New York, 1974.
- [97] G. Wybourne “*Classical Groups for Physicists*,” Wiley, New York, 1974.
- [98] A. Arima, T. Otsuka F. Iachello, and I. Talmi, Phys. Lett. B66(1977) 205.
- [99] T. Otsuka, A. Arima, F. Iachello, and I. Talmi, Phys. Lett B76 (1978) 139.
- [100] P. J. Brussaard and P. W. M. Glaudemans, *Shell Model Applications in Nuclear Spectroscopy*, North Holland 1977.
- [101] F. Iachello and I. Talmi, Rev. Mod. Phys. 50 (1987) 339.
- [102] T. Hübsch, and V. Paar, Z. Phys. A310 (1984) 111, T. Hübsch, V. Paar, and D. Vertenar , Phys. Lett., B151 (1985) 320.

References

- [103] P. Van Isacker, J. Jolie, K. Heyde, A. Frank, Phys. Rev. Lett. 54 (1985) 653.
- [104] D. D. Warner, R. F. Casten and A. Frank, Phys. Lett. B180 (1986) 207.
- [105] P. Van Isacker, J. Math. Phys. 28 (1987) 957.
- [106] J. Jolie, P. Van Isacker, K. Heyde and A. Frank, Phys. Rev. Lett. 55 (1985) 1457.
- [107] R. Bijker, *Computer program ODDPAR*, University of Groningen (1983).
- [108] C. E. Alonso, J.M. Arias, R. Bijker and F. Iachello, Phys. Lett. B 144 (1984) 141.
- [109] M. Sambataro, O. Scholten, A. E. L. Dieperink and P. Piccitto, Nucl. Phys. A423(1984) 333.
- [110] ENSDF, [http:// www. nndc. bnl. gov/ensdf](http://www.nndc.bnl.gov/ensdf) (Nuclear data sheet) (2012).
- [111] F. X. Xu, C. S. Wu and J. Y. Zeng, Phys. Rev. C 40 (1989) 2337.
- [112] E. Browne and J. Huo, Nucl. Data Sheets, 87 (1999) 94.
- [113] A. M. S. Basuni, Nucl. Data Sheets, 107 (2006) 865.
- [114] K. Atalay and M. Kaan, Math. Comp. App. 10(1) (2005) 9.
- [115] J. Lang, K. Kumar and J. H. Hamilton, Rev. Mod. Phys. Vol.54 No. 1 (1982).
- [116] D. Bonatsos, D. Lenis, N. Pietralla, P. A. Terziev, Phys. Rev. C 74 (2006) 44306.
- [117] ENSDF, [http:// www. nndc. bnl. gov/ensdf](http://www.nndc.bnl.gov/ensdf) (Nuclear data sheet) (2010).
- [118] Ph. Hubert, C. Roulet, H. Sergolle, P.Colombani, J. M. Lagrange, J. Vanhorenbeeck and N. R. Johnson, Nucl. Phys. A321 (1979) 213.
- [119] Ass'ad I. Ass'ad, Asian Journal of Applied Sciences, 8(1) (2015) 79.
- [120] T. Otsuka, A. Arima and F. Iachello, Nucl. Phys. A309 (1978) 1.
- [121] A. V. Aldushchenkov and N. A. Volnova, Data Tables 11 (1972) 299.
- [122] G. M. Kalvius and G. K. Shenoy, Nucl. Data Tables 14 (1974) 639.
- [123] R. Barrett and D. Jackson, "Nuclear Size and structure" (Oxford University Press, Oxford, 1977).
- [124] K. Heilig and A. Steudel, Nucl. Data Tables 14 (1974) 613.

References

- [125] S. Pittle, P. D. Duval and B. R. Barrett. *Ann. Phys. (N.Y)* 144 (1982) 168.
- [126] O. Scholten, K. Heyde , P. Van Isacker and T. Otsuka *Phys. Rev. C* 32(1985) 1729.
- [127] R. Bijker, A. E. L. Dieperink, O. Scholten and R. Spanhoff *Nucl Phys. A* 344 (1980) 207.
- [128] C. Gunter, P. Klienheinz, and R. F. Casten, *Nucl. Phys. A*172 (1971) 273.
- [129] P. Van Isacker *et al.*, *Ann. Phys.*2 (1985) 253.
- [130] A. E.L.Dieperink, O.Scholten and D.D.Warner, *Nucl. Phys. A*469 (1987) 173.
- [131] N. Pietralla, P. von Brentano, R.-D. Herzberg, U. Kneissl, J. Margraf, H. Maser, H. H. Pitz, and A. Zilges, *Phys. Rev. C* 52, (1995)2317.
- [132] J. N. Ginocchio, *Phys. Lett. B* 265 (1991) 6.
- [133] Pramila Raghavan, *At. Data Nucl. Data Tables* 42 (1989) 189.
- [134] M. Veskovic, W. D. Hamilton, and K. Kumar, *Phys. Rev. C* 41 (1990) R1.
- [135] W. D. Hamilton, A. Irback and P. Elliott, *Phys. Rev. Lett.* 53 (1984) 2469.
- [136] O. Scholten, *International Report KVI 252 computer code ODDA*, University of Groningen (1980).

(المزدوج التناظر) ومن قيم نسبة الخلط بعضها مقارب
وهي حساسة لقيم M1.

وهنا تم الاعتماد على طرق جديدة في حساب الشحنات المؤثرة للبوزونات (e_π, e_ν)
لغرض استخدامها في حساب الانتقالات الكهربائية رباعية القطب. وكذلك الاعتماد على طرق
جديدة وحديثة بأخذ g-factor لحساب الانتقالات المغناطيسية M1.

ع نيوترون بالاعتد برامج متقدمة وجديد

ع $X(E0/E2)$ لكلا السلسلتين.

NPBOS

الجزء الاخر من الدراسة تم تحليل مستويات الطاقة الموجبة و مستويات الطاقة السالبة
لنظائر الهافنيوم والتنكستن الزوجية الفردية باستخدام نموذجي تفاعل - الفيرميون
(IBFM-1) (IBFM-2) يث تم ايجاد مستويات او مدارات الجسم المنفرد ذات

$2f_{5/2}, 3p_{3/2}, 3p_{1/2}$. وهنا تم استخدام برنامج ODDA

PBEFM لحساب مستويات الطاقة والانتقالات الكهرومغناطيسية ونسب الخلط بينهما
مقارنة النتائج النظرية مع القيم العملية المتوفرة.

وكذلك تم اعتماد طرق جديدة في حساب الشحنة الفعالة للفيرميون (e_F)

العامل الجيرومغناطيسي للفيرميون (g_F) والذين استخدمناهما في دراسة الانتقالات
الكهرومغناطيسية في نوى الهافنيوم والتنكستن الزوجية والفردية باستخدام (IBFM)

الهافنيوم التركيب النووي IBM $^{172-180}\text{Hf}$ $^{180-190}\text{W}$ حيث تم تحديد قيم الهاملتونيد H

IBM-1 لكل نظير من IBM-2 لكل نظير من نظائر الهافنيوم والتنكستن عن طريق الموازنة (fitting) مع مستويات الطاقة التجريبية المتوفرة. وكذلك تم استخدام هذه الـ لكل نظير لدراسة الانتقالات الكهربائية رباعية القطب $B(E2)$ والانتقالات ثنائية القطب المغناطيسي $B(M1)$ والعزوم رباعية القطب الكهربائي للمستويات المثيعة الأولى $Q(2_1^+)$ والثانية $Q(2_2^+)$ وكذلك نسب الخلط بين الانتقالات الكهرومغناطيسية $\delta(E2/M1)$ والانتقالات احادية القطب الكهربائية $B(E0)$ الايزوميرية وازاحة النظائر وتمت مقارنة النتائج النظرية (بنتائج IBM-1 IBM-2) مع القيم العملية المتوفرة وكان هناك جيد بينهما.

تم دراسة المستويات المزدوجة التناظر ذات البرم العالي في IBM-2 ماجيرون ومنها مستويات ايريسست ومستويات ايرير حيث هذه المستويات تتميز بانها ذات طاقة عالية و E2 ضعيف مع انتقال M1 قوي مع تحديد البرم $F(F - \text{Spin})$. المستويات $1^+, 3_2^+, 2_5^+, 2_4^+, 2_3^+$ هي المستويات المزدوجة التناظر في نظائر Hf W وهي المستويات التي تتميز بانها مستويات ذات د او فونونين -soft التي لها نيوترونية N قريبة من 82 النظائر المشوهه

مستويات الطاقة $B(E2)$ $B(M1)$ والمستويات المزدوجة التناظر وتأثير عوامل ماجيرون على مستويات الطاقة المثيعة العليا لنظائر $^{180-190}\text{W}$ IBM-2. لتغير هذه تأثير كبير على خواص المستويات المزدوجة التناظر نة جميع النتائج التي حصلنا عليها مع القيم العملية المتوفرة وحصلنا على مقارنة جيدة. 2_5^+ ^{180}W ^{182}W هو اول مستوي مزدوج التناظر بينما 2_4^+ ^{184}W ^{186}W هو اول المستويات المزدوجة التناظر في هاتين النواتين. تم حساب خصائص $B(M1)$ $u(E2/M1)$ $g\text{-factors}$ $M1$ strength للنوى الزوجية للتنكستن $^{180-188}\text{W}$ IBM-2

نظائر الهافنيوم ($Z=72$) تقع في المنطقة المشوهه بينما نظائر التنكستن ($Z = 74$) المنطقة الانتقالية باتجاه المنطقة المشوهة العليا. نسبة الخلط $E2/M1$ تم حسابها لمستويات الطاقة المنخفضة الموقع وكذلك المستويات العليا $^{180-188}\text{W}$ $^{172-180}\text{Hf}$

الإهداء

إلى من يسعد قلبي بلقيها إلى روضة الحب التي تنبت أزكى الأزهار بدعائها لي

أمي الغالية

إلى رمز الرجولة والتضحية إلى من دفعني إلى العلم وبه ازداد افتخار برضاه عني

أبي العزيز

إلى شريكة حياتي ورفيقة دربي ، لجميل صبرها وإصرارها وهمتها

زوجتي الحبيبة

إلى من تقر الاعين بهم ويفرح بوجودهن القلب

جنى وجمانة

إلى من هم اقرب ألي من روعي إلى من شاركني حزن الأم وبهم استمد عزتي وإصراري

اخوتي وأخواتي

إلى من أنسني في دراستي وشاركني همومي تذكراً وتقديراً

أصدقائي

اليكم جميعاً أهدي ثمرة جهدي المتواضع

عمار

﴿ بِسْمِ اللَّهِ الرَّحْمَنِ الرَّحِيمِ ﴾

اقْرَأْ بِاسْمِ رَبِّكَ الَّذِي خَلَقَ ﴿١﴾ خَلَقَ الْإِنْسَانَ

مِنْ عَلَقٍ ﴿٢﴾ اقْرَأْ وَرَبُّكَ الْأَكْرَمُ ﴿٣﴾ الَّذِي

عَلَّمَ بِالْقَلَمِ ﴿٤﴾ عَلَّمَ الْإِنْسَانَ مَا لَمْ يَعْلَمْ ﴿٥﴾

سورة العلق الآيات ١-٥



جمهورية العراق
وزارة التعليم العالي والبحث العلمي
جامعة النهرين
كلية العدا
قسم الفيزياء

الخصائص الطيفية لسلاسل نظائر الهافنيوم

IBFM IBM

مجلس كلية العلوم – جامعة النهرين
وهي جزء من متطلبات نيل دكتوراه فلسفة في الفيزياء

عمار عبدالستار زغير الراوي

بكالوريوس فيزياء | كلية العلوم | جامعة النهرين 2000
ماجستير فيزياء | كلية العلوم | جامعة النهرين 2004

أ.د. ليث عبدالعزيز العاني

..

2017

1438 هـ